# Acta morphologica et anthropologica (22)

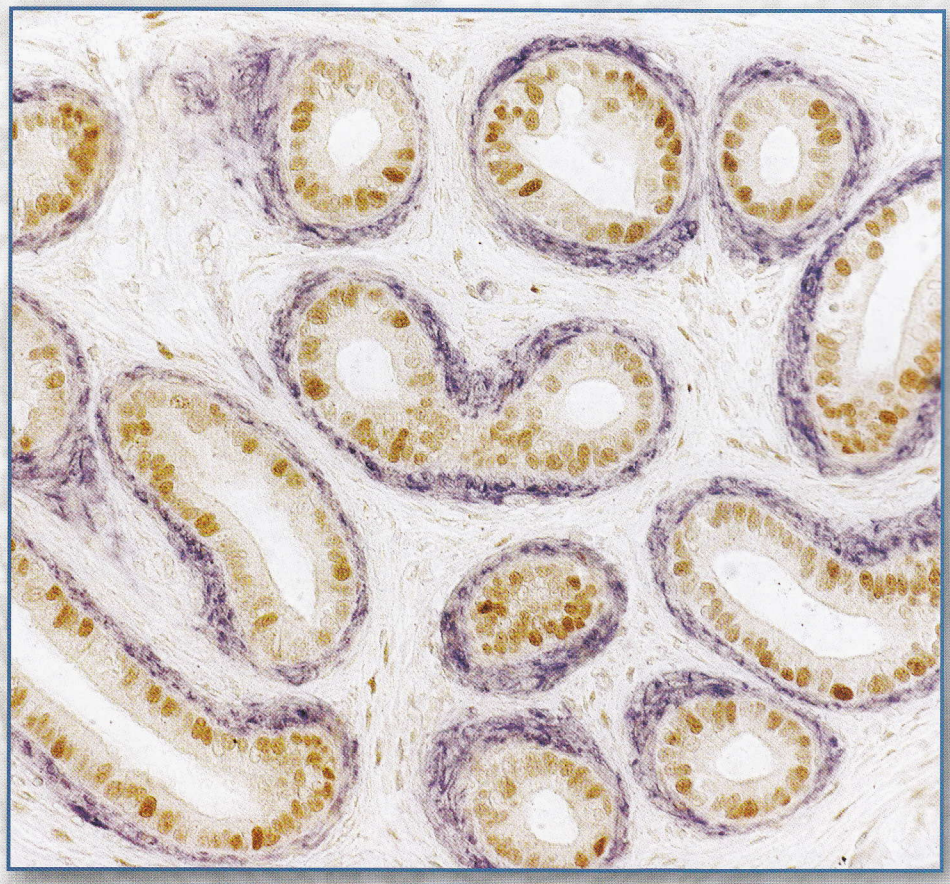

Prof. Marin Drinov Publishing House
of Bulgarian Academy of Sciences

# Acta morphologica et anthropologica

**is the continuation of**
**Acta cytobiologica et morphologica**




*Издаването на настоящия брой на списанието е осъществено с финансовата подкрепа на Фонд „Научни изследвания".*





Prof. Marin Drinov Publishing House of Bulgarian Academy of Sciences
Bulgaria, 1113 Sofia, Acad. Georgi Bonchev Str., Bl. 6

Editor *B. Kremenski* Graphic designer *Desislava Georgieva*
Format 70×100/16 Printed sheets 11

Printing-office of Prof. Marin Drinov Publishing House of Bulgarian Academy of Sciences
1113 Sofia, Acad. Georgi Bonchev Str., Bl. 5

ISSN 0861-0509

# Acta morphologica et anthropologica (22)

22 ● Sofia ● 2015
Institute of Experimental Morphology, Pathology and Anthropology with Museum
Bulgarian Anatomical Society

## Contents

Institute of Experimental Morphology, Pathology and Anthropology with Museum
Bulgarian Anatomical Society

Acta morphologica et anthropologica, 22
Sofia ● 2015

*Morphology*

# Vasoprotective Properties of Aronia Melanocarpa – a Histological and Morphometric Study

*E. Daskalova[1], S. Delchev[1], I. Bivolarski[2], P. Denev[3,4], M. Kratchanova[3,4], P. Cvetkov[5], M. Kaluch[5]*

[1] *Department of Anatomy, Histology and Embryology, Medical University of Plovdiv, Bulgaria*
[2] *Department of General and Clinical Pathology, Medical University of Plovdiv, Bulgaria*
[3] *Laboratory of Biologically Active Substances, Institute of Organic Chemistry with Centre of Phytochemistry, Bulgarian Academy of Sciences, Plovdiv, Bulgaria*
[4] *ITC – Innovative-Technological Centre Ltd., Plovdiv, Bulgaria*
[5] *Medical University of Plovdiv, Plovdiv, Bulgaria*

The social significance of age-related diseases is determined by their global role in mortality and morbidity, particularly in economically developed countries. Changes in elastic and muscular arteries walls, resulting from age-related restructuring and progression of atherosclerotic lesions, underlie coronary heart disease and cerebrovascular disease. Their prevention through administration of natural products is a research area with huge potential, and application of natural antioxidants is one of the leading strategies to retard vascular aging. *Aronia melanocarpa* juice is a rich source of polyphenols and is characterized by very high antioxidant activity *in vitro*. The aim of the current study was to investigate the effect of aronia juice intake on age-related vascular changes of rat aortic walls. We used a model of aging male rats, whose thoracic aorta walls were subjected to macroscopic, histological (hematoxilyn-eosin), histochemical (orcein) and morphometric studies. The comparative analysis between the target group of old animals supplemented with aronia juice; young untreated rats and old controls (not supplemented), revealed that aronia-supplemented animals were characterized with reduced atherosclerotic lesions and a lower level of restructuring of aortic walls. These data confirm that *Aronia melanocarpa* juice successfully retards age-related vascular aging, and can be recommended as a prophylactic tool for healthy aging.

*Key words*: vascular aging, antioxidants, Aronia melanocarpa.

## Introduction

Age-related diseases are social problem with global significance and their prevention through natural products is a research field with great potential. Cardiovascular damage is among the main causes of morbidity and mortality in relation to the aging process.

The morphological changes of the wall of the large arteries, including the aorta are result from age-related restructuring and virtually create pathophysiological conditions for deterioration of their functions leading to pathological changes [9]. The application of antioxidants is one of the strategies to slow the process of vascular aging [4, 5, 6, 7, 8]. *Aronia melanocarpa* juice is a rich source of polyphenols and as such exhibits a very high antioxidant activity [2].

The aim of the current experimental study was to investigate the effect of *Aronia melanocarpa* intake in the age-related vascular changes in the aortic wall.

## Materials and Methods

*Black chokeberry (Aronia melanocarpa) fruit juice:* Commercially available sterilized black chokeberry juice, packed in glass bottles (250 ml), was provided by Vitanea Ltd, Plovdiv, Bulgaria.

In the experiment 22 male Wistar rats were divided into three groups. 14 of them aged 10 months with initial body weight 418 ± 57 g were divided into 2 groups: **control old (CO)**, which were on a standard diet and tap water *ad libitum*, and **Aronia group (A)**, which received *ad libitum* chokeberry juice diluted 1:1 in drinking water and a standard rodent chow. The daily dose of fruit juice ingested by the animals was 10 ml/kg. The **control young group (CY)** consisted of 8 animals aged 2 months with body weight 147 ± 12 g. The experiment lasted 90 days. The experimental protocol was approved by the Committee on Ethical Treatment of Animals of the Bulgarian Agency for Food Safety. In the end of experiment animals were euthanized with i.m. Ketamin/Xilazine and the thoracic aortas were separated and prepared for examination.

*Macroscopic and histology examination:* Descending thoracic aortas from CY, CO and A groups of rats were harvested and fixed in 10% formalin. Aorta thoracica was cleared of the visible connective tissue, cut longitudinally and pressed between two glass slides. Parts of fixed aortic segments were embedded in paraffin and sectioned at 5 μm. Sequential sections were stained with hematoxylin/eosin and orcein. The photomicrographs enclosed were taken on Nikon Microphot SA microscope (Japan), equipped with a Camedia-5050Z digital camera (Olympus, Japan).

*Morphometric analysis:* All quantitative image analysis was performed using software"DP-Soft" 3.2, Olympus, Japan. For each study, analysis of histology sections was performed using at least 5 randomly chosen high-power fields from 5 different sections from each young (n = 8) and old (n = 7) rat. The thickness of aortic tunica media (μm) was measured from the internal elastic lamina to the adventitial border. Cell density (cells/50μm$^2$) in the tunica media of aortic wall was calculated as mean by counting the number of nuclei in 50/50μm areas of tunica media tissue from 5 sections from every young (n = 8), old (n = 7) and Aronia supplemented (n = 7) rat.

*Statistical analysis:* The results were analyzed with SPSS 13.0 statistical program. Statistical significance between experimental groups was determined by Student's t-test and differences were considered significant at $P < 0.05$. The intergroup comparison was made with one-way ANOVA.

## Results

From gross appearance of the intimal surface of the longitudinal section of thoracic aorta (**Fig. 1A**) was evident that there were no visible pathological changes in the intima of the thoracic aorta in the group of young controls. In the group of elderly controls

(**Fig. 1B**), initial fibrous plaques and focal hemorrhages in atherosclerotic plaques were observed. There were also single lipid stripes and spots. In aronia-supplemented group

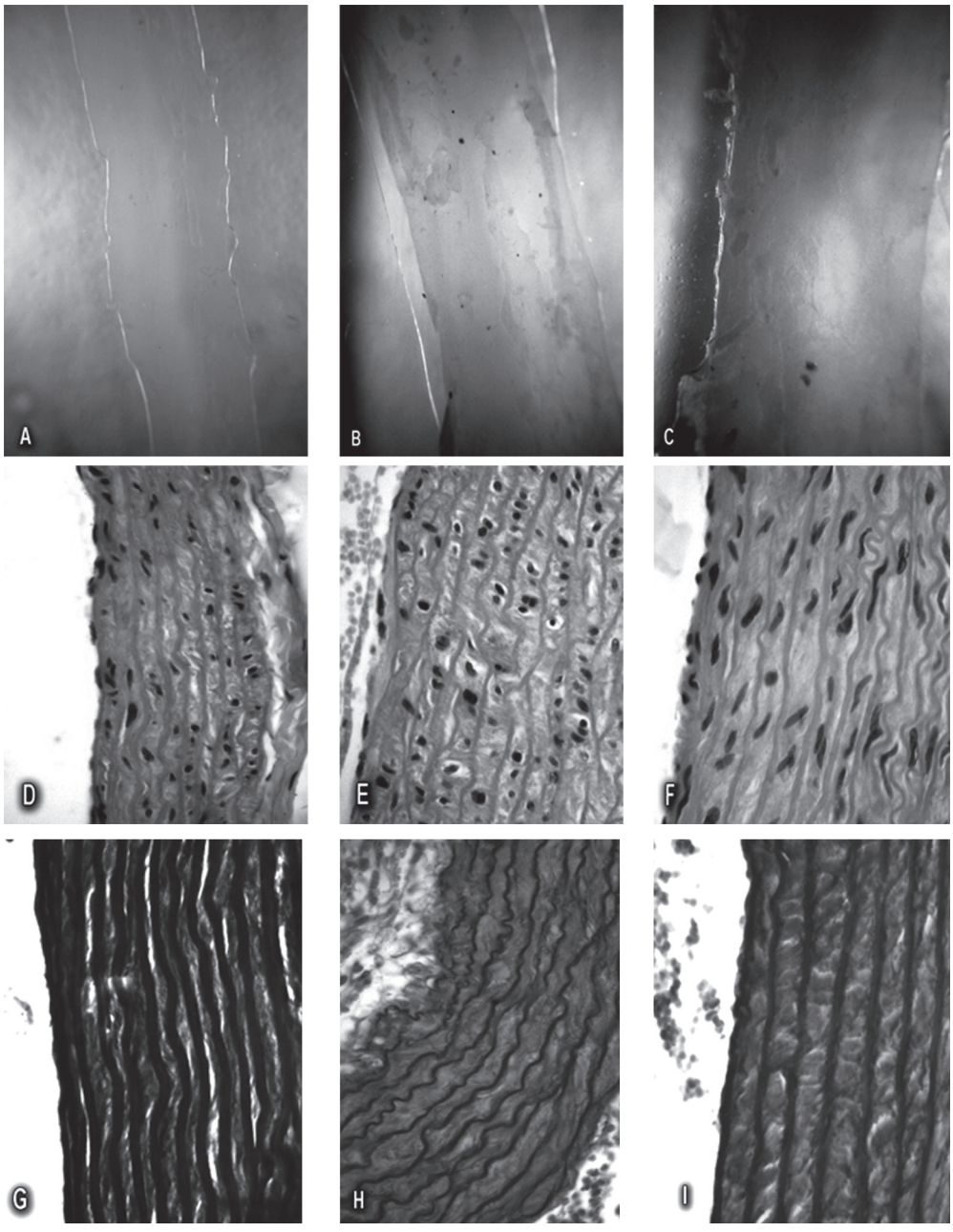


**Fig. 1. Gross appearance** of the intimal surface of the longitudinal section of thoracic aorta of the experimental groups: **A:** controls young, **B:** controls old, **C:** Aronia supplemented group, (magn. × 20), **Hematoxylin/eosin staining D:** controls young, **E:** controls old, **F:** Aronia supplemented group, (magn. × 400), **Orcein staining G:** controls young , **H:** controls old, **I:** Aronia supplemented group, (magn. × 400)

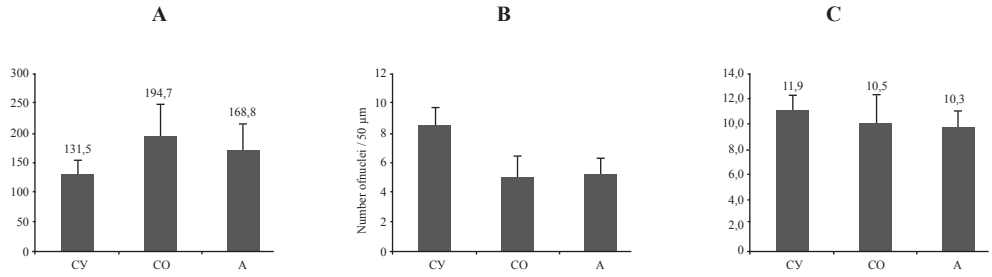


**Fig. 2. A:** Thickness of aortic tunica media, CY in comparison with CO $p < 0.05$; **B:** Cell density of aortic tunica media, CY in comparison with CO $p < 0.05$; **C:** Number of elastic membranes in aortic tunica media

(**Fig. 1C**) the intima was smooth and homogeneous and only single lipid stripes and spots were observed.

The hematoxylin/eosin stainings of thoracic aorta of the experimental groups are shown in **Fig. 1D, E, F**. In the cross-sections of aorta of the young controls (**Fig. 1D**), the tunica intima was smooth without abnormal depositions, the tunica media was presented with evenly and parallel elastic membranes. Their thickness and density were preserved. Smooth muscle cells, located between the elastic membranes were normal in size, shape and density, with normochromatic spindle cores. Tunica adventitia was represented by the usual loose connective tissue. In the crosscut of aorta of the old controls (**Fig. 1E**) the tunica intima was with uneven edges with focal plaque-like thickening. The tunica media was expanded, elastic membranes were separated, and considerably loosen and thinned, and bended serpentine. Smooth muscle cells were enlarged, with perinuclear vacuoles and pale cytoplasm. The nuclei of the cells were reduced in size, with polymorphism and polihromaziya. Some of them had pyknotic form, their orientation was transverse relative to the elastic membrane. In the crosscut of aorta of aronia group (**Fig. 1F**), the tunica intima was smooth, with protrusion of single endothelial cells to the lumen. The tunica media was presented by evenly placed parallel elastic membranes in the inner half of the aorta and serpentine bended – in the outer half. The thickness of the elastic membranes was slightly reduced and their density was stored. Smooth muscle cells had a normal spindle shape, longitudinally oriented, with preserved size, shape and density.

From **Fig. 1G** it is evident that tunica media in young controls was represented by smooth, thick elastic membranes, intensely dyed by orcein. The orcein staining in old controls (**Fig. 1H**) showed loosening and fragmentation of the paler-colored elastic membranes. Orcein staining in the Aronia group (**Fig. 1I**) showed smooth and straight elastic membranes with preserved integrity and staining intensity closer to that of young controls.

Data in **Fig. 2** demonstrated the results of the morphometric study of tunica media of aorta thoracica**.** Regarding the thickness of tunica media (**Fig. 2A**), statistically significant differences were established between younger and older controls ($p < 0.05$). Differences between old controls and aronia group did not reach statistical significance. In terms of the number of nuclei in tunica media (**Fig. 2B**), statistically significant differences were detected only between younger and older controls ($p < 0.05$). Regarding the number of the elastic membrane in the tunica media, differences between groups did not reach statistical significance.

## Discussion

Our findings demonstrate convincingly that in aronia-supplemented animals, age-related changes are discrete and structure of the vascular wall is visibly preserved. This finding demonstrates the delay in the age changes and the preservation of the vessel wall under the influence of supplementation with Aronia melanocarpa juice.

Our data confirm that with advancing age the thickness of the aortic tunica media is increasing statistically significant [9]. Supplementation with Aronia juice leads to a reduction in its dimensions, though not significantly.

Our data confirms findings from other authors [1, 9] that with increased age, a decreased quantity of smooth muscle cells is found inside the tunica media, which are responsible for synthesizing elastin within the aorta.

As recognized by other authors, the amount of elastic membrane does not change with age [1, 3, 9]. Our results confirm the findings that the quantity of the elastin membranes remains inchanged during aging on account of the deterioration of their quality, which is clearly demonstrated by staining with orcein. However, as it is evident from the microphotographs, their quality visibly deteriorates in untreated adult controls and partially improves in aronia-treated rats.

Age-related physiological changes to the aorta are associated with a progressive decline in the elastic properties of the aortic wall [1, 3]. Greenwald [3] reported that conduit arteries become stiffer with age because elastin becomes fragmented, degraded and replaced by much stiffer collagen. Furthermore, both proteins become stiffer because of cross-linking and calcification, and these changes are accelerated by uraemia, hyperglycaemia and oxidative stress [10]. Our results demonstrates that supplementation with aronia melanocarpa juice preserves the structure of the elastic membranes.

## Conclusion

Age-related structural changes in the aortic wall lead to increased aortic stiffness, increasing its diameter and length, reducing its compliance and contractility of the aortic wall [1, 3]. These amendments violate its functions and are a prerequisite for the emergence of pathologies, some of them fatal. Preservation of aortic wall and delay of age-related changes are an essential preventive measure for cardiovascular diseases such as hypertension, aortic dissection, aneurysm and rupture, congestive heart failure, complications of ischemia and stenosis. Achieving this with non-pharmacological agents is one of the latest strategies in the fight against aging. As a functional food juice, *Aronia melanocarpa* shows convincing vaso-protective properties and can be recommended as a prophylactic tool for healthy aging.

## References


1. **Collins, J. A., J. V. Munoz, T. R. Patel, M. Loukas, R. S. Tubbs.** The anatomy of the aging aorta. – Clin. Anat., **27**, 2014, 463-466.
2. **Denev, P., Ch. Kratchanov, M. Ciz, A. Lojek, M. Kratchanova.** Bioavailability and antioxidant activity of Black chokeberry (Aronia melanocarpa) polyphenols: in vitro and in vivo evidences and possible mechanisms of action: a review. – Compr. Rev. Food Sci. F., Vol. **11**, 2012, 472-489.
3. **Greenwald, S. E.** Ageing of the conduit arteries. – J. Pathol., **211**, 2007, 157-172.
4. **Medina-Remón, A., R. Estruch, R. M. Lamuela-Raventós, A. Vallverdú-Queralt**. The effect of polyphenol consumption on blood pressure. – Mini Rev. Med. Chem., **13**, 2013, 1137-1149.

5. **Miquel, J.** Nutrition and ageing. – Public Health Nutr., **4**, 2001, 1313-1314.
6. **Moline, J., I. F. Bukharovich, M. S. Wolff, R. Phillips.** Dietary flavonoids and hypertension: is there a link? – Med. Hypotheses, **55**(4), 2000, 306-309.
7. **Pase, M. P., N. A. Grima, J. Sarris.** The effects of dietary and nutrient interventions on arterial stiffness: a systematic review. – Am. J. Clin. Nutr., **93**, 2011, 446-454.
8. **Sanchez-Roman, I., G. Barja.** Regulation of longevity and oxidative stress by nutritional interventions: Role of methionine restriction. – Exp. Gerontol., **48**, 2013, 1030-1042.
9. **Wheeler, J. B., R. Mukherjee, R. E. Stroud, J. A. Jones, J. S. Ikonomidis.** Relation of murine thoracic aortic structural and cellular changes with aging to passive and active mechanical properties. – J. Am. Heart Assoc., **4**(3), 2015 (in press).
10. **Zarkovic K., P. Larroque-Cardoso, M. Pucelle, R. Salvayre, G. Waeg, A. Nègre-Salvayre, N. Zarkovic.** Elastin aging and lipid oxidation products in human aorta. – Redox. Biol., **4**, 2015, 109-117.

Institute of Experimental Morphology, Pathology and Anthropology with Museum
Bulgarian Anatomical Society

Acta morphologica et anthropologica, 22
Sofia ● 2015

# Study on Fibroblast Activation Protein-a Activity in an *In Vivo* Mouse Model of Ehrlich Ascites Carcinoma

*M. Dimitrova[1], I. Iliev[1], V. Pavlova[1], V. Mitev[2], I. Ivanov[2]*

*[1]Institute of Experimental Morphology, Pathology and Anthropology with Museum, Bulgarian Academy of Sciences, Sofia*
*[2]Department of Medical Chemistry and Biochemistry, Medical University of Sofia, Bulgaria*

Fibroblast activation protein-a (FAP-a) is a membrane-associated serine type post-proline cleaving protease with a very restricted normal tissues distribution but highly active in tumor tissues. In human breast cancer, FAP-a is expressed both in the reactive stromal fibroblasts and tumor cells. However, the enzyme role in pathogenesis of the breast cancer is unknown and its association with the prognosis is controversial varying from better to very poor. Animal models could help in elucidating the enzyme involvement in mammary gland carcinoma. In this study we present our results for FAP-a imaging in normal mouse mammary gland and in a murine *in vivo* model of Ehrlich ascites carcinoma (EAC) using a fluorogenic enzyme histochemical method recently developed by us. We show that FAP-a is not expressed in normal mouse mammary gland but is highly active in EAC cells. This result proves that mouse *in vivo* EAC model can be useful in studies of FAP-a diagnostic/prognostic value for human breast cancer.

*Key words:* fibroblast activation protein-a, Ehrlich ascites carcinoma, *in vivo* model, mouse, enzyme cytochemistry.

## Introduction

Fibroblast activation protein-a (FAP-a; EC 3.4.21.B28) is a 170 kDa integral membrane protease belonging to the S9b subfamily of post-proline cleaving enzymes [14]. This class of peptidases is known to modify bioactive peptides thus changing their cellular functions and to have important roles in cancer [16]. Some of the natural FAP-a substrates include collagen type I, α2-antiplasmin, neuropeptide Y, B-type natriuretic peptide, substance P and peptide YY [7]. Both immunohistochemical [15] and mRNA expression [3] studies have shown that in humans and mammals FAP-a has a highly restricted normal tissue distribution. It has been found only in fetal mesenchymal tissues as well as in healing wounds, single reactive fibroblasts and a distinct set of glucagon producing pancreatic islet cells (A cells) in adults. On the other hand, FAP-a is present in stromal fibroblasts of over 90% of epithelial tumors and some sarcomas [for review see 17]. Based on the above findings, the enzyme is largely considered to be a valuable marker and a potential therapeutic target for different types of carcinomas. Although malignant epithelial, neural and haematopoietic cells have generally been found to be

FAP-a-negative, some studies have revealed that the enzyme is expressed also in neoplastic cells of mesenchymal origin [15] and epithelial tumor cells of breast, gastric, and colorectal cancers [reviewed in 9]. It is commonly believed that the over-expression of FAP-a contributes to the tumor invasion capacity and facilitates sprouting of tumor blood capillaries [9, 13, 17].

In one of the earliest studies on FAP-a expression in human breast cancer using the F19 monoclonal antibody, the enzyme molecule has been identified only in the reactive tumor stroma [5]. Later on, by applying FAP-specific antisera, it has been shown that the enzyme is expressed in breast cancer cells, as well [8]. Presently, despite the widely recognized role of FAP-a in human breast cancer, its value as a prognostic marker is greatly controversial and varies from better [1] to very poor outcomes [6, 8]. Therefore, more studies on the marker importance of the enzyme in mammary gland carcinoma are needed, including use of appropriate animal models.

Mouse Ehrlich ascites carcinoma (EAC) is one of the commonly used *in vivo* animal models of mammary gland cancer, due to its resemblance with the most rapidly growing undifferentiated and chemotherapy sensitive human breast tumors [12]. It represents a spontaneous murine mammary adenocarcinoma adapted to ascites form and carried in outbred mice by serial intra-peritoneal (i.p.) passages. This model has been widely used for the evaluation of alternative approaches in cancer therapy [10] as well as the therapeutic significance of natural extracts and synthetic compounds [reviewed in 12]. However, FAP-a expression has not been studied in EAC, thus far.

The aim of the present paper is to compare FAP-a distribution in normal mouse mammary gland and in tumor cells of EAC in an *in vivo* mouse model using the fluorescent enzyme cytochemical method recently developed by us.

## Materials and Methods

*The FAP-α substrate* 4-(β-Ala-Gly-Pro-hydrazido)-N-hexyl-1,8-naphthalimide (βAGP-HHNI) was synthesized according to the previously described reaction scheme [2]. The precise chemical syntheses as well as the spectral analyses of the compounds will soon be published elsewhere.

### *Animals and Tissue Treatment*

All the experiments were performed in compliance with the Institutional Guidelines for Animal Experiments of IEMPAM – Bulgarian Academy of Sciences.

Female BALB/c mice were sacrificed by cervical dislocation 10 days after weaning of the pups. Thoracic and abdominal mammary glands were extracted and immediately frozen in liquid nitrogen. Cryostat sections (10 μm) were cut on cryotome Reichert-Jung (Germany) at –26 °C and mounted on gelatinized glass slides. The sections were air-dried, covered with 0.5% collodion (Sigma-Aldrich) in acetone: diethyl ether: absolute ethanol (4:3:3) for a minute at room temperature and used for the histochemical visualization of FAP-α activity.

Ehrlich tumor cell line was maintained in female albino mice, 5 to 7 weeks old with live body weight 25 g to 30 g, throughout serial weekly intraperitoneal injections of $1 \times 10^6$ viable tumor cells suspended in 0.2 ml phosphate buffered saline (PBS) per mouse. Mice were sacrificed by cervical dislocation 8-10 days after inoculation and Ehrlich ascites carcinoma (EAC) cells were collected by a syringe from the abdominal cavity together with the ascitic fluid. Smears of the aspired EAC cells were made on gelatinized glass slides, air-dried and fixed in paraformaldehyde vapors for 4 minutes at

room temperature. Some of the smears were stained with haematoxylin-eosin according to the classical methods of histology. Other smears were covered with 0.5% collodion as above and used for the visualization of FAP-α activity.

*Incubation Solutions and Controls*

Tissue sections and EAC smears were incubated in solutions containing 0.5 mM FAP-α substrate βAGP-HHNI and 0.5 mg/ml piperonal in 0.1 M phosphate buffer, pH 7.4, supplied with 100 mM NaCl at 37 °C for 16 h. After the incubation, they were post-fixed in 4% neutral formalin for 15 min at room temperature, slightly counter-stained with haematoxylin and embedded in glycerol/jelly. Control samples were treated in the same manner but in the lack of substrate in the incubation solutions. All the preparations were observed under the fluorescent microscope Leica DM5000B (USA).

## Results and Discussion

Fibroblast activation protein-a is widely recognized as one of the most valuable tumor markers and is considered an important target for developing innovative and more effective anti-cancer therapies. Although the enzyme is mainly known as a common characteristic of tumor stromal fibroblasts, a huge number of recent studies have revealed that it is expressed in many types of epithelial tumor cells [for review see 9]. FAP-a capacity to hydrolyze collagen type I and a2-antiplasmin is believed to contribute to tumor invasiveness and metastatic ability not only by opening free spaces in extracellular matrix, but also by releasing different growth factors in the tumor vicinity thus recruiting them in outspread of the tumor cells and blood vessels [9, 17].

In human breast cancer, FAP-a expression has been documented both in the reactive stromal fibroblasts [1, 5] and tumor cells [6, 8]. However, the precise role of the enzyme in this type of cancer is largely unknown and the enzyme association with the prognosis is controversial varying from better [1] to very poor [6, 8]. Animal models of human breast cancer could help in elucidating the enzyme involvement in the development of mammary gland carcinoma. The most commonly used mouse model of breast cancer is Ehrlich ascites carcinoma (EAC) [12]. EAC firstly appeared as a spontaneous breast cancer in a female mouse and was used for sub-cutaneous transplantations to produce solid tumors. Later, it has been adapted to a liquid form and injected i.p. to produce ascites form of the mouse breast cancer. EAC is known to possess great resemblance to highly undifferentiated human mammary gland carcinomas and is widely used to evaluate innovative anti-cancer therapies [for review see 12]. However, FAP-a distribution in EAC has not been studied yet. Additionally, it is well known that FAP-a is a highly conservative protein and mouse enzyme has 89% similarity to its human analogue [11].

Recently, we developed a novel fluorogenic substrate for FAP-a-4-(β-Ala-Gly-Pro-hydrazido)-N-hexyl-1.8-naphthalimide (βAGP-HHNI) and used it successfully for the *in situ* imaging of the enzyme activity in normal and tumor mouse fibroblasts [2]. In this paper we present our results from FAP-a distribution studies in a mouse *in vivo* model of EAC. In our experiments we used female mice, which were inoculated i.p. by EAC cells. The animals were examined every day and their abdominal circumferences were compared to those of non-treated controls. The experiments showed that 8-10 days after inoculation the mice developed ascites cancer in the peritoneal cavity. After the animal sacrifice, tumor cells were aspired and FAP-a activity was visualized in cell smears using our novel substrate βAGP-HHNI according to the cytochemical proce-

dure described before [2]. Histochemical preparations of freshly frozen healthy mature animals' mammary glands were used as controls by applying the same fluorogenic substrate. No FAP-a activity was detected in the healthy mouse mammary gland (**Fig. 1**).

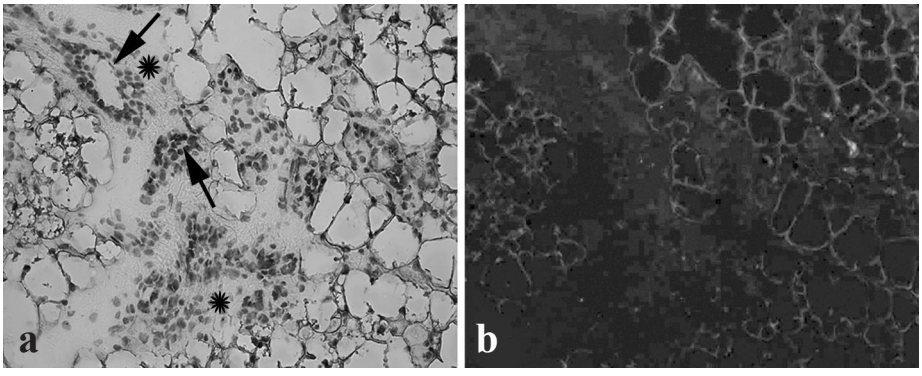


**Fig. 1.** Lack of FAP-α activity in the mammary gland of a mature female mouse as revealed using the FAP substrate βAGP-HHNI. Ductal epithelial cells (arrows) and dense connective tissue elements asterisks are all FAP-α-negative. a – light microscopy; b – fluorescent microscopy (× 200)

Both alveolar epithelial cells and dense connective tissue elements proved to be FAP-a-negative. This result is in compliance with previous findings that normal adult tissues of humans and mammals do not express the enzyme [3, 15].

The haematoxylin-eosin staining of EAC cells revealed the well-known previously observed morphological features of this type of tumor cells [4]. EAC cells possessed comparatively large nuclei and moderate amounts of basophilic vacuolated cytoplasm (**Fig. 2**). Different stages of mitosis were also to be seen in the smears.

In our enzyme histochemical study, all the EAC cells proved to be highly FAP-a-positive (**Fig. 3**). This result is to show that mouse breast carcinoma cells are FAP-a-positive just like human mammary gland carcinoma cells.

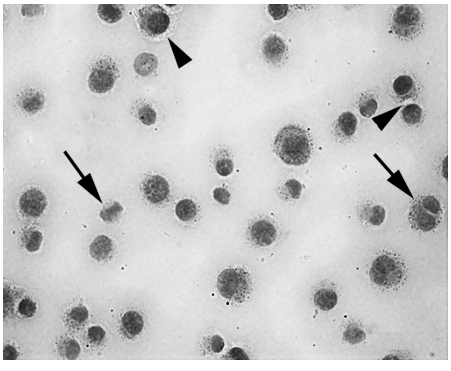

**Fig. 2.** Haematoxylin – eosin stained smear of Ehrlich ascites tumor cells. Cells in different stages of mitosis (arrows); cytoplasmic vacuoles (arrowheads) (× 400)

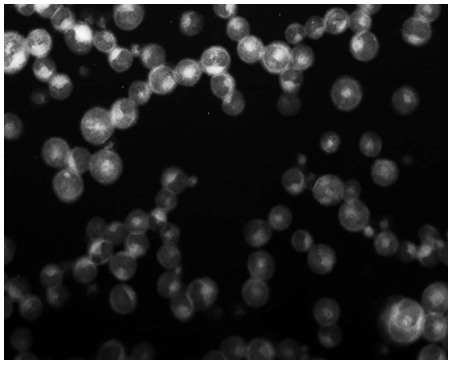

**Fig. 3.** FAP-a activity in a smear of Ehrlich ascites tumor cells visualized by means of the newly developed fluorogenic substrate βAGP-HHNI. All the cells are highly positive for the enzyme (× 400)

In conclusion, our results show that tumor cells of mouse breast carcinoma express FAP-a, which represents one more similarity between mouse EAC and human breast tumors. On the other hand, this result proves that mouse *in vivo* EAC model could be useful in the studies of FAP-a diagnostic/prognostic value for human mammary gland carcinoma.

*Acknowledgements:* This work is financially supported by the National Science Fund at the Bulgarian Ministry of Education and Science, Grant No T02/25 2014.

## References

1. **Ariga, N., E. Sato, N. Ohuchi, H. Nagura, H. Ohtani.** Stromal expression of fibroblast activation protein/seprase, a cell membrane serine proteinase and gelatinase, is associated with longer survival in patients with invasive ductal carcinoma of breast. – Int. J. Cancer, **95**, 2001, 67-72.
2. **Dimitrova, M., I. Iliev, V. Pavlova, V. Mitev, S. Dimitrova, D. Aleksandrova, I. Ivanov.** Development and application of a specific fluorogenic substrate for the cytochemical study of fibroblast activation protein alpha. – Proceedings of VI$^{th}$ Workshop on Experimental Models and Methods in Biomedical Research, 2015, in press.
3. **Dolznig, H., N. Schweifer, C. Puri, N. Kraut, W. Rettig, D. Kerjaschki, P. Garin-Chesa.** Characterization of cancer stroma markers: in silico analysis of an mRNA expression database for fibroblast activation protein and endosialin. – Cancer Immunity, **5**, 2005, 10-18.
4. **Freitas, E. S., E. Leite, A. Silva, N. Ocarino, E. Ferreira, M. Gomes, G. Cassali, R. Serakides.** Effect of thyroxine and propylthiouracil in Ehrlich ascitic tumor cells. – Int. J. Morphol., **24**, 2006, 665-671.
5. **Garin-Chesa, P., L. Old, W. Rettig.** Cell surface glycoprotein of reactive stromal fibroblasts as a potential antibody target in human epithelial cancers. – Proc. Natl. Acad. Sci. USA, **87**, 1990, 7235-7239.
6. **Huang, Y., S. Wang, T. Kelly.** Seprase promotes rapid tumor growth and increased microvessel density in a mouse model of human breast cancer. – Cancer Res., **64**, 2004, 2712-2716.
7. **Keane, F. M., N. Nadvi, T. Yao, M. Gorrell.** Neuropeptide Y, B-type natriuretic peptide, substance P and peptide YY are novel substrates of fibroblast activation protein-α. – J. FEBS, **278**, 2011, 1316-1332.
8. **Kelly, T., S. Kechelava, T. Rozypal, K. West, S. Korourian.** Seprase, a membrane-bound protease, is overexpressed by invasive ductal carcinoma cells of human breast cancers. – Mod. Pathol., **11**, 1998, 855-863.
9. **Kelly, T., Y. Huang, A. Simms, A. Mazur.** Fibroblast activation protein-α: a key modulator of the microenvironment in multiple pathologies. – In: International review of cell and molecular biology, Academic Press – Elsevier, USA, UK, The Netherlands, 2012, 83-116.
10. **Kiziltan, H. S., A. Bayir, G. Yucesan, A. H. Eris, I. Karatoprak, T. Aydin, A. Akcakaya, A. Mayadagli.** Medical ozone and radiotherapy in a peritoneal Ehrlich ascites tumor cell model. – Altern. Ther. Health Med., **21**, 2015, 24-29.
11. **Niedermayer, J., M. Scanlan, P. Garin-Chesa, C. Daiber, H. Fiebig, L. Old, W. Rettig. A. Schnapp.** Mouse fibroblast activation protein: molecular cloning, alternative splicing and expression in the reactive stroma of epithelial cancers. – Int. J. Cancer, **71**, 1997, 383-389.
12. **Ozaslan, M., I. Karagoz, I. Killic, M. Guldur.** Ehrlich ascites carcinoma. – Afr. J. Biotech., **10**, 2011, 2375-2378.
13. **Park, J. E., M. Lenter, R. Zimmermann, P. Garin-Chesa, L. Old, W. Rettig.** Fibroblast activation protein, a dual specificity serine protease expressed in reactive human tumor stromal fibroblasts. – J. Biol. Chem., **274**, 1999, 36505-3651.
14. **Pineiro-Sanchez, M. L., L. Goldstein, J. Dodt, L. Howard, Y. Yeh, H. Tran, W. Argraves, W. Chen.** Identification of the 170-kDa melanoma membrane-bound gelatinase (seprase) as a serine integral membrane protease. – J. Biol. Chem., **272**, 1997, 7595-7601.

15. **Rettig, W. J., S. Su, S. Fortunato, M. Scanlan, B. Raj, P. Garin-Chesa, J. Healey, L. Old.** Fibroblast activation protein: purification, epitope mapping and induction by growth factors. – Int. J. Cancer, **58**, 1994, 385-392.
16. **Rosenblum, J. S., J. Kozarich.** Prolyl peptidases: a serine protease subfamily with high potential for drug discovery. – Curr. Opin. Chem. Biol., **7**, 2003, 496-504.
17. **Yu, D. M. T., T. Yao, S. Chowdhury, N. Nadvi, B. Osborne, W. Church, G. McCaughan, M. Gorrell.** The dipeptidyl peptidase IV family in cancer and cell biology. – J. FEBS, **277**, 2010, 1126-1144.

Institute of Experimental Morphology, Pathology and Anthropology with Museum
Bulgarian Anatomical Society

Acta morphologica et anthropologica, 22
Sofia ● 2015

# Round Immature Spermatogenic Cells in Semen Fluids of Infertile Men with Diagnosis "Migrating Testis". Two Casuistic Cases in Adults

*I. Ilieva[1], P. Tzvetkova[2], M. Kacarov[3], I. Sainova[1], P. Taushanova[2], I. Vladov[1], E. Zvetkova[4]*

*[1]Institute of Experimental Morphology, Pathology and Anthropology with Museum, Bulgarian Academy of Sciences, Sofia, Bulgaria*
*[2]Institute of Biology and Immunology of Reproduction "Acad. Kiril Bratanov", Bulgarian Academy of Sciences, Sofia, Bulgaria*
*[3]Medical Center "Doverie", Sofia, Bulgaria*
*[4]Bulgarian Biorheological Society*

The spermatological analysis of ejaculates from two patients suffering of low male fertility and with diagnosis "migrating" testis syndrome (casuistic cases in adults), reveals cytological characteristics of different immature spermatogenic cells ("round cells") as precursors of spermatozoa. The high quantity of undifferentiated spermatocytes/spermatides in ejaculates is important for early diagnoses of andrological diseases related to male fertility (sub-fertility, infertility). The results from semen assays showed a high percent (7.3% and 13.5%) of immature ("round") spermatogenic cells in the ejaculates of patients – in correlation with the elevated number of abnormal spermatozoa in probes. The morphological analysis of sperm samples in patients with ascending testis could serve as additional diagnostic and prognostic tool in the routine everyday andrological practice.

*Key words:* spermatogenesis, immature spermatogenic cells ("round cells"), ascending testis syndrome.

## Introduction

In the process of spermatogenesis, spontaneous degenerative changes in the separated zones of the seminiferous tubules are possible. These features affect individual cell types – spermatogonia, spermatocytes (primary and/or secondary), spermatids and spermatozoa, and some of them pass in the seminal fluid. In pathology of the genital tract, which could be a result of congenital factors (cryptorhidism, anorhidism, etc.) or of the influence of different diseases, these changes can include larger regions of the testicular tissue [7, 14, 20]. In normal conditions, the amount of the degenerated gametes in the ejaculate is approximately 25% (WHO, 2010). However, in stress conditions, significant increase is possible, which could influence the inseminal qualities of the fluid. The morphological assessment of the seminiferous assay includes the determination of the mature spermatozoa, but also of other – both cytologically and functionally different

cell types. In most cases these are immature germ cells – precursors of spermatozoa, but also leucocytes (e.g. granulocytes, monocytes/macrophages) or epithelial cells from the urogenital tract. The immature germ cells, together with the leucocytes, usually are beyond the general group of so called "round cells" [4, 11, 14]. The exact determination of the cell types and their differentiation in spermatogenic or non-spermatogenic mature cells is important not only for a correct diagnosis, but also for the therapeutic approach. According to the recommendations of the World Health Organization (WHO), if the "round cells" in the ejaculate probe are more than $1 \times 10^6$/ml, they should be determined as "presenting leucocytes", because their increased amount could be a sign for inflammation process in the urogenital tract [6, 19]. In this connection, it is of interest to study the cytological content of the seminal fluid in patients with diagnosis "migrating" testis – two casuistic cases in adult men. In the scientific literature, the term "migrating" (elevator) testis ("retractile tests") [2, 12, 23] is also described as a "retractile testis" and/or as "a syndrome of ascending testis" [12, 20, 23]. This abnormal gonad state is usually diagnosed in boys (child and juvenile age – most often around 10 years), but it is extremely rare in adult men. Unlike in cases of cryptorhidism, despite the scrotal position of the testes there is a risk of migrating testes (they remain in inguinal duct and later descend into the scrotum) due to external conditions like cold, nerve stress of cremaste muscle. As a result, abnormalities in the spermatogenesis are possible, which are similar to those, established in diagnosed cryptorhidism and/or varicocelle, due to the abnormal gonad thermoregulation [20, 23].

In this connection, the aim of the present study is to evaluate the quantity and to characterize the morphology of "round cells" in the samples from semen fluids of patients with more rare diagnosis *ascending testis*. The methods of qualitative and quantitative semen analysis, applied by us, after *in situ* staining of "round cells" in ejaculates, could be an important diagnostic tool applicable in the treatment of patients with disturbances in spermatogenesis and subfertility/infertility-related problems.

## Materials and Methods

Semen liquids (ejaculates) from two andrological patients (average 23 and 30 years) with *ascending testis*, are examined, and the results are compared with data, obtained from a control group of 20 fertile healthy men (average $32.45 \pm 1.59$ years).

For a precise clinical diagnosis, in each case the patient's data (anamnesis), together with his local clinical status, are carefully investigated.

### *Sperm Analysis*

Spermatological assay includes the qualitative and quantitative analyses of ejaculates and investigations of individual cells (spermatogonia, spermatocytes, spermatids, spermatozoa and other, so-called "round cells", in seminal plasma – assessed according to WHO criteria, 2010).

For cytological analysis, the smears from ejaculates are stained by the standard methods of Papanicollaou and Hematoxyllin/Eosin. The slides are examined light-microscopically with microscope Leica DM 5000B (at different magnifications).

On the basis of morphological characteristics, the spermatogenic and non-spermatogenic ("round") cells in ejaculates are identified, as:

- spermatogonia (Spg);
- primary spermatocytes (Spc-I);
- secondary spermatocytes (Spc-II);
- spermatids (Spt);

– round spermatids – rSpt;
– elongated spermatids – elSpt;
- other (non-spermatogenic) round cells:
  – granulocytes;
  – monocytes/macrophages;
  – lymphocytes.

*Statistical Analysis*

Statistical significance is verified by Student's *t*-test. The results are given as MEAN ± SD.

## Results

In the course of the spermatological analysis we obtained a reduced number of morphologically normal spermatozoa in the ejaculates of two andrological patients (with ascending testis), in comparison with the normal values for the control group. The quantitative results are presented in **Table 1**.

**Table 1.** Cell number and presence of spermatozoa (including abnormal), as well as undifferentiated (immature) spermatogenic cells in ejaculates of patients with *ascending testis*, versus data for the control group

| | **Number of spermatozoa (million/ml)** | **Normal spermatozoa (%)** | **Abnormal spermatozoa (%)** | **Immature germ cells (million/ml)** | **Immature germ cells (%)** |
|---|---|---|---|---|---|
| Ascending testis (n = 2) | (n = 1) Normospermia 67 | 38.3 | 54 | 5.59 | 7.3 |
| | (n = 1) Oligospermia 19 | 22.95 | 63.45 | 2.97 | 13.5 |
| Control group (n = 20) | 84.79 ± 13.57 | 80.63 | 18.37 | 0.86 ± 0.09 | 1.0 |

In one of the patients, the results show *oligospermia* – significantly decreased total spermatozoa number (19 million/ml) in the ejaculate, and in the other – *normospermia* (67 million/ml). In both cases, especially in that with *oligospermia* we assessed increased (> 50%) percent of the spermatozoa with abnormal morphology (**Table 1**). The highest percent is established for the spermatozoa (18.46%), possessing deformations in the head, but gametes with combined abnormalities also reach significant percent (25.71%) (**Fig. 1**).

According to our results, simultaneously with the decrease of total number of spermatozoa, an increase in the percent of the spermatogenic "round cells" in the ejaculates was found, which correlates with the higher percent of the abnormal gametes. The percentage of the immature "round" spermatogenic cells in the samples of both patients is

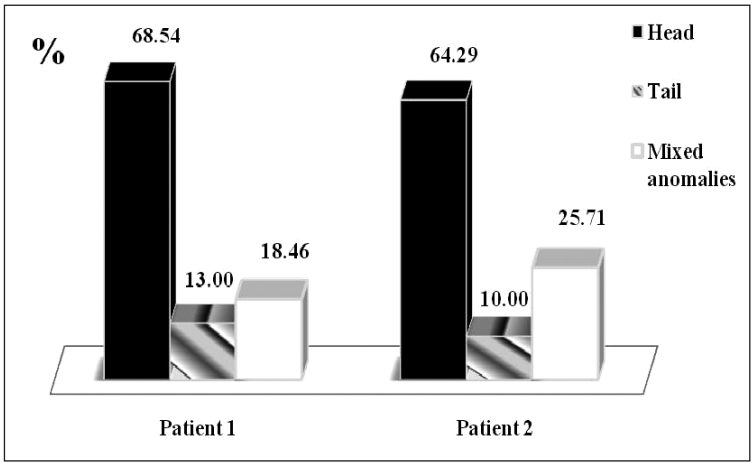


**Fig. 1.** Percent (%) distribution of the morphological spermatozoa abnormalities (in head, tail, mixed anomalies) in the two patients with ascending testis (Patient 1 – *normospermia*, Patient 2 – *oligospermia*)

significantly increased (7.3% and 13.5%, respectively), in comparison with the control group (1%). In **Table 2** is presented the percent distribution of the morphologically immature spermatogenic cells on cytological smears from the patients with "ascending testis".

**Table 2.** Percent (%) distribution of immature spermatogenic cells in the ejaculates of patients with "ascending testis" (Patient 1– *normospermia*, Patient 2 – *oligospermia*)

| % | Spg | Spc-I-II | Spt |
|---|---|---|---|
| Patient 1 | 3.6 | 20.7 | 75.7 |
| Patient 2 | 3.7 | 21.4 | 74.9 |
| Control group (n = 20) | – | 6.8 | 93.2 |

The distribution in **Table 2** shows higher percent of the spermatids in all cases, but unlike in the control group, in both patients we established increased number of spermatogonia, and spermatocytes. In all ejaculates tested, the leucocytes amounts vary (0:0.4%).

The microscopical investigations of semen fluids resulted in a precise morphological characterization and identification of spermatogenic cells at different stages of cell maturiration/differentiation: from undiferentiated spermatogonia to mature spermatozoa (**Figs. 2, 3**).

Spermatids (with round or oval nuclear shape) and spermatocytes are the most often spermatogenic "round cells" identified in the ejaculates of patients with "ascending testis" (**Fig. 2**).

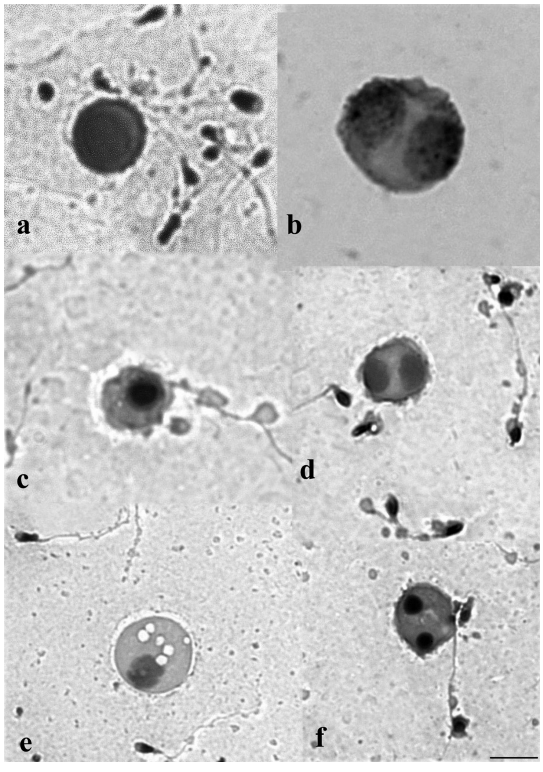


**Fig. 2.** Spermatocytes and spermatids: a) Spc I; b) Spc I with two nuclei; c) round Spt; d) Spc II with two nuclei; e) degenerating Spt with vacuoles in cytoplasm; f) degenerating Spt with two picnotic nuclei. Papanicolaou (× 400; × 600)

Spermatogonia and secondary spermatocytes are also found, but much seldom than the other spermatogenic cell types. A common morphological feature in the ejaculates of these patients is the high amount of primary (Spc I) and secondary spermatocytes (Spc II), possessing two nuclei, probably in result of abnormal mitoses (**Figs. 2b, d, f**).

The presence of similar round cells, but with larger size, possessing four nuclei, (probably spermatocytes), is more often observed in the patient with *oligospermia* than in that with *normospermia* (**Figs. 3d, 3e**).

Multinuclear cells, containing two, three or more picnotic spermatide nuclei, are also established (**Figs. 3a, c**), as well as the presence of groups (clusters) of cells or couples of cells, connected to each other by intra-cellular links ("cytoplasmic bridges") (**Figs. 3g, h**).

Another often met finding is the presence of large round cytoplasmic residues (cytoplasmic droplets), around the mature spermatozoa, with or without agglutination. Similar accumulation of mature spermatozoa is also established around the round immature germ cells (**Figs. 3f, i**).

The morphological characterization of the most spermatids (with round or oval shape of the nucleus) illustrates a high degree of male gamete degeneration, associated with injured nuclear chromatin condensation and cytoplasm vacuolization (probably due to apoptotic changes), (**Fig. 2e**).

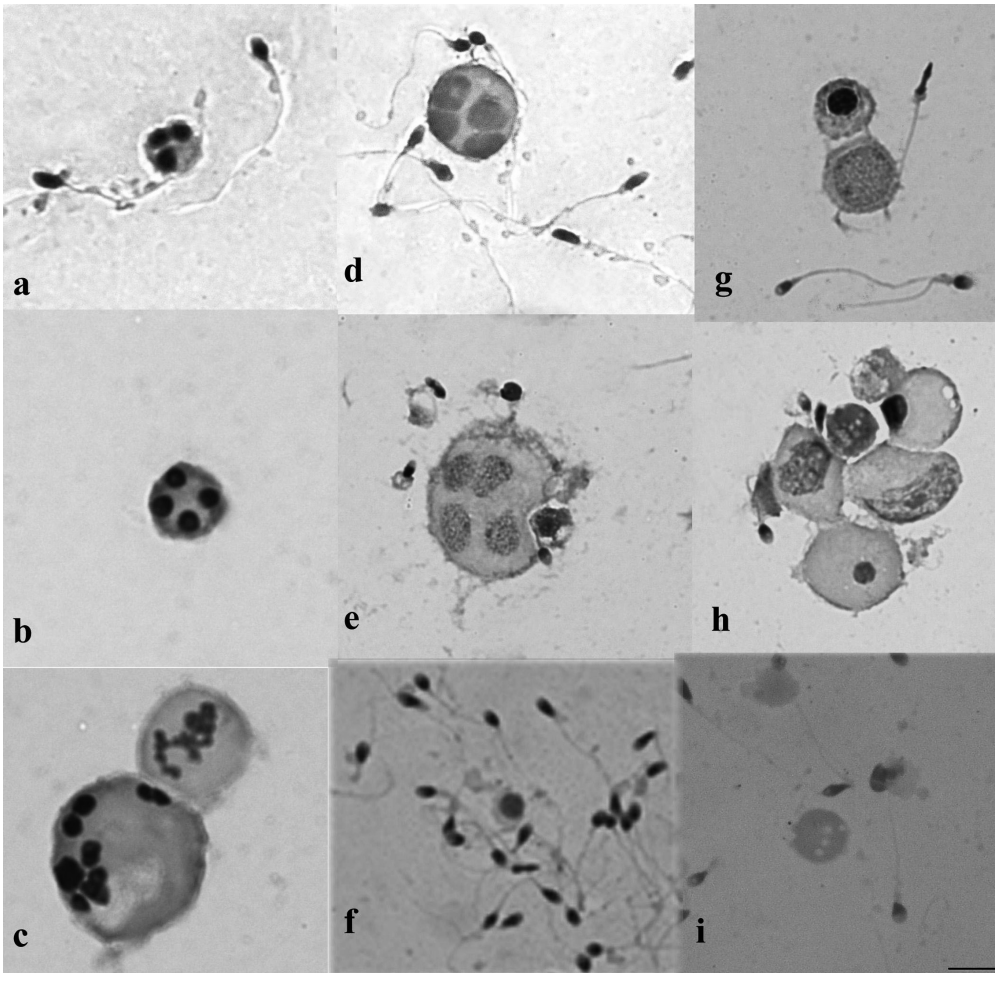


**Fig. 3.** Round cells and clusters: multi-nuclear cells (a – c) with picnotic nuclei (d – e); with four nuclei (non-finished cell division) (Spc); (f) Spc I and agglutination; (g – h) couple of cells and group (cluster) of cells; (i) cytoplasmic remedy (droplet). Papanicolaou, HE (× 400; × 600)

The spermatological assays of the ejaculates from both patients demonstrated a decreased seminal ability with sub-fertility in the case with *normospermia*, and infertility in *oligospermia*, respectively.

## Discussion

Undescended testis or cryptorchidism represents the most common congenital abnormality in boys. The main reason of infertility in cryptorchidism is hyperthermia related to the abnormal position of testis that impaired spermatogenesis [16]. From the clinical (andrological) and pathological point of view the ascending (migrating) testis demonstrates similar features to these of cryptorhidism – with impaired gonadal thermo-regulation and abnormal spermatogenesis, falling by this way into the categories of "similar

diseases" [13, 14, 20]. If these disorders are not treated for a prolonged time period, they could lead to an increased risk for infertility, but also to development of testicular tumors in adults [3, 5].

In the current spermatological study, a high percent of immature spermatogenic cells in the ejaculates of both patients with "migrating testis" diagnosis, is established – 7.3% and 13.5%, respectively. Although we obtained results from two patients only, the increased amounts of spermatids and spermatocytes in the seminal probes might be due to pathological seminiferous tubules. The observed groups (clusters) of two, three or more cells, connected to each other by cytoplasmic connections ("bridges"), but also the presence of two- and multi-nuclear spermatids (most often with picnotic nuclei), show an interesting cytological pattern in both *oligospermia*- and *normospermia*-diagnosed patients. In both cases, the reduced inseminal possibility is associated with the increased percentage of abnormal spermatozoa, in particular such with deformations in the head, as well as with mixed anomalies. These results are similar to our previous data from investigations of patients with pathologies of the male reproductive system [9, 10], where we also established increased amount of gametes with head anomalies. In cases with *cryptorchidism* the spermatozoa with elongated and round heads were prevailed, but increased number of cells with two heads was also observed. However, in comparison with the patients with ascending testis, significantly lower amount of the gametes with mixed anomalies was assessed in the cases with *cryptorchidism*.

According to many authors [8, 20, 22], the results from histological studies indicate that the spermatogenesis could be affected and injured in all stages of the male reproductive system development (ontogenesis, puberty and adult age). Different etiological factors could lead to the same and/or to similar structural abnormalities in the testicular tissue, manifested by decreased germ cells proliferation, abnormal differentiation and hence appearance of "teratological forms" among the mature spermatozoa as well as elimination of many immature spermatogenic cells. The gametogenesis abnormalities in cases with *cryptorhidism*, are often characterized by blocking of the process at the different phases of spermatocytes and/or spermatids' development in the different regions of the seminiferous ducts. The blocking is depending on the susceptibility of the respective cell populations to the increased temperature in the scrotum, as well as to the subsequent hypoxia and oxidative stress [3, 14, 18]. Depending on the pathological conditions and factors, however, changes in the spermatogenesis are possible not to occur or they could be in non-equal degree in all tubules, and intact spermatogenesis might also be established. On the other hand, the changes could be transitive, in non-constant hypospermatogenesis, associated with intra-tubular disorganization, suppression and/or arrest of the germ cells maturation process. Moreover, changes could be definitive, characterized by germinal aplasia, tubular sclerosis and/or progressive peritubular fibrosis in the testis, leading to *azoospermia* [1, 17]. In the patients with *ascending testis*, the cytological observations suggested cell apoptosis activation in early stages of germ cells development (depending on the time period of the gonads in hyperthermia conditions), rather than a concrete affection in any spermatogenic stage.

The established in the current study high percentage of abnormal spermatozoa, as well as in other disorders of the male reproductive system, suggests altered function of the *epididymis*, responsible for further proceses of the spermatozoa capacitation, and acquisition of motility. The defects in the spermatozoa formation are often connected with injuries in the cellular DNA and nuclear chromatin structure [15, 24], important in application of technologies for *in vitro*-insemination.

Assisted reproduction technologies required precise identification of immature germ cells sub-populations, for subsequent application in the intra-cytoplasmic injec-

tions on ICSI technique [21]. The results from the current investigation indicate an increased content of degenerating spermatids with picnotic nuclei and vacuolized cytoplasm, which are not appropriate for such purposes. The nuclear/chromatin defects that might occur in germ cells and their subpopulations as well as in mature spermatozoa demand careful choice in their using for ICSI procedures.

Additional studies are necessary in cases with *ascending testis* or similar pathologies (hyperthermia, cryptorhidism, varicocele), for a better clarification of the seminal fluid cytology and, hence, of the injuries in the human spermatogenesis.

## Conclusion

The increased secretion of germ cells (spermatogonia, spermatocytes and spermatids) in the seminal fluid might be good indicators for the abnormal functions of the testis, and in this way, could provide information for the stage, in which the arrest in the germ cells development occurs. Further investigations are necessary due to limited information in the literature about the "round cells" presence in the seminal fluid, which also play a prognostic role for determination of the spermatogenesis defects and could be useful in the choice of appropriate therapeutic strategies in andrology.

*Acknowledgments:* This work was supported by the European Social Fund and Republic of Bulgaria, Operational Programme "Human Resources Development" 2007-2013 framework, Grant No BG-051PO001-3.3.06-0048 from 04.10.2012.

## References

1. **Agoulnik, A. I., Z. Huang, L. Ferguson.** Spermatogenesis in cryptorchidism. – Meth. Mol. Biol., **825**, 2012, 127-147.
2. **Clarnette, T. D., D. Rowe, S. Hasthorpe, J. Huston.** Incomplete disappearance of the processus Vaginalis as a cause of ascending testis. – J. Urol., **157**, 1997, 1889-1891.
3. **Cobellins, C.** Spermatogenesis and cryptorchidism. – Front. Endocrinol. (Lausanne), **5**, 2014, 63.
4. **Fedder, J.** Nonsperm cells in human semen: with special reference to human leucocytes and their possible influence on fertility. – Arch. Androl., **36**, 1996, 41-65.
5. **Ferguson, L., A. I. Agoulnik.** Testicular cancer and cryptorchidism. – Front. Endocrinol. (Lausanne), **4**, 2013, 32.
6. **Gandini, L., A. Lenzi, F. Lombardo, F. Pacifici, F. Dondero.** Immature germ cell separation using a modified discontinuous Percoll gradient technique in human semen. – Hum. Reprod., **14**, 1999, 1022-1027.
7. **Giwercman, A., J. Bonde.** Declining male fertility and environmental factors. – Endocr. Metab. Clin. of North America, **27**, 1998, 807-830.
8. **Holstein, A., W. Schulze, M. Davidoff.** Understanding spermatogenesis is a prerequisite for treatment. – Reprod. Biol. Endocrinol., **1**, 2003, 16 p.
9. **Ilieva, I., P. Tzvetkova.** Morphological and ultrastructural changes in the tail of the sperm abnormalities of mixed type and infertility. – Andrology, **16**, 2007, 14-19.
10. **Ilieva, I., St. Ivanova, I. Chavdarov, S. Rangelov, P. Tzvetkova.** Scanning electron microscopic studies of abnormal sperm in the pathology of the male reproductive system. – Compt. rend. Acad. bulg. Sci., **65**, 2012, 1095-1098.
11. **Johansson, E., A. Campana, R. Luthi, A. de Agostini.** Evaluation of "round cells" in semen analysis: a comparative study. – Hum. Reprod. Update, **6**, 2000, 404-412.
12. **Mouriquand, P.** The nomad testis. – Arch. Dis. Childhood, **92**, 2007, 3.
13. **Nierderberger, C.** Re: Oral administration of retinoic acid receptor antagonist reversibly inhibits spermatogenesis in mice. – J. Urol., **187**, 2012, 1509 p.

14. **Paul, C., S. Teng, T. Saunders.** A single, mild, transient scrotal heat stress causes hypoxia and oxidative stress in mouse testes, which induces germ cell death. – Biol. Reprod., **80**, 2009, 913-919.
15. **Ringertz, N., B. Gledhill, Z. Darzynkiewicz.** Changes in deoxyribonucleoproteins during spermatogenesis in the bull. – Exp. Cell Res., **62**, 1970, 204-218.
16. **Robin, G., F. Boitrelle, X. Leroy, M. C. Peers, F. Marcelli, J. Rigot, V. Mitchell.** Assessment of azoospermia and histological evaluation of spermatogenesis. – Ann. Pathol., **30**(3), 2010, 182-95.
17. **Ross, M., W. Pawlina.** Histology: a text and atlas: with correlated cell and molecular biology. – Baltimore MD: Lippincott Williams & Wilkins, 2006.
18. **Thorp, J., K. Kvist, E. Clasen-Linde, B. Petersen, D. Cortes.** The relation between adult dark spermatogonia and other parameters of fertility potential in cryptorchid testes. – J. Urol., **190**, 2013, 1566-1571.
19. **Tomilson, M., A. Whitte, C. Barratt, A. Bolton, L. Cooke.** The removal of morphologically abnormal sperm forms by phagocytes: a positive role for seminal leukocytes? – Hum. Reprod., **7**, 1992, 517-522.
20. **Tzvetkov, D., P. Tzvetkova.** Congenital disorders of ducts deferens. – In: Cogenital malformation of male reproductive system. – Bulg. Sci. Found. Androl., Sofia, 1999, 93-100.
21. **Vernaeve, V., G. Verheyen, A. Goossens, A. Van Steirteghem, P. Devroey, H. Tournaye.** How successful is repeat testicular sperm extraction in patients with azoospermia? – Hum. Reprod., **21**, 2006, 1551-1554.
22. **Yin, Y., W. De Wolf, A. Morgentaler.** Experimental cryptorchidism induces testicular germ cell apoptosis by p53-dependent and-independent pathways in mice. – Biol. Reprod., **58**, 492-496.
23. **Yoshida, T., K. Ohno, Y. Morotomi, T. Nakamura, T. Azuma, H. Yamada, H. Hayashi, S. Suehiro.** Clinical and pathological features of ascending testis. – Osaka City Med., **55**, 2009, 81-87.
24. **Цветкова, П.** Морфо-функционални характеристики на епидидима и мъжки инфертилитет. – Андрология, **10**, 2001, 21–30.

Institute of Experimental Morphology, Pathology and Anthropology with Museum
Bulgarian Anatomical Society

Acta morphologica et anthropologica, 22
Sofia ● 2015

# Clinical Case of a Patient with RRMS and Acute Inflammatory Response Following Vaccination against Tetanus

*V. Kolyovska[1], D. Maslarov[2]*

*[1]Institute of Experimental Morphology, Pathology and Anthropology with Museum, Bulgarian Academy of Sciences, Sofia*
*[2]Medical University of Sofia, Neurology Clinic, First MHAT – Sofia*

Multiple sclerosis (MS) is an inflammatory disease in which the myelin sheaths around the axons of brain and spinal cord's neurons are damaged by autoantibodies, resulting in demyelination and scarring. The aim of this investigation was to show clinical significance of the tetanus vaccination and risk of autoimmune reactions in patients with MS. The risks associated with a number of vaccines have been investigated in patients with MS. Many patients with MS received immunosuppressive or immunomodulatory therapy, which could make them more susceptible to infectious diseases and might also affect their ability to respond to immunization. Here, we review the indications for and possible adverse effects of vaccines in patients with MS, and address issues of vaccination in the context of immunomodulatory therapy for MS. It is recommended that vaccines in patients with long time suppressed immune system to be applied very carefully, only if there is proven necessity and close monitoring.

*Key words:* multiple sclerosis, multiple sclerosis treatment, Glatiramer acetate, tetanus vaccination, autoimmune reaction.

## Introduction

Multiple sclerosis (MS) is primarily an inflammatory disorder of the brain and spinal cord in which focal lymphocytic infiltration leads to damage of myelin and axons. Initially, inflammation is transient and remyelination occurs but is not durable. Hence, the early course of disease is characterized by episodes of neurological dysfunction that usually recover. However, over time the pathological changes become dominated by widespread microglial activation associated with extensive and chronic neurodegeneration, the clinical correlate of which is progressive accumulation of disability. Preclinical investigations show abnormalities that indicate the distribution of inflammatory lesions and axonal loss (MRI); interference of conduction in previously myelinated pathways (evoked electrophysiological potentials); and intrathecal synthesis of oligoclonal antibody (examination by lumbar puncture of the cerebrospinal fluid) [2].

The initial MS therapeutic strategies were directed at immune modulation and inflammation control. Disease-modifying drugs (DMDs) require long-term, regular injec-

tion or monthly parenteral infusions, which may impact the patient's compliance. The aim is to prevent demyelination and to reduce axonal loss. During the different MS phases patients use various drugs: in attacks – Corticosteroids; immunomodulators – Interferon beta-1a, Interferon beta-1b (INFs), Glatiramer acetate and Fingolimod [11].

Glatiramer acetate (licensed in 1996) is an immunomodulatory drug currently used to treat relapsing-remitting MS (RRMS). It is a random polymer of four amino acids found in myelin basic protein, namely glutamic acid, lysine, alanine, and tyrosine, and may work as a decoy for the immune system. Glatiramer acetate (GA) is approved by the Food and Drug Administration (FDA) for reducing the frequency of relapses, but not for reducing the progression of disability. GA has also been shown to limit the formation of new MS-related lesions in the central nervous system (CNS) and to reduce brain atrophy [10]. The role of vaccinations in risk of developing MS or in risk of relapse has not been well established. The aim of the studies was to estimate the effect of immunizations and the risk of developing MS in adults as well as in subsequent risk of relapse [4].

Several studies have demonstrated an effect of GA on T regulatory cells (Tregs), which are potent immunosuppressor cells pivotal in the maintenance of self-tolerance. However, the role of this cell population in the therapeutic effect of GA has not been clarified. To clarify the requirement of Treg cells in the therapeutic activity of GA in an animal model of multiple sclerosis is experimental autoimmune encephalomyelitis (EAE) was used. GA treatment induces elevation of T-regulatory cells. Selective depletion of these Tregs reduces but does not eliminate the ability of GA to ameliorate EAE. These findings support the role of Tregs, but not in an exclusive fashion, in the therapeutic effect of GA. [1].

## Materials and Methods

The patient is a 40-year-old woman. MRI performed with 20 years confirmed clinical diagnosis of MS, relapsing-remitting variant, satisfying McDonald MRI criteria, with assigned level 1.5-2 Kurtzke Disability Status. The patient was on therapy with GA from ten years. From 2005 until year 2014 the patient has been in a remission with two or three weak exacerbations.

During the normal procedure with GA patient was bitten by a street dog. Doctors have implemented vaccination with tetanus vaccine. Some time thereafter (2-3 weeks) suddenly appeared bumps and severe, excruciating pain in the joints. Ultrasound appeared effusion of synovial fluid in the joints of the knees, ankles and wrists. Expressed were effusions on superolateral bursae and soft proliferation of the synovial membrane. The complete blood count of the patient is normal. The level of C-reactive protein (CRP), a marker of long-term inflammatory response in the body is normal – less than 10 mg/L (SI). Symptomatic treatment with medication Movalis (15 mg) was appointed for ten days. Then, there was a sharp decline in the swelling of the joints. Doubts for gout were also rejected. Most likely acute pain, swelling and indispositions in the body are available because of suppressed immune system many years. Perhaps this is a reaction of poorly purified proteins in the vaccine.

The study was conducted in compliance with the principles of the Declaration of Helsinki 1964 and its amendments (Tokyo 1975, Venice 1983, Hong Kong 1989). Similar studies have not been performed so far.

In the current investigation, clinical studies were focused on the type, morphology and evolution of MS lesions using conventional MRI in a patient with RRMS before GA treatment (**Fig. 1**) and during the therapy (**Fig. 2**). MRI was designed to assess the frequency, extent, and rate of cortical lesions formation in RRMS and their relationship

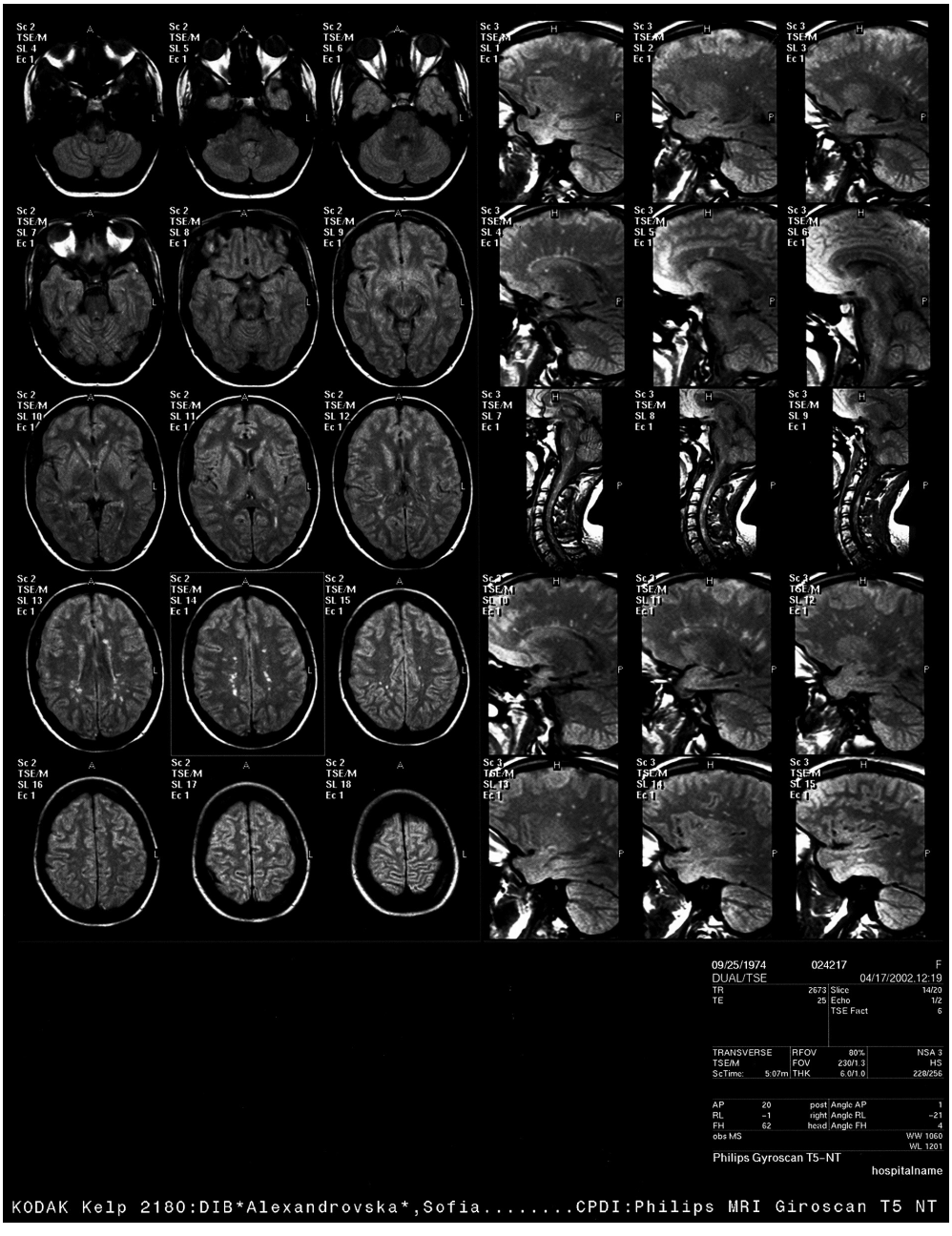


**Fig. 1.** MRI in a patient with RRMS before Glatiramer acetate treatment

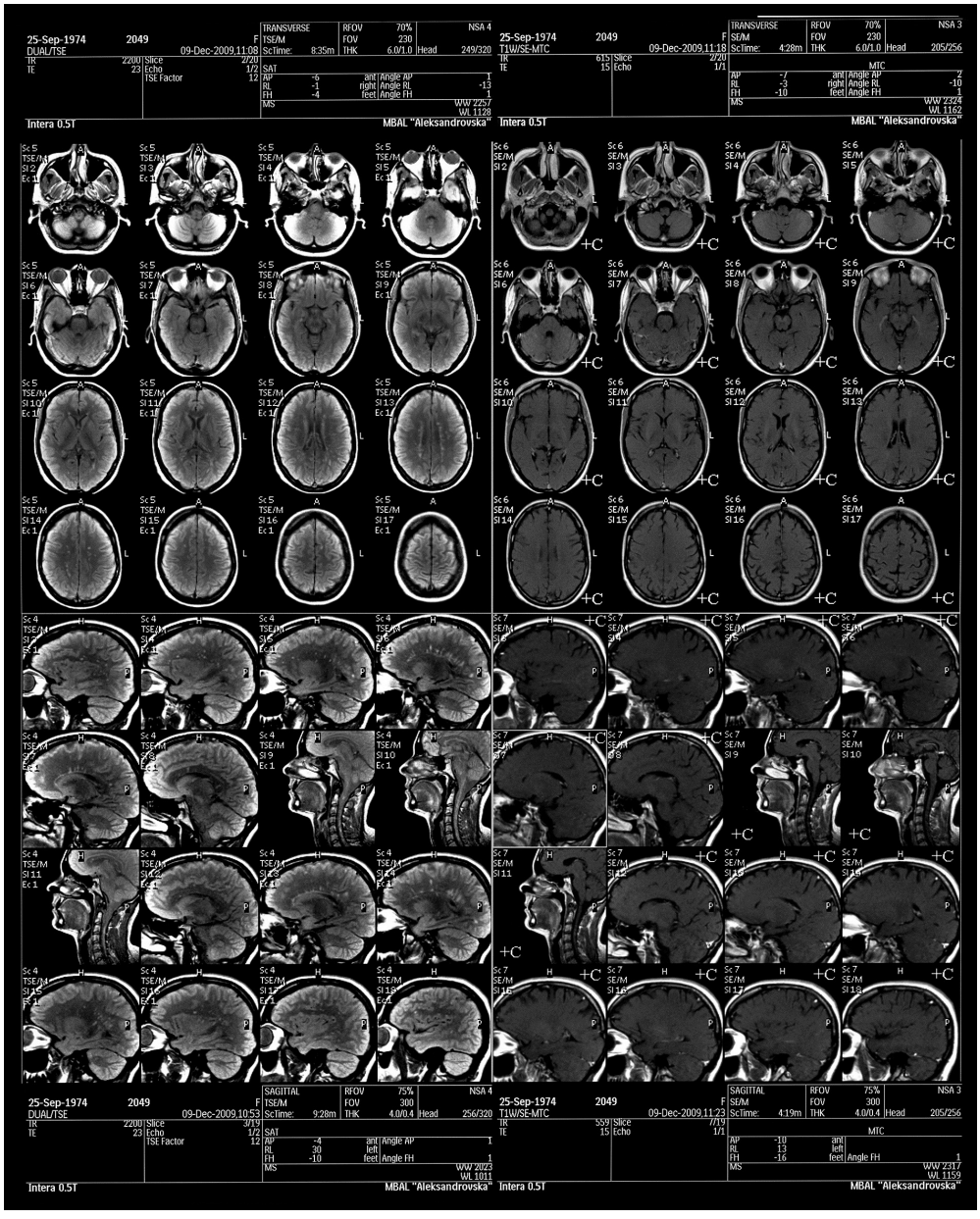


**Fig. 2.** MRI in a patient with RRMS after Glatiramer acetate treatment

with T2 lesion volume, white matter atrophy, and disability. Regrettably, MRI has not been investigated after the inflammatory response.

## Results

*MRI results from a longitudinal study*

*Year 2002 – MRI brain and spinal cord in axial and sagittal planes*

Multiple, predominantly small hyperintense foci in the brain white matter located bilaterally periventricularly and subcortically towards the convexity, in the basal ganglia and capsula interna, in all parts of corpus callosum, in the cerebellum, pons, craniospinal junction and along the cervical spinal cord. These changes are usually seen in a demyelinating process such as MS with cranial and spinal involvement with corresponding clinical and immunologic evidence (**Fig. 1**).

*Year 2005 – Brain MRI in axial plane and cervical spine in sagittal plane*

Compared to previous MRI study from 2002 – no dynamic changes; no evidence of disease progression based on "lesion load on T2".

*Year 2009 – MRI brain and spinal cord in axial and sagittal planes with gadolinium contrast enhancement (0.1 mmol Gd/kg)*

Compared to previous MRI findings from 2005 – no evidence of disease progression based on "lesion load on T2". Intact blood-brain and blood-spinal fluid barriers (**Fig. 2**).

*Year 2011 – MRI brain: T2 imaging in axial and sagittal planes, FLAIR axial and T1 sagittal planes*

Subarachnoid space and brain ventricles – normal. Supra- and subtentorial hyperintense foci documented previously on T2 and FLAIR imaging from 2009 persist. Hyperintense foci noted in cervical cord at C2 level. Pontocerebellar angles appear normal. Brain ventricular system – normal shape, size and location. No evidence of MRI findings progression compared to MRI study from 2009 – cerebrospinal demyelinating process.

The fact that there is no progression on MRI imaging findings from 2005 until 2012 based on brain "T2 lesion load" suggests the protective role of GA treatment.

## Discussion

Vaccination against infection becomes important in patients with neuromyelitis optica spectrum disorder (NMOSD) because they are at an increased risk of infection due to long-term immunosuppressive therapy. However, it is unclear whether NMOSD patients under immunosuppression therapy show proper antibody formation after vaccination. Thus the antibody formation after influenza A (H1N1) vaccination in patients with NMOSD receiving rituximab was evaluated [9]. This study shows a severely hampered humoral immune response to H1N1 influenza vaccine in patients with NMOSD treated with rituximab, although the vaccination itself is safe in these patients [9].

Bacterial and viral infections have been shown to induce relapses and accelerate the progression of MS. Vaccination to prevent communicable disease in such patients is, therefore, of key importance. Reports of potentially detrimental effects of immuni-

zation on the course of MS, however, have prompted patients and physicians to adopt a cautious attitude towards the use of vaccines. The risks associated with a number of vaccines have been investigated in patients with MS. Many patients with MS receive immunosuppressive or immunomodulatory therapy, which could make them more susceptible to infectious diseases and might also affect their ability to respond to immunization. The researchers reviewed the indications for and possible adverse effects of vaccines in patients with MS, and address issues of vaccination in the context of immunomodulatory therapy for MS [12]. Tetanus vaccination is associated with a low risk of multiple sclerosis in healthy people [6].

That is not indicative of patients with permanently suppressed immunity as patients treated with GA. The question of a connection between vaccination and autoimmune illness (or phenomena) is surrounded by controversy. A heated debate is going on regarding the causality between vaccines, such as measles and anti-hepatitis B virus (HBV), and MS. Brain antibodies as well as clinical symptoms have been found in patients vaccinated against those diseases [13].

Post-vaccination acute disseminated encephalomyelitis (ADEM) has been associated with several vaccines such as rabies, diphtheria-tetanus-polio, smallpox, measles, mumps, rubella, Japanese B encephalitis, pertussis, influenza, hepatitis B, and the Hog vaccine. Researchers review ADEM with particular emphasis on vaccination as the precipitating factor [7]. In the current study investigations were focused on the tetanus vaccination and risk of autoimmune reactions in patients with RRMS. The aim of the MS treatment is to prevent demyelination and to reduce axonal loss. Vaccination against hepatitis B (HB), influenza, tetanus, measles, or rubella is not associated with an increased risk of multiple sclerosis or optic neuritis [3].

This is a statement in healthy subjects. In the cases of patients with permanently suppressed immune response the reaction of vaccination is not the same. Several hundred cases of an acute central demyelinating event following HB vaccination were reported to the pharmacovigilance unit, leading to a modification of vaccination policy in the schools and the initiation of several studies designed to examine the possible relationship between the vaccine and the central demyelinating events. The results of these studies failed to establish the causality of the HB vaccine. Nevertheless, molecular mimicry between HB antigen(s) and one or more myelin proteins, or a non-specific activation of autoreactive lymphocytes, would constitute possible pathogenetic mechanisms for these adverse neurological events [5].

Farez and Correale [4] suggest that no significant change in the risk of developing MS after vaccination was found for BCG, Hepatitis B, Influenza, Measles-Mumps-Rubella (MMR), Polio and Typhoid fever. They found decreased risk of developing MS for Diphtheria and Tetanus. Influenza immunization was also associated with no change in risk of MS relapse. Risk of developing multiple sclerosis remained unchanged after BCG, Hepatitis B, Influenza, MMR, Polio and Typhoid fever immunization, whereas diphtheria and tetanus vaccination may be associated with a decreased risk of MS. Further research is needed for the remaining vaccines [4].

Kappos et al. [8] evaluated the immune responses in Fingolimod-treated patients with MS against influenza vaccine (to test for responses against anticipated novel antigens in seronegative patients) and recall (tetanus toxoid booster dose) antigens. Most Fingolimod-treated patients with MS were able to mount immune responses against novel and recall antigens and the majority met regulatory criteria indicating seroprotection. However, response rates were reduced compared with placebo-treated patients. This should be kept in mind when vaccinating patients on Fingolimod [8]. In some patients with MS receiving immunizations, concurrent Fingolimod treatment in comparison to placebo decreases vaccination-induced immune responses.

## Conclusion

Two problems must be considered in regard to the relationship between vaccinations and MS: Do vaccinations favor the first attack of MS? Do they increase the short- or long-term risk in patients with known disease? Answers to these questions are difficult due to the paucity of reported cases, our ignorance of the precise frequency of neurological adverse events in vaccines based on prospective studies, and finally by the lack of a well established pathophysiology.

In most instances, the role of the vaccine is based on a temporal link between the injection and the onset of neurological disease, and more rarely to a positive reintroduction. The mechanism (or mechanisms) of autoimmune reactions following immunization has not yet been elucidated. One of the possibilities is molecular mimicry; when a structural similarity exists between some viral antigen (or other component of the vaccine) and a self-antigen. This similarity may be the trigger to the autoimmune reaction. Other possible mechanisms are discussed. Even though the data regarding the relation between vaccination and autoimmune disease is conflicting, it seems that some autoimmune phenomena are clearly related to immunization (e.g. Guillain-Barre syndrome).

It is recommended that vaccines in patients with long time suppressed immune system to be applied very carefully, only if there is proven necessity and close monitoring. As their immune system is permanently suppressed, it does not respond in the way that reacts in healthy people.

## References


1. **Aharoni, R., T. Feferman, D. Bar Lev, G. Shakhar, M. Sela, R. Arnon.** The role of T regulatory cells in the therapeutic effect of glatiramer acetate in experimental autoimmune encephalomyelitis. – J. Multiple Sclerosis, **20**, 2014, 326.
2. **Compston, A., A. Coles.** Multiple sclerosis. – Lancet, **372**(9648), 2008, 1502-1517.
3. **DeStefano, F**., **T. Verstraeten**, **L. Jackson**, **C. Okoro**, **P. Benson**, **S. Black,** H. **Shinefield**, **J. Mullooly**, **W. Likosky**, **R. Chen**. Vaccinations and risk of central nervous system demyelinating diseases in adults. – Arch. Neurol., **60**(4), 2003, 504-509.
4. **Farez, M., J. Correale.** Immunizations and risk of multiple sclerosis: systematic review and meta-analysis. – J. Neurol., **258**(7), 2011, 1197-1206.
5. **Gout, O.** Vaccinations and multiple sclerosis. – Neurol. Sci., **22**(2), 2001, 151-154.
6. **Hernán, M., A. Alonso, S. Hernández-Díaz.** Tetanus vaccination and risk of multiple sclerosis: a systematic review. – Neurology, **67**(2), 2006, 212-215.
7. **Huynh, W., D. Cordato, E. Kehdi, L. Masters, C. Dedousis.** Post-vaccination encephalomyelitis: literature review and illustrative case. – J. Clin. Neurosci., **15**(12), 2008, 1315-1322.
8. **Kappos, L., M. Mehling, R. Arroyo, G. Izquierdo, K. Selmaj, V. Curovic-Perisic, A. Keil, M. Bijarnia, A. Singh, P. von Rosenstiel.** Randomized trial of vaccination in fingolimod-treated patients with multiple sclerosis. – Neurology, **84**(9), 2015, 872-879.
9. **Kim, W., S. H. Kim, S. Y. Huh, S. Y. Kong, Y. J. Choi, H. J. Cheong, H. J. Kim.** Reduced antibody formation after influenza vaccination in patients with neuromyelitis optica spectrum disorder treated with rituximab. – J. Eur. Neurol., **20**(6), 2013, 975-980.
10. **Kolyovska, V., S. Todorov, D. Maslarov.** New perspectives in multiple sclerosis treatment. – Medical Data, **5**(3), 2013, 241-244.
11. **Kolyovska, V., D. Maslarov, I. Dokova, S. Todorov, I. Iliev, S. Engibarov, R. Eneva.** Serum IgG antibodies to GM1, GM3 and GD1a gangliosides in patients with relapsing remitting multiple sclerosis under treatment with Interferon, Glatiramer acetate and Laquinimod – preliminary data. – Acta morphol. et anthropol., **21**, 2015, 62-66.
12. **Löebermann, M., A. Winkelmann, H. Hartung, H. Hengel, E. Reisinger, U. Zettl.** Vaccination against infection in patients with multiple sclerosis. – Nat. Rev. Neurol., **8**(3), 2012, 143-151.
13. **Shoenfeld, Y, A. Aron-Maor.** Vaccination and autoimmunity-'vaccinosis': a dangerous liaison? – J Autoimmun., **14**(1), 2000, 1-10.

Institute of Experimental Morphology, Pathology and Anthropology with Museum
Bulgarian Anatomical Society

Acta morphologica et anthropologica, 22
Sofia ● 2015

# Morphometrical Study of the Choroid Plexus Blood Vessels in Experimental Hamster *Graffi* Tumor Model

*V. Ormandzhieva, R. Toshkova*

*Institute of Experimental Morphology, Pathology and Anthropology with Museum, Bulgarian Academy of Sciences, Sofia, Bulgaria*

The choroid plexus consists of epithelial cells, fenestrated blood vessels, and the stroma, dependent on various physiological or pathological conditions. In the present study the blood vessels, divided in four subgroups of the choroid plexus of control and tumor bearing hamsters (TBH), were morphometrically investigated. The investigations were performed on semithin sections examined with the light microscope using a square grid system. Brain tumor can be classified into two major classes, namely, primary brain tumor that start in the brain and secondary brain tumor that are generated by the cancer cells that migrated from tumor developed in other parts of the body. In the present study were observed statistically significant increase of the luminal diameter of the blood vessels in TBH on the $10^{th}$ and $30^{th}$ day of examination in comparison with control hamsters and metastasis near the brain ventricles. The morphological changes in the choroid plexus vasculature and structure are evidence for alteration of the blood-cerebrospinal fluid barrier and probably were a result of secondary metastasis in the brain.

*Key words:* choroid plexus morphological and morphometrical studies, experimental hamster *Graffi* tumor model, brain metastasis.

## Introduction

Secondary brain tumors are more common than primary ones and are the most common cause of tumors in the intracranial cavity. This means that a cancerous neoplasm has developed in another organ elsewhere in the body and that cancer cells have leaked from that primary tumor and then entered the lymphatic system and blood vessels. They then circulate through the bloodstream, and are deposited in the brain. How the metastatic process is regulated also largely remains a mystery. The development of new therapeutic approaches for this disease is a difficult challenge, and there is no effective treatment for almost all the brain diseases. In most of the cases, the major cause of the failure in the development of drugs to treat brain diseases is the presence of blood-brain barrier (BBB) [1]. The cerebrospinal fluid (CSF) circulatory system is involved in the neuroimmune regulation, cerebral detoxification, and delivery of various endogenous and exogenous substances [2]. The barriers of the brain play critical roles in controlling the movement of various metabolites, but also drugs, between the blood and the brain (Blood-Brain Barrier) and the blood and the CSF (Blood-CSF-Barrier). Fundamental to all brain barrier mechanisms is the presence of intercellular tight junctions between

intimately opposed cells comprising these interfaces (endothelial cells of the brain vessels – BBB and choroid plexus epithelial cells – B-CSF-B) [8].

Plexus choroideus is highly vascularised structure in the brain ventricles. It produces cerebrospinal fluid and involves in the synthesis and transport of numerous CSF components. Choroid plexus has an important role in the homeostasis of nutrients in the CSF [13]. The transplantable myeloid tumor used in this study originated as a Graffi murine leukemia virus-induced tumor in newborn hamsters, adapted and maintained to mature Golden Syrian hamsters [3, 9].

The *aim* of the present study is to investigate the morphometric changes of the choroid plexus blood vessels in the experimental hamster *Graffi* tumor model.

## Materials and Methods

*Experimental hamster Graffi tumor model*

Golden Syrian hamsters, 2 months old, were used in experiments. The experimental Graffi tumor was primary created by the Graffi-virus in new-born hamsters, and maintained monthly *in vivo* by subcutaneous transplantation of live tumor cells ($2\times10^6$/ml PBS) in the interscapular area of hamsters, for keeping the tumor's survival [3, 9, 10]. The tumor is 100% cancerous, and the animals die usually up to the $30^{th}$ day after transplantation. The animals were kept under standard conditions with free access to food and water.

*Histopathological examination*

Brain samples from control (healthy) and tumor bearing hamsters (TBH) were taken, fixed in Carnoy's solution and embedded in paraffin using routine histological practice. Tissue sections (5–7 μm) were stained by hematoxylin-eosin and examined under light microscope Leica DM5000B.

*Morphometric analysis*

We obtained morphometric data from the light microscope Carl Zeiss Jena at 1000 × magnification using a square grid system. The luminal diameter was measured as perpendicular distance across the maximum chord axis of each vessels of control ($n = 446$) and TBH ($n = 431$ on the $10^{th}$ and $n = 467$ on the $30^{th}$ day after tumor implantation).

*Statistical analysis:* Results are reported as mean values ± SEM and statistically analyzed by Student's t-test using statistical package (STATISTICA, ver.6, Stat-Soft Inc., 2001), and differences were regarded as significant at $p < 0.05$.

All studies were performed in accordance to the Guide for Care and Use of Laboratory Animals, as proposed by the Committee on Care Laboratory Animal Resources, Commission on Life Sciences and National Research Council, and a work permit No. 11130006.

## Results

In the present study changes in the luminal diameter of the choroid plexus blood vessels divided in four subgroups in control (healthy) and tumor-bearing hamsters were determined. These findings are shown in **Fig. 1.** Significant changes were observed in the luminal diameter of capillaries (vessels < 15.0 μm in diameter) and large vessels

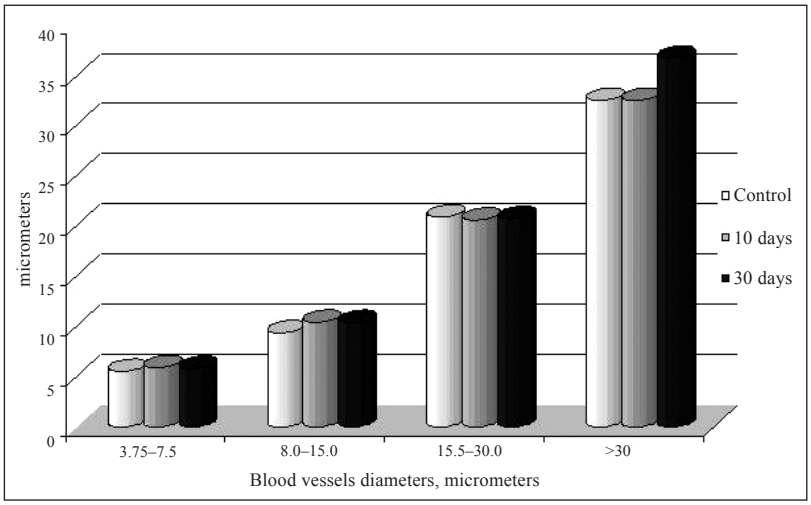


**Fig. 1.** Comparison of morphometric data of choroid plexus blood vessels in control and experimental hamster tumor model

(> 30.0 μm in diameter) in TBH on the 10th ($p < 0.001$) (blood vessels diameter of the 3.75-7.5 μm: 5.90 ± 0.10 μm and 8.0-15.0 μm: 10.42 ± 0.24 μm) and 30th ($p < 0 .001$) (blood vessels diameter of the 3.75-7.5 μm: 5.83 ± 0.11 μm and 8.0-15.0 μm: 10.40 ± 0.25 μm; blood vessels > 30.0 μm in diameter: 36.70 ± 1.23 μm) day of examination in comparison with control hamsters (blood vessels diameter of the 3.75-7.5 μm: 5.54 ± 0.09 μm and 8.0-15.0 μm: 9.38 ± 0.21 μm; blood vessels > 30.0 μm in diameter: 32.50 ± 0.91 μm). The mean luminal diameter of capillaries (blood vessels diameter of the 3.75-15.0 μm) was not statistically changed in TBH in comparison with control.

The choroid plexus lies in the brain ventricles as a fibrous network of tissue and vasculature. It consists of single layer of large cuboidal light and dark epithelial cells, connective tissue elements and capillary with many fenestrations (**Fig. 2**). The histopathological studies of the brain on the 10th and the 30th day after tumor implantation are shown in **Figs. 3** and **4**. Many brain vessels and choroid plexus cappilaries with destructive changes were seen in the present TBH study. Some endothelial cells of the choroid plexus blood vessels were destroyed. There were many dark epithelial cells and macrophages in the apical part of the choroid plexus epithelial cells. Massive accumulation of tumor metastatic cells were detected in the brain tissue,

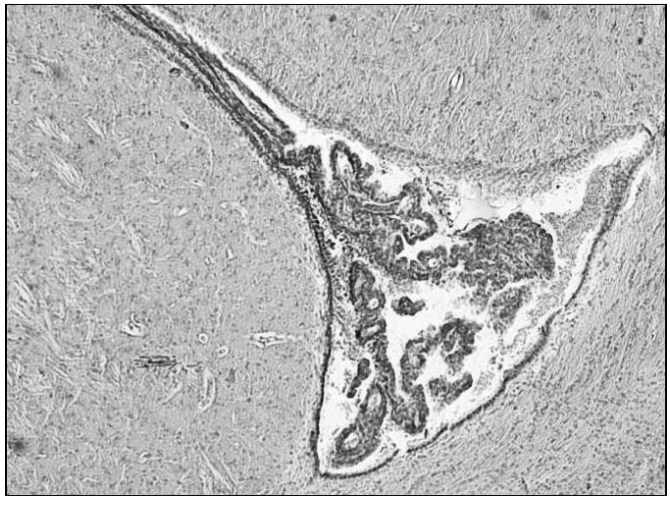

**Fig. 2.** Light microscopic micrograph of the plexus choroideus of control hamster in the lateral ventricle. H&E stain (× 5)

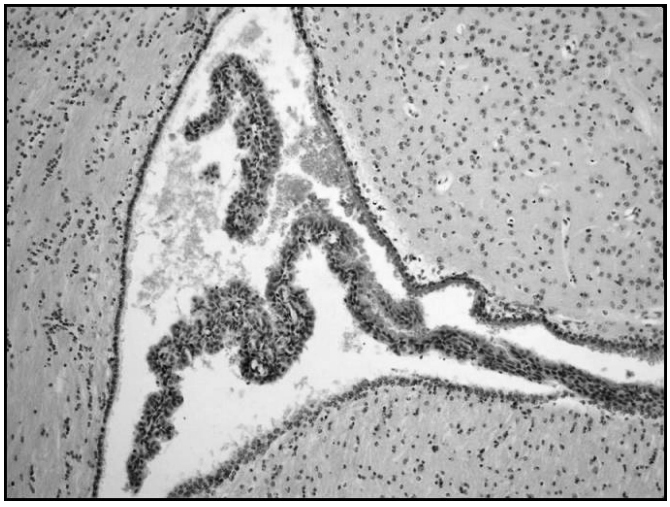

**Fig. 3.** Light microscopic micrograph of the plexus choroideus of tumorbearing hamster (10 days after tumor implantation). H&E stain (× 10)

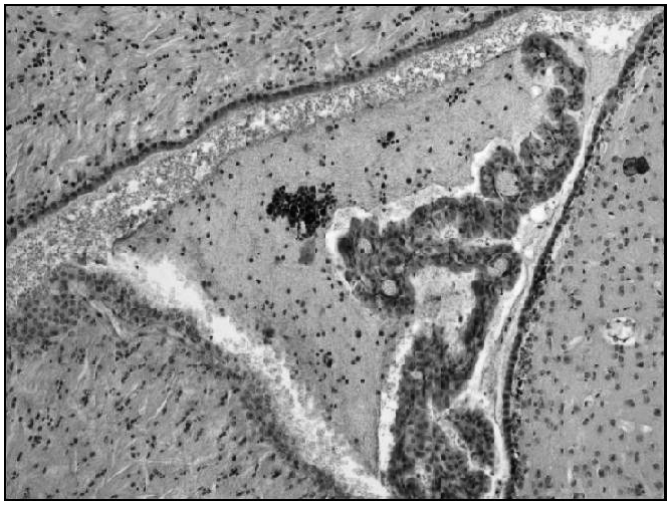

**Fig. 4.** Light microscopic micrograph of the plexus choroideus of tumorbearing hamster (30 days after tumor implantation). H&E stain (× 10)

lateral ventricle and under ependyma in TBH on the 30$^{th}$ day of examination. Tumor cells have a similar morphological characteristic to that described in the primary tumor.

## Discussion

For the first time brain was examined in experimental hamsters with Graffi tumor to establish morphological changes in the choroid plexus and brain metastases during tumor progression. Up to present time little quantitative information has been available

regarding the vessels of the brain, in particular, regarding the vessels of the rat choroid plexus. The capillaries of the choroid plexus have a large diameter and sinusoidal dilations, and showed the presence of occasional short, blind sprouts indicative of angiogenesis. Short anastomoses between arterioles supplying the plexuses and venules draining them were only rarely observed [12].

It was found that the tumor metastasizes lymphatic and haematogenous route. In our previous studies metastases were observed in regional and non-regional lymph nodes, in the lung, liver and spleen of TBH. Massive accumulation of tumor metastatic cells were detected in the brain tissue, lateral ventricle and under ependyma in TBH on the 30$^{th}$ day of examination. Tumor cells in metastatic lesions have a similar morphological characteristic to that described in the primary tumor, reported in our previous studies [9, 11].

Remarkable changes were found in choroid plexus morphology in all tumorbearing hamsters. The significant increases were observed in the luminal diameter of capillaries and large vessels in TBH on the 10$^{th}$ (vessels diameter of the 3.75-7.5 μm by 6.50% and 8.0-15.0 μm by 11.09%) and 30$^{th}$ (vessels diameter of the 3.75-7.5 μm by 5.23% and 8.0-15.0 μm by 10.87%; blood vessels > 30.0 μm in diameter by 12.92%) day of examination in comparison with control hamsters. Destructive changes of the brain vessels and choroid plexus capillaries, many macrophages in the apical part of the choroid plexus epithelial cells and in the CSF, and increased number of dark epithelial cells, were seen in the present study. Most blood vessels in the plexus choroideus are wide-calibre (10-15 μm) fenestrated capillaries, wich included non-fenestrated endothelial segments with some vesicles [4]. Similar changes in the rat choroid plexus blood vessels and epithelial cells we observed in our previous investigations after low doses ionizing irradiation [5, 6]. Statistically significant changes in the choroid plexus blood vessels established in this study are in support of our previous research in which we found metastatic lesions in the brain ventricles and brain tissue [7]. The choroid plexus epithelium constitutes a physical barrier between blood and cerebrospinal fluid (the blood – CSF barrier – BCSFB) by virtue of the complexity of the tight junctions between adjacent epithelial cells.

## Conclusion

Our morphological study of the TBH experimental model clearly demonstrated that the brain metastasis provoked significant destructive changes in the plexus choroideus. These morphological changes led to the damage of the BBB and B-CSF-B.

*Acknowledgements:* This research was financially supported by the Bulgarian National Science Fund (Grant BO2/5-2014). The authors wish to thank M. Pavlova, medical laboratory assistant, for the excellent technical assistance of the histological preparation of tissue.

## References

1. **Bhowmik A., R. Khan, M. K. Ghosh.** Blood brain barrier: A challenge for effectual therapy of brain tumors. – BioMed. Research International, 2015, (http://dx.doi.org/10.1155/2015/320941).
2. **Ghersi-Egea, J., A. Babikian, S. Blondel, N. Strazielle.** Changes in the cerebrospinal fluid circulatrory system of the developing rat: quantitative volumetric analysis and effect on blood-CSF permeability interpretation. – Fluids and Barriers of the CNS, **12**(8), 2015, DOI 10.1 186/s12987-015-0001-2.

3. **Jakimov, M., Z. Mladenov, A. Konstantinov, I. Yanchev.** Transplantable myeloid tumor in hamsters (MTH) induced by Graffi virus. – Gen. Compar. Pathol., **6**, 1979, 24-35.
4. **Ormandzhieva, V.** Rat choroid plexus blood vessels: morphometric characteristics. – Med. Data Rev., **3**(3), 2011, 229-232.
5. **Ormandzhieva, V.** Effect of radiation with low doses fast neutrons and high energy oxygen ions on the rat choroid plexus blood vessels. – Acta Morphol. Anthropol., **13**, 2008, 22-25.
6. **Ormandzhieva, V.** Choroid Plexus after Low Doses Ionizing Irradiation. – Med. Data Rev., **5**(2), 2013, 111-119.
7. **Ormandzhieva, V., R. Toshkova.** Brain metastasis in *Graffi* hamster experimental model. – Proceedings of the Fifth workshop experimental models and methods in biomedical research, 2015, 12-14 May, (http://www.iempam.bas.bg/).
8. **Saunders, N., R. Daneman, K. Dziegielewska, S. Liddeow.** Transporters of the blood-brain and blood-CSF interfaces in development and in the adult. – Molecular Aspects of Medicine, **34**, 2013, 742-752.
9. **Toshkova, R.** Attempts for immunomodulation in hamsters with transplanted myeloid tumor, previously induced by Graffi virus. PhD Thesis, 1995, Sofia, Bulgaria, p.168.
10. **Toshkova, R., N. Manolova, E. Gardeva, M. Ignatova, L. Yossifova, I. Rashkov, M. Alexandrov.** Antitumor activity of quaternized chitosan-based electrospun implants against Graffi myeloid tumor. – J. Intern. Pharm., **400**(1-2), 2010, 221-233.
11. **Yanchev, I., R.Toshkova, E. Ivanova.** Immunomorphological changes in hamsters with progressing myeloid tumor induced by Graffi virus. – Comptes rendus de l'Academie bulgare des Sciences, **49**(3), 1996, 95-98.
12. **Zagorska-Swiezy K., J. Litwin, J. Gorczyca, K. Pitynski, A. Miodonski.** The microvascular architecture of the choroid plexus in fetal human brain lateral ventricle: a scanning electron microscopy study of corrosion casts. – J. Anatomy, **213**(3), 2008, 259-265.
13. **Орманджиева, В**. Електронномикроскопски и хистометрични изследвания на plexus choroideus в мозъка на плъх в онтогенеза и при експериментални въздействия. – София, АИ „Проф. М. Дринов", 2014. 152 с.

Corresponding author:
*e-mail: vormandzhieva@abv.bg*

Institute of Experimental Morphology, Pathology and Anthropology with Museum
Bulgarian Anatomical Society

Acta morphologica et anthropologica, 22
Sofia ● 2015

# Effects of Aging on Sperm Morphology and Fertility

*M. Pencheva[1], Y. Koeva[1], A. Aleksandrov[2] , N. Atanassova[3]*

*[1] Department of Anatomy, Histology and Embryology, Medical University of Plovdiv, Bulgaria*
*[2] AG Center "Salmanida", Plovdiv, Bulgaria*
*[3] Institute of Experimental Morphology, Pathology and Anthropology with Museum, Bulgarian Academy of Sciences, Sofia, Bulgaria*

Infertility affects about 14% of the couples of childbearing age. Several studies show that in about 40% of couples infertility is due to changes in spermatogenesis. Infertility itself does not threaten the physical health of men, but it has a major impact on mental and social well-being of married couples. The aim of our study was to determine the infertility distribution among a group of men with fertility problems, age range when it is observed, the associated morphological defects in comparison to the WHO criteria and possible reasons for infertility. The study examines the extent of infertility in age groups and morphological characteristics of semen analysis. The results obtained clearly reflect the global trend of harmful factors affecting spermatogenesis associated with lower sperm quantitative and qualitative indicators in human males.

*Key words:* infertility men, semen analysis, sperm morphology, reproduction.

## Introduction

Infertility affects about 14 % of couples of childbearing age [1]. For many years infertility is attributed mainly to female factor, whereas the role of the male is highly underestimated. Several studies show that about 40% of couples infertility is due to changes in spermatogenesis. Infertility itself does not threaten the physical health of men, but has a major impact on the mental and social well-being of married couples. Infertile men are more susceptible to depression and aggression. Crucial in such cases is exactly prepared semen analysis and adequate treatment plan. The first step after detecting abnormal semen analysis is to precise the reason for infertility. Only comprehensive evaluation of the data and the relationship between them can give a prognosis for fertility ejaculate.

In Bulgaria the first studies of male infertility began in the middle of the last century. In 1978 Nalbanski conducted extensive research among childless couples and found that in 33.19% of them direct cause of infertility is male infertility [8]. Today, the percentage is even higher, according to a report by the Ministry of Health [10]. In year 2010, couples with fertility problems are about 270 000 [9]. The reasons for these alarming data are probably changed lifestyle and diet, the use of ionizing devices, stress and many others.

## Objective

The aim of the study was to determine the influence of age on sperm morphological defects and sterility among group of men.

## Materials and Methods

The study was conducted among 74 males, average age of 34.9 years (20-51 years old.) Families with long (primary or secondary) infertility from Plovdiv that visited "Salmanida" AG Center (Obstetrics and Gynaecology Center) in the period from May to September 2014 were included in the present study.

Each patient signed written informed consent. Semen for seminologic study was obtained by masturbation after 3-5-day sexual abstinence in a sterile container and stored at room temperature 18-20 °C. Qualitative and quantitative studies were carried out to determine the volume of ejaculate and concentration of spermatozoa in 1 ml. Total sperm count, evaluation of motility and morphology in Kruger strict criteria [3] were investigated using a light microscope (Olympus) and camera for counting cells (Makler).

The evaluation of the results was carried out according to the criteria of the World Health Organization (WHO) [11].

All data were processed with statistical program SPSS 17.0, by applying descriptive and variation analysis

## Results

Our study found that only 40.54% of the men have normal sperm parameters respectively with normal fertility (normozoospermia), while the remaining 59.46% expressed varying degrees of infertility and reduced or lack of fertility.

The largest percentage of patients were with oligoastenozoospermia (25.68%), followed by those with astenoteratozoospermia (16.22%). Significantly rarely are diagnosed men with oligozoospermia (6.7%) and azoospermia (6.7%), and only at 4.05% with astenozoospermia and oligoastenoteratozoospermia **(Fig.1)**.

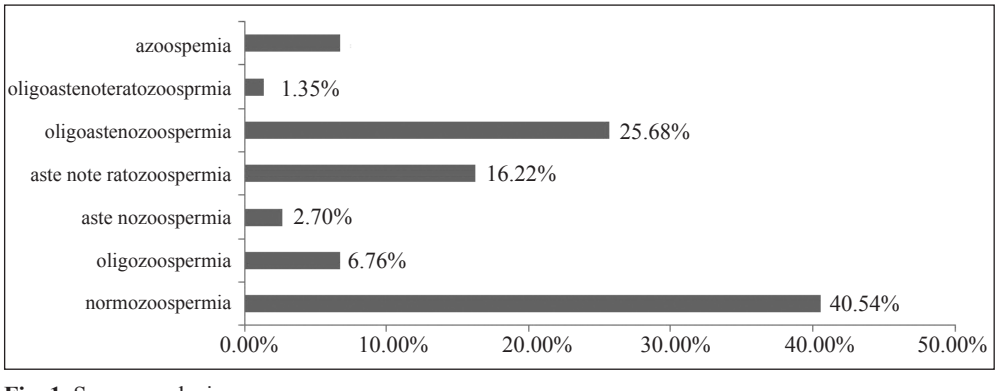


**Fig. 1.** Semen analysis

By analysis of the distribution of different types of infertility in age groups we found oligoastenozoospermia-minute diagnosed with approximately equal frequency in men between 31-40 years (28.85%) and 41-50 years (30.77%). All other types of infertility occur mainly in the age group 41-50 years (46.15%) **(Fig. 2)**

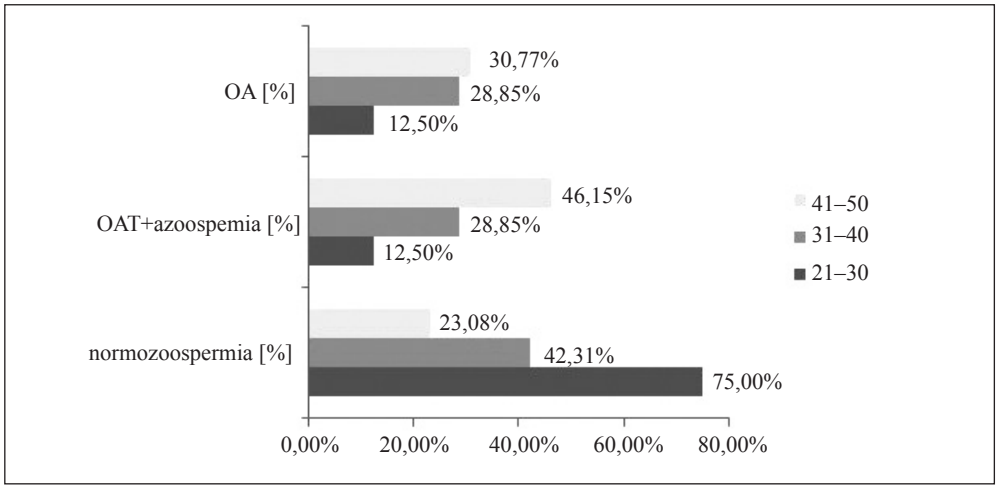


**Fig. 2.** Distribution of patients by age

The results of the morphological characteristics of semen analysis are shown in the diagram below:

N – Normozoospermia

OA – Oligoastenozoospermia

OAT – Oligoastenoteratozoospermia

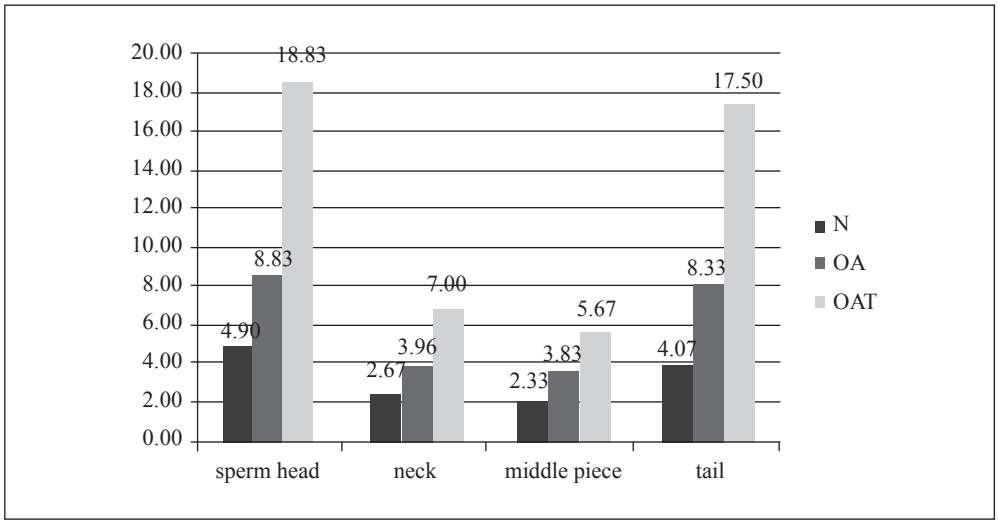


**Fig. 3.** Morphological characterization of sperm

The highest percentage of defects was reported in sperm head and sperm flagellum apparatus in patients with:

- Normozoospermia – sperm head (4.9%), tail (4.07%)
- Oligoastenozoospermia – sperm head (8.83%), tail (8.33%)
- Oligoastenoteratozoospermia – sperm head (18.83%), tail (17.5%).

## Discussion

The present study demonstrates that the number of sperm reaching its peak in men aged 21-30 years and it is reduced after 50 years of age. Also it was found that sperm motility is highest around the age of 25 and lowest after age 50. Comparing the number of spermatozoa with normal morphology in ejaculate in men aged 21-30 years to men aged over 50 it was found that the sperm motility decreased by about 50%. Sperm morphology determines success in fertilization and embryo development. In sperm morphological assessment, the percentage of sperm with normal and abnormal shape, analyzing the head, the volume of acrosome, neck, middle and caudal part were evaluated. Normally, more than 14% of sperm should have a normal shape and structure, according to the criterion by Kruger et al. (1986, 1988, 2010), the deviations are considered abnormal forms [3]. According to Ilieva and Tsvetkova [6], anomalies in the shape of the head of the sperm are combined with the pathology of the genital tract, cryptorchidism, epididymal cysts, prostatitis, epididymitis, varicocele, torsio testis. Incorrect placement of the head, its shape and size can lead to abnormalities in sperm motility and penetration ability. Numerous studies prove that the violations in the neck and middle part of the sperm due to anomalies in the construction of axonema – lack of protein dynein, microtubule and fibrils and improper disposal of mitochondria are result of genetic defects. Morphological studies reported that abnormalities in sperm tail were found in a higher percentage in diseases such as chronic epididymitis, epididymal cyst and postparotidic orchitis [5]. It is well known that the cellular or physiological changes in the urogenital tract increased with age. Testicular biopsies demonstrate narrowing and sclerosis of the lumen of the seminiferous tubules, reduced spermatogenesis and increased degeneration of germ cells, and atrophy with diminished function of Leydig cells [2].

Changes in the prostate that occur with age, such as smooth muscle atrophy and reduced water and protein content can lead to reduction in the semen volume and sperm motility. In addition, changes in the epididymis, associated with age, suppress energetic movement sperm capacity. Epididymitis is hormonally sensitive tissue that plays an important role in sperm maturation [7]. Thus, the reduction of the hormonal levels associated with age may lead to a decrease in mobility in older men.

Second, the aging provides a longer period of impact of exogenic factors on the reproductive system. Older men have been exposed longer to the carcinogenic effects of smoking, possibility of diseases, including genitourinary infections than younger men.

Other parameters that may be affected by age include sperm morphology, which is shown to be a sensitive indicator of status and changes in the epididymis. Several studies have shown age-related defects in the genetic integrity of sperm. For example, age is associated with increased aneuploidy in sperm production in humans [4] and mice, as well as increasing in the frequency of the *de-novo* gene mutations.

## Conclusion

The results obtained clearly reflect the global trend of harmful factors affecting spermatogenesis associated with lower sperm quantitative and qualitative indicators in human males.

## References


1. **Adams, J. A., T. S. Gallowa, D. E. Mondial, S. C. Esteves, F. Matthews.** Effect of mobile telephones on sperm quality: a systematic review and meta-analysis. – Environ Int., 2014 Sep; 70: 106-112.
2. **Barbutska, D., Iv. Koeva, M. Bakalska, N. Atanasova, E. Detchev.** Aging and steroidogenesis in testicle-morphological analysis. – MU, Plovdiv, IEMPAM-BAS, 2014.
3. **Cooper, T. G., E. Noonan, S. von Eckardstein, J . Auger, H. Baker, H. Behre, T. Haugen, T. Kruger, Wang, M. Mbizvo, K. Vogelsong.** World Health Organization reference values for human semen characteristics. – Human Rep. Up., **16**(3), 2010, 231-234.
4. **Friedman, J.** Genetic disease in the offspring of older fathers. – Obstet. Gynecol., 57, 1981, 745-749.
5. **Hancock, A., D. de Kretser.** The axonemal ultrastructure of spermatozoa from men astenospermia. – Fertility Sterility, **57**, 1992, 661-664.
6. **Ilieva, I., P. Tsvetkova.** Morphological changes in the head of the sperm and infertility. – Repr. Health, **14**, 2008, 20-24
7. **Lowe, X., Br. Eskenazi, D. Nelson, Sh. Kidd, A. Alme, A. Wyrobek.** Frequency of XY sperm increases with age in fathers of boys with klinefelter syndrome. Correspondence, Medical Center, San Francisco, – J. Am. Hum. Genet., **69**(5), 2001, 1046-1054.
8. **Nalbanski, B.** Male infertility as a cause of infertility in the family: medico-biological, seminologic and medical and social studies. Sofia, 1978.
9. Annual report on the activities of the "I Want a Baby", 2010, Plovdiv.
10. "Investigation of the frequency and causes of infertility," Report of the Ministry of Health, National Institute of Statistics on Population Fund and the UN, Sofia, 2005.
11. World Health Organization Laboratory Manual for Examination of Semen and Sperm-Cervival Mucus Interaction, 4th Edition, 1999. Cambridge University Press, Cambridge.

Institute of Experimental Morphology, Pathology and Anthropology with Museum
Bulgarian Anatomical Society

Acta morphologica et anthropologica, 22
Sofia ● 2015

# Immunohistochemical Expression of Ghrelin Receptor GHS-R1 in the Gastrointestinal Tract

*N. Penkova, P. Atanassova*

*Department of Anatomy, Histology and Embryology, Medical University, Plovdiv*

Ghrelin is a gastrointestinal hormone which performs the function of a ligand for secretory receptors of growth hormone in the adenohypophysis. In recent years, studies reveal the presence of ghrelin receptors outside the CNS. The aim of the study is an immunohistochemical proof of the presence and localization of ghrelin receptor GHS-R1 in the human gastrointestinal tract. Biopsy specimens from stomach – body and antrum pylorus and duodenum are subjected for the expression of ghrelin receptor GHS-R1. Immunohistochemical study of GHS-R1 found its expression in biopsy material from three locations. The presence of receptors for ghrelin in the gastrointestinal tract indicates its paracrine action. There are ghrelin receptors in the epithelial cells of gastric glands and Lieberkuhn crypts of the duodenum that can directly affect their secretion. By binding to receptors in smooth muscle cells ghrelin also influences motility of the gastrointestinal tract.

*Key words:* ghrelin, ghrelin receptor, GHS-R1, gastrointestinal tract.

## Introduction

Ghrelin is a gastrointestinal hormone which performs the function of a ligand for secretory receptors of growth hormone in the adenohypophysis (growth hormone secretagogue receptor, GHSR). As a releasing factor for growth hormone ghrelin intervenes in the regulation of many metabolic processes. In recent years, studies reveal the presence of ghrelin receptors outside the CNS, in peripheral tissues. Ghrelin receptor GHS-R1 is established in placenta, lung, uterine myometrium, in vegetative afferent nerve fibers in the gastrointestinal tract.

The aim of the study is an immunohistochemical proof of the presence and localization of ghrelin receptor GHS-R1 in the human gastrointestinal tract.

## Materials and Methods

The materials about the morphologic research of the EC cells were obtained by fibrogastroscopy performed on 6 female patients, 45-72 years old, from the MBAL "St. George" Clinic of Gastroenterology in Plovdiv. The biopsy specimens were taken from the body

and antrum pylorus of the stomach and superior portion of the duodenum. There were no endoscopic pathological changes in the gastric mucosa of these patients.

The material is studied by immunohistochemistry using the ABC method with primary antibody for ghrelin receptor GHS-R1 (rabbit polyclonal antibody Ghrelin – Santa Cruz Biotechnology USA) at a dilution of 1:100. Positive response to ghrelin is presented by fine brown granulation. The specificity of the immunohistochemical reaction was confirmed by negative controls, the specific antibody was replaced with a buffer (PBS) or normal non-immune serum.

## Results

Immunohistochemical study of ghrelin receptor GHS-R1 found its expression in biopsy material from three locations – in the stomach body and antrum pylorus and in the duodenum. In the stomach body mucosa GHS-R1 receptors were visualized by brown fine granulation in some cells of the fundic glands. These cells were few in number.

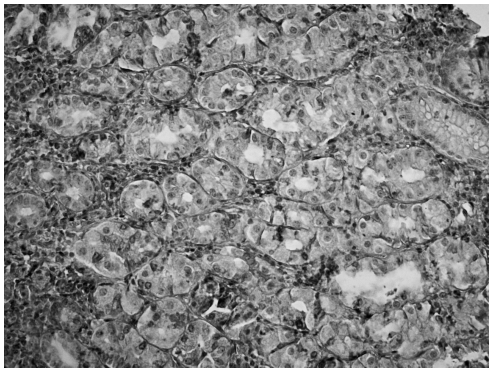

**Fig. 1.** Biopsy specimens from the body of the stomach. Immunohistochemical expression of GHS-R1 in the fundic glands. Paraffin preparation. Magnification × 20

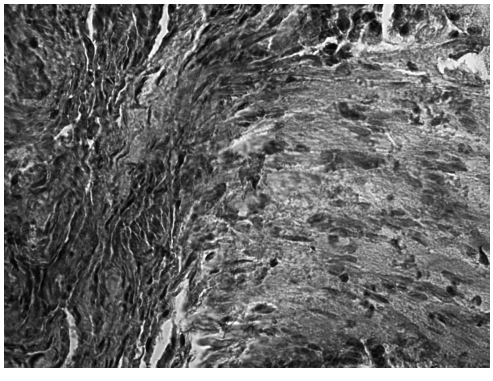

**Fig. 2.** Biopsy specimens from the antrum of the pylorus. Immunohistochemical expression of GHS-R1 in the smooth muscle cells of the gastric wall. Paraffin preparation. Magnification × 40

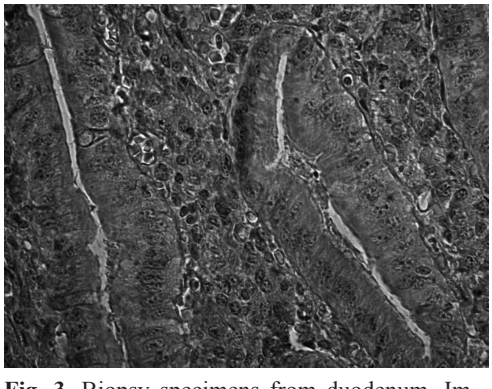

**Fig. 3.** Biopsy specimens from duodenum. Immunohistochemical expression of GHS-R1 in the epithelial cells of the duodenal villus. Paraffin preparation. Magnification × 40

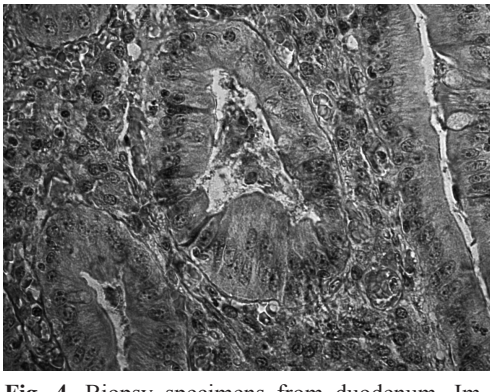

**Fig. 4.** Biopsy specimens from duodenum. Immunohistochemical expression of GHS-R1 in the glandular cells of the crypts of Lieberkuhn. Paraffin preparation. Magnification × 40

They were located mainly in the central parts of the glands unevenly among other epithelial cells (**Fig. 1**). In the antrum biopsy immunohistochemical reaction is positive for smooth muscle cells. Bundles of parallel leyomyocytes showed brown granulations that can cover whole cells (**Fig. 2**). In the duodenum the receptor is expressed in both the epithelial cells coating the intestinal villi, and in the glandular cells of the crypts of Lieberkuhn (**Figs. 3, 4**).

## Discussion

Ghrelin receptor GHS-R1 is a G-coupled peptide. It was first cloned in 1996 from adenohypophysis and hypothalamus [1]. Binding of ligands to this receptor leads to the secretion of growth hormone. In 1999 ghrelin was identified as an endogenous ligand for this receptor [5]. The receptor has two isoforms – GHS-R1a and GHS-R1b. GHS-R1a is a mature polypeptide of 366 amino acid sequences and 7 transmembrane domains. GHS-R1b is an immature polypeptide with 289 amino acid residues and 5 transmembrane domains. Recently some authors found the presence of ghrelin receptors outside of the CNS. O'Brien et al. [4] reported the expression of ghrelin and GHS-R1 in the smooth muscle cells of myometrium of the uterus during pregnancy, childbirth and in the uterine wall outside of pregnancy. Ghrelin has autocrine and paracrine effects that decrease contractility of the leyomyocytes and provide protection of pregnancy [4]. Ghrelin has a number of effects on the cardiovascular system. In vitro and in vivo it has a powerful vasodilatating effect. Ghrelin decreases the tonus of smooth muscle cells of the vascular wall. Endothelial cells of the microcirculatory bed express ghrelin and GHS-R1. *In vitro* ghrelin stimulates cell proliferation, migration and angiogenesis [3]. There is evidence of GHS-R1 receptor in the gastrointestinal tract of rats and guinea pigs that affect gastrointestinal motility [2].

## Conclusion

The presence of receptors for ghrelin in the gastrointestinal tract indicates its paracrine action. There are ghrelin receptors in the epithelial cells of gastric glands and Lieberkuhn crypts of the duodenum that can directly affect their secretion. By binding to receptors in smooth muscle cells ghrelin also influences motility of the gastrointestinal tract. Evidence of the existence and distribution of ghrelin receptors in the human gastrointestinal tract is important for the clinical practice – possible therapeutic use of ghrelin analogues; agonists and antagonists of ghrelin receptors and knowledge of their side effects and complications.

## References


1. **Howard, A., S. Feighner, D. Cully, J. Arena, P. Liberator, C. Rosenblum, M. Hamelin, D. Hreniuk, O. Palyha, J. Anderson, P. Paress, C. Diaz, M. Chou, K. Liu, K. McKee, S. Pong, L. Chaung, A. Elbrecht, M. Dashkevicz, R. Heavens, M. Rigby, D. Sirinathsinghji, D. Dean, D. Melillo, A. Patchett, R. Nargund, P. Griffin, J. DeMartino, S. Gupta, J. Schaeffer, R. Smith, L. Van der Ploeg.** A receptor in pituitary and hypothalamus that functions in growth hormone release. – Science, **273**, 1996, 974-977.
2. **Kitazawa, T, T. Nakamura, A. Saeki, H. Teraoka, T. Hiraga, H. Kaiya.** Molecular identification of ghrelin receptor (GHS-R1a) and its functional role in the gastrointestinal tract of the guinea-pig. – Peptides, **32**(9), 2011, 1876-86.

3. **Li, A., G. Cheng, G. Zhu, A. Tarnawski.** Ghrelin stimulates angiogenesis in human microvascular endothelial cells: Implications beyond GH release. – Biochem. Biophys. Res. Commun., **353**(2), 2007, 238-243.
4. **O'Brien, M., Earley, J. Morrison, T. Smith.** Ghrelin in the human myometrium. – Reprod. Biol. Endocrinol., **8**, 2010, 55.
5. **Wren, A., C. Small, H. Ward, K. Murphy, C. Dakin, S. Taheri, A. Kennedy, G. Roberts, D. Morgan, M. Ghatei, S. Bloom.** The novel hypothalamic peptide ghrelin stimulates food intake and growth hormone secretion. – Endocrinology, **141**(11), 2000, 4325-4328.

Corresponding author:
*Nadya Penkova*
*Department of Anatomy, Histology*
*and Embryology*
*Medical University, Plovdiv*
*15A, Vassil Aprilov Blvd.*
*4002 Plovdiv, Bulgaria*
*GSM: 0898 274 344*
*e-mail: nadja_penkova@abv.bg*

Institute of Experimental Morphology, Pathology and Anthropology with Museum
Bulgarian Anatomical Society

Acta morphologica et anthropologica, 22
Sofia ● 2015

# Therapeutic Activity of Albendazole on a Murine Experimental Model of the Muscle Stage of Trichinellosis

*S. Petkova, V. Dilcheva, E. Gabev*

*Institute of Experimental Morphology, Pathology and Anthropology with Museum, Bulgarian Academy of Sciences, Sofia, Bulgaria*

A comparative study on the anti-Trichinella efficiency of liposomal Albendazole (LA) and free (unincorporated in liposomes) Albendazole (A) has been carried out on an experimental murine model of the muscle stage of trichinellosis, i.e. when parasite larvae are encapsulated into the muscle tissue and routine therapy has proven inadequate. The results showed that (LA) yields a 69% efficiency compared to a slight 36% for (A) applied at equal doses.

*Key words:* liposomes, Trichinellosis, Albendazole, fitting analysis.

## Introduction

Trichinellosis is one of the most detrimental parasitic ailments in the animals and the human caused by representatives of the Trichinella genus (Nematoda class – roundworms).

The epidemic outbursts in their character-massiveness and unpredictability resemble the ones of many infectious diseases (dysentery, typhoid, tularemia) the complications being very perilous both in its acute and chronic forms. In the literature known to us to the present moment no successful treatment of the muscle stage has ever been reported [2, 3, 4]. That is why our investigations were aimed at the treatment of this phase of the disease.

Based on the liposomal theory for transferring therapeutic substances to damaged organs and cells [1] the mechanism of the improved therapeutic activity of (LA) as compared with (A) is explained by the "delivery" of Albendazole in the muscle cell in close proximity to the parasite. Thus, the larvae are found at a constant concentration of the anthelmintic which is detrimental to them while at routine application a higher concentration of the drug is reported in the patient's blood while in situ concentration is insufficient and dwindling very fast with time. The period of demi-elirainationfor most drugs is several hours. A paradox is observed when the parasite is attacked by an insufficiently high concentration of the anthelmintic which hasn't capacity to destroy it and the concentration in the target cell rapidly decreases being at the same time comparatively high which leads to toxic effects for the healthy tissues. After the liposome comes

in contact with the cell either through adsorption or fusion it supplies the intracellularly active therapeutic substance (Albendazole in our case). Its release gradually started from the liposome either via the action of the intracellular enzymes (lipases) found in the liposomes or by diffusion (it passes through the liposome and cell lipid membranes). This deposition of the active therapeutic substances in situ in the affected organs and cells provides the increased therapeutic activity as well as for the typical of the liposomal preparations depot-effect, i.e. their retarded and long-term action. This allows for the preparations to be introduced only once or twice a week. The depot-effect of the liposomal action is explained by the slow degradation of millions of liposomal vesicles and the slow diffusion through the bi-layer lipid membrane, especially in the case of the multilamellar liposomes used in our experiments.

## Materials and Methods

*Animal Experiments*

White mice, weighing around 30 g, were infected per os with 100 Trichinella larvae of *T. spiralis* species. On day 35 following the infection, when the muscle stage is well-expressed, five experimental groups with 30 mice each were formed.

Group 1 – controls, injected with saline i.p. once a week;

Group 2 – experimental, injected with Albendazole dose of 24 mg/kg i.p. once a week;

Group 3 – experimental, injected with Albendazole encapsulated in liposomes at a dose of 24 mg/kg i.p. once a week.

Three mice of each group were sacrificed each week. The number of live *Trichinella larvae* has been recorded in the diaphragms of the mice preliminarily processed by the compressor method and the effect of application of the preparation has been assessed after the diaphragms have been separately digested in artificial stomach juice and the number of live and dead *Trichinella larvae* has been registered.

*Preparation of liposome Encapsulated Albendazole (LM)*

Albendazole substance of pharmaceutical grade (Cipla, India) was encapsulated in the lipid phase of extrusion type of liposomes. Briefly, freeze-thawed multilamellar liposomes were subjected to high pressure of argon gas jet homogenization with subsequent in line extrusion through l00 nm pore size polycarbonate membrane implemented by Emulsi-Flex C5 apparatus (Avestin, Canada). Lipid phase consists of 20 mg/ml total egg yolk lipids. Sodium saline (150 mM NaCl) dissolved in double distilled and sterile water was used as an aqeous phase of the liposomes. The resulted liposome sterile suspension was used for treatment of the experimental animals.

*Preparation of Non-liposome Encapsulated (free) Albendazole*

Albendazole substance of the same quality as above was dissolved in sodium saline using intermittent sonification (2 × 20 s with 1 min pause between). Bath type sonifier B220, 125 W (Branson, USA) was used.

## Results and Discussion

The experimental results of the investigation are presented in **Fig. 1**. The number of live *Trichinella larvae* in the target organ - the diaphragm (data are placed on the ordinate axis) served as criteria for anti-Trichinella activity during the recording

period (abscissa). The interpretation of the results is carried out in two aspects - an intuitive-visual one which readily shows the advantage of LA as compared to A and a mathematical one which through a detailed statistcal analysis proves the significance of the obtained data.

**Figure 1** shows the diminution of the live *Trichinella larvae* number under the action of A and LA in dose (24 mg/kg bw). A linear decrease of the parasite numbers is registered until their final extermination is accomplished by week 9 to 10.

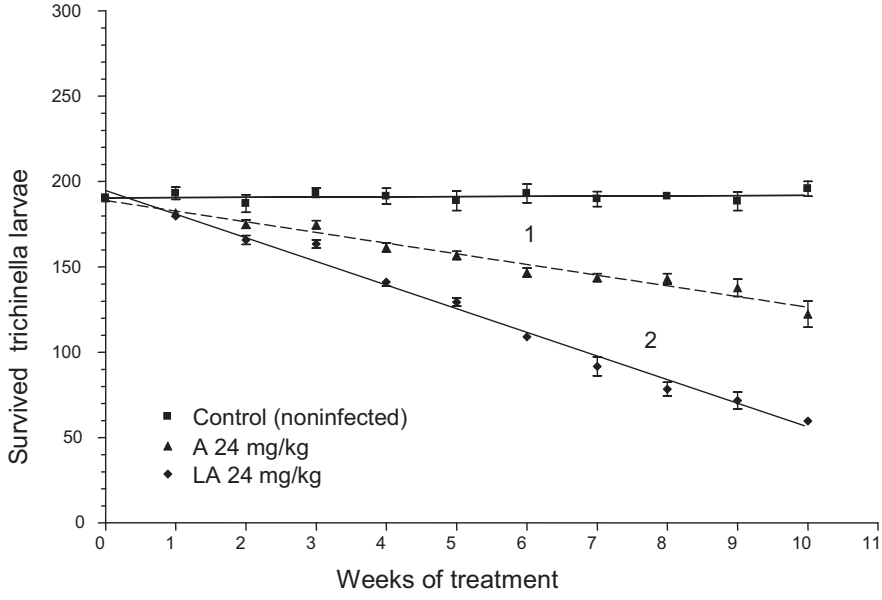


**Fig. 1.** Treatment of experimental muscle phase of trichinellosis with liposomized Albendazole (LA) and free Albendazole (A). Treatment started 35 days after the infection

The results obtained from the mice treated with liposome-free Albendazole and liposomal Albendazole are presented in **Fig. 1**. It is quite clear that after the application of free Albendazole (A) the larvae number decreases much more slightly, and the most important – they do not reach zero level despite continuing the treatment. After about 4 to 5 weeks we observed an inefficiency of the therapy, without tendency to reach the zero level (unlike the case with LA). At the dose of 24 mg/kg A the efficacy is 36%.

The results interpretation shows that LA at a dose of 24 mg/kg leads to a complete annihilation of *Trichinella larvae* compared to A at the same dose and there is an upward trend which proves an impossibile annihilation of *Trichinella larvae* encapsulated in the muscle cell by free Albendazole. At the dose of 24 mg/kg the efficacy of liposomal Albendazole (LA ) is 69%.

This fact explains the unsatisfactory results obtained in the practice of treating muscle trichinellosis [7, 6]. The applied analysis clearly demonstrates the advantages of liposomal Albendazole compared to free one but does not provide strict proofs for the significance of data which imposed the undertaking of a detailed statistical analysis which provoked the above-presented conclusions.

All experimental data have been pretested for correspondence to the normal Gauss distribution. The data were also checked for presence of extreme values by Grubb on line test (these are usually very low or very high values compared to others left unconsidered). The Curve Expert version 1.36 (Hans Development, USA) for preliminary automatic fit with 36 models and interpolation of the viral load with time was used. The Prism version 2.01 [5] for further detailed analysis of the best fitting linear regression line and estimation of the best fit parameters and calculation of the theoretical end point time necessary for obtaining different viral loads was used. The Prism version was also implemented for construction of the graphs. For data obtained from the therapy with LA a linear equation was formulated

$$y = a + bx, \quad (1)$$

and for those obtained from the treatment with free A the equation

$$y = a \exp(bx) + c \quad (2)$$

is exponential with a residual coefficient c differing from the aero with a biological value, meaning that it defines the number of the live larvae left in spite of the treatment with the preparation and demonstrates the impossibility for a radical extermination of the parasite.

From the analysis it has been established that the parameters showing a degree of correspondence between the experimental data (goodness of fit) and the data of the theoretical linear curve have a big importance and also prove that the liposomal preparation leads to a significant extermination of the larvae for a short period of treatment (about 10 weeks).

Linear-regression analysis of the control for LA shows that it is absolutely horizontal and related to the abscissa (period of treatment), i.e. there is no loss of larvae upon incubation with saline which means that the anti-Trichinella effect is solely due to the preparation rather than other factors.

From the analyses is clear that liposomal encapsulation of Albendazole leads to a considerably improved therapeutic efficiency compared to the one displayed by free, routinely applied Albendazole. It is expressed not only in the quantitative augmentation of the larvocidal effect but also in the cardinal alteration of the model (equation) of the mechanism of action of LA compared to A. The latter kills the larvae after an exponential dependency (equation 2) with lack of efficiency (plateau) despite the continuation of drug administration. The mathematical model LA shows the effect as a linear regression with a progressive diminishing of larvae number accomplishing their total annihilation in the end.

## References


1. **Ball, P.** Designing the molecular world: Chemistry at the frontier. – Princeton, USA, Chichester, West Sussex, UK, Princeton University Press, 1994, 232-238.
2. **Campbell, W., A. Cuckler.** Effect of thiabendazole upon theenteral and parenteral phases of trichinosis in mice. – J. Parasitol, **50**(4), 1964, 481-488.
3. **Campbell, W., A. Cuckler.** Further studies on the effect of thiabendazole on trichinosis in swine, with notes on the biology of the infection. – J. Parasitol., **52**, 1966, 260-279.
4. **Lopez-Garcia, M., S. Torrado-Duran.** Albendazole versus ricobendazole (albendazole-sulphoxide) against enteral and parenteral stages of *Trichinella spiralis* in mice. – J. Int. Parasitol, **27**, 1997, 781-785.

5. **Motulsky, H.** Analyzing data with graph pad prism. – San Diego, Graph Pad Software Inc., 1999.
6. **Pozio, E.** Trichinellosis in the European Union: Epidemiology, Ecology and Economic Impact. – Parasitol. Today, **14**, 1998, 35-38
7. **Pozio, E**., **D**. **Sacchini, L. Sacci, A. Tamborrmi, F. Alberici.** Failure of mebendazole in the treatment of humans with *Trichinella spiralis* infection at the stage of encapsulating larvae. – Clinical Infectious Diseases, **32**, 2001, 638-642.

Institute of Experimental Morphology, Pathology and Anthropology with Museum
Bulgarian Anatomical Society

Acta morphologica et anthropologica, 22
Sofia ● 2015

# Homology of Heat Shock Protein 70 (HSP70) in Human and Mouse Testis

*S. Zaprianova, P. Rashev*

*Institute of Biology and Immunology of Reproduction "Acad. Kiril Bratanov", Bulgarian Academy of Sciences,* Sofia, Bulgaria

The 70kDa family of stress proteins is highly conserved showing structural and functional homology. In mammals several isoforms exist: a constitutive isoform of Hsp70 (Hsp73) is thought to act as chaperones for other cellular proteins under non-stress conditions. By contrast, the stress-inducible isoform of Hsp70 (Hsp72) is generally not expressed in unstressed cells; however, upon exposure to stressful conditions, Hsp72 is highly inducible. During the conditions of stress, both Hsp73 and Hsp72 are thought to bind to damaged and misfolded polypeptides, and facilitate their repair. Extracts from mouse, heat-treated and non-treated testes, as well as human testes were obtained, separated electrophoretically, and the Hsp70 protein expression was studied by Western blot analysis. Homology of the two isoforms was detected by employing an absorption method. Polyclonal anti-Hsp70 antibody (DACO) recognized both isoforms in mouse heat-treated testis while in non-treated only constitutive Hsp73 protein was expressed, suggesting that inducible Hsp72 protein appears to repair the proteins whose conformation is altered by stress. After absorption of the antibody with heat-treated mouse testes extracts no specific reaction was registered by Western blotting of mouse and human extracts providing evidence for homology of the Hsp72 and Hsp73 isoforms in these mammalian species.

*Key words:* heat stress, heat shock proteins, Hsp70, homology, mouse and human testis.

## Introduction

The cellular stress response is an evolutionarily conserved defense mechanism characterized by a transcriptionally controlled induction of the synthesis and accumulation of heat shock or stress proteins (HSPs) following exposure of cells to high temperatures or other environmental challenges [5, 10]. The protective effect is the ability of HSPs to act as molecular chaperones, interacting with denatured proteins and helping them to restore their native structure and their function [1]. The stress proteins of the family of 70kDa (HSP70s) are amongst the most highly induced proteins of the cellular stress response in mammals [10]. Hsp70 family encoded by 11 genes in human cells and by 8 genes in murine cells [9]. One of these genes is known to encode the major cytosolic/nuclear constitutive isoform HSP73, whereas two other genes encode the inducible isoform HSP72 [3]. HSP70 shares the property of binding ATP and polypeptides. In the testis, a number of HSP have been identified and characterized, of which HSP70 family

comprises stress-inducible Hsp70 (HSP72) and constitutively expressed Hsc70 (HSP73) [6]. The two isoforms show extensive sequence homology (over 95%), but their expression and functions in male germ cells are still unknown [11]. HSP72 (HSP70) and HSP73 (heat shock cognate, HSC70) have been located within the cytoplasm and, following stress, in the nucleus. High level of Hsp70 expression not only in heat stressed but in normal germ cells during different stages of spermatogenesis suggests its role both in stress conditions and in testis maturation and function [4]. Under physiological conditions, constitutively expressed HSP73 acts as molecular chaperone that assists proper folding, assembly, and intercellular trafficking of newly synthesized proteins. In response to stressful stimuli, HSP72 is induced and involved in cellular repair and protective mechanism [2]. In the last few years it has been demonstrated that this protective effect is in part the result of inhibition of apoptosis or cell suicide [8]. Hsp72 inhibits apoptosis by blocking release of cytochrome *c* from mitochondria. On the other hand, HSP72 is known to inhibit mitochondrial apoptosis-inducing factor (AIF) release, thus decreasing partly cell injury [7]. Heat shock proteins may also regulate the apoptotic pathway downstream of cytochrome *c* release and prior to caspase activation. Binding of cytochrome *c* to Apaf-1 requires significant structural changes to facilitate binding and cleavage of pro-caspase-9 to generate the active enzyme. These structural changes may be inhibited by some Hsps since maintenance of protein structure is a well-established property of Hsps in their role as chaperones. Despite many reports on the protective effects of HSPs, the possible mechanisms by which they negatively modulate the apoptotic process are poorly investigated [8]. The present study focused on monitoring the homology of expressed Hsp73/72 in mouse and human normal mature testis.

Studies on the role of heat shock proteins during human spermatogenesis are still insufficient due to ethic reasons. In this context experiments on homology between certain stress proteins in human and mouse testis are often used as a model system. Our study on homology between human and mouse stress proteins gives the possibility for extrapolation of the results from mouse spermatogenesis towards human spermatogenesis.

## Materials and Methods

Extracts from mouse and human testes were used. Pieces from testes of 60-day-old male conventional mature mice (not-treated and treated-incubated under high temperature), and pieces from normal human testes (surgically derived) were prepared in cold Tris-buffered solution (TBS, pH 7.4), homogenized in presence of Protease inhibitors (Sigma Co., St. Louis, USA), and centrifuged. Protein contents were evaluated with Ultraspec 1000.

Protein fractions in extracts from control or heat-treated sexually mature mouse and normal human testes were separated and the expression of homologous antigens was achieved by means of SDS-PAGE and Western blot analysis. Testes extracts were prepared in 6 × Sample buffer in ratio 3:1. Equal amounts of lysate were resolved by 10% SDS polyacrylamide gel under reducing conditions. Protein fractions were visualized by Coomassie Brilliant blue (Sigma Co., USA) and their molecular weight were determined according to standard molecular markers. This was followed by blotting onto nitrocellulose membranes (Amersham Pharmacia Biotech, UK) for 1 hour. Nonspecific binding sites were blocked with 5% nonfat dry milk in TBS for 1 hour. The blots were incubated with primary antibody – rabbit, polyclonal serum against HSP70 (DAKO) at 1:500 overnight at 4 °C. The expression of homologous antigens was detected with the same antibody prepared in two variants: non-absorbed at 1:500, and absorbed extracts from heat treated mouse testis at 1:1000 overnight. Thereafter, the blot was washed and

incubated with biotin-conjugated anti-rabbit IgG at 1:2000 in blocking buffer followed by washing and incubation in streptavidin-alkaline phosphatase for 1 hour. Immunodetection of proteins and homologous antigens were revealed using alkaline-phosphatase buffer (containing 0.1 M Tris, 0.1 M NaCl, 0.005 M $MgCl_2$, pH 9.5) in which were added nitroblue tetrazolium (NBT) and 5-bromo-4-chloro-3-indolyl-phosphate (BCIP). The reaction was stopping in $dH_2O$.

## Results and Discussion

The present study was conducted to detect the homology of expression of HSP70 in normal and heat-treated mouse, and normal human mature testes. There are described two isoforms of HSP70 – a constitutive HSP73 and an inducible HSP72. Both isoforms share 95% sequence identity and are present in cytosol and nucleus in resting cells, and become predominantly nuclear during or soon after heat stress. We performed SDS-PAGE electrophoresis and corresponding Western blot to detect the expression of HSP70 in extracts of normal mouse and human mature testes (**Fig. 1**).

We observed that under normal conditions antibody against HSP70 recognized

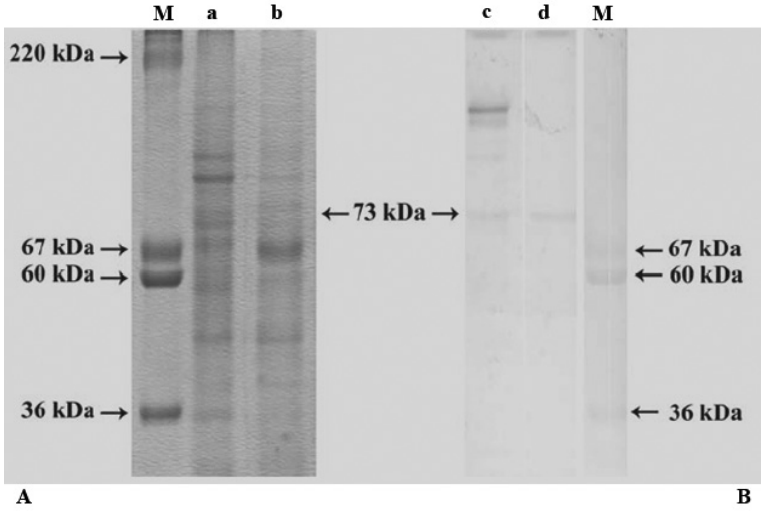


**Fig. 1.** SDS-PAGE (A) and corresponding Western blot (B) analysis to detect the expression of Hsp70 in extracts of non-treated mouse testis (a, c), and human testis (b, d). Polyclonal anti-Hsp70 antibody recognized protein band corresponding to approximately 73kDa molecular weight in both samples – the constitutive isoform of Hsp70 (Hsp73); (M) – protein molecular weight marker

protein band corresponding to approximately Hsp73 kDa molecular weight – the constitutive isoform of Hsp70 (Hsp73). The results showed that under physiological spermatogenesis, when the process of spontaneous apoptosis exists, Hsp73 is expressed. We assumed that the constitutive isoform Hsp73 has important functions as a molecular chaperone at the time of mouse and human spermatogenesis.

After heat shock the results received from SDS-PAGE and corresponding Western blot of normal and heat-treated mouse testicular extracts revealed protein band respective to Hsp73 isoform. Under hyperthermia conditions the specific reaction of antibody against Hsp73 is increased. We observed enhancement of Hsp73 levels following ex-

posure to heat stress simultaneously with the presence of an additional band, indicates the expression of the inducible Hsp72. We allowed that in male germ cells exists not only the constitutive Hsp70 but also the inducible isoform of this protein. There is evidence that Hsp72 is expressed only under heat inducible apoptosis and probably related with protective functions in spermatogenesis at the time of temperature stress (**Fig.2**).

In our previous study we analyzed the specific expression of the two isoforms

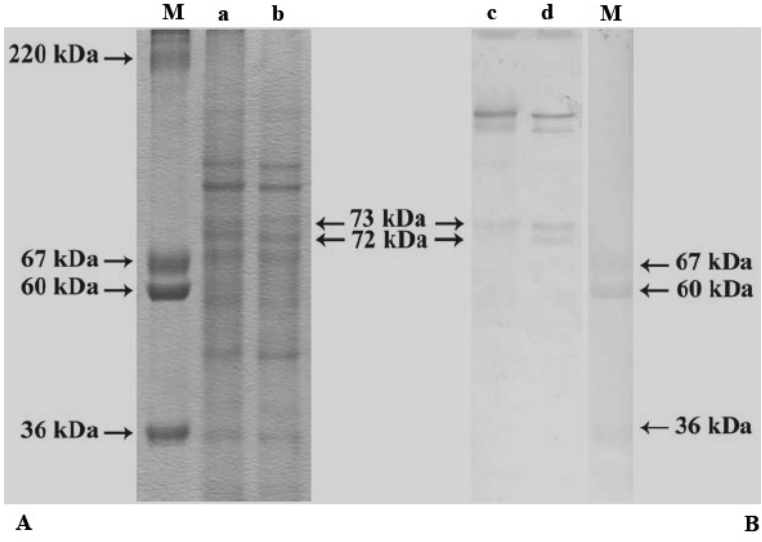


**Fig. 2.** SDS-PAGE (A) and Western blot (B) of non-treated mouse testis extract (a, c), as well as heat-treated mouse testis extract (b, d). The specific reaction of the antibody against Hsp73 isoform increased after hyperthermia. Note the presence of an additional band in sample from heat-treated tissue, indicates the expression of Hsp72 isoform following the exposure to high temperature. (M) – protein molecular weight marker

(Hsp72/Hsp73) of the Hsp70-gene family during postnatal development of mouse testis and testicular hyperthermia in adult animals, using immunocytochemistry. The obtained results showed expression of Hsp70 in germ cells during all stages of spermatogenesis. Our results confirmed predominant cytoplasmic localization of Hsp70 in spermatogonial cells and in pachytene spermatocytes. Round spermatids expressed Hsp70 not only in the cytoplasm but in the nucleus as well. After heat shock the labeling of the nucleus of spermatocytes and round spermatids was significantly increased, probably due to the movement of Hsp70 from cytoplasm to nucleus. Nuclear translocation of Hsp70 triggers the cascade in signal transduction events leading to realization of chaperone activity of Hsps [4].

We performed SDS-PAGE and respective immunoblot with non-absorbed Ab against Hsp70 in heat-treated mouse, and normal mouse and human testes extracts. The reaction of constitutive Hsp73 isoform was detected in all cases while inducible Hsp72 was expressed only in heat-treated mouse testis (**Fig. 3A**). After absorption of the antibody with heat-treated mouse testes extracts and subsequent Western blot, no specific reaction was registered (**Fig. 3B**). The results obtained with absorption methods together with SDS-PAGE and Western blot analysis are clear evidence for homology

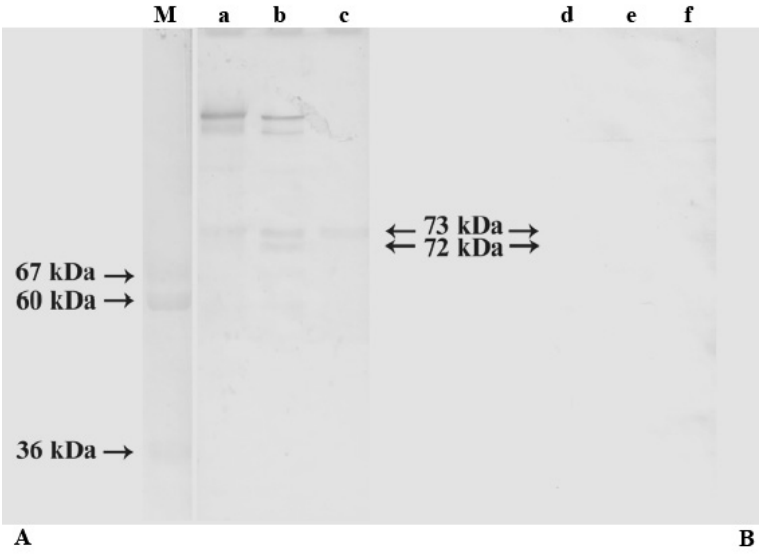


**Fig. 3. (A).** Western blot analysis of non-treated (a), and heat-treated (b) mouse testes, as well as normal human (c) testes extracts. The reaction of Hsp73 isoform was seen in all samples while the inducible Hsp72 isoform was detected only after heat stress (b); **(B).** Detection of the homology of Hsp70 in mouse and human testes was performed by absorption of the antibody against Hsp70 with heat-treated mouse testis, and subsequent Western blot. After absorption, no specific reaction of the antibody was registered in non-treated (d), heat-treated (e) mouse testes, and normal human testes (f). (M) – protein molecular weight marker

between the two isoforms, Hsp73 and Hsp72, of heat shock protein 70 in mouse and human testes.

## Conclusion

In conclusion, the results reported in this paper show that Hsp70 Ab absorbed with heat-treated mouse testis extract in immunoblot does not react with both mouse and human extracts, and provide evidence for homology of Hsp72/73 isoforms in human and mouse testes. Under stress conditions the protein expression of the constitutive isoform Hsp73 increased, simultaneously with the activation of the inducible isoform Hsp72 in order to ensure germ cell survival and to avoid subsequent male infertility problems.

## References

1. **Buchner, J.** Supervising the fold: functional principles of molecular chaperones. – J. FASEB, **10**, 1996, 10-19.
2. **De Maio, A.** Heat shock proteins: facts, thoughts, and dreams. – Shock, **11**(1), 1999, 1-12.
3. **Ellis, S., R. Killender, R. L. Anderson.** Heat-induced alterations in the localization of HSP72 and HSP73 as measured by indirect immunohistochemistry and immunogold electron microscopy. – J. Histochem. Cytochem., **48**, 2000, 321-331,
4. **Mollova, M., S. Zaprjanova, P. Rashev, Y. Martinova.** Developmental and hyperthermia-related

expression of heat shock protein 70 (HSP 70) in mouse testis. – Comp. rend. Acad. bulg. Sci., **60**(8), 2007, 903-906.
5. **Morimoto, R.** Cell in stress: Transcriptional activation of heat shock genes. – Science, **259**, 1993, 1409-1410.
6. **Neuer, A., S. Spandorfer, P. Giraldo, S. Dieterle, Z. Rosenwaks, S. Witkin.** The role of heat shock proteins in reproduction. – Human Reproduction Update, **6**(2), 2000, 149-159.
7. **Ruchalski, K., H. Mao, K. Singh, Y. Wang, D. D. Mosser, F. Li, J. H. Schwartz, S. C. Borkan.** HSP72 inhibits apoptosis-inducing factor release in ATP-depleted renal epithelial cells. – J. Am. Physiol. Cell Physiol., **285**(6), 2003, 1483-1493.
8. **Samali, A., S. Orrenius.** Heat shock proteins: regulators of stress response and apoptosis. – Cell Stress Chaperones, **3**(4), 1998, 228-236.
9. **Tavaria, M., T. Gabriele, I. Kola, R. L. Anderson.** A hitchhiker's guide to the human Hsp70 family. – Cell Stress Chaperones, **1**(1), 1996, 23-28.
10. **Welch, W.** Mammalian stress response: cell physiology, structure/function of stress proteins, and implications for medicine and disease. – Physiol. Rev., **72**(4), 1992, 1063-1081.
11. **Xu, M., W. Wright, R. Higashikubo, J. Roti.** Intracellular distribution of hsp70 during long duration moderate hyperthermia. – J. Int. Hypertherm., **14**(2), 1998, 211-225.

Institute of Experimental Morphology, Pathology and Anthropology with Museum
Bulgarian Anatomical Society

Acta morphologica et anthropologica, 22
Sofia ● 2015

*Anthropology and Anatomy*

# Paleopathological Changes in the Human Postcranial Skeletal Remains from the Necropolis in the Locality of Saint Spas, in the Varosh Quarter, Town of Pernik, Western Bulgaria (15th-19th Centuries)

*N. Atanassova-Timeva, B. Galabova*

*Institute of Experimental Morphology, Pathology and Anthropology with Museum, Bulgarian Academy of Sciences, Sofia, Bulgaria*

Rescue archaeological excavations were undertaken in the locality of St. Spas situated in the Varosh Quarter, town of Pernik in 2003 and 2004. A sector of wide necropolis was examined, which had been in use within the periods of the 11th-12th and the 14th-19th c. The 2014 field season excavated fifty-one burial pits with inhumation, dated in 15th-19th c. Bone remains of a total eighty-seven individuals were identified. The aim of present study comprised identifying the age and sex of buried and the pathological changes on postcranial skeletal in the series of the necropolis. The percentage distribution between adults and subadults is almost equal but children in early childhood prevail. Pathological changes were observed in 31.51% of the postcranial skeletons: 65.22% were males, 30.43% were females and 4.35% unsexed individuals (a child). Fractures, arthritis, pathology on the limbs, vertebral pathology, ossified insertionitis and *myositis* were registered.

*Key words*: paleopathology, palaeoanthropology, necropolis, human postcranial skeletal remains.

## Introduction

Rescue archaeological excavations were undertaken in the locality of St. Spas situated in the Varosh Quarter, town of Pernik in 2003 and 2004 under the direction of Vasilka Paunova from the Regional Historical Museum - Pernik. During the field work it was ascertained that this localization had been considered a holy place for centuries. Here, three churches had existed which were situated in cultural layers one above the other – Early Christian from the 6th c. AD, Late Medieval and from the beginning of 20th c. (a chapel). A sector of wide necropolis was examined around them, which had been in use within the periods of the 11th-12th and the 14th-19th c. [19].

The 2014 field season excavated fifty-one burial pits with inhumation, dated in 15th-19th c. Most of them are used repeatedly or overlap each other. People were buried

directly in the ground as in some cases stones of various sizes were placed along the periphery of bottom of gravel pit. Small coals were discovered in all graves. All buried were placed in supine position (lying on the back). Many different positions can be observed for upper limbs: they can lie both along the sides, or one along the side (equally left or right) and one on the chest or on the pelvis; also hands can be crossed on the chest or on the pelvis. The lower limbs are usually outstretched. The majority of the skeletons are placed in northwest-southeast orientation [20].

## Materials and Methods

The study includes bone material unearthed in 51 graves from the excavation season 2014. Bone remains of a total eighty-seven individuals were identified. The skeletal remains are in good condition. Their cortical layers are well preserved. Despite the good condition of the bones, there are completely preserved skulls only in six individuals.

The anthropological analysis was carried out in the laboratory of the National Anthropological Museum at the Institute of Experimental Morphology, Pathology and Anthropology with Museum – BAS. The analysis of the human skeletal remains followed procedures defined by Martin–Saller [9], Алексеев [15, 16], Герасимов [17], Simpson, Olivier [16], Kühl [7], Bass [2], Facchini, Veschi [5].

Sex and age at death were estimated using standard non-destructive procedures and are divided into two groups – for immature and for adults. Skeletal remains have been classified into six general age groups: Early childhood (*Infans* I) – 0-7 years; Late childhood (*Infans* II) – 7-14 years; Adolescence (*Juvenis*) – 14-18/20 years; Adults (*Adultus*) – 20-40 years; Matures (*Maturus*) – 40-60 years; Elderly (*Senilis*) – over 60 year.

For the immature group age at death, dental formation and eruption [6, 15] were utilised whenever possible. Other criteria included bone development [2, 5]. Main data used to estimate adult age at death included morphology of the pubic symphysis [14] and the ossification of cranial sutures [6, 10, 14, 16]. Epiphyseal union, dental attrition and other [3, 1] general age indicators [2, 4, 6] were also used.

When possible, sex was determined from pelvis morphology (the shape of *incisura ischiadica major*), the value of the pubic angle, pelvic inlet shape (*foramen obturatum*), the breadth and length of the sacrum (*os sacrum*). When the pelvis was not available or was too fragmentary for use, the size of other bones and cranial elements (development of supercilary arches (*arcus superciliaris*) and *glabella*, the shape of orbital edge and the bottom view of the lower jaw [2, 4, 7, 8, 13] were used.

During anthropological analysis some pathological changes and natural variation were noticed: fractures, arthritis, pathology on the limbs, vertebral pathology, *spina bifida*, etc. All diagnoses of pathological conditions followed the recommendations of important clinical journals, books and paleopathological texts [1, 8, 11, 12].

Tooth wear (*abrasio*) is the term used to describe the progressive loss of a tooth's surface due to actions other than those which cause tooth decay or dental trauma. Tooth wear increases with age. In the archaeological researches dental attrition is an aging indicator and of dietary behaviors and/or health problems in earlier human populations [3, 17].

## Results and Discussion

The aim of present investigation comprised identifying the age and sex of buried and the pathological changes on postcranial skeletal in the series of the necropolis in locality of St. Spas, Varosh Quarter, town of Pernik (15$^{th}$-19$^{th}$ c.).

## Age at death estimation

The eighty-seven individuals excavated in the necropolis in Varosh Quarter, town of Pernik were classified into six age groups based on anthropological analysis: thirty-two individuals are in **early childhood group (*Infans* I**); ten individuals are identified in **late childhood (*Infans* II)**; three were **Juveniles (*Juvenis***); fourteen were **Adults (*Adultus***); twenty-one of them were **Matures (*Maturus***) and three are in **elderly** group (**Table 1**).

**Table 1.** Age distribution of buried in the excavated graves from the necropolis in locality of St. Spas, Varosh Quarter, town of Pernik, season 2014

| **Infans I** | **N** | **Infans II** | **N** | **Juvenis** | **N** | **Adultus** | **N** | **Maturus** | **N** | **Senilis** | **N** | **Adultus +** | **N** | |
|---|---|---|---|---|---|---|---|---|---|---|---|---|---|---|
| Fetus | 2 | 7–8 y | 3 | 14–15 y | 0 | 20–25 y | 6 | 40–45 y | 2 | 60–70 y | 3 | | 4 | |
| 0–6 m | 4 | 8–9 y | 2 | 15–16 y | 0 | 25–30 y | 2 | 45–50 y | 9 | | | | | |
| 6m–1y | 3 | 9–10 y | 1 | 16–17 y | 0 | 30–35 y | 3 | 40–50 y | 1 | | | | | |
| 1–2 y | 7 | 10–11 y | 2 | 17–18/20 | 3 | 35–40 y | 3 | 50–55 y | 5 | | | | | |
| 2–3 y | 3 | 11–12 y | 1 | | | | | 55–60 y | 3 | | | | | |
| 3–4 y | 5 | 12–13 y | 1 | | | | | 50–60 y | 1 | | | | | |
| 4–5 y | 1 | 13–14 y | 0 | | | | | | | | | | | |
| 4–6 y | 1 | | | | | | | | | | | | | |
| 5–6 y | 0 | | | | | | | | | | | | | |
| ≈ 6 y | 2 | | | | | | | | | | | | | |
| 6–7 y | 2 | | | | | | | | | | | | | |
| Inf I | 2 | | | | | | | | | | | | | |
| **Total** | 32 | | 10 | | 3 | | 14 | | 21 | | 3 | | 4 | **87** |

Diagnostic bone fragments for more accurate age determination were not preserved in four adults individuals. Therefore, they are defined as individuals with uncertain age group (*Adultus* +).

The percentage distribution between adults and subadults is almost equal (48.28-51.72%) but children in early childhood prevail (**Fig. 1**).

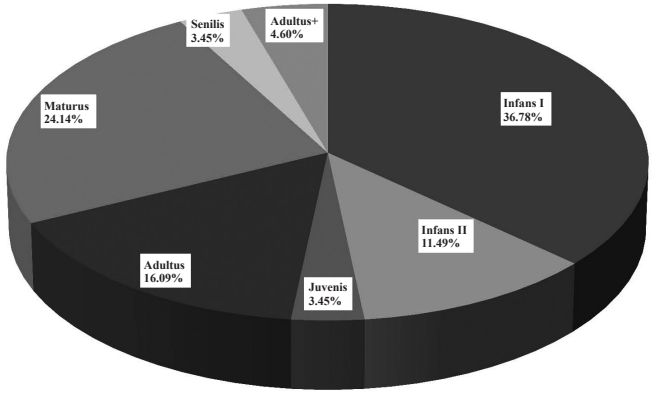


**Fig. 1.** Percentage of age groups from the necropolis in locality of St. Spas Varosh Quarter, season 2014

## Sex determination

Sex is determined in 46 out of 87 individuals: 25 were male and 15 were female. Five individuals are determined probably as male and one probably as female, because the sexual characteristics are not clearly expressed and/or gender diagnostic bone fragments are not preserved. In one case because of the lack of diagnostic fragments the sex of the individual is undetermined.

The age and sex distribution of the St. Spas skeletal sample is as follows: thirty-two individuals are in early childhood group; a female child, one probably male child and eight with undetermined sex in late childhood group; two male and a female in Juvenile group; four male, two probably male, six female, one probably female and one with undetermined sex in *Adultus* group; sixteen male, one probably male and four female in mature group and three female in elderly group. In the group of adults with undetermined age there are three male and one probably male (**Table 2**).

**Table 2.** Sex and age distribution of buried in the excavated graves from the necropolis in locality of St. Spas, Varosh Quarter, town of Pernik, season 2014

| **Age group** | | | | | | | | | | | | | | | | | | | | | **Total** |
|---|---|---|---|---|---|---|---|---|---|---|---|---|---|---|---|---|---|---|---|---|---|
| **Infans I** | **Infans II** | | | **Juvenis** | | **Adultus** | | | | | **Maturus** | | | | **Senilis** | | | **Adultus+** | | | |
| | ♂? | ♀ | ♂♀ | ♂ | ♀ | ♂ | ♂? | ♀ | ♀? | ♂♀ | ♂ | ♂? | ♀ | ♂♀ | ♂ | ♀ | ♂♀ | ♂ | ♂? | ♀ | |
| 32 | 1 | 1 | 8 | 2 | 1 | 4 | 2 | 6 | 1 | 1 | 16 | 1 | 4 | – | – | 3 | – | 3 | 1 | – | **87** |

## Pathologies and traumas

The postcranial skeletons are preserved in 73 individuals (83.91%) (**Table 3**).

Pathological conditions were observed in 31.51% of the skeletal remains: 65.22% were males, 30.43% were females and 4.35% undetermined individuals (children).

**Table 3.** Pathological changes of buried in the necropolis in locality of St. Spas, Varosh Quarter, town of Pernik, season 2014

| Disease | N (number of individuals) | Percentage distribution |
|---|---|---|
| Destructive-degenerative diseases of the spine | **17** | **23.29%** |
| Degenerative-destructive diseases of the limbs | 12 | 16.44% |
| Insertionitis | 8 | 10.96% |
| Traumas | 4 | 5.48% |
| Myositis ossificans | 3 | 4.11% |
| Ankylosis | 3 | 4.11% |
| Osteochondrosis | 2 | 2.74% |
| *Spina bifida* | 1 | 4.35% |
| Rickets | 1 | 1.37% |

In both sexes destructive-degenerative diseases of the spine were the most common pathology registered in 23.29% (17 individuals). This pathology is typical for buried in mature and elderly, and was identified at only one individual in the age group *Adultus*. Eleven of males and six of females suffered from vertebral arthritis with different degrees of seriousness, from initial degradation to very severe damages. It should be noted that destructive-degenerative diseases of the spine occur in almost all females (85.71%) over 40 years (**Fig. 2**).

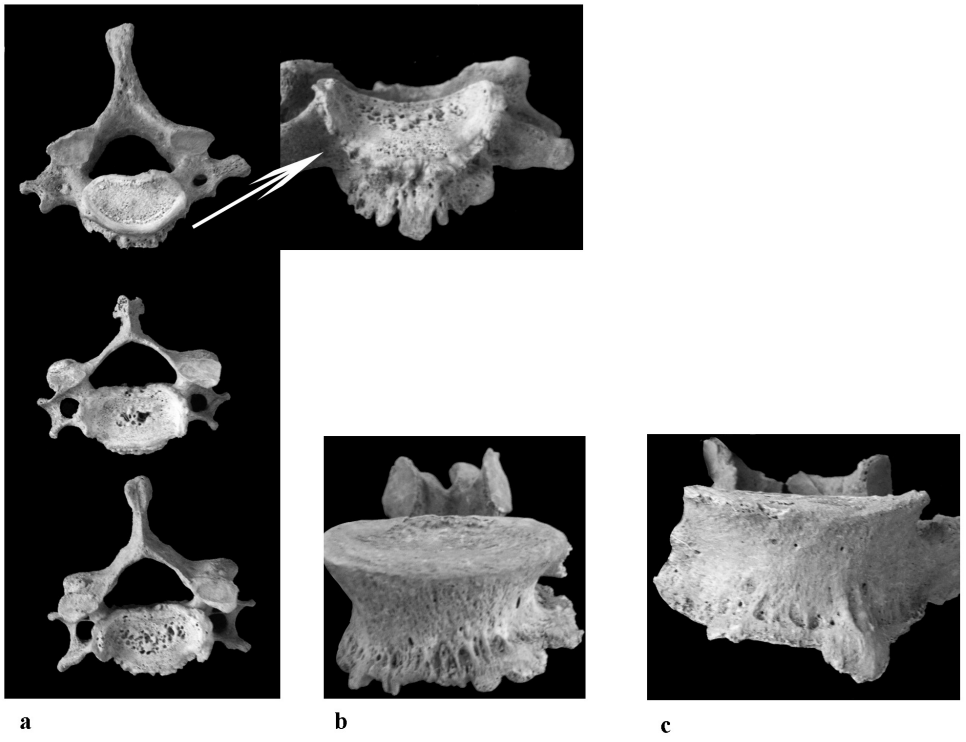


**Fig. 2.** Destructive degenerative diseases of the spine: a) 50-55-year-old female*;* b) 55-60-year-old male; c) 45-50-year-old male

The distribution of degenerative-destructive diseases of the limbs between male and female is equally (6 individuals of both genders). This type of pathology was not observed in any individual under 40 years. A high percentage of buried women were affected by a different type of arthritis on the limbs. It could be explained by the heavy physical labor (**Fig. 3**).

Ossified insertionitis represents dystrophic disease affecting mostly muscle-ligament areas of bone. These are sites of stress concentration at the region where tendons and ligaments attach to the bone. Consequently, they are commonly subject of overuse injuries (enthesopathies), physical overexertion or excessively strong movements received by hard work, sports etc. The ossified insertionitis is documented at a total of eight individuals including seven men and only one woman. This type of bone changes are identified in the buried in the age range 40 to 60 years, with the exception of a young male aged 20-25 years at death (**Fig. 4**).

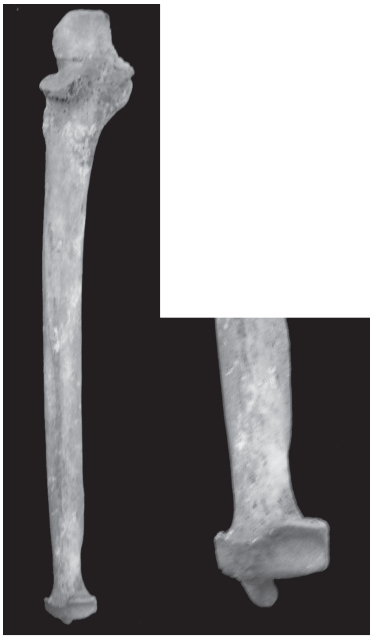

**Fig. 3.** Degenerative-destructive diseases of the upper limb – 55-60-year-old male

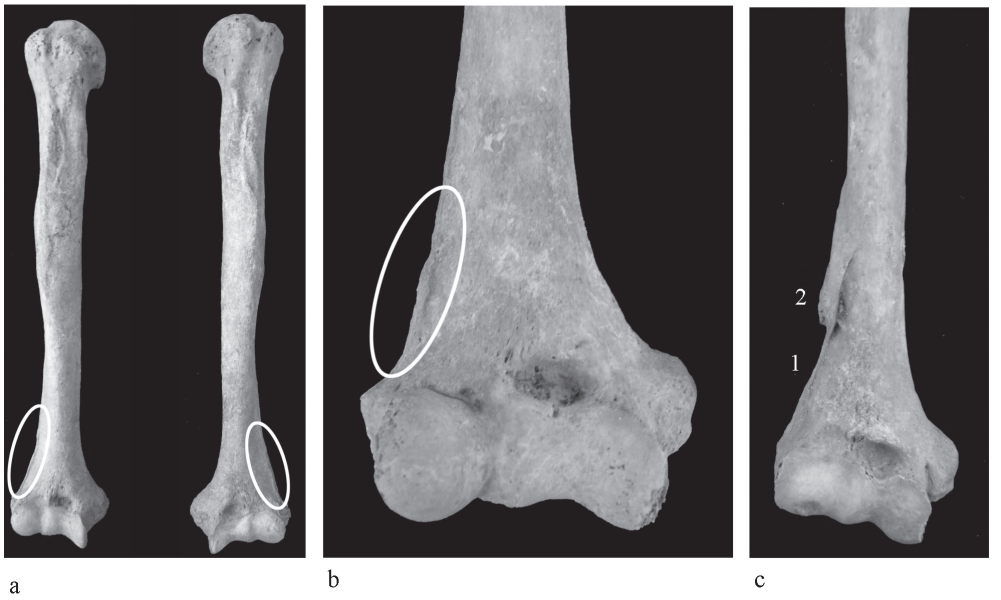


**Fig. 4.** Insertionitis on the upper limbs: a) 50-55-year-old male; b) 60-70-year-old female; c) 55-60-year-old male

Myositis ossificans is an unusual condition that often occurs in people who sustain a blunt injury that causes deep tissue bleeding. The soft-tissues that were injured in the traumatic event initially develops a hematoma, and subsequently develop the myositis ossificans. The myositis ossificans means that bone forms within the muscle, and this occurs at the site of the hematoma. Myositis is detected in three individuals from necropolis in locality of St. Spas. (**Fig. 5**).

Traumatic marks on bones from postcranial skeleton are also identified only in male skeletons (**Fig. 6**).

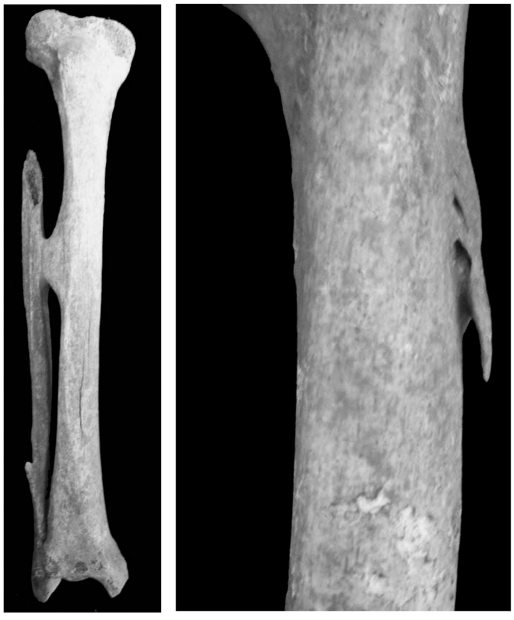


**Fig. 5.** Myositis: a) on the tibia et fibula dextra in 50-55-year-old male; b) on the femur dexter in 55-60-year-old male

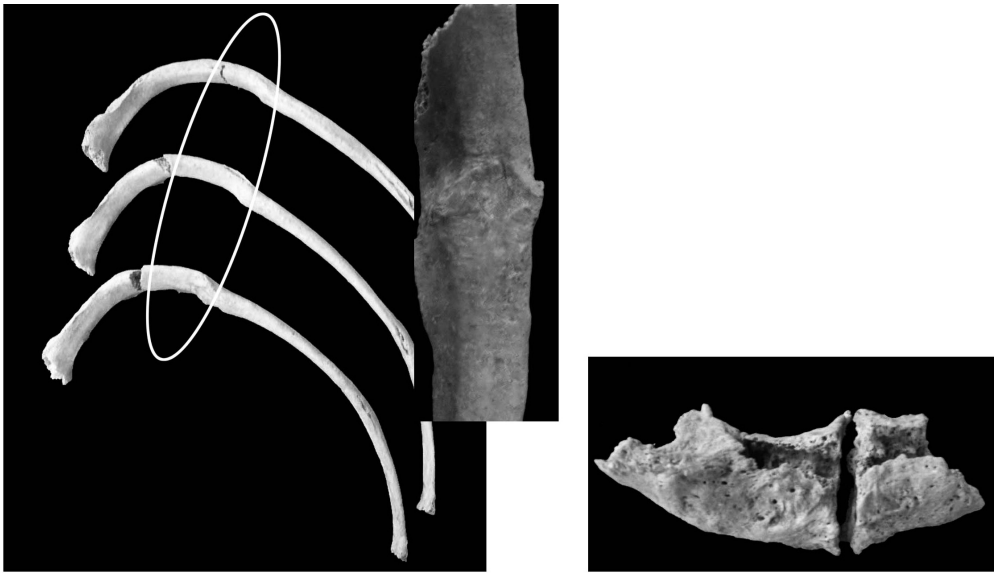

**Fig. 6.** Trauma on the ribs – 50-55-year-old male

## Conclusion

This report on 87 studied individuals gives information about burial rituals, anthropometry and paleopathology and it must be considered preliminary until the end of the systematic excavation in the necropolis.

Results of anthropological analysis of the necropolis from locality of St. Spas, Varosh quarter, town of Pernik, strongly suggest a high mortality rate in the early childhood and mostly in the age range of 1-2 years. This fact most probably could be explained by systematic infections that children were exposed to (for example cholera, smallpox etc.), possibly because of immunity weakened by malnutrition, poor medical care as well as low life standards.

The children in early childhood had a weak immunity, so only the strongest survived who in most cases lived through the late childhood and adolescence (in these age groups in the studied necropolis mortality decreased sharply).

What makes an impression in adult individuals is the large number of female, for which death occurred in the range between 20 to 30 years. This is the active childbearing age and higher mortality for the young women could be associated with problems during the pregnancy, childbirth and postpartum period as well as the large number of successive births. In the necropolis were discovered skeletal remains of a pregnant woman.

Pathological changes in the postcranial bones, a result of various diseases, including injuries, were identified mainly in buried in mature and elderly age groups, as the most affected have been male individuals.

## References


1. **Aufderheide, A. C., C. Rodríguez-Martín.** The Cambridge Encyclopaedia of Human Paleopathology. Cambridge University Press, Cambridge, 1989.
2. **Bass, W.** Human Osteology: A Laboratory and Field Manual. Special Publication, 2. The Missouri Archaeological Society, 5th edition, 2005.
3. **Barthwell, D. R.** Digging up bones. Ithaca, New York: Cornell University Press, 1965.
4. **Buikstra, J. E., D. H. Ubelaker.** Standards of data collection from human skeletal remains. – Arkansas Archaeological Survey Research Series, 44, Fayetteville, 1984.
5. **Facchini, F., S. Veschi.** Age Determination on Long Bones in a Skeletal Subadults Sample (b – 12 Years). – Collegium Antropologicum, **28**(1), 2004, 89-98.
6. **Ferembach, D., I. Schwidetzky, M. Stloukal.** Recommendations for age and sex diagnosis of skeletons. – J. Hum. Evol., **9**, 1980, 517-549.
7. **Kühl, I.** Skelettreste aus prähistorischen Brandbestattungen und ihre Aussagemöglichkeiten, mit Hinweisen auf spezielle Fragestellungen in Schlesvig-Holstein. – Mitteilungen der Anthropologischen Gesellschaft in Wien, 15, 1985, 113-137.
8. **Mann, R., D. Hunt.** Photographic regional atlas of bone disease. A guide to pathologic and normal variation in the human skeleton. Charles Thomas Publisher Ltd., Illinois, 2005.
9. **Martin, R., K. Saller.** Lehrbuch der Anthropologie in sistematischer Darstellung, Band I. G. Fischer, Stuttgart, 1957.
10. **Meindl, R., C. Lovejoy.** Ectocranial suture closure: a revised method for the termination of skeletal age at death based on lateral-anterior sutures. – American Journal of Physical Anthropology, 68, 1985, 57-66.
11. **Merbs, C. F. Trauma.** In: Reconstruction of Life, Iscan M. Y., Kennedy, K. (eds). Alan R. Liss, New York; 1989, 161-189.
12. **Ortner, D. J., J. Putschar.** Identification of pathological conditions in human skeletal remains. Smithsonian Institution Press, Washington, 1981.
13. **Todd, T. W.** Age changes in the pubic bone I: the male white pubis. – American Journal of Physical Anthropology, 3, 1920, 285-334.

14. **Valois, H. V.** L'omoplate humaine: Étude anatomique et anthropologique. – Bulletins et Mémoires de la Société d'Anthropologie de Paris, **3**, 1932, 3-153.
15. **Алексеев, В.** Остеометрия. Методика антропологических исследований. Москва, 1966.
16. **Алексеев, В., Г. Дебец.** Краниометрия. Методика антропологических исследований. Москва, 1984.
17. **Герасимов, М.** Восстановление лица по черепу. – ТИЭ, 25, 1955.
18. **Зубов, А.** Одонтология. Москва, 1968.
19. **Паунова, В.** Археологическо проучване на църкви № 9 и № 10 в подножието на хълма Кракра в град Перник (XIV–XX век), с. 120–138.
20. **Паунова, В.** Раннохристянска базилика, късносредновековен и възрожденски некропол в м. Св. Спас, кв. Варош, гр. Перник. – Археологически открития и разкопки през 2014 г. София, 2015, 742–744.

Institute of Experimental Morphology, Pathology and Anthropology with Museum
Bulgarian Anatomical Society

Acta morphologica et anthropologica, 22
Sofia ● 2015

# Psoriasiform Keratosis – a Case Report

*V. Broshtilova [1], V. Mihailova [2], M. Gantcheva [3]*

*[1]Department of Dermatology and Venereology, Faculty of Medicine, Sofia Medical University, Sofia, Bulgaria*
*[2] Department of Dermatology and Venereology, Tokuda Hospital Sofia, Sofia, Bulgaria*
*[3] Institute of Experimental Morphology, Pathology and Anthropology with Museum, Bulgarian Academy of Sciences, Sofia, Bulgaria*

Psoriasiform keratosis is a unique clinico-pathological entity which was first reported in 2007. To date, no more than 30 cases have been reported worldwide. The condition is presented by a solitary keratotic papule or plaque with typical psoriasis histology. Obligatory, the patients have no pre-existing and current skin changes suggestive for psoriasis. We describe a 43-year-old man with a single scaly yellow-to-gray lesion localized to his body. Focal psoriasiform inflammatory pattern was found on routine histology. He claimed to have no personal or family history of psoriasis. Based on patient's history and clinical manifestation we raise the hypothesis that psoriasiform keratosis should be considered a lesion sui generis rather than a rudimentary manifestation of psoriasis.

*Key words:* psoriasis, keratosis.

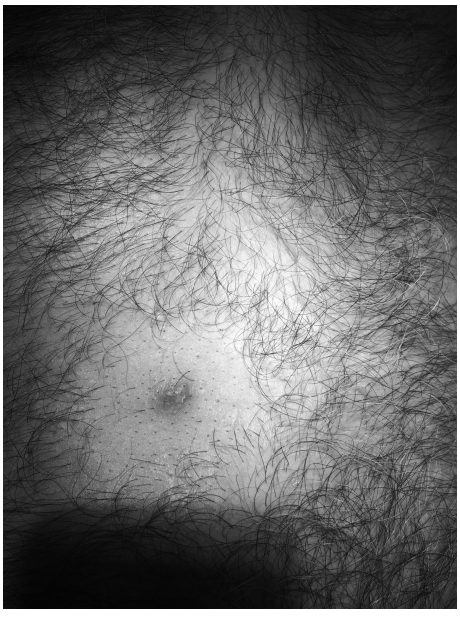

**Fig. 1.** A scaly erythematous papule with elevated borders

## Introduction

In 2007 Walsh et al. [5] described a new entity that clinically represents a solitary scaly, erythematous plaque, which showed histological features of psoriasis [5]. The term "psoriasiform keratosis" was coined for these peculiar lesions, which seem to be exceptionally rare. To date, no more than 30 cases have been reported worldwide. Herein, a male patient with psoriasiform keratosis, localized on the body, is described.

### *Case Report*

A 43-year-old Caucasian man complaining of a small lesion on his presternal zone with a 3-week duration. The lesion was intermittently itchy, and grew peripherally at

a very slow pace. The patient had neither personal nor family history of psoriasis. On physical examination a single one-centimeter in diameter erythematous scaly papule with elevated borders was presented (**Fig. 1**). Antibiotic and mild-potent corticosteroid preparations were used with no effect for the last 3 weeks. Mycological and bacterial cultures were negative. Histopathological examination showed papillomatosis, psoriasiform acanthosis, focal agranulosis, vacuolated and pale superficial keratinocytes and

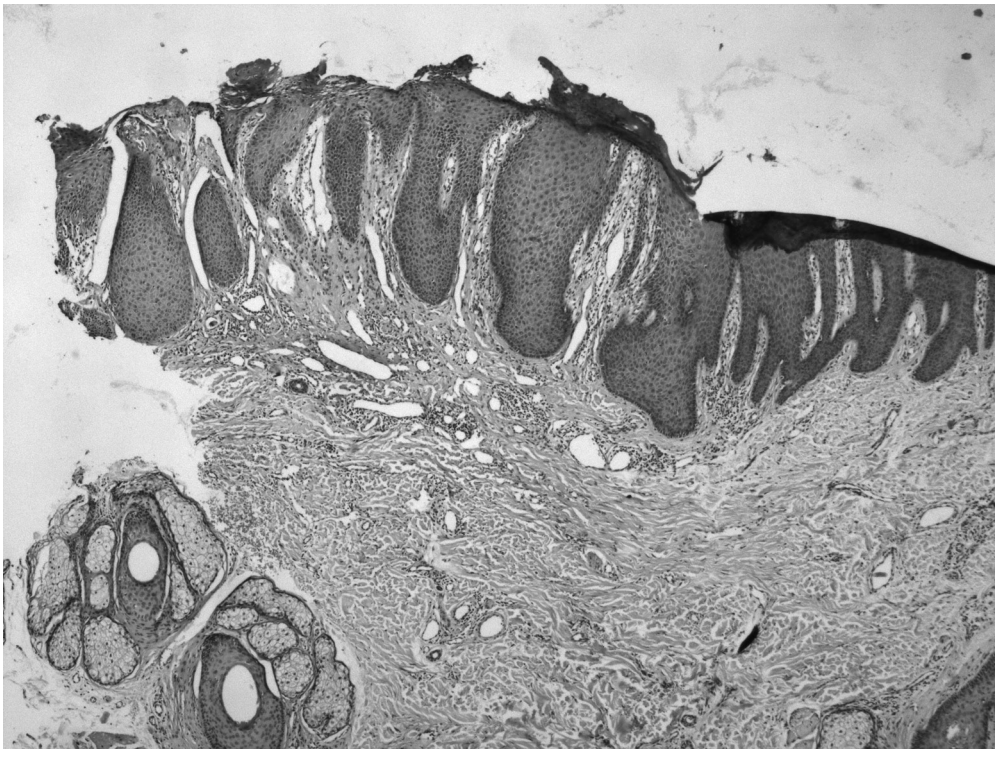

**Fig. 2.** Focal parakeratosis, lack of granular cell layer, psoriasiform acanthosis, reduction of suprapapillary segments (HE × 100)

suprapapillary epidermal atrophy (**Fig. 2**). No atypical keratinocytes were present. The papillary dermis was filled-in with mild perivascular lymphocytic infiltrate. Ectatic capillaries were seen in the subepidermal segment of the dermis. Based on the clinical and histology findings the diagnosis of psoriasiform keratosis was concluded. The patient was advised to undergo a radical excision, which was scheduled duly.

## Discussion

Psoriasiform keratosis is a rare clinic entity. It is characterized by solitary, scaly keratotic papule, or plaque mainly located on the extremities. Other sites that can be involved are scalp, neck, shoulders, and back [3]. Usually the lesions evolve in 6 to 7 months. They can be associated with burning sensation, itch or mild pain. All patients are in good general health. Slight men preponderance is noticed. There is no personal or family history of psoriasis. The etiopathogenesis of the disease remains unknown.

Clinically, most lesions are averagely less than one centimeter. They are dome-shaped, scaly and yellow-to-gray. The diagnosis is based on histopathological findings, which are unrecognizable from psoriasis. Focal segmental parakeratosis, lack of granular cell layer, regular acanthosis and suprapapillary reduction is typical for the disease. Sometimes neutrophilic microabscesses and Kogoj pustules can be found. Vascular dilatation and lymphocytic chronic inflammation are usually present in the superficial dermis. Periodic acid-Schiff (PAS) stain should be performed to rule out yeast or dermatophyte infection [1]. Recently, human papilloma virus 6 was verified by tissue polymerase chain reaction in a 74-year-old woman with a typical psoriasiform keratosis on the left arm [4]. Interestingly, this finding did not correspond to any nuclear inclusion bodies or specific koilocytes in the epidermis of the tissue samples on routine HE staining

Psoriasiform keratosis is usually refractory to topical modalities [2]. Destructive chemical substances are not useful, together with electrodesiccation and cryotherapy. Radical surgical excision is a first-line therapy with minimal relapse rate.

In conclusion, we described the first case of psoriasiform keratosis in Bulgaria. The lesion shows very rare localization and typical therapeutic resistance. Based on patient's personal history and clinical manifestation we believe psoriasiform keratosis should be considered a lesion sui generis rather than a rudimentary manifestation of psoriasis.

## References


1. **Carbone, A., C. De Simone, F. Valenzano, P. Amerio, G. Massi.** Psoriasiform keratosis. – J. Eur. Dermatol., **19**, 2009, 631-632.
2. **Mutasim, D.** Psoriasisform keratosis: A lesion mimicking psoriasis. – J. Am. Dermatopathol., **29**, 2007, 482.
3. **Pires, C., B. Sousa, C. Nascimento, M. Moutinho et al.** Psoriasiform keratosis – case report. – An. Bras. Dermatol., **89**, 2014, 318-319.
4. **Sezer, E., A. Boer, T. Falk.** Identification of human papilloma virus type 6 in psoriasiform keratosis. – J. Am. Dermatopathol., **32**, 2010, 492-494.
5. **Walsh, S., M. Hurt, D. Santa Cruz.** Psoriasiform keratosis. – J. Am. Dermatopathol., **29**, 2007, 137-140.

Institute of Experimental Morphology, Pathology and Anthropology with Museum
Bulgarian Anatomical Society

Acta morphologica et anthropologica, 22
Sofia ● 2015

# Characteristic on the Arterial Blood Supply of Dog Mammary Glands

*L. Hristakiev[1], G. D. Georgiev[1], G. I. Georgiev[1], E. Sapundzhiev[1], I. Raychev[2]*

*[1]Department of Anatomy, Histology and Physiology, Faculty of Veterinary Medicine, University of Forestry, Bulgaria*
*[2]Department of Surgery, Radiography, Obstetrics and Gynecology, Faculty of Veterinary Medicine, University of Forestry, Bulgaria*

Knowing the location of the arterial blood vessels and their eventual deviations is indispensable in teaching normal morphology, carrying out surgical procedures and angiography of the dog mammary glands. The purpose of this study was arterial supplying of the mammary glands in female dog species to be examined. Three bitches with approximately 15 kg body weight in diestrum condition were used during investigation. By anatomical section and preparation of the main blood vessels and injection of hardening substances or a gypsum solution, the specific blood vessels pathways, branches and features were traced. Simultaneously in comparative aspect standard orthogonal projections by contrast radiography were performed. The circulatory trace of subclavian and external pudendal arteries and their branches which predominantly supplied the mammary complexes were established and visualized and their characteristics are described.

*Key words:* dog, arteries, mammary gland, blood supply, radiography.

## Introduction

The bitch normally has five pairs of mammary glands. They are divided into three groups: thoracic (cranial and caudal), abdominal (cranial and caudal), and inguinal, respectively. There is a lack of morphological information about their blood supply in dog instead of productive species. In spite of this the mammary glands neoplastic processes are about 25-35% of all neoplasia which occur in dogs. According to this, knowing the location of the arterial blood vessels and their eventual deviations is indispensable in connection of carrying out surgical procedures and corresponding angiography of dog mammary glands. The investigation of mammary glands arterial supply in different dog species was the purpose of this study.

## Materials and Methods

Three adult female dogs with approximately 15 kg body weight in diestrum condition were used for examination. They previously were diagnosed as disadvantageous exit of accident or exhibited aggressive behavior.

Radiography by *"Eickemeyer Vet – E 7239X"* was performed on a first euthanized dog with use of barium sulfate as a contrast. After that the dog was dissected and the specific blood vessels of the mammary glands were traced.

Second dog was used for a corrosion cast of a. pudenda externa sinistra and a. thoracica interna dextra. The plastic solution – *"Duracryl (Spofa)"* was prepared according to manufacturer's recipe and injected with a syringe manually in the arteries.

Third dog was injected with gypsum solution through a. carrotis communis and after solidification the specific blood vessels of the mammary glands were traced.

The results from dissections were compared with radiography from the first dog.

## Results and Discussion

The internal thoracic artery according to Dyce et al. [1], supply ventral abdominal wall and part of the thoracic organs. It gives rami perforantes, which are branched to rami sternales, rami musculares and rami mammarii that exit through intercostal spaces. Close to diaphragm it gives musculophrenic artery and cranial epigastric artery and the last one gives a. epigastrica cranialis superficialis [1]. By radiography method we confirm that the common arterial supply of the cranial thoracic mammary glands arise from perforating branches of the a. thoracica interna, which gives mammary branches (**Fig. 1**).

These facts are also traced by corrosion cast and the blood vessels were presented (**Fig. 2**).

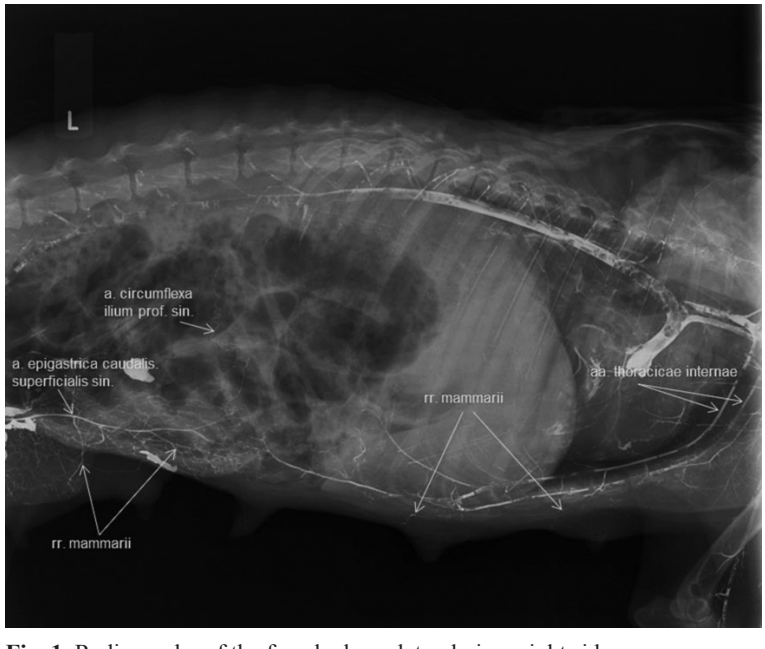


**Fig. 1.** Radiography of the female dog – lateral view, right side

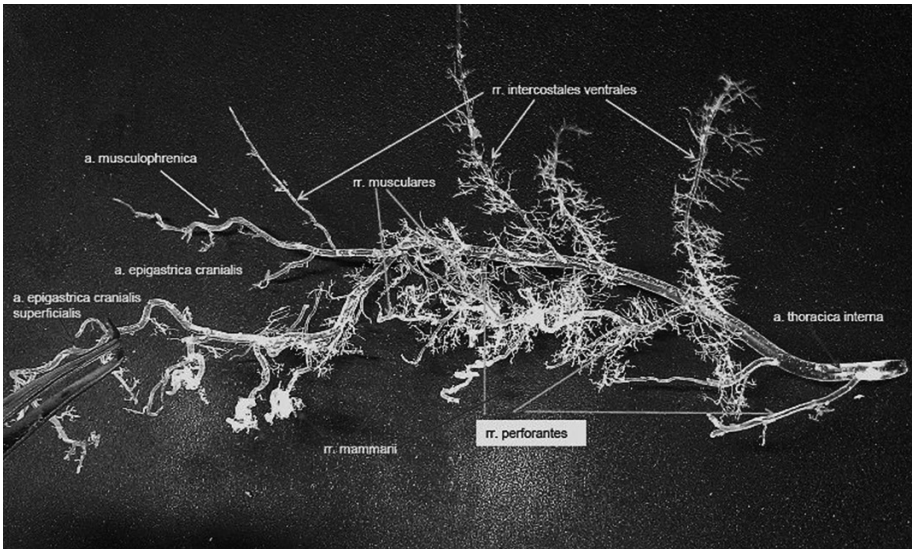


**Fig. 2.** Corrosion cast of a. thoracica interna dextra in dog

The lateral thoracic artery is a branch of axillar artery and supply thoracic wall distal to thoracodorsal artery. Dorsal intercostal arteries give lateral cutaneous branches for the lateral thoracic wall.

According to Silver [6], a. circumflexa ilium profunda plays important role of the caudal abdominal wall supply.

Arteria pudenda externa close to the superficial inguinal lymph nodes gives two branches, respectvely a. epigastrica caudalis superficialis and ramus labialis ventralis [1, 2, 3, 4].

On the cadaver sample it is also seen that the second thoracic complex is supplied from perforating branches of the internal thoracic arteries and rami mammarii from aa. intercostales dorsales (**Fig. 3A**).

The cranial and caudal abdominal complexes are supplied from a. epigastrica cranialis superficialis, which is weak in no lactating dogs. The artery makes anastomosis [1, 6] with superficial caudal epigastric artery, as they supply both the caudal pair of abdominal mammary complexes. According to Silver [6], abdominal complexes may receive blood from phrenicoabdominal arteries. In investigated dogs we did not observed this fact.

We have confirmed that dorsal intercostal arteries (VII-XII) supply caudal thoracic and cranial abdominal complexes, thus were traced $6^{th}$, $7^{th}$ and $8^{th}$ dorsal intercostal arteries (**Fig. 3B**). The cranial mammary complexes are also supplied from branches from a. thoracica lateralis what is visible on the native sample (**Fig. 4**) and this artery we have seen that supply the periphery parts and skin area of the glands. We observed that lateral thoracic artery gives well distinct blood vessels towards mammary glands as seen on gross dissection. We supposed that these branches are well developed in lactating bitches because our model was previously in this condition. The lateral thoracic artery is visualized also on the radiograph.

Caudal abdominal complexes are supplied from a. epigastrica caudalis superficialis which originates from a. pudenda externa. The artery gives rr. mammarii to the caudal abdominal and inguinal glands (**Fig. 5**).

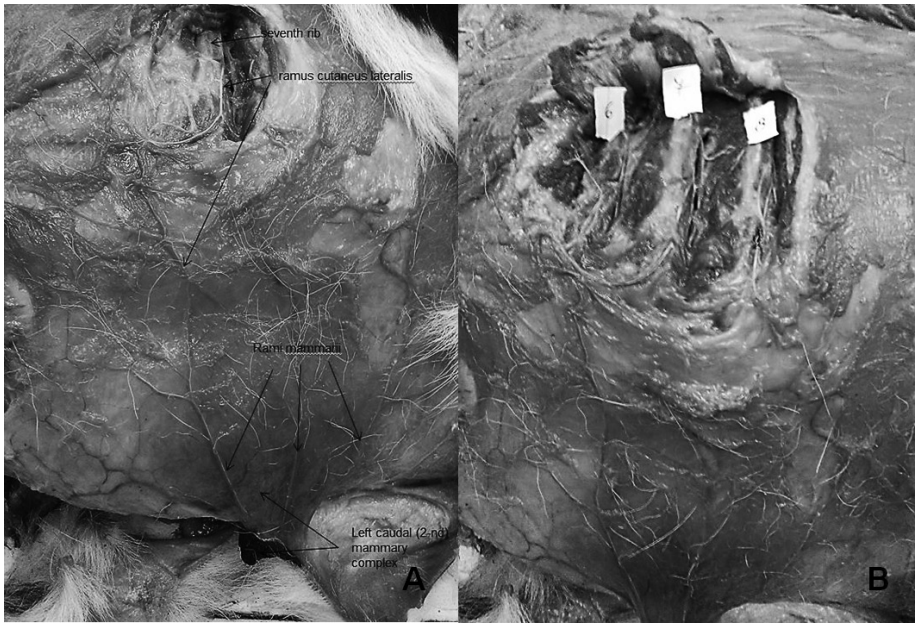


**Fig. 3. A –** Native sample, caudal abdominal mammary gland, lateral view. **B** – Native sample, caudal abdominal mammary gland, lateral view. The number of the ribs are written on small pieces of paper

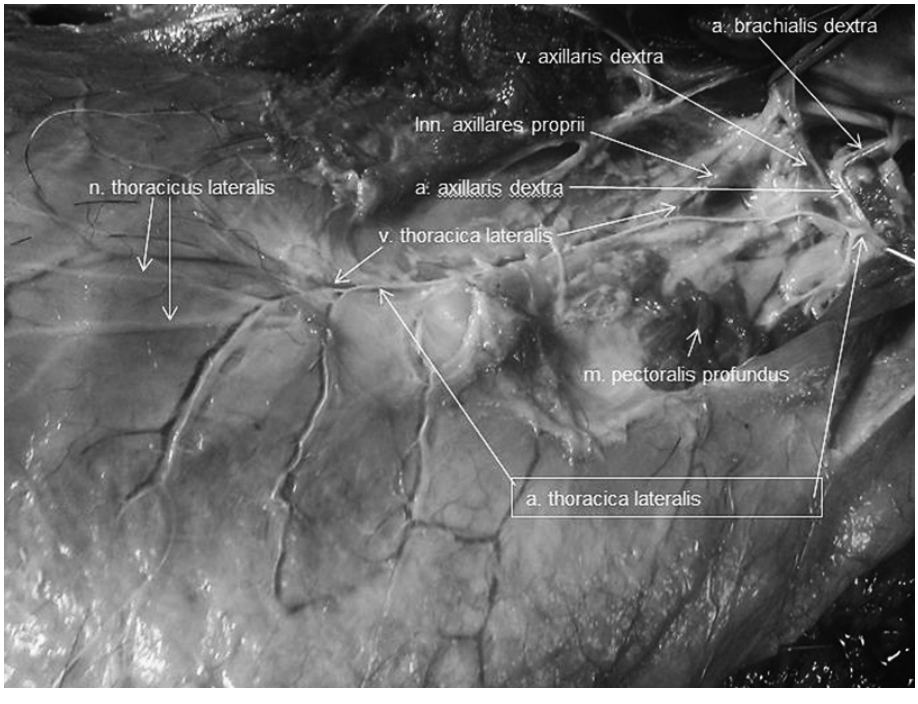


**Fig. 4.** Dissection of a right thoracic wall of a dog. Lateral view

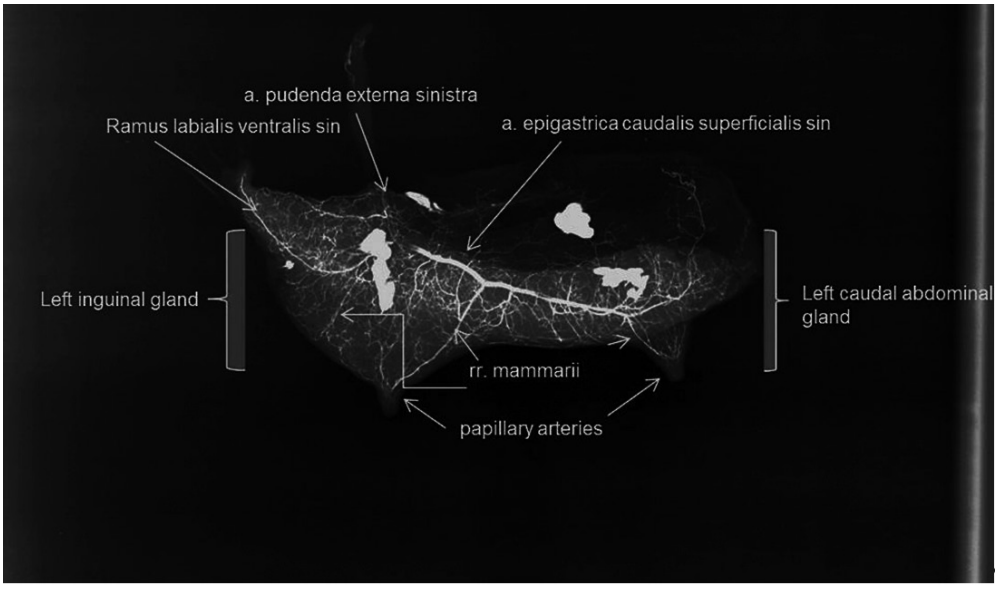


**Fig. 5.** Contrast radiography of mammary gland in dog (left inguinal and caudal abdominal glands). Lateral view

Silver [6] wrote that a. circumflexa ilium profunda contribute to the blood supply of caudal abdominal mammary complex. We confirm that this artery with its caudal branches gives subcutaneous ventral ramifications, which are visualized on the radiograph.

The arterial supply of the inguinal mammary glands is derived from branches of a. pudenda externa as it is seen on the radiographs (**Fig. 5**). There is a branch from a.epigastrica caudalis superficialis that directly goes into the inguinal mammary glands. In each part of the mammary complex it was established that there are between 5-7 main mammary branches. They converge and make vascular circle network which is arteriolar, because the diameter of these vessels is smaller. This is located on the base of the mammary teat. From that network 4-7 straight papillary arterioles are branched and directed toward the tip of the teat.

## Conclusion

The parenchyma of mammary glands receives their main blood supply from perforating branches which arise from a. thoracica interna also from the mammary branches of a. epigastrica cranialis superficialis and a. epigastrica caudalis superficialis. The mammary complexes receive also additional blood supply from a. thoracica lateralis, aa. intercostales dorsales and a. circumflexa ilium profunda. Additional arterial supply is related to the skin and periphery of the glands.

The mammary teats are supplied from vascular network situated on the base of papilla mammaria and it gives several straight branches directed toward the teat apex.

## References


1. **Dyce, K., W. Sack, C. Wensing.** Textbook of veterinary anatomy. – 4th edition, Saunders, Elsevier, 2010.
2. **Evans, H. and A. de Lahunta.** Miller's anatomy of the dog. – 4th edition, Elsevier, 2013
3. **Konig, H., H. Liebich.** Veterinary anatomy of domestic mammals, 2004.
4. **Miller, M., G. Christensen, H. Evans.** Anatomy of the Dog. W. B. Saunders Company, 1964.
5. **Schaller, O.** Illustrated veterinary anatomical nomenclature. – 2nd edition, Enke Verlag, Stuttgart, 2007.
6. **Silver, I. A.** Symposium on mammary neoplasia in the dog and cat – The anatomy of the Mammary Gland of the Dog and Cat. I, 1966.
7. **Ковачев, Г., Г. Георгиев, А. Воденичаров.** Анатомия на домашните животни. Том 3. Съдова, нервна система и сетивни органи. Стара Загора, Кота, 2010.

Institute of Experimental Morphology, Pathology and Anthropology with Museum
Bulgarian Anatomical Society

Acta morphologica et anthropologica, 22
Sofia ● 2015

# Extensor Indicis Brevis Muscle: Anatomical and Clinical Considerations

*A. Iliev[1], G. P. Georgiev[2*], I. N. Dimitrova[3], B. Landzhov[1]*

*[1]Department of Anatomy, Histology and Embryology, Medical University – Sofia, Bulgaria*
*[2]University Hospital of Orthopaedics "Prof. B. Boychev", Medical University – Sofia, Bulgaria*
*[3]Department of Cardiology, University Hospital "St. Ekaterina", Medical University – Sofia, Bulgaria*

During the routine anatomical dissection a rare muscular variant, the extensor indicis brevis muscle was observed of the left hand of an adult Caucasian male cadaver. The variant muscle originated from the joint capsule and ligaments of scaphoid and lunate ran across the third metacarpal and the second dorsal interosseous muscle and inserted as a single tendon to the ulnar side of the index extensor digitorum communis tendon. It was innervated by the posterior interosseous nerve. Different anatomical variations and the clinical importance of the aberrant muscle are also discussed.

*Key words:* extensor indicis brevis muscle, anatomical characteristics, clinical significance.

## Introduction

Variations of the extensor muscles and tendons of the hand are very common. They are often discovered incidentally during surgery. However, these variations rarely could be associated with clinical significance, especially when the variant muscle impinge and occupy the narrow dorsal compartments of the wrist. The knowledge of the existing muscular variations of the hand and is mandatory in cases of reconstructive surgeries planned in this region [1].

The extensor indicis brevis muscle (EIB) is a variant muscle found on the dorsum of the wrist and hand. This muscle is found in approximately 2% to 3% of the population with a slight male predominance and is easily mistaken for other dorsal hand pathology [2, 8]. This variant muscle has been described mostly in cadaver dissections and rarely in distinct clinical case reports mimicking dorsal wrist ganglions [3, 5, 6, 9, 12].

In this report, we describe a rare case of EIB, review the current literature and emphasize on its possible clinical significance.

## Case report

During a routine anatomical dissection, approved by the Medico-Legal Office and Local Ethic Committee, of the left upper extremity of a 69-year-old formol-carbol fixed

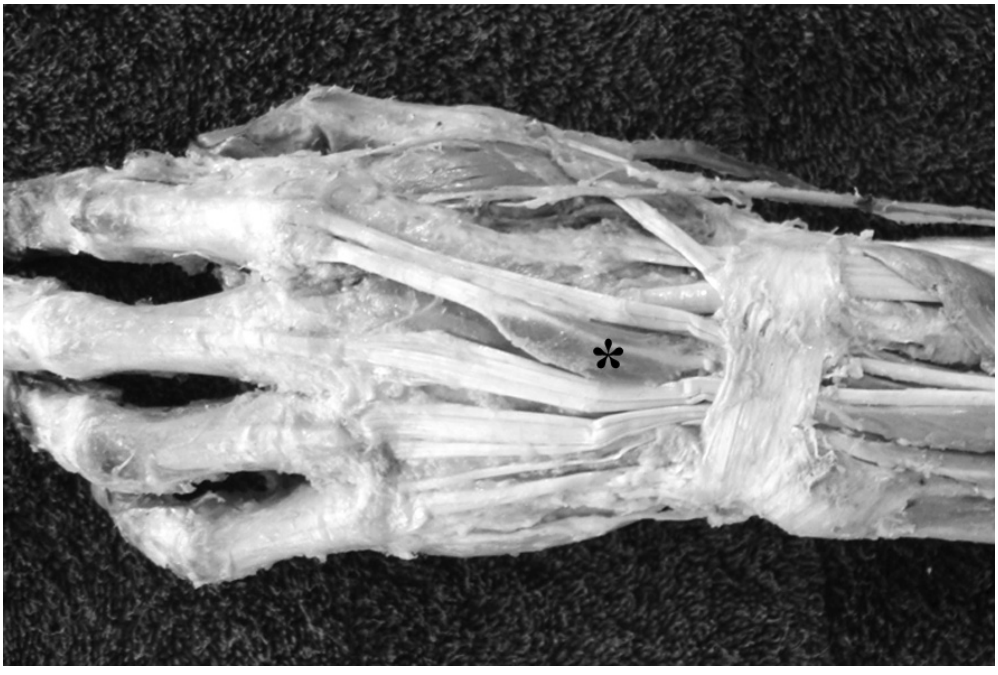

**Fig. 1.** Photograph of the extensor indicis brevis muscle (asterisk)

Caucasian male cadaver, from the autopsy material available at the Department of Anatomy, Histology and Embryology of the Medical University of Sofia, an unusual muscular variation was observed (**Fig. 1**). After the removal of the skin and superficial fascia, the extensor retinaculum was longitudinally opened to expose the dorsum of the hand. The variant muscle originated from the joint capsule and ligaments of scaphoid and lunate bones. It ran across the third metacarpal and the second dorsal interosseous muscle and inserted as a single tendon to the ulnar side of the index extensor digitorum communis tendon. The muscle belly was fusiform, 4.4 cm long and 0.55 cm wide. It was innervated by the posterior interosseous nerve and its blood supply was provided by the posterior interosseous artery. Due to its morphological characteristics, innervation, and apparent function we deem the muscle to be an EIB.

There is no information, concerning history of previous diseases for the dissected subject. No other clinical signs of trauma or surgical scars were noticed.

## Discussion

Despite the fact that the muscle and tendon variations on the dorsum of the hand and wrist are common, the variation of the EIB reported here, is relatively rare. In 1734, Albinus was the first to describe this muscular variation [6]. The main contribution to the popularization of the term EIB is Kadanoff [4]. It is also known as extensor digitorum brevis manus muscle [12]. The EIB is thought to be atavistic and a remnant from the amphibians. The digital joints of amphibians are entirely controlled by intrinsic muscles, and the EIB could represent a homologue of the extensor digitorum brevis on the dorsum of the foot [11].

The EIB generally consists of a single belly, but cases with two bellies with variable sizes also have been reported [8]. Different variations of the EIB have been described. It could arise from the distal end of the radius, the dorsal radiocarpal ligament, the wrist joint capsule, the dorsal metacarpal surface or from the extensor tendons. Different insertions to the middle finger; to the second and third fingers; to the ulnar side of the middle and ring finger; one to the middle and two slips to the fifth finger; to the second, third, and fourth fingers have also been described. The most common insertion of this muscle was into the index finger, followed by that into the middle finger, and those into the index and middle fingers. The nerve and blood supply of the EIB have been ensured by the posterior interosseous nerve and artery [3, 5, 6].

Ogura et al. [7] classified this variant muscle into three types based on its insertion and relationship with extensor indicis proprius (EIP). Type I –inserted onto the dorsal aponeurosis of index finger with absence of EIP. Type II – together with both EIP inserted on the index finger. Type III – EIP inserted on the index finger and EIB inserted on the long finger [7].

The muscular belly of the EIB commonly lies distal to the distal edge of the extensor retinaculum. Usually, the clinical examination reveals an elongated swelling in the proximal part of the dorsum of the hand, between the middle and index finger extensor tendons. In clinical case reports, the EIB is commonly misdiagnosed as a dorsal wrist ganglion [5, 6, 9]. In the case of Murakami and Todani, together with a dorsal wrist ganglion an EIB was found lying over the ganglion [5]. Slavchev and Georgiev, also described a case of a ganglion cyst within the extensor digitorum brevis manus muscle diagnosed by sonography in an eighteen-year-old girl [10]. In some cases the EIB could be asymptomatic, whereas in others it may cause pain and swelling of the dorsum of the hand, especially in heavy manual workers [5, 6, 9].

In differential diagnosis, the EIB could also simulate an exostosis, a tendon sheath cyst, tenosynovitis of extensor tendons, a hemangioma, rheumatoid tenosynovitis or a benign soft tissue tumor [6]. For differentiation of the EIB from a ganglion cyst, a detailed clinical examination could be of use. In a case of an anomalous muscle, it usually becomes more prominent with active extension of the wrist and fingers, while the ganglion cyst is better outlined by wrist flexion [1]. The new imaging techniques such as magnetic resonance imaging could clearly identify the variant muscle [6]. Sonography readily detects fluid-filled ganglion cysts but it requires substantial operator experience to reliably visualize fine structures like aberrant muscles of the hand [10].

Knowledge of these variants is not only important for differential diagnosis of doctors but also might eliminate a surgical procedure.

In conclusion, the EIB is a muscle structure without essential function for delicate movements of the hand. To know this anatomic variation is important for the upper limb specialist not only for surgical procedures at the level of the hand but also because its hypertrophy can cause incapacitating symptoms.

## References


1. **Cauldwell, E., B. Anson, R. Wright.** The extensor indicis proprius muscle. A study of 263 consecutive specimens. – Quart. Bull. Northwestern Univ. Med. School, **17**, 1943, 267–269.
2. **Coudert, X., A. Deghrar, G. Lavarde.** Supernumerary muscle on the dorsal surface of the hand. A case report. – Ann. Chir. Main Memb. Super., **12**, 1993, 230-232.
3. **Fernandez Vazquez, J., R. Linscheid.** Anomalous extensor muscles simulating dorsal wrist ganglion. – Clin. Orthop. Relat. Res., **83**, 1972, 84-86.
4. **Kadanoff, D.** Über die Erscheinungen des Umbildungsprozesses der Finger- und Zehenstrecker beim Menschen. – Gegenbaurs Morphol. Jahrb., **99**, 1958, 613– 661.

5. **Macalister, A.** Additional observations on muscular anomalies in human anatomy (third series), with a catalogue of the principal muscular variations hitherto published. – Trans. Roy. Irish Acad., **25**, 1875, 1-130.
6. **Murakami, Y., K. Todani.** The extensor indicis brevis muscle with an unusual ganglion. – Clin. Orthop. Relat. Res., **162**, 1982, 207-209.
7. **Ogura, T., H. Inoue, G. Tanabe.** Anatomic and clinical studies of the extensor digitorum brevis manus. – J. Hand Surg. Am., **12**, 1987, 100-107.
8. **Paraskevas, G., B. Papaziogas, S. Spanidou, A. Papadopoulos.** Unusual variation of the extensor digitorum brevis manus: a case report. – J. Eur. Orthop. Surg. Traumatol., **12**, 2002, 158-160.
9. **Rodríguez-Niedenführ, M., T. Vázquez, P. Golanó, I. Parkin, J. Sañudo.** Extensor digitorum brevis manus: anatomical, radiological and clinical relevance. A review. – Clin. Anat., **15**, 2002, 286-292.
10. **Slavchev, S., G. Georgiev.** Ultrasound diagnosis of a ganglionic cyst within an extensor digitorum brevis manus muscle. – Chir. Main, in press.
11. **Straus, W. L.** The phylogeny of the human forearm extensors. – Hum. Biol., **13**, 1941, 203-238.
12. **Voigt, C., H. Breyer.** The extensor indicis brevis muscle-a rare anatomic variant. A case example and critical review of the literature. – Handchir. Mikrochir. Plast. Chir., **21**, 1989, 276-278.

*Corresponding author:
*Georgi P. Georgiev, MD*
*University Hospital of Orthopaedics*
*Medical University, Sofia*
*56 Nikola Petkov Blvd.*
*1614 Sofia, Bulgaria*
*Tel.: +359 884 493 523*
*Fax: +359 29 555 312*
*E-mail: georgievgp@yahoo.com*

Institute of Experimental Morphology, Pathology and Anthropology with Museum
Bulgarian Anatomical Society

Acta morphologica et anthropologica, 22
Sofia ● 2015

# Qualitative Dermatoglyphic Traits in Twins

*I. Maslarski*

*Department of Human Anatomy, Histology and Pathology, Medical Faculty,*
*University of Sofia St. Kliment Ohridski, Bulgaria*

Palm and finger prints are an important element of the Twin Method, whereby we use both qualitative and quantitative indicators. It has been established with the qualitative indicators that the papillary image refers to polygenic hereditary characteristics, and that they are to be detected more easily than the quantitative ones. The main place in the study is the dermatoglyphic morphology of the hands, represented in two groups: monozygotic twins (MZ) and dizygotic twins (DZ). The material of the study included palm prints of both hands of 21 pairs of MZ twins and 22 pairs of DZ twins. Fingerprints and palms were obtained by a standard method. The Twin Method researches differences in MZ and DZ twins, using the "Similarity Method". Quantitative indicators demonstrate a relationship with zygosity, concerning the left and right hand.

*Key words:* monozygotic twins, dizygotic twins, twin method, total ridge count, ridge count triradii.

## Introduction

The Twin Method appeared due to the necessity of juxtaposing the genetic predisposition and the influence of one's environment. Already in 1875, Francis Galton [6] had made a series of experiments with twins to establish the extent of influence in environmental and genetic factors. He had prepared hundreds of questionnaires addressed to parents of the twins in order to achieve his goal and to understand the power of heredity. Nowadays, we can rely on findings from other disciplines, such as morphology, genetics and psychology, to explore the above-mentioned discourse and for our analysis to be more authentic.

Palm and finger prints are an important element of the Twin Method, whereby we use both qualitative and quantitative indicators. It has been established with the qualitative indicators that the papillary image refers to polygenic hereditary characteristics and that they are to be detected more easily than the quantitative ones (**Fig. 1**). The application and the development of the Twin Method, as well as of the finger-palm prints, leads to the advance of the following disciplines: medical genetics (used to establish a relationship between changed in skin relief and hereditary chromosomal diseases, as well as to determine the zygosity of twins), ethnic anthropology (used to establish a common origin of two separate groups of a population) and criminology (used to solve debatable questions, such as paternity rejection or identification of an individual).

Particularities of fingerprints have been noticed ever since the Ancient times The Chinese, for example, used their fingerprints instead of a stamp when validating docu-

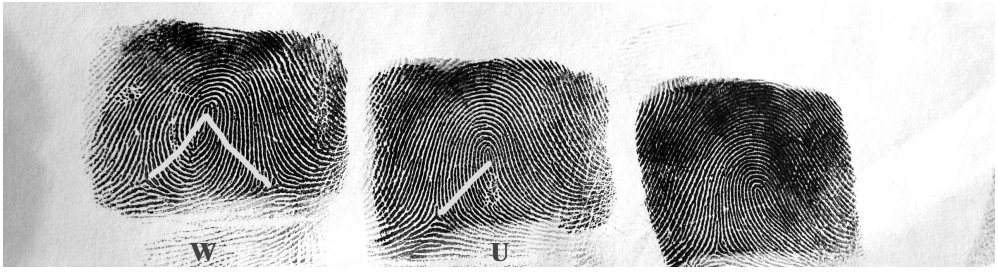


**Fig. 1.** Ridge count triradii of the fingers, W – whorl; U – ulnar loop; Line – ridge count triradii

ments. The use of friction ridge skin as a signature in China, Japan, India, and possibly in other states prior to European discovery is thus well documented. The German doctor and anatomist C. A. Mayer wrote: "Although the arrangement of skin ridges is never duplicated in two persons, never the less the similarities are closer among some individuals. In other, the differences are marked, yet in spite of their peculiarities of arrangement all have a certain likeness" (Cummins and Midlo, 1943), [3]. Mayer was the first to write that friction ridge skin is unique.

The birth of dermatoglyphics was possible thanks to works of Galton, Herschel (1880) [8] and Faulds [4], which researched fingerprints of people and primates. They establish the individuality and uniqueness of the images, as well as the possibility of human identification using finger-palm prints [5]. A few years later, Kallman (1885) made the first dermatoglyphic description of a foot. Following his example, a series of scientists continued studying the foot dermatoglyphics (Hepburn 1893, 1895; Wielder, 1904, 1913, 1916, 1922). Cummins and Middlo (1943), [3] publish two important monographs: about the skin relief in primates (1942) and about general dermatoglyphics (1943). Bansal (1968), [1] reports the bilateral symmetry, measuring the distance between the triradii of the third and the fourth finger.

The literature review demonstrates that twin research has not been extensive, perhaps due to the difficulty of obtaining anthropological material. The majority of twin research is based on physical development of twins and on causes for multiple pregnancies (J. Bertrand Petit, A. Marin, 1988). Imaizumi (1987), [9] and co-authors make a series of experiments on the influence of parents' age and the birth sequence on a multiple pregnancy. They establish that with parents' age increase, the chance of twin birth is higher.

## Materials and Methods

The main place in the study is the dermatoglyphic morphology of the hands, represented in two groups: monozygotic twins (MZ) and dizygotic twins (DZ). The material of the study included palm prints of both hands of 21 pairs of MZ twins and 22 pairs of DZ twins. Most data was collected in the area surrounding the town of Shumen, Bulgaria. Fingerprints and palms were obtained by a standard method. Fingerprinting was done by covering the hand palmar surface with topographic ink, and by using a glass plate and a roller. The recording of fingerprinting was done in a passive way, as the researcher helped with the data collection. A rotary tool was used to cover palms and fingers, always starting from the 1$^{st}$ finger on the right hand and finishing with the 5$^{th}$ finger on the left hand. Palmar surface was greased with topographic ink and fingerprints were left on a white sheet of paper, placed on a convex cylindrical surface. Such

method provided an accurate print of the palmar surface, including the central part of the palm. The establishment of dermatoglyphic differences was performed with the aid of a binocular loupe.

## Results and Discussion

Every developing trait depends both on hereditary and environmental factors. The goal of the Twin Method is to establish the relative role of both in the variability of different traits. This method is used in medicine when studying the hereditary predisposition to specific diseases (Down syndrome, cerebral gigantism, diabetes, schizophrenia, chromosomal abnormalities and others).

The Twin Method study differences in monozygotic (MZ) and dizygotic (DZ) twins, using the "Similarity Method". MZ twins are juxtaposed with DZ twins of the same gender, while taking into account that all differences in MZ twins are a product of external factors and in DZ twins – partly due to genetic factors and partly because of environmental ones. When taking heredity into account, one must determine the type of zygosity in twin research with great accuracy.

Two MZ embryos have the same hereditary potential, but develop as two independent individuals. They have the same gender, the same blood group and the same serum factors. This applies to many other hereditary physical traits. When it comes to intrauterine development, there are a couple of conditions, which can lead to differences in MZ twins. The exact time of zygote division is of great importance. We distinguish three ways of zygote division, depending on the time of its occurrence.

• MZ I (dichorionic diamniotic) – the separation happens between 0 to 3 days after fertilization. MZ I type occurs approximately 28.3%).

• MZ II (monochorionic diamniotic) – the separation happens during the developed morula stage (from day 4-5 to day 7 after fertilization). This type of separation is the most typical for the monozygotic twins (about 70%).

• MZ III (monochorionic monoamniotic) – the separation takes place after the 7$^{th}$ day following fertilization, which is when the embryo of the internal membranes (amnion) is already formed and the process of division stopped. MZ III type occurs rarely (1.2%).

The so called 'Siamese twins' are of great interest, as they do not have the possibility of full zygote division and remain connate to different extents. This takes place if the division starts after the 9$^{th}$ day post-fertilization.

Qualitative dermatoglyphic results shown that the ridge count between the four finger triradii has been defined: "a-b", "b-c" and "c-d" separately on each hand, the total ridge count (TRC) for both hands and the total ridge count. When there was an extra triradius, we also took into account the finger triradius "a" or "d".

The size of the "atd" angle has been measured by connecting finger triradii "a", "t" and "d" with two straight lines, and reported using an octant and a protractor. If extra triradii "a1" and "d1" existed, we also noted the most radial and most ulnar triradii. If extra axis triradii existed, we noted the most distal triradii.

When comparing the finger ridge quantity, we observed the following patterns. MZ twins with highest values have a unique IV finger on the left hand in both groups (I born twins – 15.55%; II born twins – 16.45%). We observed a high degree of similarity in the researched trait distribution also in the rest of the fingers (**Table 1**). The distribution of this trait in DZ twins is quite different. The highest ridge quantity was observed on the 1st finger of right hand in the group of 1st born twins. As a whole, this trait is characterized with higher values in the group of 1st born DZ twins and in both types of group twins (**Table 2**).

**Table 1.** Quantitative indicators of the monozygotic twins (MZ)

| Index | Birth order | N | $\bar{x}$ ($\mu_x$) mean value | Standard deviation S. | Sample standard deviation Sx | Variance (V) |
|---|---|---|---|---|---|---|
| TRC a-d | I | 22 | 190.2727 | 45.1571 | 9.6275 | 23.73 |
| | II | 22 | 187.8636 | 43.1115 | 9.1914 | 22.94 |
| TRC I-V | I | 22 | 132.5 | 32.9657 | 7.0283 | 24.87 |
| | II | 22 | 135.4091 | 33.3262 | 7.1052 | 24.61 |
| ∑ RT I-V dex | I | 22 | 66.5455 | 15.6714 | 3.3412 | 23.55 |
| | II | 22 | 67.4545 | 17.1012 | 3.6460 | 25.35 |
| ∑ RT I-V sin | I | 22 | 65.9545 | 18.9246 | 4.0347 | 28.69 |
| | II | 22 | 67.9545 | 17.3356 | 3.6960 | 25.59 |
| ∑ RT d-a dex | I | 22 | 97.4545 | 19.2965 | 4.1140 | 19.79 |
| | II | 22 | 98.2727 | 17.7635 | 3.7872 | 18.07 |
| ∑ RT d-a sin | I | 22 | 96.2273 | 19.3364 | 4.1225 | 20.10 |
| | II | 22 | 99.7273 | 13.2564 | 2.8263 | 13.30 |
| RT d-c dex | I | 22 | 33.2273 | 10.2443 | 2.1841 | 30.82 |
| | II | 22 | 36 | 7.6158 | 1.6237 | 21.14 |
| RT d-c sin | I | 22 | 31.5 | 10.5413 | 2.2474 | 33.46 |
| | II | 22 | 33.5455 | 8.3821 | 1.7871 | 24.89 |
| RT c-b dex | I | 22 | 26.8182 | 7.9560 | 1.6962 | 29.68 |
| | II | 22 | 27.3636 | 5.2513 | 1.1196 | 19.19 |
| RT c-b sin | I | 22 | 25.7727 | 7.5589 | 1.6116 | 29.33 |
| | II | 22 | 27.5909 | 4.7675 | 1.0164 | 17.29 |
| RT b-a dex | I | 22 | 38.0909 | 4.5136 | 0.9623 | 11.84 |
| | II | 22 | 37.7273 | 4.7927 | 1.0218 | 12.72 |
| RT b-a sin | I | 22 | 38.9545 | 5.5419 | 1.1815 | 14.22 |
| | II | 22 | 38.4091 | 6.5659 | 1.3998 | 17.08 |
| RT I dex | I | 22 | 14.227 | 6.5096 | 1.3878 | 45.75 |
| | II | 22 | 15.1364 | 6.5268 | 1.3915 | 43.13 |

| | | | | | | |
|---|---|---|---|---|---|---|
| RT I sin | I | 22 | 14.8182 | 5.5689 | 1.1873 | 37.52 |
| | II | 22 | 15.2273 | 4.6284 | 0.9868 | 30.33 |
| RT II dex | I | 22 | 13.2273 | 3.6506 | 0.7783 | 27.58 |
| | II | 22 | 12.7273 | 4.4420 | 0.9470 | 34.88 |
| RT II sin | I | 22 | 10.9545 | 6.0826 | 1.2968 | 55.52 |
| | II | 22 | 11.2273 | 5.8386 | 1.2448 | 52.00 |
| RT III dex | I | 22 | 12.0909 | 4.5660 | 0.9735 | 37.76 |
| | II | 22 | 12.7727 | 5.2001 | 1.1087 | 40.71 |
| RT III sin | I | 22 | 12.1818 | 5.6285 | 1.2000 | 46.21 |
| | II | 22 | 12.5 | 4.0679 | 0.8673 | 32.54 |
| RT IV dex | I | 22 | 14.6818 | 4.2693 | 0.9102 | 29.08 |
| | II | 22 | 14.8182 | 4.6867 | 0.9992 | 31.63 |
| RT IV sin | I | 22 | 15.5455 | 4.8573 | 1.0356 | 31.24 |
| | II | 22 | 16.4545 | 3.5821 | 0.7637 | 21.77 |
| RT V dex | I | 22 | 12.2273 | 4.6284 | 0.9868 | 37.85 |
| | II | 22 | 12.1364 | 4.6629 | 0.9941 | 38.39 |
| RT V sin | I | 22 | 12.7727 | 4.5558 | 0.9713 | 35.71 |
| | II | 22 | 13 | 4.6188 | 0.9847 | 35.53 |
| < atd dex | I | 22 | 46.1818 | 6.5001 | 1.3858 | 14.07 |
| | II | 22 | 47.0909 | 6.7040 | 1.4293 | 14.24 |
| < atd sin | I | 22 | 46.2273 | 7.4446 | 1.5872 | 16.10 |
| | II | 22 | 47.0455 | 7.9491 | 1.6948 | 16.90 |

**TRC** – total ridge count
**RT** – ridge count triradii
**dex** – right
**sin** – left

**Table 2.** Quantitative indicators of the dizygotic twins (DZ)

| Index | Birth order | N | $\bar{x}$ ($\mu_x$) mean value | Standard deviation S. | Sample standard deviation Sx | Variance (V) |
|---|---|---|---|---|---|---|
| TRC a-d | I | 21 | 199.7619 | 22.7638 | 4.9675 | 11.36 |
| | II | 21 | 192.0952 | 34.8782 | 7.6111 | 18.16 |
| TRC I-V | I | 21 | 138.9048 | 31.9467 | 6.9713 | 23.00 |
| | II | 21 | 122.8095 | 47.0836 | 10.2745 | 38.34 |
| ∑ RT I-V dex | I | 21 | 69.1429 | 16.6201 | 3.6268 | 24.04 |
| | II | 21 | 63.6190 | 22.9945 | 5.0178 | 36.14 |
| ∑ RT I-V sin | I | 21 | 69.7619 | 17.0555 | 3.7218 | 24.45 |
| | II | 21 | 59.1905 | 25.3882 | 5.5402 | 42.90 |
| ∑ RT d-a dex | I | 21 | 101.0952 | 12.8876 | 2.8123 | 12.75 |
| | II | 21 | 94.8571 | 23.5803 | 5.1456 | 26.97 |
| ∑ RT d-a sin | I | 21 | 103.3333 | 11.2665 | 2.4585 | 11.00 |
| | II | 21 | 101.4286 | 18.6884 | 4.0781 | 18.43 |
| RT d-c dex | I | 21 | 35.5238 | 6.5316 | 1.4253 | 18.38 |
| | II | 21 | 35.5238 | 4.7076 | 1.0273 | 13.26 |
| RT d-c sin | I | 21 | 35.2857 | 5.5690 | 1.2153 | 15.79 |
| | II | 21 | 34.0952 | 11.2067 | 2.4455 | 32.87 |
| RT c-b dex | I | 21 | 25.5238 | 5.6800 | 1.2395 | 22.26 |
| | II | 21 | 26.5714 | 6.6225 | 1.4451 | 24.91 |
| RT c-b sin | I | 21 | 26.1905 | 4.3545 | 0.9502 | 16.61 |
| | II | 21 | 26.3810 | 8.0838 | 1.7640 | 30.63 |
| RT b-a dex | I | 21 | 39.4286 | 7.0041 | 1.5284 | 17.75 |
| | II | 21 | 38.4286 | 4.8946 | 1.0681 | 12.72 |
| RT b-a sin | I | 21 | 41.8571 | 6.5596 | 1.4314 | 15.67 |
| | II | 21 | 40.3333 | 4.6940 | 1.0243 | 11.65 |
| RT I dex | I | 21 | 15.7619 | 5.2240 | 1.1400 | 33.12 |
| | II | 21 | 16.4762 | 4.5345 | 0.9895 | 27.50 |

| | | | | | | |
|---|---|---|---|---|---|---|
| RT I sin | I | 21 | 14.8095 | 4.8023 | 1.0479 | 32.41 |
| | II | 21 | 13.5238 | 4.8334 | 1.0547 | 35.72 |
| RT II dex | I | 21 | 12.0000 | 6.3246 | 1.3801 | 52.67 |
| | II | 21 | 11.5238 | 6.0052 | 1.3104 | 52.10 |
| RT II sin | I | 21 | 12.3333 | 6.6508 | 1.4513 | 53.94 |
| | II | 21 | 10.4762 | 6.4158 | 1.4000 | 61.24 |
| RT III dex | I | 21 | 13.0000 | 4.4159 | 0.9636 | 33.97 |
| | II | 21 | 10.4762 | 5.9213 | 1.2921 | 56.52 |
| RT III sin | I | 21 | 13.9048 | 5.3843 | 1.1749 | 38.72 |
| | II | 21 | 10.6667 | 7.3643 | 1.6070 | 68.98 |
| RT IV dex | I | 21 | 15.1905 | 4.4229 | 0.9652 | 29.12 |
| | II | 21 | 13.1905 | 6.2500 | 1.3639 | 47.38 |
| RT IV sin | I | 21 | 15.6667 | 3.5963 | 0.7848 | 22.92 |
| | II | 21 | 13.0952 | 7.2726 | 1.5870 | 55.88 |
| RT V dex | I | 21 | 13.2381 | 4.7001 | 1.0256 | 35.50 |
| | II | 21 | 12.2381 | 6.2202 | 1.3574 | 50.82 |
| RT V sin | I | 21 | 13.0476 | 4.3986 | 0.9599 | 33.71 |
| | II | 21 | 11.4286 | 6.1284 | 1.3373 | 53.62 |
| < atd dex | I | 21 | 45.9524 | 7.2696 | 1.5864 | 15.82 |
| | II | 21 | 42.4286 | 13.0674 | 2.8515 | 20.16 |
| < atd sin | I | 21 | 45.3810 | 7.6972 | 1.6797 | 16.96 |
| | II | 21 | 45.8095 | 8.6811 | 1.8944 | 18.95 |

**TRC** – total ridge count
**sin** – left
**RT** – ridge count triradii
**dex** – right

There have not been established any differences in ridge count distribution in interdigital fields neither in the MZ and DZ twins comparison, nor in the order of birth comparison. The highest ridge quantity for the entire excerption was observed in the field d-a, with the second highest observed in the field b-a, and the lowest – in c-b.

The average value of the total ridge count (TRC) is highest in I-born twins group (138.90%) and lowest in II-born DZ twins group (122.81%). This trait in MZ twins was almost identical for both I-born and II-born twins (I-born – 132.5%, II-born – 135.41%). When comparing the total ridge count trait, the difference is minimal in I-born and II-born MZ twins (2.41%). The two DZ twin groups show a bigger difference (7.67%). The highest total ridge count is observed in I-born twins (199.76%) and the lowest – in II-born MZ twins (187.86%).

When comparing the maximal values of the angle atd, we have not observed any significant differences between the two researched groups. The highest maximal value of the angle has been reported in II-born MZ twins in both hands, while the lowest maximal value was observed on the right hand in II-born DZ twins (**Tables 1, 2**).

The analysis of connections and dependencies in MZ twins demonstrates that all researched quantitative indicators (ridge count of interdigital triradii (RT), ridge quantity of finger phalanges (RT – I-V), total right count and the angle atd) are distributed normally (**Tables 1, 2**). By performing Levene's test, we also established that all indicators are over 0.05% (first order error) and, subsequently, there is no connection between the indicators and the I-born and II-born MZ twins (T-test).

We have performed the same test for DZ twins, and the results are similar and show the expected distribution, with the exception of the indicator RT III dex (Kolmogorov-Smirnov test). A non-parametrical test for this indicator demonstrates lack of a relationship with the relevant groups of I-born and II-born DZ twins. The indicators RT d-c sin, RT c-b sin, RT III sin and RT IV sin in Levene's test reject the null hypothesis. Despite the existing relationship, it is not statistically significant, because the null hypothesis may not be rejected in a T-test. The calculated extent of the relationship is under 0.3, i.e. the difference between the two researched groups is very weak with these indicators in mind.

The comparison of groups as a whole, MZ on the one hand, and DZ on the other, demonstrates that, on average, all indicators have a normal distribution (Kolmogorov-Smirnov test). Levene's test confirms the null hypothesis, which is rejected only by the RT d-c dex indicator (T test). Only with this indicator is it possible to search for a difference between MZ and DZ twins, but the calculated effect is minimal.

The second variant in researching MZ and DZ twins as an median difference between I-born and II-born twins was more successful. The distribution of indicators TRC a-d, TRC I-V, ∑ RT I-V dex at sin, ∑ RT d-a dex. et sin., RT d-c dex, RT I dex, RT II dex, RT V dex. < atd dex. is not normal. For these indicators we used Mann Whitney's non-parametrical test. The above-mentioned indicators, with the exception of RT d-c dex, RT I dex., ∑ RT d-a sin, RT V dex. < atd dex., demonstrate the existence of a connection in twin zygosity.

Parametrical indicators are investigated with Levene's test and T-test. With Levene's test we found that the following indicators have a connection with zygosity: RT b-a dex., RT I sin, RT III sin, RT IV dex et sin. The aforementioned indicators reject the null hypothesis in the T-test. Significant values are the sum of 1-5 phalanges ridges on the left hand (0.67%) and the TRC of finger phalanges. The least significant value is possessed by the indicators ∑ RT d-a dex and TRC a-d. The most significant individual indicator was the ridge count of the 5$^{th}$ finger phalanx on the left hand.

## Conclusion

Based on the current research and after analysing the results, the following conclusions can be made:

1. MZ twins with highest values in finger ridge quantity have a unique IV finger on the left hand in both groups (I born twins – 15.55%; II born twins – 16.45%). The highest ridge quantity in DZ was observed on the 1st finger of the right hand in the group of I-born twins;

2. Quantitative indicators demonstrate a relationship with zygosity, concerning the left and right hands are as following: five indicators on the left hand (∑ RT I-V sin, RT I sin, RT III sin, RT IV sin, RT V sin), five indicators on the right hand (∑ RT I-V dex., ∑ RT d-a dex., RT b-a dex., RT II dex., RT IV dex.) and two total indicators (TRC a-d, TRC I-V);

3. The distribution of indicators TRC a-d, TRC I-V, ∑ RT I-V dex at sin, ∑ RT d-a dex. et sin., RT d-c dex, RT I dex, RT II dex, RT V dex. < atd dex. is not normal;

4. The significant individual indicator was the ridge count of the 5th finger phalanx on the left hand.

## References


1. **Bansal, I. J. S.** Palmar dermatoglyphics in maharashtrians in India. – Acta geneticae medicae et gemellologiae, **14**(4), 1965, 431-437.
2. **Boklage, C.** Race, zygosity and mortality among twins: interaction of myth and method. – Acta geneticae medicae et gemellologiae, **6**(3), 1987, 275-288.
3. **Cummins, H., C. Midlo.** Finger prints, palms and soles: an introduction to dermatoglyphics. New York, Dover Publications, 1961, 319.
4. **Faulds, H.** Guide to Finger-print Identification. Hanley, Wood, Mitchell & Co Ltd, 1905, 75.
5. **Fournier, N., H. Ross.** Sex, ancestral, and pattern type variation of fingerprint minutiae: A forensic perspective on anthropological dermatoglyphics. – J. Am. Phys. Anthrop., **158**(3), 2015, 78-84.
6. **Galton, F.** The history of twins, as a criterion of the relative powers of nature and nurture. – Fraser's Magazine, **12**, 1875, 566-576.
7. **Hepburn, D.** The Papillary Ridges of the Hands and Feet of Monkeys and Men. – Royal Dublin Society, 1895, 538.
8. **Herschel, W. J.** The Origin of Finger-Printing. Oxford University Press, London, 1916.
9. **Imaizumi, Y.** Infant mortality rates in single, twin and triplet births, and influencing factors in Japan. – Paediatric and perinatal epidemiology, **15**(4), 2001, 346-351.



Corresponding author:
*Maslarski, Ivan Ilkov*
*Tel.: +359-882-000-809*
*e-mail: maslarsky@gmail.com*

Institute of Experimental Morphology, Pathology and Anthropology with Museum
Bulgarian Anatomical Society

Acta morphologica et anthropologica, 22
Sofia ● 2015

# The Papillary Images as Part of the Twin Method

*I. Maslarski[1*], L. Belenska[2]*

[1]*Department of Human Anatomy, Histology and Pathology, Faculty of Medicine, University of Sofia St. Kliment Ohridski*
[2]*Department of Biology, Medical Genetics and Microbiology, Medical Faculty, University of Sofia St. Kliment Ohridski*

The "Twin Method" is attempting to answer questions linked with the extent of influence of genetic information as opposed to the environment over various diseases, behaviors and level of intelligence. The material of the study included palm prints of both hands of 21 pairs of MZ twins and 22 pairs of DZ twins. Most data was collected in the area surrounding the town of Shumen, Bulgaria. Fingerprints and palms were obtained by a standard method. The distribution of ulnar loops on fingers in MZ and DZ twins shows that its frequency is the highest on the 5th distal phalanx (87.5% in MZ twins and 69.04% in DZ twins). The percentage of spirals compared to other fingerprint images is greater in DZ twins (40.47%) than in MZ twins (29.77%). The difference in zygosity can be observed in triradii t', t', 0.

*Key words:* monozygotic twins, dizygotic twins, papillary images, twin method, hypothenar image.

## Introduction

In the past few years, the interest towards twin research has significantly increased. Almost 150 years have passed since Francis Galton expressed for the first time the necessity to study twins when studying their illnesses. He also found a correlation between hereditary factors and the environment, while researching the extent and duration of their influence. The "Twin Method", developed as a natural continuation of Galton's works, is still being perfected. This method is attempting to answer questions linked with the extent of influence of genetic information as opposed to the environment over various diseases, behaviors and level of intelligence. It is known that monozygotic twins (MZ) have 100% identical genetic information and thus environmental factors are predominant for such analysis. The dizygotic twins (DZ), on the other hand, have 50% genetic identity and thus the genetic information is the most important factor. The analysis of fingerprints requires the use of qualitative indicators more common. They are bound by specific genetic markers that define the form of papillary images. The implementation of dermatoglyphic analysis requires knowledge in various fields of science, such as ethnic anthropology, medical genetics, forensics and others.

A literature review shows that twin studies are not numerous, mainly due to the difficulties linked with the acquirement of anthropological material. Most of the re-

search is related to physical development and reasons of multiple pregnancies. The effect of parents' age and birth sequence over multiple pregnancies has been studied by J. Bertranpetit, A. Martin and Y. Imaizumi [1, 7]. They establish that with the age increase age of parents, there is also an increase in the percentage of twins being born as a result. Moreover, with every subsequent birth, the possibility of twin birth is increasing as well. In 1982 and 1987, Boklage et al. [2] researched the mortality rate of twins. They lay down that the twin mortality during the first labor is much lower than during second or third, taking into account also the age variation of mothers. Eriksson and Bressers [4] demonstrate that the twin birth rate also increases during wars and famines. It was also shown that in rodents (lemmings), type of food influences the birth of twins. The studies by Miara et al. [5] provide interesting data in relation to birth sequence and intervals between labors. Recently research shows the relationship between dermatoglyphic traits and the electrical activity in the brain of a healthy person [6].

## Materials and Methods

The main place in the study is the dermatoglyphic morphology of the hands, represented in two groups: monozygotic twins (MZ) and dizygotic twins (DZ). The material of the study included palm prints of both hands of 21 pairs of MZ twins and 22 pairs of DZ twins. Most data was collected in the area surrounding the town of Shumen, Bulgaria. Fingerprints and palms were obtained by a standard method. Fingerprinting was done by covering the hand palmar surface with topographic ink, and by using a glass plate and a roller. The recording of fingerprinting was done in a passive way, as the researcher helped with the data collection. A rotary tool was used to cover palms and fingers, always starting from the 1$^{st}$ finger on the right hand and finishing with the 5$^{th}$ finger on the left hand. Palmar surface was greased with topographic ink and fingerprints were left on a white sheet of paper, placed on a convex cylindrical surface. Such method provided an accurate print of the palmar surface, including the central part of the palm. The establishment of dermatoglyphic differences was performed with the aid of a binocular loupe.

In this study we used the Galton's [8] classification scheme (1892) of the fingerprints. This classification includes three types of the terminal phalanges of the fingers images: whorls (W), loops (L) and arches (A).

Whorls are images that must have two triradii. They consist of a closed figure, in which the papillary lines run around the center of the image. Some whorls have two centers (**Fig. 1**). Loops represent a semi-closed figure. The loop, opened towards the radial direction is notated with the letter R, and the loop, pointing towards the ulnar direction is notated with the letter U. The T-shaped arch (T) has a triradius, the two proximal radiants of which are pointed in the ulnar (ulnaris) and radial (radialis) direction, and its distal radiant is interrupted and is accompanied by papillary lines, appearing as a distally convex arch.

Palmar images were recorded on the hypothenar (Hy) and on the thenar (Th) areas of the palm with 1$^{st}$ (Th/I), 2$^{nd}$, 3$^{rd}$ and 4$^{th}$ interdigital fields [9]. The hypothenar (Hy) skin relief is normally presented with a system of arch-like papillary lines, arranged obliquely relative to the longitudinal axis of the hand and opened towards the ulnar side of the hand. They are noted as ulnar arches (Au). In rare cases, arches are opened in the radial direction (Ar) or in the carpal direction (carpalis) (Ac). Even rarer to be found are skin ripples, which form an image on the hypothenar, appearing as a whorl (W), a loop or a T-shaped image [3]. The presence of loops on the hypothenar, depending on the direction of opening, can be ulnar (Lu), radial (Lr), and carpal (Lc).

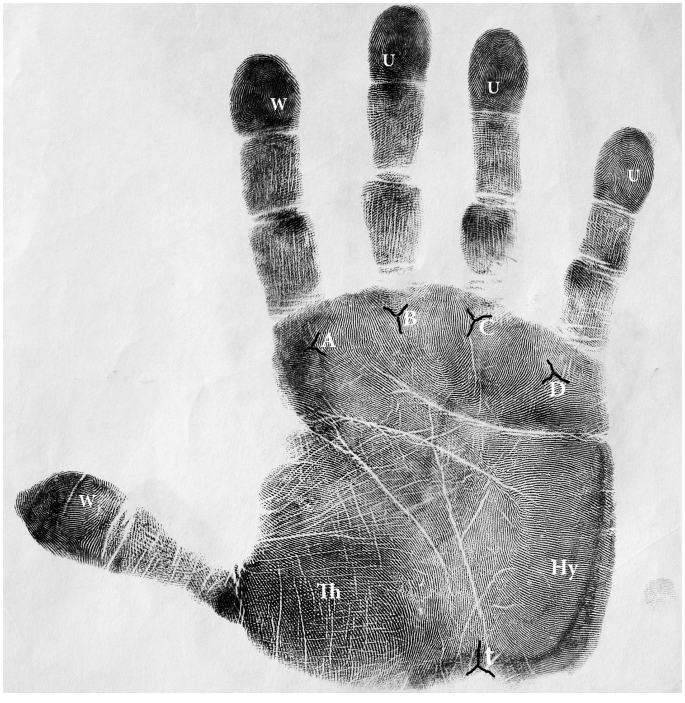


**Fig. 1.** Finger and palm prints; W – whorl; U – ulnar loop; A, B, C, D – types of triradii; t – axial triradius; Th – thenar; Hy – hypothenar

Images on the thenar and first interdigital area are always noted together. The lack of an image is marked with 0. When the papillary line ridges form an image, it is marked with symbols similar to those of the hypothenar. Traces of images are noted with the letter V. In the event of a double image, the result is noted first on the thenar, and then, separated by a slash, we record the image from the first interdigital area. When skin ripples do not form an image with a specific form on any of the interdigital fields, we record the result 0. Should there be a loop of not more than five papillary lines, we record the result "1". If the loop has more than five papillary lines, the observation is "L". The loop in the interdigital fields is always distally open. It is possible that the loop of the proximal ending finishes with a triradius, while spirals are rare.

The axial triradius is located on the second field of the palm, between the thenar and the hypothenar. To identify it, we used Gaipel's method [10]. There exist various forms of the axial triradius: carpal (t), intermediate (t') and central (t"). In rare cases, the palm surface may have two triradii (tt', tt" and t' t") and even more rarely three (tt't"). In the absence of an axial triradius, we write "0" in the formula.

## Results

The qualitative analysis of fingerprints show that loops (L) are most frequently found in fingerprint images of MZ and DZ twins, whereby this frequency is more pronounced in monozygotic twins (62.27%) than in dizygotic twins (52,37%). Interesting results were

**Table 1.** Fingerprints at MZ twins

| Type of fingerprints | | Fingers of MZ twins | | | | | | | | | | | | | | |
|---|---|---|---|---|---|---|---|---|---|---|---|---|---|---|---|---|
| | | I | | | II | | | III | | | IV | | | V | | | |
| | LH n = 44 | RH n = 44 | BH n = 88 | LH n = 44 | RH n = 44 | BH n = 88 | LH n = 44 | RH n = 44 | BH n = 88 | LH n = 44 | RH n = 44 | BH n = 88 | LH n = 44 | RH n = 44 | BH n = 88 | |
| A + T | value | 0 | 4 | | 2 | 0 | | 2 | 6 | | 0 | 0 | | 0 | 0 | |
| | % | – | 9.1 | 4.54 | 4.54 | – | 2.27 | 4.54 | 13.63 | 9.1 | – | – | – | – | – | – |
| R | value | 0 | 0 | | 7 | 4 | | 0 | 0 | | 0 | 2 | | 1 | 0 | |
| | % | – | – | – | 15.9 | 9.1 | 12.5 | – | – | – | – | 4.54 | 2.27 | 2.27 | – | 1.13 |
| U | value | 32 | 26 | | 14 | 21 | | 37 | 31 | | 22 | 22 | | 37 | 40 | |
| | % | 72.72 | 59.09 | 65.9 | 31.81 | 47.72 | 39.77 | 84.1 | 70.45 | 77.27 | 50 | 50 | 25 | 84.1 | 90.9 | 87.5 |
| W | Value | 12 | 14 | | 21 | 19 | | 5 | 7 | | 22 | 20 | | 6 | 4 | |
| | % | 27.27 | 31.81 | 29.54 | 47.72 | 43.18 | 45.45 | 11.36 | 15.9 | 14.77 | 50 | 45.45 | 47.72 | 13.63 | 9.1 | 11.36 |
| DL10 | % | 12.72 | 12.27 | 24.99 | 14.31 | 14.31 | 28.62 | 10.68 | 10.22 | 20.8 | 15 | 14.54 | 29.54 | 11.36 | 10.9 | 22.26 |
| L= R + U | % | 72.72 | 59.09 | 65.9 | 47.71 | 56.82 | 52.27 | 84.1 | 70.45 | 77.27 | 50 | 54.54 | 27.27 | 86.37 | 90.9 | 88.63 |

LH – left hand
RH – right hand
BH – both hands

A – arcus
L – loops (R-radial, U-ulnar)
W – whorl

**Table 2.** Fingerprints at DZ twins

| Type of fingerprints | | Fingers of DZ twins | | | | | | | | | | | | | | |
|---|---|---|---|---|---|---|---|---|---|---|---|---|---|---|---|---|
| | | I | | | II | | | III | | | IV | | | V | | | |
| | LH n = 44 | RH n = 44 | BH n = 88 | LH n = 44 | RH n = 44 | BH n = 88 | LH n = 44 | RH n = 44 | BH n = 88 | LH n = 44 | RH n = 44 | BH n = 88 | LH n = 44 | RH n = 44 | BH n = 88 | |
| A + T | value | 2 | 3 | | 6 | 6 | | 5 | 3 | | 2 | 1 | | 0 | 2 | |
| | % | 4.76 | 7.14 | 5.95 | 14.28 | 14.28 | 14.28 | 11.9 | 7.14 | 9.5 | 4.76 | 2.38 | 3.57 | – | 4.76 | 2.38 |
| R | value | 1 | 0 | | 4 | 1 | | 0 | 0 | | 0 | 0 | | 0 | | |
| | % | 2.37 | – | 1.19 | 9.1 | 2.27 | 5.95 | – | – | – | – | – | – | – | – | – |
| U | value | 17 | 20 | | 13 | 17 | | 26 | 25 | | 19 | 19 | | 31 | 27 | |
| | % | 38.6 | 45.45 | 44.04 | 30.95 | 40.47 | 35.71 | 61.9 | 59.52 | 60.71 | 45.23 | 45.23 | 45.23 | 73.8 | 64.28 | 69.04 |
| W | value | 22 | 19 | | 19 | 18 | | 11 | 14 | | 21 | 22 | | 11 | 13 | |
| | % | 50 | 43.18 | 48.8 | 45.23 | 40.47 | 44.04 | 26.19 | 33.33 | 29.76 | 45.23 | 50 | 51.19 | 26.1 | 30.95 | 28.57 |
| DL10 | % | 14.1 | 13.18 | 27.27 | 13.09 | 12.85 | 25.94 | 11.16 | 12.61 | 23.77 | 14.52 | 15 | 29.5 | 12.6 | 12.6 | 25.14 |
| L= R + U | % | 41 | 45.45 | 45.23 | 40 | 42.74 | 41.66 | 61.9 | 59.52 | 60.71 | 45.23 | 45.23 | 45.23 | 73.8 | 64.28 | 69.04 |

LH – left hand;
RH – right hand;
BH – both hands;

A – arcus
L – loops (R-radial, U-ulnar)
W – whorl

**Table 3.** Axial triradii

| | | MZ | | | DZ | | |
|---|---|---|---|---|---|---|---|
| | | Left hand n = 44 | Right hand n = 44 | Both hands n = 88 | Left hand n = 42 | Right hand n = 42 | Both hands n = 84 |
| t | value | 9 | 12 | | 14 | 14 | |
| | % | 20.45 | 27.27 | 23.86 | 33.33 | 33.33 | 33.33 |
| t’ | value | 19 | 23 | | 19 | 20 | |
| | % | 43.18 | 52.27 | 47.72 | 45.24 | 47.62 | 46.42 |
| t’’ | value | 4 | 5 | | 3 | 2 | |
| | % | 9.1 | 11.36 | 10.28 | 7.14 | 4.76 | 5.95 |
| tt’’ | value | 2 | 1 | | 2 | 2 | |
| | % | 5.45 | 2.27 | 3.40 | 4.76 | 4.76 | 4.76 |
| t’t’’ | value | 1 | 0 | | | | |
| | % | 2.27 | – | 1.13 | | | |
| tt’t’’ | value | 2 | 0 | | 1 | 0 | |
| | % | 4.54 | – | 2.27 | 2.38 | – | 1.19 |
| tt | value | | | | | | |
| | % | | | | | | |
| t’t’ | value | 2 | 0 | | | | |
| | % | 4.54 | – | 2.27 | | | |
| 0 | value | | | | | | |
| | % | 6.81 | 6.81 | 6.81 | | | |

t, t’, t’’ – different types of palm triradius

obtained for distribution of ulnar loops on fingers in MZ and DZ twins shows that its frequency is the highest on the 5th finger (87.5%; 69.04%) and lowest on the 4th finger in MZ (25%) and on the 2nd finger in DZ (35.81%). The radial loops dominate the left hand in both MZ and DZ twins (**Tables 1, 2**).

When conducting similar experiments on spirals, we established large differences between MZ and DZ twins. The percentage of spirals compared to other fingerprint images is greater in DZ (40.47%) than in MZ (29.77%) (**Tables 1, 2**).

From the results it is noticeable that the amount of arches (A + T) is significantly greater than that of loops and spirals (7.14% in DZ and 3.18% in MZ twins). Arches are found more frequently in DZ than in MZ (**Tables 1, 2**).

The study of palm prints (axial triradii and palm images) showed that triradii t, t’’ is present in DZ but absent in MZ twins. In regard to palm images variant Au/Ac has the highest percent probability of occurrence in both groups (38.63% in MZ and 32.14% in DZ twins). In MZ twins, possible combinations are more numerous than in DZ twins (**Table 3**).

## Discussion

In order to use efficiently and correctly the "twin method", zygosity should be determined very precisely. There are a number of methods which aim to diagnose twins. The diagnosis of a physician during birth is one of the most widely used methods. It is based on the number of placentas. Such method, however, can be quite erroneous. To understand the high probability of errors during this diagnosis, one should look at the way twins are created. There are known to be three different ways: MZ I (dichorionic diamniotic) – the separation happens between 0 to 3 days after fertilization and the frequency of occurrence is approximately 28.3%); MZ II (monochorionic diamniotic) – the separation happens during the developed morula stage (from day 4-5 to day 7 after fertilization and the frequency is about 70%); MZ III (monochorionic monoamniotic) – the separation takes place after the 7th day following fertilization, which is when the embryo of the internal membranes (amnion) is already formed and the process of division stopped. MZ III type occurs rarely (1.2%).

The situational (distribution analysis) and diagnostic (analysis of relationships and dependencies between phenomena) statistical analysis were used. Many individual results were received as a product of the study. These have to be summarized in such a way as to appropriately suit the analysis. In such synthesis, one has to move away from information about the individual units to statistical data, which relates to the quality of homogeneous groups. It is important to note that one does not search for a specific numeric expression evaluation, but only checks whether the empirical data confirms or refutes the preliminary assumption (hypothesis) on some properties (parameters) of the distribution of random variables.

The results obtained from a qualitative analysis of fingerprints as we mentioned earlier show that loops (L) are most frequently found in fingerprint images of MZ and DZ twins. The ulnar loops prevail in both MZ and DZ twins, with the respective percentages: 59.09% and 50.95%. Radial loops (R) are less frequent than ulnar ones in terms of percentage. They are however more frequent in MZ twins than in DZ twins (3.18% and 1.43% respectively). When it comes to loops, there is an absolute difference of 10%, with 8% in ulnar loops and with radial – 2%. This difference demonstrates that there is a difference in zygosity to a small extent (refer to tables). Distribution of ulnar loops on fingers in both groups MZ and DZ twins shows that its frequency is the highest on the 5th finger (87.5% and 69.04% respect.) and lowest on the 4th finger in MZ (25%) and on the 2nd finger in DZ (35.81%). Radial loops in MZ and DZ twins with the highest percentage frequency are found on the 2nd finger (12.5% and 5.95%), while they are completely absent on the 1st and the 3rd fingers in MZ twins and on the 3rd, 4th and 5th fingers in DZ twins. The frequency of ulnar loops in MZ is almost identical on both hands with a slight preponderance on the left hand (64.55%) (On the right hand, the frequency is 63.63%). Similarly, in DZ twins there is also a little difference, but there is a slight preponderance on the right hand (50.10% and 51%).

From the data recorded in the results of this paper, it is clear that radial loops dominate the left hand in both MZ and DZ twins and large differences of the spirals between the same group of twins (40.47%) in MZ twins than (29.77%) in DZ twins. There is an absolute difference of 11%. In both experimental groups, this image is most frequently found on the 4th finger (MZ twins – 47.72% and 51.19%). Spiral images are almost equally distributed on the left and right hands in both MZ and DZ twins (**Table 1**, **Table 2**).

The amount of arches (A + T) are found more frequently in DZ than in MZ twins. There is an absolute difference of 4%. In MZ twins, arches are missing on the 4th and 5th fingers on both hands and are most numerous on the 3rd finger (9.1%). Arches in

DZ twins, though few in number, are located on all finger phalanges. They are most numerous on the 2nd phalanx (14.28%) and least numerous on the 5th phalanx (2. 38%). Arches in MZ twins prevail on the right hand, while in DZ twins they are almost equally distributed on both hands.

The data of frequencies of axial triradii are represented in **Table 3**. The research analysis concludes that the encounter of single axial triradii t, t' and t'' is the highest in both groups of twins. Triradius variant t, t is the only one, which is not to be found in both kinds. The difference in zygosity can be observed in triradii t', t'', 0 and only in MZ twins, while absent completely in DZ twins. Triradius variant t, t'' is present in DZ but absent in MZ twins. Most frequently found triradius is triradius t' and it is found in both kinds of twins (47.72% in MZ twins and 46.42% in DZ twins). The lower percentage probability is for triradius variant t, t' and t'' (2.27% in MZ twins and 1.19% in DZ twins).

The results obtained from a qualitative analysis of palm images (table 4) variant Au/Ac has the highest percent probability of occurrence in both groups (38.63% in MZ twins and 32.14% in DZ twins). This image is more pronounced on the left hand (40.9% in MZ and 38.1% in DZ twins). The difference between both hands is less significant in MZ twins (4%) and more significant in DZ twins (12%). From the images represented in the table, images Au/Lr and Lr/Lc are missing. In DZ twins there are five images that are missing: S, W/Lu, T, R and Au/Au/Ac. The least pronounced images are S, W, W/Lu, Ws, T and Au/Au/Ac (1.13% in DZ twins), and Ar, Au/Lu, Au/Lr, Lr/Lc, W (1.19% in MZ twins).

## Conclusions

Based on the current research and after analysing the results, the following conclusions can be made:

1. The distribution of ulnar loops on fingers in MZ and DZ twins shows that its frequency is the highest on the 5th distal phalanx (87.5% in MZ twins and 69.04% in DZ twins). The percentage of spirals compared to other fingerprint images is greater in DZ twins (40.47%) than in MZ twins (29.77%).

2. The palm image Au/Ac has the highest percent probability of occurrence in both groups (38.63% in MZ twins and 32.14% in DZ twins). This image is more pronounced on the left hand (40.9% in MZ and 38.1% in DZ twins). The difference between both hands is less significant in MZ twins (4%) and more significant in DZ twins (12%).

3. In MZ twins the group variability of researched features is almost evenly distributed, while in DZ twins the variability is higher in the second-born twins.

4. The difference in zygosity can be observed in triradii t', t'', 0 and only in MZ twins, while absent completely in DZ twins. The lower percentage probability is for triradius variant t, t' and t'' (2.27% in MZ twins and 1.19% in DZ twins).

## References


1. **Bertranpetit, J., A. Martin.** Demographic parameters and twinning: A study in Catalonia, Spain. – Acta geneticae medicae gemellologiae, **37**(2), 1988, 127-135.
2. **Boklage, C.** Race, zygosity and mortality among twins: interaction of myth and method. – Acta geneticae medicae et gemellologiae, **36**(3), 1987, 275-288.
3. **Cummins, H., C. Midlo.** Finger prints, palms and soles: an introduction to dermatoglyphics. – New York, Dover Publications, 1961, p. 319.
4. **Ericsson, A., W. Bressers, P. Kostense.** Twinning rate in Scandinavia, Germany and the Netherlands during years of privation. – Acta geneticae medicae et gemellologiae, **37**(3-4), 1988, 277-297.

5. **Galton, F.** The history of twins, as a criterion of the relative powers of nature. – Fraser's Magazine, **12**, 1875, 566-576.
6. **Hepburn, D.** The Papillary Ridges of the Hands and Feet of Monkeys and Men. – Royal Dublin Society, 1895, p.538.
7. **Imaizumi, Y.** Infant mortality rates in single, twin and triplet births, and influencing factors in Japan. – Pediatric and perinatal epidemiology, **15**(4), 2001, 346-351.
8. **Miura, T., H. Kawana, K. Nonaka.** Twinning in New England in the 17th-19th centuries. – Acta geneticae medicae et gemellologiae, twin research, **36**(3), 1987, 355-364.
9. **Rocha, L., P. Fernandes.** Motor features, dermatoglyphic and EEG periods of girls in pre and post menarche. – Portlogia, **9**(1), 2013, 34-45.
10. **Sharma, A.** A methodological study on angle atd (t, t', t") distribution on the palmar prints. – Zeitschrift für Morphologie und Anthropologie, **55**(2), 1964, 24-31.

*Corresponding author:
*Maslarski, Ivan Ilkov*
*Tel.: +359-882-000-809*
*e-mail: maslarsky@gmail.com*

Institute of Experimental Morphology, Pathology and Anthropology with Museum
Bulgarian Anatomical Society

Acta morphologica et anthropologica, 22
Sofia ● 2015

# A Case of Skeletal Dysplasia in Bone Remains from a Contemporary Male Individual

*S. Nikolova[1], D. Toneva[1], I. Georgiev[2,3]*

*[1]Department of Anthropology and Anatomy, Institute of Experimental Morphology, Pathology and Anthropology with Museum, Bulgarian Academy of Sciences, Sofia, Bulgaria*
*[2]Department of Scientific Computations, Institute of Information and Communication Technologies, Bulgarian Academy of Sciences, Sofia, Bulgaria*
*[3]Department of Mathematical Modeling and Numerical Analysis, Institute of Mathematics and Informatics, Bulgarian Academy of Sciences, Sofia, Bulgaria*

The skeletal dysplasias are a large heterogeneous group of disorders characterized by generalized abnormalities of the skeleton. The severity of skeletal dysplasias ranged from individuals with normal stature and survival but early-onset osteoarthrosis to perinatal lethality. This study aimed to investigate bone remains with obvious skeletal abnormalities and to make a differential diagnosis. The remains belonged to a young male individual preserved in the Military Mausoleum with Ossuary, National Museum of Military History (Sofia, Bulgaria). It was established that the abnormalities were due to skeletal dysplasia with increased bone density and *craniometadiaphyseal dysplasia, wormian bone type* was suspected as a probable diagnosis. The individual was fit for service, which suggests a normal stature and mental development without severe malformations.

*Key words:* skeletal dysplasia, increased bone density, craniometadiaphyseal dysplasia, wormian bone type, Brodie's subacute osteomyelitis.

## Introduction

The skeletal dyspasias, or *osteochondrodysplasias*, are a large heterogeneous group of disorders characterized by generalized abnormalities of the skeleton. A chromosomal classification of the skeletal dysplasias is in elaboration, but traditionally they are classified by parts of the skeleton which are involved [15]. Each dysplasia is rare, but the overall birth incidence is estimated to be 1/5000 live births [1]. The most frequent clinical implication is a disproportionate short stature, but it is not uniformly present. The severity of skeletal dysplasias ranged from individuals with normal stature and survival but early-onset osteoarthrosis to perinatal lethality. These disorders can be associated with a variety of orthopedic, neurologic, auditory, visual, pulmonary, cardiac, renal, and psychological complications [8]. Most skeletal dysplasias are associated with normal intellectual development, but there are exceptions to this rule [15].

Differential diagnosis of the skeletal dysplasias required radiographs and complete skeletal survey as well as assessment of the size, structure, and shape of the individual

bones. The region of the skeleton that is affected along with the pattern of skeletal abnormalities and bone density are crucial for a differential diagnosis [15]. Thus, the aim of the present study was to investigate in detail bone remains with obvious skeletal abnormalities and to make a differential diagnosis.

## Materials and Methods

The objects of the present study were bone remains of a soldier who served and died in the wars from the beginning of the 20th century. The remains were preserved in the Military Mausoleum with Ossuary, National Museum of Military History (Bulgaria). The remains belonged to a young male individual and consisted of a skull with previously cut out calvaria, right and left humeri, left ulna, right and left tibiae. The mandible and the other postcranial bone were not available.

The physiological age of the individual was determined according to the cranial and postcranial bone development, observation of the cranial sutures and dentition [2, 7, 13, 17].

The skull and the available postcranial bones were macroscopically observed and measured. The characteristics of the angels and indices were given after Martin and Saller scales [9]. The categories "very small", "small", "middle", "large" and "very large" were used after Alekseev and Debets [16]. The stature was calculated based on the lengths of the limb long bones according to the method of Pearson and Lee [11]. A digital radiography was performed on a Nikon XT H 225 system.

## Description and discussion of the case

*Estimation of the physiological age*

The remains belonged to a juvenile individual (16-18 years). It was inferred taking into account that all cranial sutures were open without traces of obliteration and the sphenooccipital synchondrosis was discernible. Furthermore, the third molars were not erupted as well as the second left molar. The radiographs showed an agenesis of these teeth, i.e. missing tooth germs in the maxilla, resulting in hypodontia. The available teeth showed minimal degree of dental attrition without abnormalities except for caries on the mesial surface of the second right molar.

Dental formula:

| Right | Left |
|---|---|
| 6 5 X X X X | X X X X 5 6 7 |

*X – postmortem loss of the tooth

The epiphyses of the long bones had the appearance of separated segments, even though they were fused with the diaphyses except for the distal epiphysis of the ulna, which was detached and missing (**Fig. 1**).

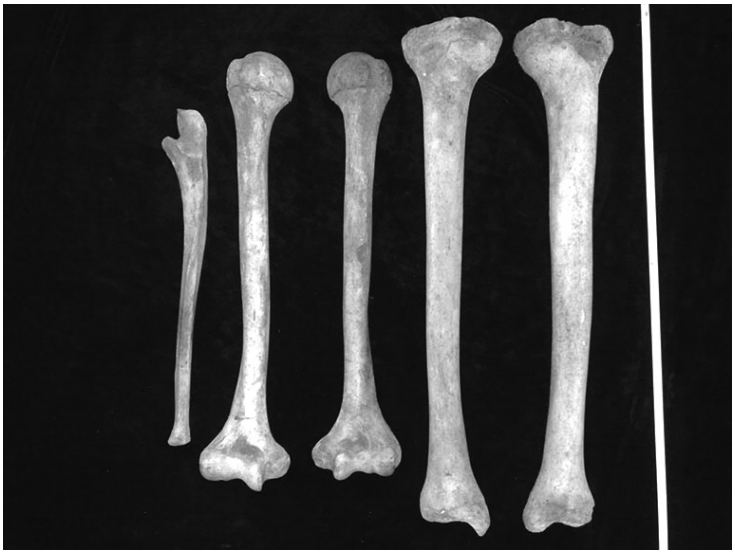

**Fig. 1.** The available long bones of the skeleton

*The skull*

The metric, angular and index characterizations of the skull were presented in **Tables 1, 2, 3**. The viscerocranium was broad but short and feebly profiled, i.e. it did not project significantly when the cranium was oriented in the Frankfurt plane (**Fig. 2**). The facial bones were small and underdeveloped. The nasal bones were noticeably wide and depressed, which was precondition for a broad and flat nasal bridge (**Fig. 2a**). The maxillary arch and hard palate were unusually broad and short, which probably was related to the observed hypodontia (**Fig 2c**). In addition, the canine fossae were very deep (**Fig. 2a**).

**Table 1.** Measurements of the skull after Martin and Saller [9]. The categories were given after Alekseev and Debets [16]

| No | Measurements | mm | Category |
|---|---|---|---|
| 1 | Maximum cranial length | 183 | Medium |
| 5 | Cranial base length | 93 | Very small |
| 7 | Foramen magnum length | 47 | Very large* |
| 8 | Maximum cranial breadth | 144 | Medium |
| 9 | Minimum frontal breadth | 108 | Very large |
| 10 | Maximum frontal breadth | 134 | Very large |
| 12 | Biasterionic breadth | 116 | Large |
| 16 | Foramen magnum breadth | 33 | Very large |
| 17 | Basion-bregma height | 132 | Medium |
| 20 | Porion-bregma height | 112 | Small |
| 23 | Cranial circumference | 530 | Large |

| | | | |
|---|---|---|---|
| 26 | Frontal arc | 127 | Medium |
| 27 | Parietal arc | 129 | Medium |
| 28 | Occipital arc | 112 | Medium |
| 29 | Frontal chord | 106 | Small |
| 30 | Parietal chord | 114 | Medium |
| 31 | Occipital chord | 92 | Small |
| 38 | Cranial capacity /by Pearson for male skull/ | 1449.87 cc | Medium |
| 40 | Basion-prosthion length | 85 | Very small |
| 43 | Upper facial breadth | 109 | Large |
| 45 | Bizygomatic breadth | 133 | Medium |
| 46 | Middle facial breadth | 101 | Large |
| 48 | Upper facial height | 67 | Small |
| 51 | Orbital breadth | 39 | Very small |
| 52 | Orbital height | 34 | Medium |
| 54 | Nasal breadth | 26 | Medium |
| 55 | Nasal height | 50 | Small |
| 56 | Nasal bones length | 18 | – |
| 49a (DC) | Dacrial chord | 27 | Very large |
| 57 (SC) | Simotic chord | 11 | Large |
| DS | Dacrial subtense | 7.5 | Very small |
| SS | Simotic subtense | 2.5 | Small |
| 60 | Maxilloalveolar length | 45 | Very small |
| 61 | Maxilloalveolar breadth | 67 | Large |
| 62 | Palatal length | 31 | Very small* |
| 63 | Palatal width | 43 | Large |
| 64 | Palatal height | 12 | – |
| FC | Canine fossa depth | 10 | Very large |

* The value of the measuremant is out of the borderlines of the category

**Table 2.** Angular characterization of the skull after Martin and Saller [9]. The categories were given after Alekseev and Debets [16]

| No | Measurements | Degree | Category | Rubrication |
|---|---|---|---|---|
| 72 | Total facial angle | 85° | Large | Orthognathous |
| 73 | Middle facial angle | 87° | Large | Orthognathous |
| 74 | Alveolar angle | 84° | Very large | Mesognathous |
| 75 | Nasal bones angle | 66° | – | – |
| 75(1) | Angle of nasal projection | 21° | Small | – |
| 77 | Naso-malar angle | 153° | Very large | |
| < zm | Zygomaxillar angle | 148° | Very large | – |

**Table 3.** Index characterization of the skull after Martin and Saller [9]. The categories were given after Alekseev and Debets [16]

| Indices | | % | Characterisctics | Category |
|---|---|---|---|---|
| 8:1 | Cranial index | 78.69 | Mesocranic | Medium |
| 17:1 | Height-length index | 72.13 | Orthocranic | Small |
| 17:8 | Height-breadth index | 91.67 | Tapeinocranic | Small |
| 9:8 | Frontoparietal index | 75.00 | Eurymetopic | Very large |
| 48:45 | Upper facial index | 50.38 | Mesenic | Small |
| 52:51 | Orbital index | 87.18 | Hypsiconchic | Large |
| 54:55 | Nasal index | 52.00 | Chamaerhinic | Large |
| 61:60 | Maxilloalveolar index | 148.89 | Brachyuranic | Very large* |
| 63:62 | Palatal index | 138.71 | Brachystaphylinic | Very large* |
| 40:5 | Alveolar/Gnathic index | 91.40 | Orthognathic | Small |
| DS:DC | Dacrial index | 40.74 | – | Small |
| SS:SC | Simotic index | 33.33 | – | Small |
| 16:7 | Index of foramen magnum | 70.21 | – | Very small |

* The value of theindex is out of the borderlines of the category

The neurocranium was round in shape (**Fig. 2b**) with medium size and relatively low. The frontal bone was broad and bulging with entirely preserved metopic sutures (**Figs. 2a, b**). The occipital bone was broad and slightly bulging as well. At the posterior part of the sagittal suture a depression was observed (**Fig. 2b**). Foramen magnum was extremely large with notch in its posterior margin (**Fig. 2c**). The basal angle lies at the midpoint between normal and basilar kyphosis, i.e. extensive flection (**Fig. 3**). There was also uncompleted pterygoalar foramen on the left side, formed by the partial ossification of the pterygoalar ligament. The paranasal sinuses were underdeveloped as the frontal sinus was missing. The mastoid air cells were underdeveloped as well. A mild osteosclerosis of the skull was observed.

Multiple Wormian bones (WBs) with mosaic pattern occupied an oval-shaped territory at lambda (**Fig. 4**). They were relatively large in size (**Table 4**). Separate WBs were also placed along the lambdoid suture (**Table 5**). In addition, epipteric bones, postsquamosal bones and WBs in the occipitomastoidal suture were observed bilaterally (**Table 6**). According to Cremin et al. [4], WBs are of significance and could be accepted as a possible indicator of abnormal development when they are 10 or more in number with a diameter exceeding 6 × 4 mm, and arranged in a general mosaic pattern. The association of WBs with definite pathological conditions was widely discussed in our previous work [10].

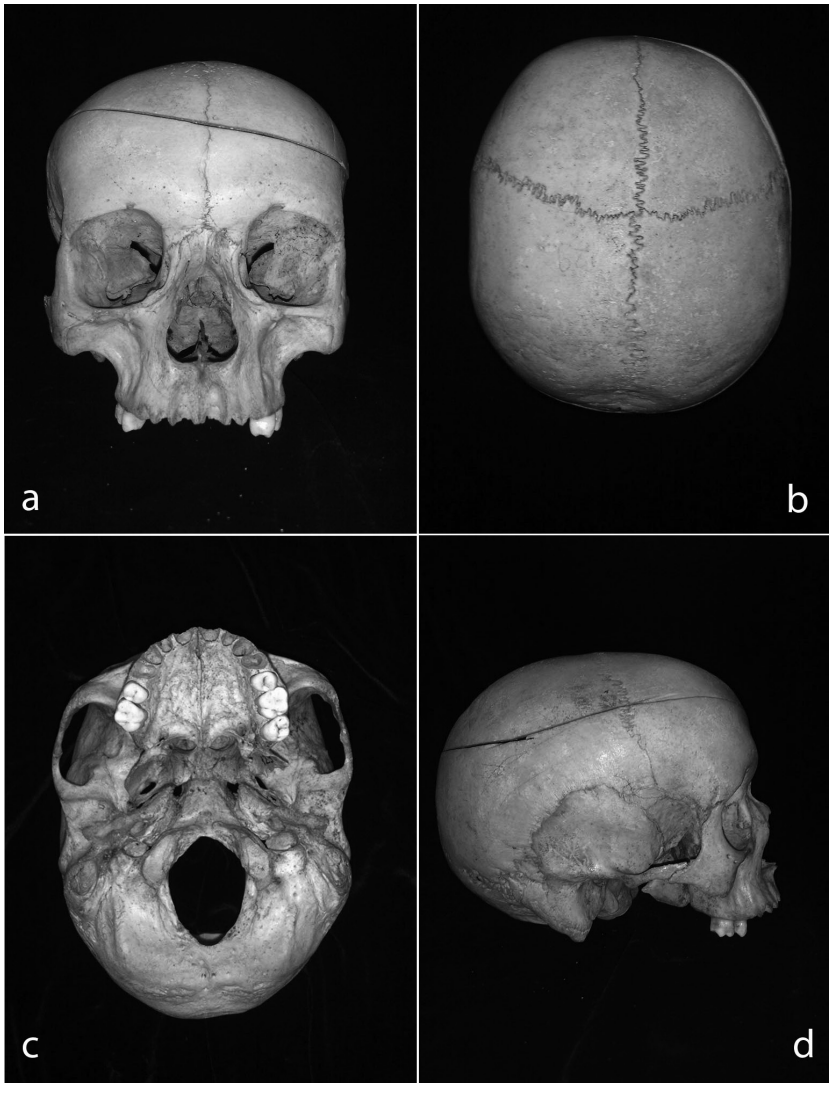


**Fig. 2.** Views of the skull: a) frontal; b) parietal; c) basilar; d) right lateral

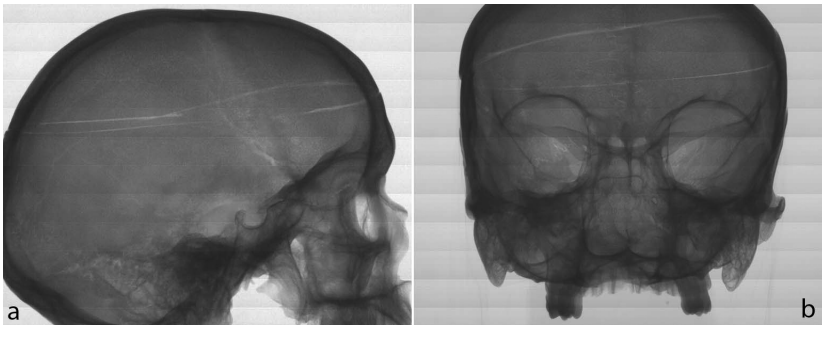


**Fig. 3.** Digital radiographs of the skull: a) lateral view; b) frontal view

**Table. 4.** Measurements of the Wormian bones in the region of lambda in mm

| No | Wormian bones in lambda | |
|---|---|---|
| | length | width |
| 1 | 26 | 11 |
| 2 | 24 | 9 |
| 3 | 15 | 6 |
| 4 | 21 | 11 |
| 5 | 25 | 12 |
| 6 | 17 | 8 |
| 7 | 16 | 4 |
| 8 | 15 | 4 |
| 9 | 19 | 7 |
| 10 | 15 | 5 |
| 11 | 18 | 15 |
| 12 | 24 | 15 |
| Total | 41 | 47 |

**Table 5.** Measurements of the Wormian bones in the lambdoid suture in mm

| Wormian bones in lambdoid suture | | | | | |
|---|---|---|---|---|---|
| Right | | | Left | | |
| No | length | width | No | length | width |
| 1 | 14 | 5 | 1 | 19 | 3 |
| 2 | 18 | 5 | 2 | 16 | 5 |
| 3 | 21 | 6 | 3 | 17 | 5 |
| 4 | 16 | 4 | 4 | 9 | 2 |
| 5 | 22 | 6 | 5 | 13 | 4 |
| 6 | – | – | 6 | 17 | 6 |
| 7 | – | – | 7 | 16 | 4 |
| 8 | – | – | 8 | 8 | 3 |
| 9 | – | – | 9 | 12 | 5 |

**Table 6.** Measurements of the other Wormian bones in mm

| Bones | Right | | Left | |
|---|---|---|---|---|
| | length | width | length | width |
| Os epiptericum | 22 | 10 | 14 | 4 |
| | – | – | 10 | 10 |
| Os postsquamosum | 16 | 14 | 14 | 9 |
| Os Wormi suturae occipitomastoidea | 5 | 6 | 20 | 12 |

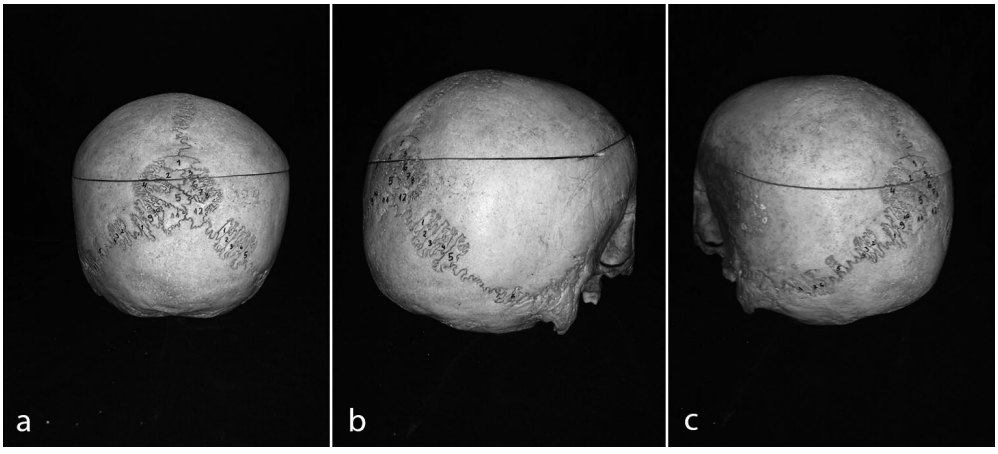


**Fig. 4.** Wormian bones: a) in lambda region; b) in lambdoid suture on the right side; c) in lambdoid suture on the left side

*Postcranial skeleton*

The available long bones did not show traces from healed fractures or perimortem inflicts, but the lack of other postcranial bones was an obstacle for complete assessment. The bones displayed thinning of the cortex and expansion of the medullary cavity. Their shape and size were normal except for both humeri whose distal ends were bowed forward (**Fig. 5**).

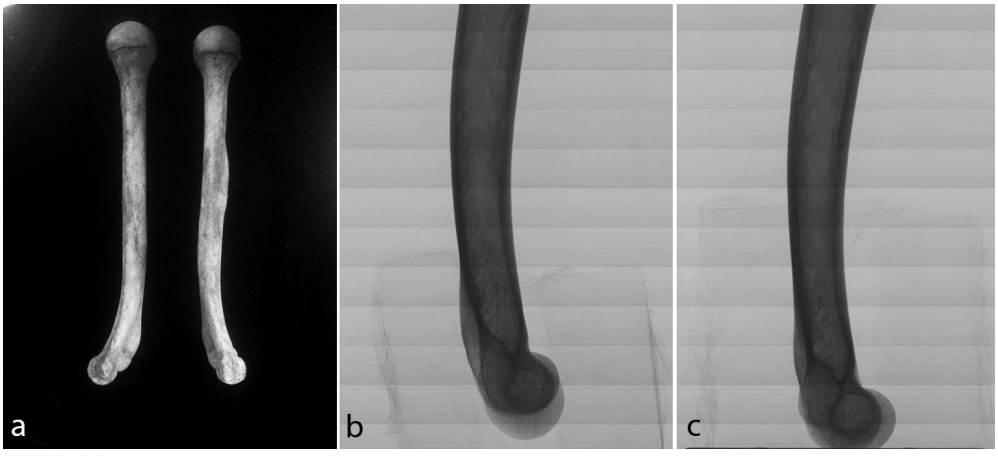


**Fig. 5.** Bowing of the distal ends of both humeri: a) right and left humeri; b) digital radiograph of the right humerus; c) digital radiograph of the left humerus

The deltoid tuberosity region of the right humerus was swollen and displayed a prolonged lesion – 22 mm long and 9 mm wide (**Fig. 6**). From the proximal end of the lesion started a 12 mm long canal that runs parallel to the bone axis. The aperture of the canal was round (6 × 6 mm). The canal did not communicate directly with the medullary cavity of the bone (**Fig. 6c**). This lesion probably is a consequence of a Brodie's abscess (subacute osteomyelitis) located on the diaphyseal cortex. Brodie's abscesses

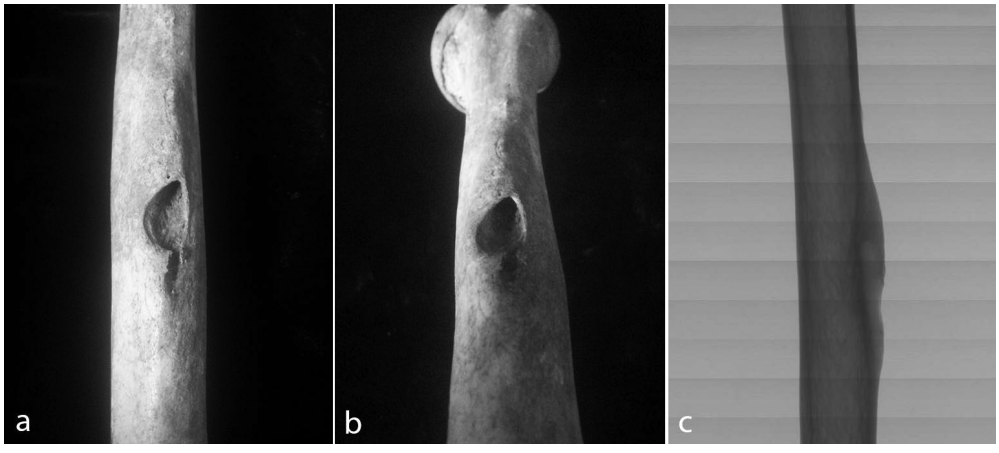


**Fig. 6.** Bone lesion on the left humerus: a-b) close views of the lesion; c) digital radiograph of the lesion, lateral view

are especially common in the metaphisis in children and occur less frequently in other tubular, flat or irregular bones, including the vertebral bodies, and are diaphyseal in location [12].

The left tibia was twice lighter in weight than the right one. The radiographs revealed excessive cortical thinning with medullary expansion (**Fig. 7**). It has been established that the immobilization causes a bone mass lost by reducing the bone mineral density in the epiphyses and by reducing the cortical wall thickness achieved by advanced endosteal resorption in the diaphyses [5]. Thus, the immobilization of the left leg of the individual due to some kind of trauma could be a reasonable explanation for this localized extra thinning.

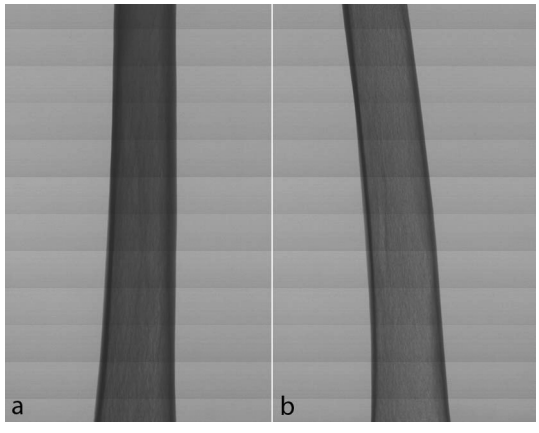


**Fig. 7.** Digital radiographs showing the cortical thickness of both tibiae: a) right tibia; b) left tibia

The stature of the individual, calculated on the basis of the lengths of the tibiae and the humeri despite the bowing (**Table 7**), was 164.4 cm. The stature was slightly below the mean body height of the recruits in Bulgaria during the period from 1897 to 1920 year which varied around 166 cm [14]. The individuals affected by skeletal dysplasias

most commonly had a disproportionately short stature due to short-trunk or short-limb. Obviously, in our case the individual was with normal length of the limbs, and bearing in mind that it was fit for service, probably was with normal trunk size as well.

**Table 6.** Lengths of the long bones in mm

| **Humerus** | | **Tibia** | |
|---|---|---|---|
| **right** | **left** | **right** | **left** |
| 321 | 315 | 367 | 370 |

The differential diagnosis showed that the observed skeletal abnormalities most probably were due to craniotubular dysplasia with increased bone density. *Craniometadiaphyseal dysplasia* (CRMDD)*, wormian bone type* is such a disorder with autosomal recessive inheritance and cranial, metaphyseal and diaphyseal involvement. The generalized manifestation on the cranium includes: a large circumference of the skull; a prominent forehead, frontal bossing and parietal bulging; multiple WBs; a delayed ossification of the cranial vault and wide open anterior fontanelle; a calvarial thickening; a mild sclerosis of the skull base; obliterated paranasal sinuses and basal skull foramina; hypoplastic malar bones; noted maxilla and mandible; high palate; increased caries and dental hypoplasia. The most frequently manifested features on the postcranial skeleton include: an abnormal modeling of tubular bones; lack of normal diaphyseal constriction and poor metaphyseal flaring; osteoporotic bones with thin cortices; bowing of lower limbs; coxa valga; wide long bones, short tubular bones; widen ribs and clavicles; chest deformity; multiple fractures causing severe scoliosis. There were also reported isolated cases of occipital horns, natal teeth, distorted pelvis and short stature [3, 6, 12]. Most of the symptoms of this rare disorder resemble to a great extent those manifested in the investigated bone remains.

Pyknodysostosis is another skeletal dysplasia with increased bone density and similar manifestation on the cranium, but the difference came from the long bones appearance with generalized osteosclerosis, narrowed medullary cavity and short stature, particularly the limbs. By this reason, we suspected CRMDD as more likely diagnosis. However, absence of the other postcranial bones was an obstacle to the complete assessment of the disorder manifestation. Certainly, even though we performed a detailed skeletal survey, an investigation based solely on bone remains has to a great extent an interpretative character, whereas the confirmation of such rare and specific disorder requires more convincing proofs.

## Conclusions

The observed abnormalities were due to skeletal dysplasia with increased bone density and CRMDD was suspected as a probable diagnosis. The individual was fit for service, which suggests a normal stature and normal mental development without severe malformations.

*Acknowledgement:* This work was partially supported by FP7 project AComIn "Advanced Computing for Innovation", grant 316087, and Bulgarian Ministry of Education and Science grant DO1-192/214. The authors would like to acknowledge the kind assistance given by the staff of the National Museum of Military History (Bulgaria).

## References


1. **Alanay, Y., R. Lachman.** A Review of the Principles of Radiological Assessment of Skeletal Dysplasias. – J. Clin. Res. Pediatr. Endocrinol., **3**(4), 2011, 163-178.
2. **Buikstra, J. E., D. Ubelaker.** Standards for data collection from human skeletal remains. – Arkansas Archeological Survey Research Series # 44. 1994.
3. **Castriota-Scanderbeg, A., B. Dallapiccoia.** Abnormal skeletal phenotypes. Berlin Heidelberg, Springer Verlag, 2005.
4. **Cremin, B., H. Goodman, J. Spranger, P. Beighton.** Wormian bones in osteogenesis imperfecta and other disorders. – Skeletal Radiology, **8**, 1982, 35-38.
5. **Eser, P., A. Frotzler, Y. Zehnder, L. Wick, H. Knecht, J. Denoth, H. Schiessl.** Relationship between the duration of paralysis and bone structure: a pQCT study of spinal cord injured individuals. – Bones, **34**(5), 2004, 869-880.
6. **Gorlin, R. J., M. M. Cohen, R. C. M. Hennekam.** Syndromes affecting bone: graniotubular bone disorders. – In: Syndromes of the Head and Neck. 4th ed., Oxford University Press, 2001, pp. 285.
7. **Işcan, M. Y., M. Steyn.** The human skeleton in forensic medicine. Springfield, Charles C. Thomas Publisher, 2013.
8. **Krakow, D., D. Rimoin.** The skeletal dysplasias. – Genet. Med., **12**(6), 2010, 327-341.
9. **Martin, R., K. Saller.** In: Lehrbuch der Anthropologie in sistematischer Darstellung. Stuttgart, Gustav Fischer Verlag, 1957.
10. **Nikolova, S. Y., D. Toneva, Y. Yordanov, N. Lazarov.** Multiple Wormian bones and their relation with definite pathological conditions in a case of an adult cranium. – Anthropol. Anz., **71**, 2014, 169-190.
11. **Pearson, K., A. Lee.** Mathematical contributions to the theory of evolution. V. On the reconstruction of the stature of prehistoric races. – Phylosophical Transactions of the Royal Society, ser. A, **192**, 1899, 169-244.
12. **Resnick, D.** Diagnosis of bone and joint disorders. – USA, W. B. Saunders Company, 2002.
13. **Scheuer, L., S. Black.** Developmental Juvenile Osteology. – London, Academic Press, 2000.
14. **Stoev, R.** Body height in recruits in Bulgaria. – Acta Morphol. Anthropol., **18**, 2012, 95-101.
15. **Unger, S., A. Superti-Furga, D. Rimoin.** A diagnostic approach to skeletal dysplasias. – In: Pediatric bone (ed. F. H. Glorieux, J. M. Pettifor and H. Jüppner), USA, Elsevier Science, 2003, 375-400.
16. **Алексеев, В. П., Г. Ф. Дебец.** Краниометрия. Москва, Наука, 1964
17. **Герасимов, М. М.** Восстановление лица по черепу. – В: Труды Инс. Этнографии, новая серия, XXVIII. Москва, АН СССР, 1955.

Institute of Experimental Morphology, Pathology and Anthropology with Museum
Bulgarian Anatomical Society

Acta morphologica et anthropologica, 22
Sofia ● 2015

# Variations in the Form of the Inferior Orbital Fissure

*S. Nikolova, D. Toneva*

*Department of Anthropology and Anatomy, Institute of Experimental Morphology, Pathology and Anthropology with Museum, Bulgarian Academy of Sciences, Sofia*

The inferior orbital fissure is a gaping cleft which extends from the temporal fossae to the orbital cavity through which the orbit communicates with the temporal, infratemporal, and pterygopalatine fossae. The outline of the IOF could be linear, narrow, moderate or wide or it may have the form of a narrow or moderate slit with a greatly enlarged lateral extremity. So, the aim of the present study was to investigate the outline of the IOF and to assess the sexual and bilateral differences of its distribution.

It was found that the outline of the IOF most commonly ranged from a narrow to a moderately wide slit as the rounded IOF was relatively rare. In most of the cases the rounded IOF was observed bilaterally, as the unilateral rounded IOF was found in few cases only on the left side. There were no significant bilateral or intergroup differences.

*Key words:* inferior orbital fissure; sphenomaxillary fissure; cranial series.

## Introduction

The inferior orbital (sphenomaxillary) fissure is a gaping cleft which extends from the temporal fossae to the orbital cavity [4]. The inferior orbital fissure (IOF) is bounded superiorly by the lower border of the orbital surface of the great wing of the sphenoid bone. Inferiorly, IOF is enclosed by the lateral border of the orbital surface of the maxilla and the orbital process of the palatine bone. Laterally, the IOF borders on a small part of the zygomatic bone and medially IOF joins at right angles with the pterygomaxillary fissure. Through the IOF the orbit communicates with the temporal, infratemporal, and pterygopalatine fossae. The fissure transmits the maxillary nerve and its zygomatic branch, the infraorbital vessels, the ascending branches from the sphenopalatine ganglion, and a vein which connects the inferior ophthalmic vein with the pterygoid venous plexus [3]. The IOF serves as an important anatomic landmark during endonasal endoscopic approaches to the skull base and orbit [1].

It was reported that the outline of the IOF could be linear, narrow, moderate or wide or it may have the form of a narrow or moderate slit with a greatly enlarged lateral extremity [8]. Thus, the aim of the present study was to investigate the outline of the IOF and to ascertain whether there were significant bilateral and sexual differences.

## Materials and Methods

The study was performed on a total of 438 adult skulls from both sexes. The skulls were grouped into three series: a contemporary male series (CMS), a medieval male series (MMS) and a medieval female series (MFS). The CMS consisted of 198 skulls from the Military Mausoleum with Ossuary, National Museum of Military History (Bulgaria). The MMS (122 skulls) and MFS (118 skulls) were part of the osteological collection of the Institute of Experimental Morphology, Pathology and Anthropology with Museum, Bulgarian Academy of Sciences. The age and sex of the individuals from the medieval series were previously determined.

The form of the IOF was macroscopically observed on both sides using the criteria suggested by Movsesyan et al. [11], i.e. slit (**Fig. 1a**) or rounded IOF (**Figs. 1b, c**). We preferred to use these simplified criteria to reduce the subjectivity in accounting of


**Fig. 1.** Forms of the inferior orbital fissure: a) bilaterally narrow inferior orbital fissure in a skull from the medieval male series; b) bilaterally rounded inferior orbital fissure in a skull from the contemporary male series; c) bilaterally rounded inferior orbital fissure in a skull from the medieval male series

the numerous borderline cases between the forms suggested by Wood-Jones [8]. The statistical significance of the bilateral and intergroup (CMS-MMS and MMS-MFS) differences in the IOF outline was assessed by chi-square ($\chi^2$) test at $p < 0.05$.

## Results

The results showed that among the three investigated series the outline of the IOF ranged predominantly from a narrow to a moderately wide slit. The rounded IOF was relatively rare. Among the CMS, rounded form of IOF was observed in total of 20 (10.10%) cases: 9 (4.55%) on the right side and 11 (5.56%) on the left one. Out of them, IOF was found to be rounded bilaterally in 9 (4.54%) cases and unilaterally in only 2 (1.01%) cases on the left side.

Among the MMS, the IOF was observed to be rounded in 6 (4.92%) cases: by 3 (2.46%) for each side, as all of them were accounted only bilaterally.

The MFS showed a rounded IOF in a total of 4 (3.39%) cases: 1 (0.85%) on the right side and 3 (2.54%) on the left one. The rounded IOF was observed unilaterally in 2 (1.69%) cases on the left side and bilaterally in only 1 (0.85%) case.

There were not established statistically significant bilateral or intergroup (CMS-MMS, MMS-MFS) differences in the form of the IOF.

## Discussion

In comparative aspect, the IOF in human and the higher mammals represents the wide communication between the orbit and the temporal fossa found in lower vertebrates [7]. According to Duckworth [2], among the Hominoids the IOF is more commonly reduced and narrower. In the Gibbon, the IOF is widely open and the infraorbital suture does not persist on the facial aspect, while in the Orang-utan it is a mere cleft of small dimensions as the infraorbital suture rarely persists long on the facial surface. In the Chimpanzee, the IOF is reduced to a narrow cleft as well. The IOF in the Gorilla is much narrowed and sometimes the malar bone does not provide the end-boundary of the fissure and then a sphenomaxillary suture occurs. In human the IOF is typically wider. In this respect, the human skull showed a more primitive feature compared to the other Hominoids, which are highly specialized and possess a narrower IOF [2].

Ontogenetically, the width of the IOF depends on the development of the maxillary sinus [5], thus the IOF is relatively large and wide in fetuses and infants [6, 7]. Furthermore, the IOF is relatively larger in the aged due to absorption of its bony margins. Either from this cause or from mal-development, the anterior end of the IOF may be abnormally large and encroach upon the lateral wall of the orbit [7].

An investigation performed by Wood-Jones [9] showed that among Hawaiian skulls from both sexes (n = 100), the IOF was narrower compared to that considered as normal in the European skull in 45% of cases and conformed to the type usual in Europeans in 15%. However, we could not find any data concerning the outline of the IOF among the different racial types. Nevertheless, according to Wood-Jones [9] the IOF in Hawaiian was wider than the normal in 15% and in 25%, although the medial portion and upper extremity of the fissure were unduly narrow, the lower lateral termination was expanded into a well-marked, often recurved, rounded dilatation. In addition, the forms for both sexes showed exact equality.

Another investigation of Wood-Jones [10] among the skulls of prehistoric inhabitants of Guam (n = 92) showed that the IOF was narrower than the European normal one in 59%. It was of normal width in 32%, wider than the average in only 2% and of the narrower type but with expanded extremity in 7%.

Our results were not exactly comparable to those of Wood-Jones [9, 10], but it could be inferred that among the investigated cranial series the outline of the IOF most commonly ranged from a narrow to a moderately wide slit and the rounded IOF was a relatively rare finding. Furthermore, in most of the cases the rounded IOF was observed bilaterally, as in few cases it was found unilaterally only on the left side. There were not established significant bilateral or intergroup (CMS-MMS; MMS-MFS) differences.

The knowledge of IOF morphology is not only of scientific interest, but it is of practical importance for both neurosurgeons and otolaryngologists who navigate in the region [1]. Obviously, further precise morphometric investigations of the IOF are necessary for a more detailed examination of its anatomy and outline.

## Conclusion

Most commonly the outline of the IOF ranged from a narrow to a moderately wide slit as the rounded IOF was a relatively rare finding. In most of the cases the rounded IOF was observed bilaterally and only in few cases it was found unilaterally on the left side. There were no significant bilateral or intergroup differences.

*Acknowledgment:* The authors would like to acknowledge the kind assistance given by the staff of the National Museum of Military History (Bulgaria).

## References


1. **De Battista, J. C., L. Zimmer, P. Theodosopoulos, S. Froelich, J. Keller.** Anatomy of the inferior orbital fissure: implications for endoscopic cranial base surgery. – J. Neurol. Surg. B. Skull Base, **73**(2), 2012, 132-138.
2. **Duckworth, W. L. H.** Morphology and anthropology: A handbook for students, **I**, 2nd ed., Cambridge, University Press, 1915.
3. **Gray, H.** Anatomy of the Human Body. (Thoroughly rev. and re-edited by Warren H. Lewis), 20th ed., Philadelphia, Lea & Febiger, 1918.
4. **Lasjaunias, P., A. Berenstein.** Functional anatomy of craniofacial arteries. – In: Surgical Neuroangiography, **1**,1987, Berlin, Springer -Verlag.
5. **Patnaik, V. V. G., B. Sanju, R. K. Singla.** Anatomy of the Bony orbit – Some Applied Aspects. – J. Anat. Soc. India, **50**(1), 2001, 59-67.
6. **Scheuer, L., S. Black.** Developmental juvenile osteology, London, Academic Press, 2000.
7. **Whitnall, S. E.** The Anatomy of the human orbit and accessory organs of vision. – London, Frowde and Hodder & Stoughton, 1921.
8. **Wood-Jones, F.** The Non-metrical Morphological Characters of the Skull as Criteria for Racial Diagnosis: Part I: General Discussion of the Morphological Characters Employed in Racial Diagnosis. – J. Anat., **65**(2), 1931, 179-195.
9. **Wood-Jones, F.** The non-metrical morphological characters of the skull as criteria for racial diagnosis: Part II: The Non-metrical Morphological Characters of the Hawaiian Skull. – J. Anat., **65**(3), 1931, 368-378.
10. **Wood-Jones, F.** The non-metrical morphological characters of the skull as criteria for racial diagnosis: Part III: The Non-metrical Morphological Characters of the Skulls of Prehistoric Inhabitants of Guam. – J. Anat., **65**(4), 1931, 438-445.
11. **Мовсесян, А. А., Н. Мамонова, Ю. Рычков.** Программа и методика исследования аномалий черепа. – Вопросы антропологии, **51**, 1975, 127-150.

Institute of Experimental Morphology, Pathology and Anthropology with Museum
Bulgarian Anatomical Society

Acta morphologica et anthropologica, 22
Sofia ● 2015

# Results from the Anthropological Investigation of Human Bone Remains from Excavations on UPI 5040 Section of Antique Necropolis of Apolonia Pontica

*V. Russeva*

*Institute of Experimental Morphology, Pathology and Anthropology with Museum, Bulgarian Academy of Sciences*

The study includes results from the investigation of human bone remains from two complexes with inhumation and three ones with cremation burial ritual, investigated during excavations of a section of the antique necropolis of Apolonia Pontica, situated in the area of Kalfata-Budzhaka, included in recent building activity. The investigated materials shed light to the history of the population, which inhabited the antique town in the 3rd-5th c. BC.

*Key words:* South necropolis, Apolonia Pontica.

## Materials and Methods

During archaeological excavation on a section of the antique necropolis of Apolonia Pontica in the area "Kalfata/Budzhaka", committed to modern construction activity, five burial complexes are uncovered [10]. Three of them, N 1, 2 and 4 are result from burials after the cremation ritual, and two, respectively N 3 and 5, after inhumation ritual. Complexes are dated in the 3rd-5th c. BC, or graves with cremation burial ritual, N 1 and 2 and the inhumations N 3 and 5 in the beginning-first quarter of the 3rd c. BC, and a complex with cremation N 4 in the 5th c. BC [10]. The anthropological investigation is held in laboratory conditions aiming to provide information about age, sex and additional individual specifics of buried according to preserved material.

In anthropological identification are used classical methods. One of the skeletons from inhumations, from grave N 5 is almost completely preserved. The one from grave N 3 is partially preserved, missing skull fragments, except a big portion from the lower jaw, vertebral column, except a fragment from a thoracic vertebra, ribs and some fragments from bones of limbs. The preserved portion of the skull vault from grave N 5 allowed use of methods for assessment of cranial sutures obliteration [7, 9]. Grave N 3 doesn't provide much data for age estimation, except auricular surface on both iliac bones, preserved in poor condition, but assessed as showing degenerative relief, and age was estimated according to it in broader limits, being impossible to precise the exact stage of development [5]. The sexual identification in both inhumations is achieved

by the form of the greater schiatic notch [1, 7]. The sexual identification of individual from grave N 5 is also confirmed by the features of cranial bones [6]. Material from complexes with cremation burial ritual is in relatively large quantities with many big, identifiable fragments, suggesting low pyre temperature. These complexes provided sufficient number of fragments with identifiable anatomical sites (**Fig. 1**), which served in anthropological identification. For age achievement in cases of cremated bone remains are applied methods for assessment of cranial sutures obliteration [7, 9]. In all complexes with cremated remains, N 1, 2 and 4, are identified fragments from bones with finished development. In material from grave N 2 are found numerous remains from permanent teeth with finished root development, which confirmed data from bones from the postcranial skeleton, which point to individual with finished skeletal development.

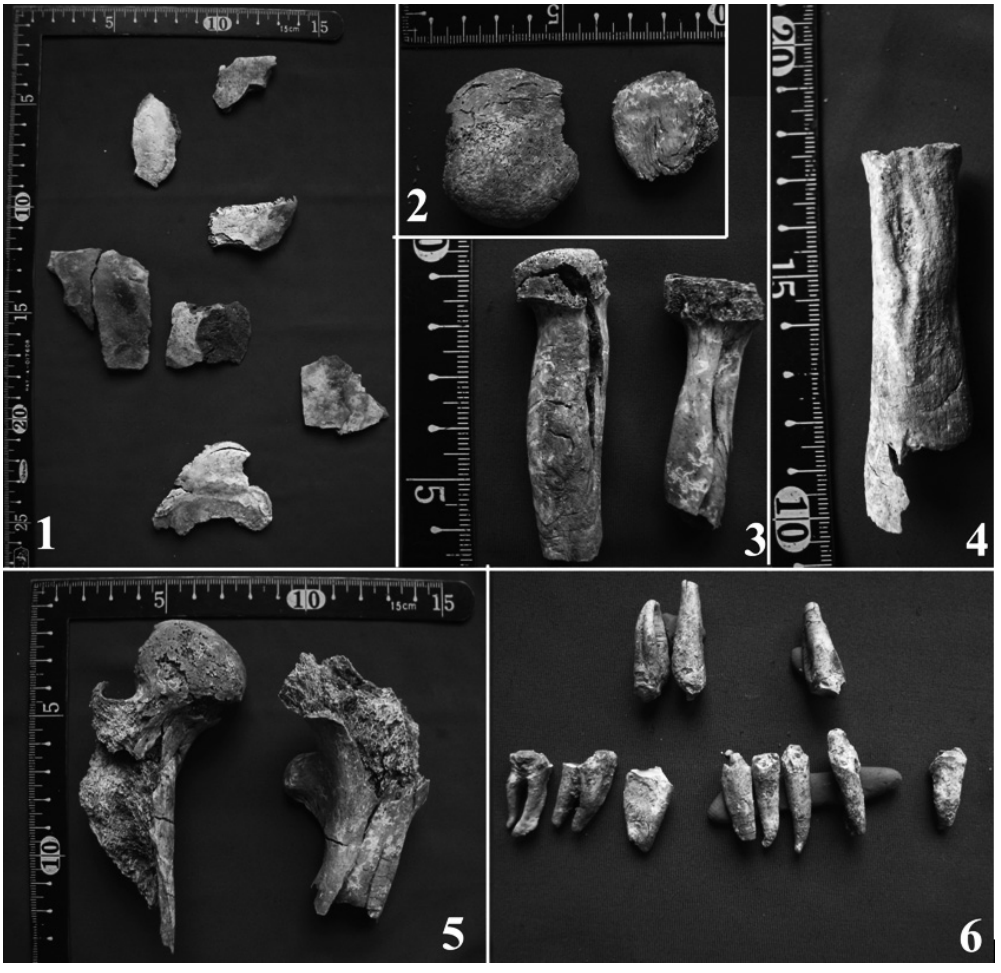


**Fig. 1.** Identified materials from cremations. **1.1.** Identified fragments from skull vault, grave, N 4. **1.2.** Left patellae with different dimensions from an adult and a child, grave N 1, presenting different individuals in the material from cremation. **1.3.** Proximal fragments from both radiuses, grave N 1. **1.4.** Fragment from diaphysis of right humerus , enthesopathic changes on the right humerus, enthesopathic lesion on the place of attachment of latissimus dorsi muscle, grave N 1. **1.5.** Proximal fragments from both femurs, grave N 1. **1.6.** Fragments from permanent dentition, grave N 2

Two of the complexes with cremated materials and both inhumations provide some metrical data for correlation to standard tables for diameters of femoral, humeral and radial heads, femoral and humeral bicondylar breadth (**Tables 1, 2**) [2, 4]. In both inhumations obtained measurements are relatively high and stay between both sexes (**Table 2**). Results for both complexes with cremations, graves N 1 and 2, don't contribute much for sexual identification, as none of the obtained dimensions is complete (**Table 1**). Nevertheless, reconstructed measurements point to male sexual identification. In one case dimensions are used in age determination after proving smaller values than expected for an adult individual. Material from both inhumations allows individual's stature reconstruction after lengths of long bones of limbs, achieved by Trotter-Glaeser's and Pearson-Lee's formulae [8]

**Table 1.** Basic measurements in cm. Complexes with cremation

| **Bone 1** | **Grave N 1** | | **Grave N 2** |
|---|---|---|---|
| | **D** | **B** | **D** |
| Femur dx/sn | > 4.00 | – | > 4.10 |
| Humerus dx/sn | > 3.90 | – | – |
| Humerus sn? | – | > 5.20 | – |
| Radius dx | > 1.90* | – | – |
| Radius sn | > 1.85* | – | – |
| Radius dx/sn | – | – | > 2.10* |
| Patella dx | 320** | 3.15 | – |

**Reconstructed measurement is characteristic for male sex; D – head diameter; B – bicondylar breadth; **height; dx – right; sn – left.*

**Table 2.** Basic measurements in cm. Complexes with inhumation. Stature estimation

| **Bone** | **Grave N 3** | **Grave N 5** | | |
|---|---|---|---|---|
| | **L** | **L** | **D** | **B** |
| Femur dx | | 44.1 | 4.55 | 7.4 |
| Femur sn | ≥ 44.8 | 43.5 | 4.6 | 7.46 |
| Tibia dx | 38.6 | 35.8 | – | – |
| Tibia sn | 38.8 | 36.0 | – | – |
| Humerus dx | | 31.0 | – | – |
| Humerus sn | | 29.9 | – | – |
| Stature *T-G* | 173.76 (170.4÷177.12)* | 163.96(160.42÷167.50)** | | |
| Stature *P-L* | 165.8* | 157.53 | | |

**Reconstructed stature after measurements of tibiae; ** Reconstructed stature after measurements of bones of lower limbs; T-G – Trotter-Glaeser's formula; P-L – Pearson-Lee's formula.*

## Results and Discussion

Preservation of the material in the graves with remains from a cremation burial ritual allows identification of the individuals approximately as three males at an age of 35-40 up to 45, 30-40 and 50-60 for graves N 1, 2 and 4, respectively. In two of the complexes is registered singular fragment from an individual at a different age. In the grave N 1 the age estimation of the additional bone, a left patella, as originating from a child at about 7 up to 14 years, highly contradicts to the determined age for the individual, presented in most fragments. In the other complex, grave N 4 difference in determined age is not as pronounced. Here the additional bone fragment is a small one, from the left parietal, from the place between the coronal and sagittal sutures, both showing complete lack of obliteration, which appears in contradiction with the observed advanced obliteration on the found lambdoid suture – complete on the endocranial surface and advanced, still visible, on the ectocranial surface. As such a situation could appear in some pathological conditions of premature, advanced obliteration in some segments of sutures here, even if most possibly can be found a second individual, presented in the singular discussed fragment, the situation is appraised as unclear. Inhumations provide more suitable material for age and sex identification and in these complexes are found remains from singular burials, containing two female individuals at an age approximately 40-50 each, age being less accurately determined for the individual from grave N 3, because of the insufficient data. As the investigated section is too small it is impossible from these results to be obtained more general conclusions for specifics in the burial ritual at the time with preference of incineration for males and, respectively, inhumations for females.

State of preservation of bones doesn't allow description of characteristics of anthropological type or physical development. Nevertheless, stature was obtained for both individuals from the inhumations (**Table 2**). The female from grave N 3 is expected to have reached at mean 173.76 cm after Trotter-Glaeser's formula and 165.8 cm after Pearson-Lee's one, being a female of a middle to high stature. The other female also reaches middle stature, being expected to have average height of 163.96 cm after Trotter-Glaeser's formula and slightly below middle stature with 157.53 after Pearson-Lee's formula for stature reconstruction. From traits, which form the anthropological type complex only on the cranial fragments from Grave N 5 is determined the form of lower margin of piriform aperture, shaped as *anthropina*.

Data for health condition of the individuals are poor. Some remains from dentitions are available in four individuals – from both inhumations and from cremations N 1 and 2 (**Fig. 1**). Only the one from grave N 5 presents full dentition (only lower left central incisor lost post-mortem). The material from grave N 3 (the other inhumation) presents a complete dentition of the lower jaw. Both individuals show relatively good dental health for determined age. In one of them there are two molars lost before death – both first molars. The other studied dentition showed no pathological changes in connection to the dental caries. Both dentitions showed periodontal changes of the alveolar processes. Both complexes with cremated bones N 1 and 2 confirm the results for good dental health of the population – the one from grave N 1 presented a fragment of mandible, on which the teeth had been present before death – these are both medial premolars, both canines and all incisors. Numerous teeth found in the material from grave N 2 point to their presence before death, too.

A specific trait, recognized on teeth – the linear enamel hypoplasia is ascertained on the dentition of individual from grave N 5. The lines correspond to 2 ½ and 3 years of age. These changes should be connected with periods, characterized by a developmental stress. They could have been caused either by a malnutrition and dietary deficiency,

or by periods of chronic, long-lasting disease during childhood. Such are not a rare finding in past populations, as childhood appeared as one of the most hazardous periods in human development in the preindustrial societies. The studied material doesn't confirm high incidence of this trait in the studied population – as the dentition from grave N 3 lacks such defects. The singular teeth from the incineration N 2 also can be assessed as unaffected of enamel hypoplasia with some degree of uncertainty. Specific changes, observed on the fragment from the frontal bone of the individual from grave N 1 point also to possibility of dietary insufficiency. Here the cortical bone from the *glabella* region and over superciliary arches shows porous structure (**Fig. 1**).

In the only fragment from a thoracic vertebra found in the remains from grave N 3 is ascertained bone reaction on the articulation surface with the rib (**Fig. 2**). Other preserved long bones of limbs show destructed places, on which the degenerative joint disease can't be observed, but lack of osteochondrotic defects point to lack or low de-

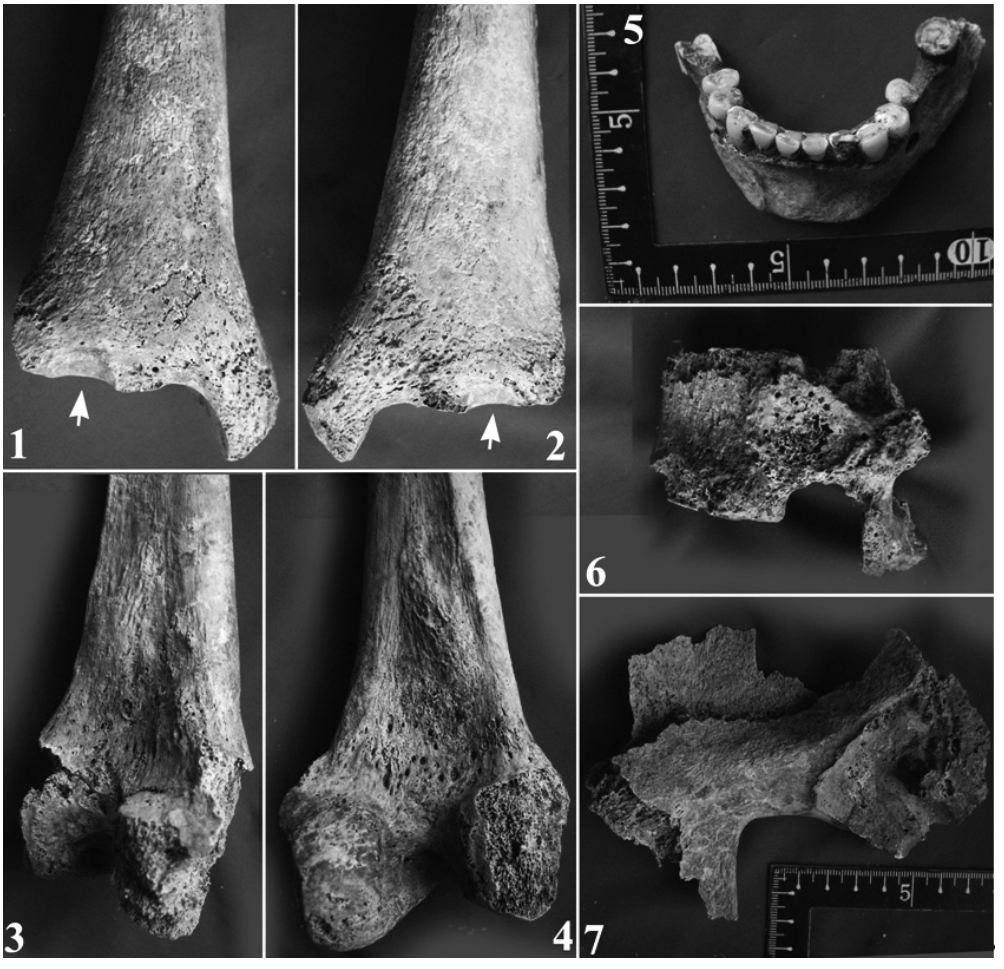


**Fig. 2.** Grave N 3. **2.1-2.** Right and left tibia. Lateral squatting facet, arrow. **2.3-4.** Right and left femur. Overdeveloped muscle relief. **2.5.** Fragment of the mandible, dentition. **2.6.** Thoracic vertebra. Bone reaction on the articulation surface with left rib. **2.7.** Fragment of right pelvic bone, form of *incisura ischiadica majo*

velopment of this pathology. The other skeleton from inhumations, the one from grave N 5, isn't affected from such changes.

Remains from two of the individuals show traces of tendon and muscle disorders. These are a fragment from the right humerus from grave N 1 with cremated bones and both femurs from grave N 3. In first case the place of the defect can be connected to the attachment site (insertion) of the latissimus dorsi muscle, where is formed a deep groove after an enthesopathic reaction (**Fig. 1**). In the other case, from grave N 3 on the dorsal side of both femurs is registered area of bone reaction and additionally grown relief (**Fig. 2**), which can be associated to adductors attachment site (insertion) possibly of adductor magnus muscle. This relief development could have been caused by overloading in habitual activity, incidental trauma, or specific health conditions. Some other clues about habitual activity are pronounced bilateral asymmetry with predominant lengths of bones of the right side of upper limbs of the only one relatively well preserved skeleton – the one from grave N 5. This points to clear right handedness. Bones of lower limbs of the other skeleton, from inhumation (grave N 3), point to reconstruction of long lasting squatting position in everyday life, pronounced in the clearly developed lateral squatting facets on both tibiae (**Fig. 2**) after methods of recognition of markers of muscolo-skeletal stress [3].

## Individual Results

**Grave N 1, cremation. Male, 35-40 to 45 years; sub-adult, 7-14 years**

Numerous fragments from cremated bones with relatively big dimensions.

*Age:* after obliteration of cranial sutures on found segments and low synostosis level of vertebrae of sacrum, which allowed their separation on pyre; ***sex:*** after massiveness of long bones, relief of muscle attachment sites, relief of occipital bone and reconstruction of big dimensions.

*Identifiable bones, cranial fragments:* occipital bone fragment, which shows developed relief; parietal bones fragments; frontal bone fragment from the *glabella* region, showing developed relief; segments from lambdoid and sagittal sutures, which show lack and initial obliteration, respectively; mandible fragment, from the chin area with alveoli of incisors, canines and first premolars, which had been lost after dead, possibly on pyre.

*Fragments from postcranial skeleton:* proximal and distal parts from both femurs (**Fig. 1: 5**); distal part from tibia; proximal parts from both humerals, radiuses (**Fig. 1: 3**) and left ulna, the latter shows massive structure and developed relief of muscle attachment sites; fragments from the articulation surface of both acetabula; fragments from seven thoracic, including first thoracic vertebra, all lumbar vertebrae and two proximal vertebrae from sacrum, separated in pyre; bones from this skeleton show massive structure, developed relief and fragments point to bones with relatively big dimensions (**Table 1**). In the material from this complex is found a left patella with small dimensions (**Table 1**).

*Pathology and specifics:* the fragment from frontal bone shows porous changes of the glabella region; the articulation surfaces of the long bones and vertebral fragments show lack of degenerative joint disease changes; a fragment from diaphysis of the right humeral bone shows deep enthesopathic lesion on the place of attachment of *latissimus dorsi* muscle (**Fig. 1: 4**).

*Individual fragment from different individual:* after dimensions of the found patella (**Fig. 1: 2**) it is associated to individual of sub-adult age, approximately *Infans II*, or 7-14 years at time of dead; there are no other identifiable bone fragment to be connected to this individual.

**Grave N 2, cremation. Male, 30-40 years.**

Numerous fragments from cremated bones with relatively big dimensions.

*Age:* after obliteration of cranial sutures on found segments; *sex:* after massiveness of long bones, relief of muscle attachment sites, relief of occipital bone and reconstruction of big dimensions.

*Identifiable bones, cranial fragments:* occipital bone fragment, which shows developed relief and segment of lambdoid suture with initial obliteration; fragment from left temporal bone with mastoid process with developed relief; fragments of teeth, from which are distinguished three canines, incisor, two premolars and roots and fragments from four molars, all teeth show finished root development and small dimensions (**Fig. 1:6**).

*Fragments from postcranial skeleton:* proximal parts from both femurs, proximal fragment from diaphysis of left tibia; distal part from both humerals; proximal parts of radius and left ulna; fragments from both taluses, which show bones with big dimensions; fragment from the first cervical (articulation surface of contact with the *dens axis*, fragment from another, unidentifiable cervical and two thoracic vertebrae.

**Grave N 3, inhumation. Female, (35) 40-50 years.**

Incomplete cranial and postcranial skeleton, many bones are not presented.

*Age:* after the relief of auricular surface of iliac bones; *sex:* after the form of greater sciatic notch.

*Cranial skeleton:* missing, except a big portion from mandible with preserved teeth; two separated from alveoli upper canine and molar (**Fig. 2:5**); the teeth show small dimensions; the mandible shows pronounced mental tubers, developed relief.

*Dentition:*

| | |
|---|---|
| 8 7 X 5 4 3 2 1 | 1 2 3 4 5 6 X 7 8 |

*Postcranial skeleton:* complete and fragmented long bones of limbs; fragment from thoracic vertebra, fragments of both pelvic bones with pronounced groove under auricular surfaces, which show degenerative relief.

*Pathology and specifics:* developed periodontal changes of the alveolar process of the mandible **(Fig. 2:5)**; on dorsal side of both femurs overgrowth of muscle attachment site, associated with adductor muscles **(Fig. 2:3-4)**; bone reaction on the place, more pronounced on the left bone.

**Grave N 4, cremation. Male, 50-60 years.**

Relatively numerous, but smaller number in relation to the material from graves N 1 and 2 fragments from cremated bones. ***Age:*** after obliteration of cranial sutures on found segments; ***sex:*** after the relief of occipital bone and form of upper margin of orbit.

*Possible additional fragment:* it appears possible that the described fragment from left parietal originates from another individual at lower age.

*Identifiable bones, cranial fragments:* occipital bone fragment, which shows developed relief and segment of lambdoid suture with advanced obliteration, fragments from parietals; fragment from left parietal between sagittal and coronal suture, both showing no obliteration; fragment from upper margin of orbit with oval shape (**Fig. 1:1**).

*Fragments from postcranial skeleton:* fragments from diaphyses of limbs; proximal fragment from left ulna; fragments from tree lumbar vertebrae.

**Grave N 5, inhumation. Female, 40-50 years.**

Relatively completely presented skeleton.

*Age:* after obliteration of cranial sutures; *sex:* after the form of greater sciatic notch and cranial features.

*Cranial skeleton:* incomplete *calva* (**Fig. 3**), missing fragment from left parietal; mandible and maxilla, with preserved dentition; sharp edge of upper orbital margins, no relief on *glabella* region, low relief of superciliary arches, advanced obliteration

**Fig. 3.** Grave N 5. Skull vault, frontal, left lateral, vertical and occipital views. Fragments from maxilla and fragment from sphenod and mandible

of cranial sutures; mandible with developed mental tubers, high angle, low relief; low abrasion of teeth; lower edge of piriform aperture is formed as *anthropina*.

*Dentition:*

| | |
|---|---|
| 8 7 6 5 4 3 2 1 | 1 2 3 4 5 6 6 7 8 |
| 8 7 6 5 4 3 2 1 | – 2 3 4 5 6 6 7 8 |

*Postcranial skeleton:* complete and fragmented bones of limbs; five cervical, including second cervical vertebrae, and all of thoracic and lumbar vertebrae, complete preserved and fragmented ribs; fragments from both pelvic bones, showing broad form of greater sciatic notch.

*Pathology and specifics:* developed periodontal changes of the alveolar processes; linear enamel hypoplasia, with lines corresponding to 2 ½ and 3 years of age; mild traces from recombined *cribra orbitalia*.

## Conclusions

The investigated material is still of small number, but it makes possible to obtain data for age and sex of the buried in the section of the necropolis and the results of this investigation point to relatively favorable conditions of survivorship for the studied period. Data about health condition of the buried are also poor, but again, results, mostly derived from presented dentitions, testify for a good health state of individuals during life.

## References


1. **Acsádi, G., J. Nemeskéri.** History of human life span and mortality. Budapest, Akademiai Kiado, 1970, 333.
2. **Bass, W.** Human osteology: a laboratory and field manual of the human skeleton. University of Missouri, 1971, 281.
3. **Kennedy K.** Skeletal markers of occupational stress. In: Iscan M. Y., Kennedy K. A. R., editors. Reconstruction of life from the skeleton. New York: Alan R. Liss. 1989, p. 129-160.
4. **Kühl, R.** Skelettreste aus prähistorische brandbestattungen und ihre aussagemöglichkeiten, mit hinweisen auf spezielle fragestellungen in schleswig-holstein. – MAGW, **115**, 1985, 113-137.
5. **Ubelaker, D.** Human Skeletal Remains: Excavation, Analysis, Interpretation. 2nd ed. Washington, D.C., Taraxacum, 1989.
6. **Walrath, D., P. Turner, J. Bruzek.** Reliability Test of the Visual Assessment of Cranial Traits for Sex Determination. – Am. J. Phys. Anthropol., **125**, 2004, 132-137.
7. **White, T., P. Folkens.** The Human Bone Manual. Elsevier, 2005, 464.
8. **Алексеев, В.** Остеометрия, методика антропологических исследований. Москва, Наука, 1966, 252.
9. **Алексеев, В., Г. Дебец.** Краниометрия, методика антропологических исследований. Москва, Наука, 1964, 228.
10. **Богданова, Т.** № 39. Спасително археологическо проучване на обект „Външен водопровод за УПИ XV-5040“, м. Калфата/Буджака, гр. Созопол. АОР за 2014 г., 360–363, София, 2015 г.

Institute of Experimental Morphology, Pathology and Anthropology with Museum
Bulgarian Anatomical Society

Acta morphologica et anthropologica, 22
Sofia ● 2015

# Anthropological Investigation of the Bone Remains from the Archaeological Site "Samuil – Tsar of Bulgaria" Monument

*D. Toneva[1], S. Nikolova[1], P. Stoyanova[2]*

*[1]Institute of Experimental Morphology, Pathology and Anthropology with Museum, Bulgarian Academy of Sciences*
*[2]Sofia History Museum*

This study presents the results from the anthropological investigation of the bone remains, revealed at the rescue archaeological excavations led on the place of the Samuil – Tsar of Bulgaria Monument. There were revealed 10 medieval graves, dated to the 11th-12th c. AD. The skeletons of 11 individuals were investigated. They were determined to belong to 6 adults (1 male, 4 female and 1 of undetermined sex), 1 juvenile and 4 children. The observation of the bone remains showed that one of the individuals was affected by spondylodiscitis and another one survived a trauma on the left leg. In addition, the skeleton of the male individual bore many traces of violence, including three depressed fractures on the skull, a tip of an arrow stuck in the left sacral ala as well as cut injuries affecting the inferior surface of the fourth lumbar vertebral body and the right humerus. None of these bone damages showed traces of healing, which suggests that the individual died a violent death.

*Key words:* bone remains, medieval, anthropological investigation.

## Introduction

At the end of 2014, rescue archaeological excavations had been performed on the place, where was put up a monument to Tsar Samuil (Sofia, Bulgaria). The archaeological site was located in the garden in front of the St. Sophia basilica within the borders of the Serdika – Sredets Historical and archaeological reserve, in the middle of the Eastern antique necropolis. The excavations were led by archaeologist Polina Stoyanova and covered an area of 13 $m^2$. There were revealed 10 medieval graves, distributed to two levels. The upper one included graves numbered from 1 to 5, and the lower one – from 6 to 10. According to the grave goods, the graves from the upper level were dated to the 11th-12th c. AD. The graves from the lower level were synchronous or a little earlier than the upper ones [12].

The results from the anthropological examination of the bone remains, revealed at the rescue archaeological excavations on the place of the Samuil – Tsar of Bulgaria Monument are presented in this study.

## Materials and Methods

The *in situ* position of the skeletons was documented on the site of the excavation and then the bones were picked up. The examination of the bone remains was performed in the Institute of Experimental Morphology, Pathology and Anthropology with Museum, BAS. The laboratory work started with cleaning and reconstruction of the fragmented bones, where it was possible. The signatures of the burials are identical with these of the archaeologists. There were two skeletons lying one on top of the other in *Grave 1*, which were marked as 1a (upper skeleton) and 1b (lower skeleton).

The sex of the individuals was determined according to the morphological characteristics of the skull and bones of the postcranial skeleton [1]. The age of the adults was determined according to the cranial sutural closure [1], Gerasimov's scale for dental attrition [11] and Todd pubic symphysis scoring system [1]. The degree of fusion of the epiphyses of the long bones and the fusion of the sacral vertebrae as well as of the pubis, ischium and ilium into single bones were also used for dating the age of the juvenile and adult individuals [6]. The age of the children was determined in accordance with the degree of bone growth and fusion between the bone segments [6], the length of the long bones of the limbs [2], and the stages of dental development and eruption [8].

The skulls and bones of the postcranial skeletons of the adult individuals were examined metrically and scopically by classical anthropological methods [3, 9, 10]. Descriptive statistics was not applied to the data, because of the small sample. The stature was calculated on the basis of the lengths of the upper and lower limb long bones according to the methods of Pearson and Lee [4] and Trotter and Gleser [7]. The long bones of the children were measured in order to be established their age after the method of Facchini and Veschi [2].

## Results

*Sex and age of the individuals*

*Grave 1.* There were two skeletons of adult individuals, lying one on top of the other. The upper skeleton (1a) belonged to an adult female with an age at death of 35-40 years. The second skeleton, lying below the other one, belonged to a female at about 30 years old.
*Grave 2.* Only the right and left tibiae and fibulae of the individual were available. They belonged to an adult, but the sex could not be determined.
*Grave 3.* The skeleton belonged to an adult female with an age at death of 30-35 years. The indexes of the skull showed that it was mesocranic (8:1), orthocranic (17:1), tapeinocranic (17:8), and metriometopic (9:8).
*Grave 4.* The bone remains belonged to an adult male. The age of the individual was determined at about 30 to 35 years.
*Grave 5.* The skeleton was determined to belong to a juvenile individual (15-16 years), probably female.
*Grave 6.* The bones belonged to a child at the beginning of the 1st year.
*Grave 7.* According to the available bone remains, the individual was determined as child around the age of 3 years and 8 months.
*Grave 8.* The skeleton belonged to a female individual. The age was determined in the age group *Adultus* (20-40 years). The indexes calculated between the skull measurements showed that the skull was hyperbrachicranic (8:1) and stenometopic (9:8).

*Grave 9.* The skeleton was determined to belong to a child at the age of 1 year and 10 months.
*Grave 10.* The bone remains belonged to a child at the age of 2 years and 7 months.

*Position of the skeletons in situ*

The burials were performed by laying of the bodies on the back with head to the west and with arms folded at the elbows and lying in the abdominal or thoracic region according to the Christian burial rite. However, two of the children deviated from the burial rite. The child from *Grave 7* was found with head on the right side, legs on the left side, the right arm turned upwards along the head and the left arm along the body. The child from *Grave 9* lied on the back in the upper part of the body, but with legs on the right side and arms along the body. On the site of the excavations, there were also found scattered human and animal bones.

*Stature of the adult individuals*

The stature of the adult individuals, calculated on the basis of the available long bones of both upper and lower limbs, is presented in **Table 1**.

**Table 1.** Stature of the adult individuals according to the methods of Pearson and Lee [4] and Trotter and Gleser [7]

| Grave | Methods | Stature |
|---|---|---|
| Grave 1a (female) | Pearson-Lee | 156.7 cm |
| | Trotter-Gleser | 161.6 cm |
| Grave 1b (female) | Pearson-Lee | 153.9 cm |
| | Trotter-Gleser | 157.8 cm |
| Grave 3 (female) | Pearson-Lee | 153.2 cm |
| | Trotter-Gleser | 158.5 cm |
| Grave 4 (male) | Pearson-Lee | 168.0 cm |
| | Trotter-Gleser | 174.5 cm |
| Grave 8 (female) | Pearson-Lee | 159.1 cm |
| | Trotter-Gleser | 165.7 cm |

*Paleopathological data*

Three of the buried individuals showed trace of some kind of pathological condition or violence.

The pathological changes observed on the bones from *Grave 2* showed that the individual probably suffered a trauma on the left leg above the ankle. The left tibia had a bony growth with an additional articular surface in the lower part of the bone. This articular surface was directed to the fibula, which also had a small bony growth with a corresponding additional articular surface (**Fig. 1a**). There were no traces of fractures on the bones. The pathological changes might have been caused by a traumatic injury affecting the muscles and tendons in this part of the leg. The injury probably led to a gait disturbance, resulting in severe osteoarthritic changes in the right knee, observed on the superior articular surface of the right tibia (**Fig. 1b**).

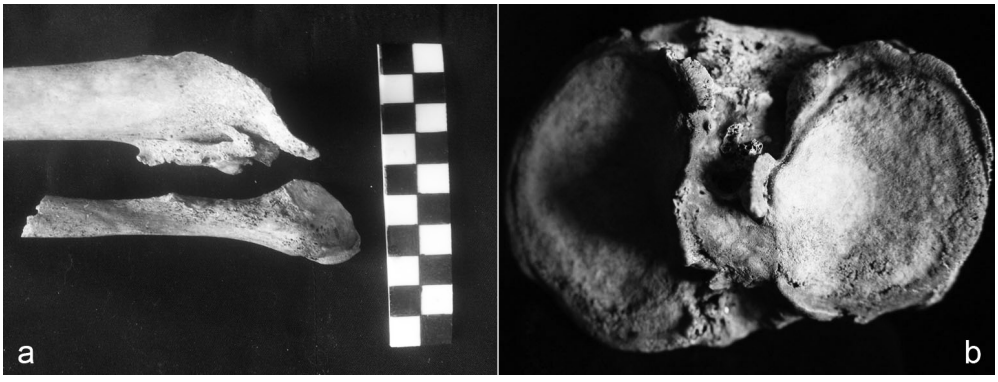


**Fig. 1.** Bones of the individual from *Grave 2*: a) The lower parts of the left tibia and fibula; b) The superior articular surface of the right tibia

The bones of the female from *Grave 3* also showed traces of pathological changes. The individual was affected by spondylodiscitis. There were lytic lesions on the vertebral bodies from the sixth thoracic vertebra to the fifth lumbar vertebra (**Fig. 2a**). The adjacent body surfaces between the twelfth thoracic and the first lumbar vertebrae and between the fifth lumbar vertebra and the body of the sacrum showed destructive changes indicative of epidural abscesses (**Fig. 2b**). The spondylodiscitis could be associated with different diseases – tuberculosis, brucellosis, staphyloccocal infections, etc [5]. Besides, the skull characterized with a complete atrophy of the maxillary alveolar process (**Fig. 2c**) and *cribra orbitalia* on the roof of the left orbit. Periostitis was observed on both tibiae and fibulae.

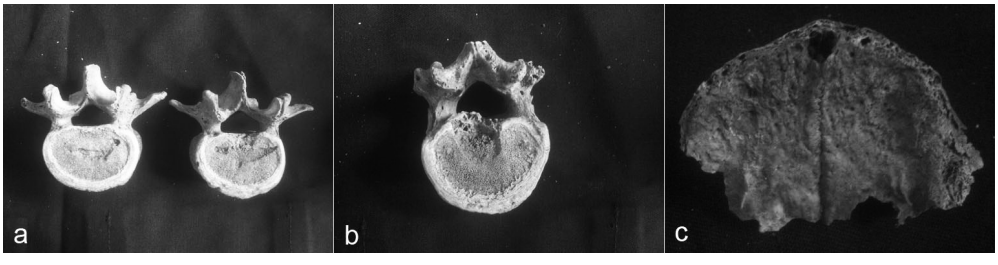


**Fig. 2.** Bones of the individual from *Grave 3*: a) The superior body surfaces of the second and third lumbar vertebrae; b) The inferior body surface of the twelfth thoracic vertebra; c) Complete atrophy of the maxillary alveolar process

According to the bone damages, observed on the bones from *Grave 4*, the individual appeared to have died a violent death (**Fig. 3**). Although the skull was fragmented and had missing parts, there were visible few damages on its outer surface. A rounded defect with an approximate diameter of 45 mm was observed on the coronal suture and adjacent areas of the frontal and left parietal bones (**Fig. 3b**). The outline of the defect was distinctly visible on the outer surface of the skull, but there were not damages on the internal table, and therefore, the underlying soft tissues were not affected directly. It is very likely that the defect was caused by striking a blow with a blunt object, which resulted in a depressed fracture. Another rounded defect was observed on the left parietal bone at a distance of 43 mm at the back of the above-described traumatic injury (**Fig. 3c**). The defect had a diameter of 27 mm on the outer surface of the skull and was smaller than the first one. On the internal table of the skull, it showed a bigger diameter than the outer one and had an

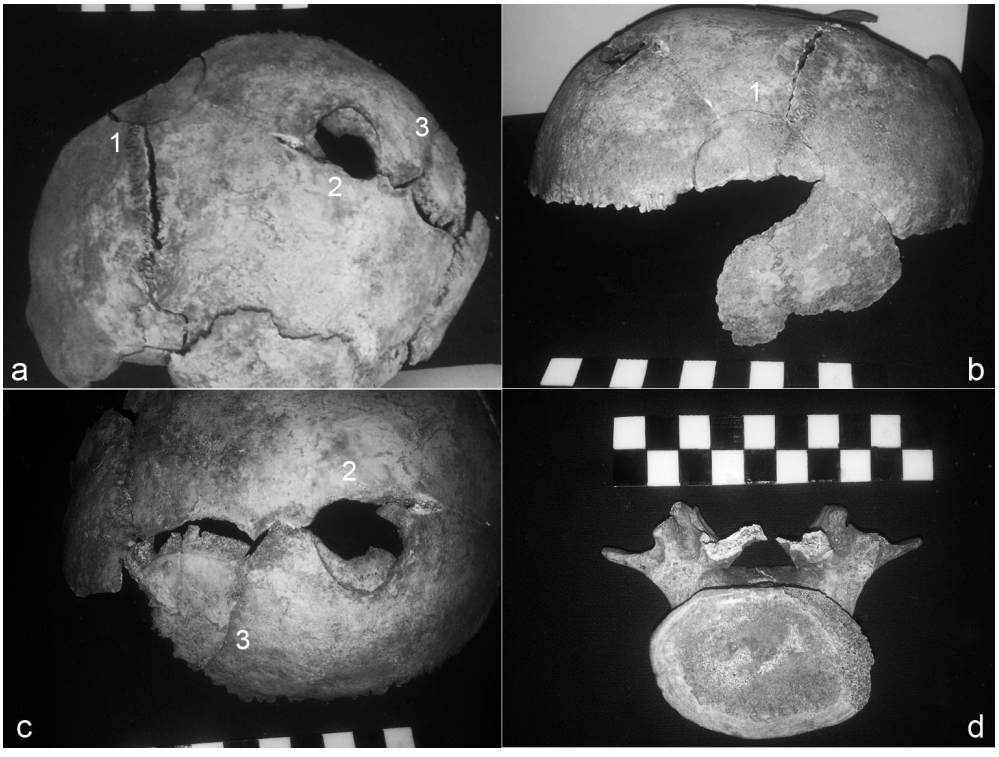


**Fig. 3.** Bones of the individual from *Grave 4*: a-c) Reconstructed parts of the skull with traces of depressed fractures, designated as 1, 2 and 3; c) The inferior body surface of the fourth lumbar vertebra

irregular outline. The depressed fracture in this case probably was also caused by a strong blow with a blunt object, but on a relatively small area. The blow caused knocking out of at least two bone fragments, which sank inwards and might have damaged the underlying meninges and brain tissue. Moreover, there was observed one more defect with semilunar shape, situated at a distance of 15 mm behind the second above-mentioned defect. It represented a crack between two bone fragments. The upper fragment had an oblique margin and was at a distance of 10 mm from the lower one, whose inner surface had a similar corresponding oblique outline. The distance between the fragments probably was a result from the strong postmortem deformation of the parietal bone. The outline of this third depressed fracture cannot be completed, because of the lack of parts of both left parietal and occipital bones (**Fig. 3c**).

Furthermore, a tip of an arrow was found stuck in the left sacral ala of this individual. It was obliquely stuck at a depth of 22 mm (**Fig. 4**). The tip laid on the left transverse process of the fifth lumbar vertebra, which might have affected the corresponding nerve and blood vessels. Besides, bone damage was observed on the inferior surface of the body of the fourth lumbar vertebra, which presented a slightly oblique section in a depth of 11 mm in the intervertebral space (**Fig. 3d**). The cut surface was smooth and suggested a blow with sharp object, inflicted almost horizontally on the right side of the waist. This blow is very likely to have affected some of the internal organs. The right humerus also showed a trace obtained by a blow with sharp object. It was observed in the middle of the diaphysis and was 20 mm long. The cut was deeper and wider on the lateral surface and became shallower and narrower towards the medial surface.

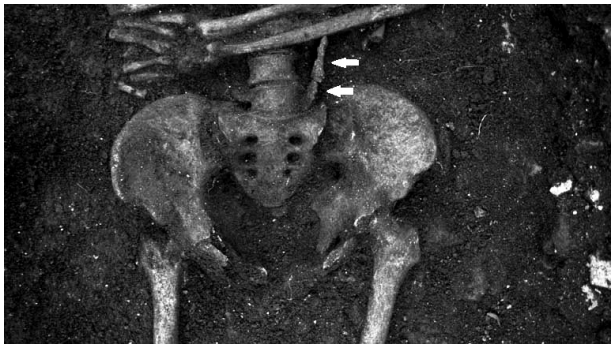

**Fig. 4.** Skeleton of the individual form *Grave 4 in situ* with a tip of arrow stuck in the left sacral ala

The described bone damages showed no traces of healing and most probably caused the death of the individual. Besides all these traumatic injuries, a bone growth was observed in the upper 1/3 of the *linea aspera* of the right femur. It might have been caused by a trauma affecting the soft tissues in this part of the thigh without bone fracture. Unlike the other injuries, this one was survived.

## Conclusion

As a whole, the results from the anthropological investigation of the bone remains revealed at the rescue archaeological excavations led on the place of the Samuil – Tsar of Bulgaria Monument showed that they belonged to 11 individuals (6 adults, 1 juvenile and 4 children). Pathological changes were observed on the bones of three of the adults.

## References


1. **Buikstra, J. E., D. H. Ubelaker.** Standards for data collection from human skeletal remains. Fayetteville, Arkansas. – Archeological Survey Research Series No. 44, 1994.
2. **Facchini, F., S. Veschi.** Age determination on long bones in a skeletal subadults sample (b-12 years). – Coll. Antropol., **28**(1), 2004, 89-98.
3. **Martin, R., K. Saller.** Lehrbuch der Anthropologie in systematischer Darstellung. – **I**, 1957, Stuttgart.
4. **Pearson, K., A. Lee.** Mathematical contributions to the theory of evolution. V. On the reconstruction of the stature of prehistoric races. – Phylosophical Transactions of the Royal Society, ser. A, 192, 1899, 169-244.
5. **Sans, N., M. Faruch, F. Lapègue, A. Ponsot, H. Chiavassa, J.-J. Railhac.** Infections of the spinal column – Spondylodiscitis. – Diagnostic and Interventional Imaging, **93**(6), 2012, 520-529.
6. **Scheuer, L., S. Black.** Developmental Juvenile Osteology. San Diego, California, Academic Press, 2000.
7. **Trotter, M., G. Gleser.** A re-evaluation of estimation of stature based on long bones after death. – J. Am. Phys. Anthrop., **16**(1), 1958, 79-123.
8. **White, T. D., P. A. Folkens.** Human Osteology. 2nd ed., San Diego, 2000, California, Academic Press.
9. **Алексеев, В. П.** Остеометрия. Москва, Наука, 1966.
10. **Алексеев, В. П., Г. Ф. Дебец.** Краниометрия. Москва, Наука, 1964.
11. **Герасимов, М. М.** Восстановление лица по черепу. – В: Труды Инс. Этнографии, новая серия, XXVIII. Москва, АН СССР, 1955.
12. **Стоянова, П.** 2015. Спасително археологическо проучване на обект „Скулптурен монумент „Самуил – цар на България“. В: АОР през 2014 г., 2015, 515–517.

Institute of Experimental Morphology, Pathology and Anthropology with Museum
Bulgarian Anatomical Society

Acta morphologica et anthropologica, 22
Sofia ● 2015

# Coexistence of a Suprascapular Notch and a Bony Canal: a Rare Anatomical Variation

*D. Toneva, S. Nikolova*

*Department of Anthropology and Anatomy, Institute of Experimental Morphology, Pathology and Anthropology with Museum, Bulgarian Academy of Sciences*

In the presents study, we report a case of coexistence of a suprascapular notch and a bony canal. It occurred in a left scapula, belonging to a male individual with an age at death of approximately 45 to 50 years. The canal was formed by the base of the coracoid process anteriorly and an ossified ligament posteriorly. Because of the posterior insertion of the ossified ligament at the base of the coracoid process, we suppose that it represents an ossified superior transverse scapular ligament and exclude the possibility for formation of the canal through ossification of an anterior coracoscapular ligament.

*Key words:* suprascapular notch, bony canal, superior transverse scapular ligament, suprascapular nerve entrapment.

## Introduction

The suprascapular notch (SSN) is a very important anatomical region of the scapula, because of its key position on the course of the suprascapular nerve (SN). Normally, the SSN serves as a passage for the SN, as the superior transverse scapular ligament (STSL) closes the upper part of the notch, converting it into a foramen. It represents a strong fibrous band extended along the superior border of the scapula, connecting the medial and lateral borders of the SSN [35]. Occasionally, another ligament may be present on the anterior side of the SSN inferior to the STSL, named anterior coracoscapular ligament (ACSL) [3]. There is a high variability in relation to the blood vessels crossing through the SSN region. The suprascapular artery (SSA) is commonly passing above the STSL, whereas the suprascapular vein (SSV) is found with a high frequency to run above [55] or below it [30, 39]. After transiting the SSN, the SN supplies motor branches to the supraspinatus and infraspinatus muscles and sensory branches to the coracoacromial and coracohumeral ligaments, subacromial bursa and acromioclavicular and glenohumeral joints [9].

There are different classifications concerning the shape of the SSN, based on scopical observations [15, 16, 41, 47] or metrical characteristics [27, 31]. In all reported classifications, there were types considered as risk factors for suprascapular nerve entrapment (SNE), such as the partial and complete ossification of STSL or the V-shaped SSN. The complete absence of the SSN was also regarded as a possible cause of SNE [28].

Based on other studies, Gosk et al. [11] noticed that the greatest risk of nerve entrapment appears in patients with a small SSN and a calcified transverse ligament. However, the coexistence of an SSN and a suprascapular foramen (SSF) is presented as a type only in the classification of Natsis et al. [27], as Type V. According to Polguj et al. [34], such coexistence narrows the space for passage of the nerve and thus increases the risk of suprascapular neuropathy.

Nevertheless, none of the classifications included the presence of a bony canal as a possible morphological variant in the SSN region. Wang et al. [54] were the first to take notice of the forming of a bony canal instead of an SSF and emphasized the very increased risk of SNE in such a case. However, there has not been reported a case of coexistence of an SSN and a bony canal, which would complicate additionally the passage of the SN through this region.

In this study, we report a case of coexistence of an SSN and a bony canal, because of the uniqueness of such a combination and the clinical importance of SNE.

## Materials and Methods

The object of this study is a scapula with coexistence of an SSN and a bony canal. The sample was part from the osteological collection at the Institute of Experimental Morphology, Pathology and Anthropology with Museum, Bulgarian Academy of Sciences. The bone remains of the individual were obtained during archaeological excavations of a medieval necropolis. The age and sex of the individual were determined by standard anthropological methods [5].

The SSN and the bony canal were examined macroscopically and metrically. The measurements of the notch and posterior wall of the canal were taken in accordance with the measurements of both SSN and bony bridge described by Polguj et al. [34] for the cases with coexistence of an SSN and an SSF. In addition, two (transversal and sagittal) diameters of both superior and inferior openings of the canal were measured. All measurements were taken with a sliding caliper.

## Results

The coexistence of an SSF and a bony canal was observed in a left scapula, belonging to a male individual with an age at death of approximately 45 to 50 years. The right scapula of the individual had a deep SSN, without formation of a SSF or a bony canal.

The SSN was shallow and its vertical diameter was only 3 mm. The transversal diameter in the upper part of the notch was 6 mm. The superior opening of the bony canal was situated below and laterally to the notch, near the root of the coracoid process. It was oval-shaped with a transversal diameter of 8.5 mm and a sagittal one of 4 mm. The canal was directed downward and laterally, following the course of the SN toward the spinoglenoid notch (**Fig. 1**). The size of the inferior opening was smaller than the superior one with a transversal diameter of 5.5 mm and a sagittal one of 3.5 mm. The canal was formed by the base of the coracoid process anteriorly and by an ossified ligament posteriorly. According to the measurements of the ossified ligament, it was 10.5 mm long, with a proximal width of 15 mm, a middle width of 12.5 mm and a distal one of 16 mm.

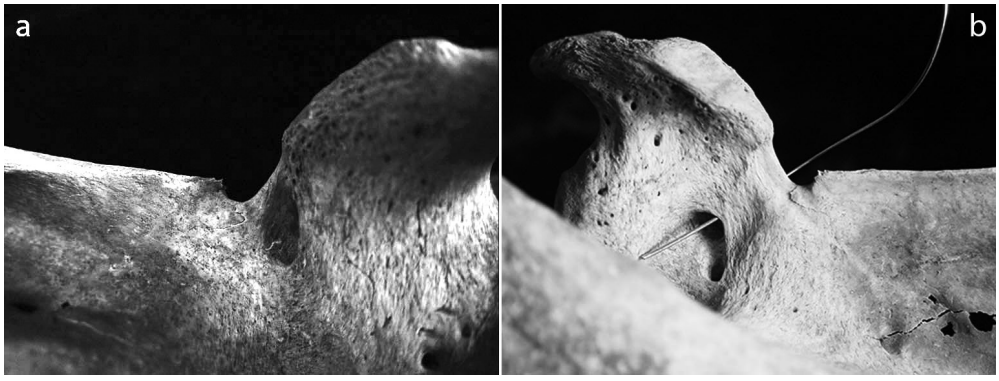


**Fig. 1.** Left scapula showing coexistence of a suprascapular notch and a bony canal: a) Anterior view; b) Posterior view

From the lower end of the canal began a sulcus, leading to a nutrient foramen, which was at a distance of 3 mm from the superior border of the base of the scapular spine.

## Discussion

The size and shape of the SSN are supposed to be predisposing factors for compression of the SN. The earliest symptom of SNE is a deep pain around the suprascapular region and shoulder [19]. The pain is often aggravated by lifting the arm above the shoulder level. Moreover, the shoulder pain may radiate medially and upward, involving the neck area, or medially and downward to the infrascapular region. Atrophy of supra- and infraspinatus muscles is frequently present, along with weakness of external rotation of the shoulder [52]. The ossification of the STSL is the most common cause of SNE. The formation of an SSF by ossification of the STSL is reported by many authors with a varying frequency from 1.5% to 30.76% in the different population groups [2, 4, 8, 17, 23, 25, 27, 31, 36, 41, 45, 46, 47, 48, 49, 53, 54]. According to Tubbs et al. [51] and Polguj et al. [38], the presence of an ossified STSL was more common in males and in the right scapulae. However, some studies reported a higher frequency in females [36, 49]. As a whole, Albino et al. [2] did not found any relation between the type of the SSN and sex of the individuals. Concerning the more common occurrence of the ossified STSL on the right side, Tubbs et al. [51] supposed that it may be due to a predilection for right-sided handedness in most people.

The coexistence of a SSN and a SSF is another interesting type of the SSN, which is more rarely observed, with a frequency often below 1%. Polguj et al. [34] supposed that the frequency of this anatomical variation depend on the population like to the frequency of completely ossified STSL. Hrdlicka [14] was first to describe such a case among a sample of 2792 dried scapulae (0.036%). Later, Natsis et al. [27] found 3 cases with coexistence of a SSN and a SSF among 432 German scapulae (0.7%). Such coexistence was reported by Sinkeet et al. [46] in one out of 138 Kenyan scapulae (0.72%). Polguj et al. [34] investigated 616 scapulae of Polish patients by CT and found this rare anatomical variation in 2 left scapulae (0.33%) as well as in a right dried one, and assumed that the ossification of a single bundle ACSL is the most probable hypothesis for the formation of a bony bridge above the SSF. According to the studies conducted on Indian scapulae, the frequency of coexistence of a SSN and a SSF varied from 0.56%

to 1.33% [25, 44, 47]. Saritha [44] also described this anatomical variation with the complete ossification of the ACSL. However, there are studies in which this type of morphology of the SSN was not observed at all [1, 54]. It is supposed that the presence of an SSF along with an SSN increases the risk of SNE, because of the additionally reduced size of the SSF, i.e. the space available for passage of the SN. According to Polguj et al. [35], the presence of a bony bridge passing through the middle part of the SSN decreases this space by about 36.5-38.6%.

Unlike the above cited studies, Wang et al. [54] observed the presence of a bony canal instead of just an SSF. They found it in 4 scapulae (1.36%), as the canal length ranged from 5.89 mm to 17.86 mm. Vyas et al. [53] also reported such a canal in 4 cases (1.33%) with a length varying from 11.83 to 14.03 mm. Taking into account the lengths of the ossified ligament measured in the described case, the length of the canal is similar to the reported long ones. According to the summed bilateral distribution of the bony canal findings [53, 54], a higher frequency came out for the right side. However, the left scapula was involved in our case.

According to Wang et al. [54] and Vyas et al. [53], the bony canal was most probably formed by the complete ossification of a wide and flat STSL. Although the attachment of the ossified ligament in our case was a bit lower on the medial border of the SSN, because of the posterior insertion of the ossified ligament at the base of the coracoid process, we also suppose that it represents an ossified STSL and exclude the possibility of formation of the canal through ossification of an ACSL. There are different studies reporting cases with bifid STSL [4, 32, 48], trifid STSL [33, 48], bifid ACSL [37], as well as classifying the types of STSL [4, 35] and ACSL [29, 37]. However, the coexistence of an SSN and a bony canal, and more precisely the formation of such a long bony canal, as in the reported case, could not be explained with any of these classifications. Classifying the types of STSL, Polguj et al. [35] obtained 15.1 mm and 13.1 mm as biggest proximal and distal width in specimens with fan-shaped ligaments and lower maximum values in these with band-shaped ones. Such high values show the presence of rather wide STSL, but obviously it is more typical of fan-shape type, which is hard to be related to our case. Besides, the proximal and distal widths of a bifid STSL with superior and inferior bands, reported by Polguj et al. [32], are comparatively smaller. In the case with trifid STSL, described by Polguj et al. [33], taking into account the summed proximal widths of the three bands comes out a quite wide ligament on the medial border of SSN, where the three bands attached separately, while the common distal part of the ligament is quite narrower. Thus, the ossified ligament in our case could not be compared to such an ossified trifid STSL. In addition, it should be considered the relation of the STSL with the fasciae of both supraspinatus and omohyoid muscles as well as with the adjacent conoid part of the coracoclavicular ligament, which might blend with it [22, 26]. Thus, these structures could also be supposed to have played a part in the canal formation.

There may be different causes for ossification of the STSL. Morrigl et al. [26] proved that both entheses of STSL are strongly fibrocartilaginous as well as the remainder of the ligament has a moderately fibrocartilaginous matrix and suggested that the frequency with which the STSL ossifies is related to its fibrocartilaginous character. According to Millela [24], age has a great impact on the expression of entheseal changes, which are probably related to such causes as the response of bone to continuous microtraumatic stress in connection with daily biomechanical stimuli, ontogenetic processes of the musculoskeletal system, and degenerative processes associated with aging. Yonemoto [56] asserted that entheseal changes are influenced by the age to a certain degree, depending on specific physical activities associated with the individual occupation. The mean age of the sample with a completely ossified STSL, reported by Polguj et al. [38],

was over 60 years. However, Zehetgruber et al. [57] announced a mean age of 37 years for individuals with SNE, caused by ligament compression, but it was not related to the ossification of the ligament. The observation of the other bones in the reported case showed a presence of osteophytes on the thoracic vertebral bodies as well as a fusion of manubrium and sternal body, which are considered age-related changes. Thus, it could be supposed that the ossification of STSL in given cases could be prompted by the age advance. However, Rogers et al. [43] noted that enthesophyte formation was associated with age, but above all enthesophytes could be considered as skeletal responses to stress. These authors also noticed that some people are more prone to form new bone in response to stress than others. Here, it should be mentioned that there is a hypothesis presuming that the ossification of STSL could be genetically predetermined. It was brought forward by Cohen et al. [7], who described a calcification of the STSL in two members of a family (father and son) with concomitant symptoms of SNE.

On the other hand, the variations in thickness and length of STSL as well as its tendency to ossify suggest that the ligament responds to changes in mechanical load [26]. Although the STSL is connecting two areas of the same bone and has no direct attachment to any joint, the nearby fascia of the supraspinatus, origin of the omohyoid muscle as well as attachment of the conoid ligament could concentrate significant stress at the STSL entheses during twisting movements and force acting on them [22]. Therefore, the ossification of STSL could be provoked by vigorous and repeating overhead upper limb movements and thus to cause SN compression. Suprascapular nerve neuropathy frequently affects individuals who have been involved in violent overhead activities [1] and is common in athletes who overuse the shoulder region [53]. The repetitive overhead motions and forceful rotational movements performed during sports activities such as volleyball, baseball, tennis, and weightlifting may cause traction upon the nerve at SSN [10, 20, 42, 58]. The regular carrying of heavy objects on the shoulder also might lead to SNE [17]. Thus, it is hypothesized that repetitive overhead motions contribute to ossification of the ligament [51]. According to Kopell and Thompson [21], the movement of abduction or horizontal adduction of the shoulder results in compression of the nerve against the STSL. Rengachary et al. [41] described the etiopathogenesis of SNE with so-called "sling effect". According to it, the SN makes only minimal transitional movements during upper limb motions, but at maximal rotation, the nerve could be pressed against the sharp bony margin of the SSF. In this way, a repeated kinking may cause nerve irritation and induce microtrauma, which to result in neuropathy.

Besides, the ossification of STSL could be a result from a microtrauma of the ligament, caused by exertion of blood pressure from the SSA in cases when it passes below the STSL along with SN and the size of the SSF is significantly reduced [38]. The SSA normally runs above the STSL, but there were reported cases with its course under the ligament [12, 39, 40, 50, 55]. It could be assumed that the presence of the notch above the canal in the described case reduced additionally the area for passing of the SN, and in case that SSA and SN passed together through the formed bony canal, the STSL might have been at serious risk of trauma. The observed groove running from the inferior opening of the bony canal to the spinoglenoid notch ended in a nutrient foramen above the scapular spine. Since the SSA gives nutrient branches, supplying the clavicle and scapula [13], there is a possibility that a nutrient artery or vein might have passed along with the SN through the bony canal. However, there is only one reported case of an accessory SSA, accompanying the SN under the STSL, while SSA was passing above the ligament [6]. So in case of passing through the canal, the SSA is more likely to have given rise to a nutrient branch immediately after going out of it. On the other hand, the SSV is more frequently observed to pass below the STSL than the SSA [12, 30, 39]. Furthermore, Podgórski et al. [30] described the presence of suprascapular

notch veins, crossing the SSN, as a separate structure from the SSV. All this goes to show that the SN is very likely to have passed through the bony canal along with any of the above-mentioned blood vessels. The reported diameter of SN ranged from 2 mm to 3.3 mm [3, 30, 39, 51]. According to Podgórski et al. [30], the diameters of the SSA and SSV were 2.3 mm and 3.4 mm, respectively and the diameter of the suprascapular notch veins varied from 0.5 mm to 3 mm. The measurements of the superior and inferior openings in our case showed a narrowing of the space within the canal. Thus, bearing in mind the reported size of the SN and blood vessels and the dimensions in the smaller lower end of the canal, the passage of the nerve along with some of the vessels might have led to its compression as well as caused exertion of blood pressure on the STSL.

Nevertheless, the real cause for ossification of the STSL in our case cannot be pointed out, i.e. if it was prompted by certain activities of the individual, age advance or the unusual morphology of the ossified ligament. However, it is very likely that this rare anatomical variation caused SNE.

The coexistence of a SSN and a bony canal is very interesting, because it has not been reported or taken into consideration by other researchers. The presence of such a case would be of significance for clinicians and surgeons dealing with suprascapular neuropathy. Furthermore, the knowledge of the morphological variations in the suprascapular region can be helpful for a better understanding the way of living and health problems of the people, living in the past. A specific morphology of the SSN could be an indicator of SNE and a supposition that the individual might have suffered from the concomitant symptoms for this pathological condition.

## References


1. **Agrawal, D., B. Singh, G. Agrawal.** Human Scapulae: Supra Scapular Notch, Morphometry and Variations. – Indian Journal of Clinical Anatomy and Physiology, **1**, 2014, 1-7.
2. **Albino, P., S. Carbone, V. Candela, V. Arceri, A. Vestri, S. Gumina.** Morphometry of the suprascapular notch: correlation with scapular dimensions and clinical relevance. – BMC Musculoskeletal Disorders, **14**, 2013, 172.
3. **Avery, B. W., F. Pilon, J. Barclay.** Anterior coracoscapular ligament and suprascapular nerve entrapment. – Clin. Anat., **15**, 2002, 383-386.
4. **Bayramoglu, A., D. Demiryurek, E. Tuccar, M. Erbil, M. Aldur, O. Tetik, M. Doral.** Variations in anatomy at the suprascapular notch possibly causing suprascapular nerve entrapment: an anatomical study. – Knee Surg. Sport Trum. Arthros., **11**, 2003, 393-398.
5. **Buikstra, J. E., D. Ubelaker.** Standards for Data Collection from Human Skeletal Remains. Fayetteville, Arkansas Archaeological Survey Research Series No. 44, 1994.
6. **Chen, D., P. Adds.** Accessory suprascapular artery. – Clin. Anat., **24**, 2011, 498-500.
7. **Cohen, S. B., D. Dines, C. Moorman.** Familial calcification of the superior transverse scapula ligament causing neuropathy. – Clin. Orthop. Rel. Res., **334**, 1997, 131-135.
8. **Cirpan, S., N. Gocmen Mas, F. Aksu, M. Edizer, S. Karabekir, A. Magden.** Suprascapular foramen: a rare varıatıon caused by ossıfied suprascapular lıgaments. – Folia Morphol., 2015. DOI: 10.5603/FM.a2015.0073
9. **Cummins, C. A., T. Messer, G. Nuber.** Suprascapular nerve entrapment. – J. Bone Joint Surg. Am., **82**, 2000, 415-424.
10. **Ferretti, A., G. Cerullo, G. Russo.** Suprascapular neuropathy in volleyball players. – J. Bone Joint Surg. Am, **69-A**, 1987, 260-263.
11. **Gosk, J., M. Urban, R. Rutkowski.** Entrapment of the suprascapular nerve: anatomy, etiology, diagnosis, treatment. – Orthop. Traumatol. Rehabil., **9**, 2007, 68-74.
12. **Gürses, İ. A., Ö. Gayretli, O. Coşkun, A. Kale, A. Öztürk.** Anatomical relations between anterior coracoscapular ligament and suprascapular neurovascular structures and a proposal for classification. – Acta Orthop. Traumatol. Turc., **49**(4), 2015, 433-437.

13. **Hinrichsen, C.** A Synopsis of Regional Anatomy. Hackensack, NJ, World Scientific Pub., 2008, 233-234.
14. **Hrdicka, A.** The adult scapula: additional observations and measurements. – J. Am. Phys. Anthropol., **29**, 1942, 363-415.
15. **Iqbal, K., R. Iqbal, S. G. Khan.** Anatomical variations in shape of suprascapular notch of scapula. – J. Morphol. Sci., **27**, 2010, 1-2.
16. **Jadhav, S. D.** The suprascapular notch: its various shapes in Indian dry scapulae. – J. Res. Pharm., Biol. Chem. Sci., **3**, 2012, 1085-1090.
17. **Kajava, Y.** Uber den Schultergiirtel der Finen. – Ann. Acad. Sci. Fenn., **21**, 1924, 1-69.
18. **Karataş, G. K., F. Göğüş.** Suprascapular nerve entrapment in newsreel cameramen. – Am. J. Phys. Med. Rehabil., **82**, 2003, 192-196.
19. **Kaye, A. H.** Essential Neurosurgery (3rd Ed.). Wiley-Blackwell, 2005, 239.
20. **Khan, A. M., M. Guillet, G. Fanton.** Volleyball: rehabilitation and training tips. – Sports Med. Arthroscopy Rev., **9**, 2001, 137-146.
21. **Kopell, H. P., W. Thompson.** Pain and the frozen shoulder. – Surg. Gynecol. Obstet., **109**, 1959, 92-96.
22. **Mahato, R.K., P. Suman.** Ossification of Superior Transverse Scapular Ligament: Incidence, Etiological Factors and Clinical Relevance. – J. Int. Health Scien. Res., **3**(9), 2013, 14-21.
23. **Mahdy, A. A., A. Shehab.** Morphometric variations of the suprascapular notch as a potential cause of neuropathy: anatomical study. – J. Am. Scien., **9**, 2013, 189-197.
24. **Millela, M.** The Influence of Life History and Sexual Dimorphism on Entheseal Changes in Modern Humans and African Great Apes. – PLoS ONE, **9**(9), 2014, e107963.
25. **Mistry, P., K. Chauhan, C. Mehta, D. Patil, M. Bansal, K. Suthar.** A study of incidence of ossification of superior transverse scapular ligament of scapula and its clinical implications. – J. Int. Basic and Appl. Med. Scien., **3**(2), 2013, 41-45.
26. **Moriggl, B., P. Jax , S. Milz, A. Büttner, M. Benjamin.** Fibrocartilage at the entheses of the suprascapular (superior transverse scapular) ligament of man – a ligament spanning two regions of a single bone. – J. Anat., **199**(5), 2001, 539-545.
27. **Natsis, K., T. Totlis, P. Tsikaras, H. J. Appell, K. Skandalakis.** Proposal for classification of the suprascapular notch: a study on 423 dried scapulas. – Clin. Anat., **20**, 2007, 135-139.
28. **Ofusori, D., R. Ude, Ch. Okwuonu, O. Adesanya.** Complete absence of the suprascapular notch in a Nigerian scapula: a possible cause of suprascapular nerve entrapment. – J. Int. Shoul. Surg., **2**, 2008, 85-86.
29. **Piyawinijwong, S., P. Tantipoon.** The anterior coracoscapular ligament in Thais: possible etiological factor of suprascapular nerve entrapment. – J. Siriraj Med., **64**, 2012, S12-S14.
30. **Podgórski, M., M. Sibiński, A. Majos, L. Stefańczyk, M. Topol, M. Polguj.** The suprascapular vein: A possible etiology for suprascapular nerve entrapment and risk of complication during procedures around the suprascapular foramen region. – Orthopaedics & Traumatology: Surgery & Research, **100**(5), 2014, 515-519.
31. **Polguj, M., K. Jędrzejewski, M. Podgórski, M. Topol.** Morphometric study of the suprascapular notch: proposal of classification. – Surg. Radiol. Anat., **33**, 2011, 781-787.
32. **Polguj, M., K. Jedrzejewski, A. Majos, M. Topol.** Variations in bifid superior transverse scapular ligament as a possible factor of suprascapular entrapment: an anatomical study. – Int. Orthop., **36**(10), 2012, 2095-2100.
33. **Polguj, M., K. Jedrzejewski, A. Majos, M. Topol.** The trifid superior transverse scapular ligament: a case report and review of the literature. – Folia Morphol., **71**(2), 2012, 118-120.
34. **Polguj, M., K. Jędrzejewski, A. Majos, M. Topol.** Coexistence of the suprascapular notch and the suprascapular foramen – a rare anatomical variation and a new hypothesis on its formation based on anatomical and radiological studies. – Anat. Sci. Int., **88**, 2013, 156-162.
35. **Polguj, M., K. Jędrzejewski, M. Podgórski, A. Majos, M. Topol.** A proposal for classification of the superior transverse scapular ligament: variable morphology and its potential influence on suprascapular nerve entrapment. – J. Shoulder Elbow Surg., **22**, 2013, 1265-1273.
36. **Polguj, M., K. Jędrzejewski, M. Topol.** Sexual dimorphism of the suprascapular notch: morphometric study. – Arch. Med. Sci., **9**, 2013, 177-183.
37. **Polguj, M., K. Jędrzejewski, M. Topol.** Variable morphology of the anterior coracoscapular ligament. A proposal of classification. – Annals of Anatomy, **195**, 2013, 77-81.

38. **Polguj, M., M. Sibiński, A. Grzegorzewski, M. Waszczykowski, A. Majos, M. Topol.** Morphological and Radiological Study of Ossified Superior Transverse Scapular Ligament as Potential Risk Factor of Suprascapular Nerve Entrapment. – Bio. Med. Research International, 2014, Article ID 613601, 1-7.
39. **Polguj, M., J. Rożniecki, M. Sibiński, A. Grzegorzewski, A. Majos, M. Topol.** The variable morphology of suprascapular nerve and vessels at suprascapular notch: a proposal for classification and its potential clinical implications. – Knee Surg. Sports Traumatol. Arthrosc., **23**(5), 2015, 1542-1548.
40. **Reineck, J. R., S. Krishnan.** Subligamentous suprascapular artery encountered during arthroscopic suprascapular nerve release: a report of three cases. – J. Shoulder Elbow Surg., **18**(3), 2009, e1-e3.
41. **Rengachary, S. S., D. Burr, S. Lucas, K. Hassanein, M. Mohn, H. Matzke.** Suprascapular entrapment neuropathy: a clinical, anatomical, and comparative study. Part 2: Anatomical study. – Neurosurgery, **5**, 1979, 447-451.
42. **Ringel, S. P., M. Treihaft, M. Carry, R. Fisher, P. Jacobs.** Suprascapular neuropathy in pitchers. – J. Am. Sports Med., **18**, 1990, 80-86.
43. **Rogers, J., L. Shepstone, P. Dieppe.** Bone formers: osteophyte and enthesophyte formation are positively associated. – Annals of the Rheumatic Diseases, **56**, 1997, 85-90.
44. **Saritha, S.** Coexistence of suprascapular notch and suprascapular foramen.A rare anatomical variation and itsclinical correlation – A Case Report. – J. Int. Med. Sci. Clin. Inv., **1**(2), 2014, 65-68.
45. **Silva, J. G., M. Abidu-Figueiredo, R. M. P. Fernandes, F. Aureliano-Rafael, E. A. Sgrott, S. F. Silva, M. A. Babinski.** High incidence of complete ossification of the superior transverse scapular ligament in Brazilians and its clinical implications. – Int. J. Morphol., **25**, 2007, 855-859.
46. **Sinkeet, S. R., K. O. Awori, P. O. Odula, J. A. Ogeng'o, P. M. Mwachaka.** The suprascapular notch: its morphology and distance from the glenoid cavity in a Kenyan population. – Folia Morphol., **69**, 2010, 241-245.
47. **Sutaria, L. K., T. Nayak, S. Patel, H. Jadav, C. Pensi.** Morphology and morphometric analysis of suprascapular notch. – J. Int. Biomed. Adv. Res., **4**(1), 2013, 35-39.
48. **Ticker, J. B., M. Djurasovic, R. J. Strauch, E. W. April, R. G. Pollock, E. L. Flatow, L. U. Bigliani.** The incidence of ganglion cysts and variations in anatomy along the course of the suprascapular nerve. – J. Shoulder Elbow Surg., **7**, 1998, 472-478.
49. **Toneva, D., S. Nikolova.** Morphology of suprascapular notch in medieval skeletons from Bulgaria. – Folia Morphol., **73**(2), 2014, 210-215.
50. **Tubbs, R. S., M. D. Smyth, G. Salter, W. J. Oakes.** Anomalous traversement of the suprascapular artery through the suprascapular notch: a possible mechanism for undiagnosed shoulder pain? – Med. Sci. Monit., **9**(3), 2003, BR116-BR119.
51. **Tubbs, R. S., C. Nechtman, A. V. D'Antoni, M. M. Shoja, M. M. Mortazavi, M. Loukas, C. Rozzelle, R. Spinner.** Ossification of the suprascapular ligament: a risk factor for suprascapular nerve compression? – J. Int. Shoulder Surgery, **7**(1), 2013, 19-22.
52. **Turner, O. A., N. Taslitz, S. Ward.** Suprascapular nerve entrapment. – In: Handbook of peripheral nerve entrapments. New York, Humana Press, 1990, 17-22.
53. **Vyas, K. K., H. B. Rajput, K. M. Zanzrukiya, I. Suttarwala, B. J. Sarvaiya, B. D. Shroff.** An osseous study of suprascapular notch and various dimensions of safe zone to prevent suprascapular nerve injury. – J. Indian Appl. Basic Med. Sci., **15a**(20), 2013, 27-39.
54. **Wang, H. J., C. Chen, L. P. Wu, C. Q. Pan, W. J. Zhang, Y. K. Li.** Variable morphology of the suprascapular notch: an investigation and quantitative measurements in Chinese Population. – Clin. Anat., **24**, 2011, 47–55.
55. **Yang, H. J., Y. Gil, J. Jin, S. Ahn, H. Lee.** Topographical anatomy of the suprascapular nerve and vessels at the suprascapular notch. – Clin. Anat., **25**, 2012, 359-365.
56. **Yonemoto, S.** Differences in the effects of age on the development of entheseal changes among historical Japanese populations. – Am. J. Phys. Anthropol., 2015. (DOI: 10.1002/ajpa. 22870).
57. **Zehetgruber, H., H. Noske, T. Lang, Ch. Wurnig.** Suprascapular nerve entrapment. A meta-analysis. – International Orthopaedics (SICOT), **26**, 2002, 339-343.
58. **Zeiss, J., L. S. Woldenberg, S. R. Saddemi, N. A. Ebraheim.** MRI of suprascapular neuropathy in a weight lifter. – J. Comput. Assist. Tomogr., **17**(2), 1993, 303-308.

Institute of Experimental Morphology, Pathology and Anthropology with Museum
Bulgarian Anatomical Society

Acta morphologica et anthropologica, 22
Sofia ● 2015

# Application of Duracryl® Plus in Making of Corrosion Casts for Macro- and Microscopical Studies of the Renal Vasculature and Collecting System in Domestic Swine

*N. S. Tsandev, I. S. Stefanov, G. N. Kostadinov, H. R. Hristov, B. K. Derventlieva, A. P. Vodenicharov*

*Department of Veterinary Anatomy, Histology and Embryology, Faculty of Veterinary Medicine, Trakia University, Stara Zagora, Bulgaria*

The lack of more concrete data about application of the acrylic resin Duracryl® Plus in making corrosion casts of renal blood vessels and collecting system motivated us to undergo undertake this study. We aimed to perform modified technique for making corrosion casts for 3-dimensional (3D) studies of the kidney blood vessels and collecting system and for replicating microvasculature using Duracryl. As a result, corrosion casts of the whole renal arterial network including glomeruli were obtained. The number of cortical glomeruli in kidney, which arteries were injected with casting media with dilution of 1:2, was significantly smaller than the dilution of 1:5. With regard to collecting system, the lower dilution of casting media allowed the filling of small calices while the media with a higher dilution – the collecting tubules system of the renal medulla and even of the cortex.

In conclusion, we found that the Duracryl is suitable for making three-dimensional casts of the renal arteries and collecting tubules and also microvascular corrosion casts for stereomicroscopy and scanning electron microscopy.

*Key words:* Duracryl® Plus, corrosion casts, kidney.

## Introduction

The anatomists have tried to improve the casting media, the method of injection, and the method of removing the surrounding tissues in order to produce more accurate replica of the biological structures for five centuries. The casting or injection media must have physicochemical properties making them appropriate for the scanning electron microscopy (SEM) study of microvessels, such as low viscosity, rapid polymerization, minimal shrinkage during hardening, resistance to corrosion, cleaning, dissection and drying procedures, allow replication of endothelial structures, electron conductivity, resistance to electron bombardment [1, 8].

Many other authors have used the microvascular corrosion casting/SEM method to study not only vascular but non-vascular structures of various organs and tissues under different conditions and during development and aging [3, 5].

The semi-polymerized methyl methacrylate resin has been considered the most appropriate casting medium for the SEM study of microvascular beds due to its low viscosity, which allows the infusion of the small vessels including the capillaries and its propriety of electron reflection [5, 9]. Duracryl as a representative of these resins is a self-polymerizable acrylic resin occurring as a bicomponent system: polymer and monomer. The polymer is a methyl polymethacrylate, in the form of low powder particles, while the monomer is liquid methyl methacrylate [13]. Duracryl is one of the most widely used dental materials in the stomatology [3, 5].

There are single data of applying Duracryl in the corrosion method. Mazensky and Danko [6] observed morphological variations in the origin and course of the rabbit arteria vertebralis using Duracryl Dental (Spofa-Dental, Czech Republic) for making corrosion casts.

The existence of many similarities in the pig and human intrarenal arteries define the swine as the best animal model for investigation of kidney function and pathology [10]. Anatomical knowledge about the macro- and microvascularisation and collecting system of kidney is important for performing intrarenal surgery with minimal blood loss and minimal injury to parenchyma [4].

In this regard, we aimed to perform modified technique for making 3-dimensional casts of the kidney renal vasculature and collecting system and for replicating microvasculature by using acrylic resin Duracryl® Plus.

## Materials and Methods

### 1. Animals and materials

The left kidneys were taken from 12 mixed breed Landras and Danube white, male pigs slaughtered at age of 6 months and weighing 97 to 105 kg. Two groups of kidneys (with almost equal weight – 183.30 ± 7.04 g for the first group, and 184.96 ± 6.47g for the second group) were chosen to be filled later with a corrosion cast medium in two different concentrations. Then the obtained kidneys were prepared for performing the renal vascular and collecting system corrosion casting method using Duracryl® Plus (Spofa/Dental Product, Czech Republic) as a medium.

### 2. Method

The corrosion casting method includes the following seven steps:

### 2.1. Precasting treatment

Before injecting the casting media into the blood vessels, the complete removal of the blood was done in order to fill the entire arterial tree with the resin. For this reason, the kidneys are perfused by syringe with saline solution through a cannula (silicone tube 5 cm long for each kidney) placed and into the renal artery and ureter, as well.

### 2.2. Injection of Duracryl® Plus

After the precasting treatment, two different concentrations of the injection medium were prepared. The first one is consisted of 1 part Duracryl's base added to 5 parts of catalyst to initiate the polymerization, but the second one – 1 part base to 2 parts catalyst. To obtain the endocasts a yellow resin (volume 15 ml) was injected manually by syringe into the ureter to fill the kidney collecting system and a red resin (volume 20 ml) was also injected into the main trunk of the renal artery to fill the arterial tree.

### 2.3. Polymerization of casting medium

Injected specimens were placed in a water bath (at room temperature) for 48 hours to complete the polymerization of the perfused casting medium.

### 2.4. Corrosive treatment

The surrounding tissues were macerated in order to obtain the renal vascular and collecting system casts. For this purpose, the injected specimens were immersed into a highly concentrated (20%) sodium hydroxide solution (at 60 °C for 24 hours).

### 2.5. Cleaning of the corrosion casts

Washing the cast in warm running water was performed to remove the white saponified materials resulted from the maceration of tissues rich of lipid.

### 2.6. Gross dissection and microdissection

For macroscopic study, cast samples were dissected longitudinally into two equal parts. Stereo microscopy (SM) which allows 3-dimensional microscopic viewing of the objects was used for microdissection.

### 2.7. Air-drying of the casts

### 3. Macrometric study

Macrometric parameters were determined by electronic digital caliper (with 0.02 mm precision), measuring the large and small diameters of major and small calices corrosion casts of porcine kidneys using two different concentrations of Duracryl® Plus.

### 4. SM observation of corrosion casts

Stereo microscope (МБС-10 USSR) was used for 3-dimensional microscopic viewing and for counting the glomeruli.

### 5. Statistical analysis

Five pieces (with area of about 2 $mm^3$ each) were obtained by microdissection from the lateral edge of each kidney opposite the transition of the ureter in the renal pelvis. The number of glomeruli was estimated by counting them on 10 microscopic fields (× 42) per each kidney. The data about glomeruli density (number/field × 42) are presented as mean ± standard deviation (SD). Large and small diameters of major and small calices corrosion casts per each kidney were measured and the data were presented as mean ± SD. Statistical data processing was done by using Student's *t*-test. The difference was considered as significant when $P < 0.05$.

## Results

The twelve corrosion casts made from normal porcine kidneys were subdivided into two groups (6 kidneys per each group) in order to establish the most suitable concentration of Duracryl® Plus for making the precision casts of the renal arterial tree and collecting system (**Table 1**). The results confirmed the existence of one more resin appropriate for corrosion casting method on kidneys. Duracryl® Plus used as a medium for corrosion casting method showed that its mechanical properties allow to make adequate casts

of the entire arterial tree of the kidney to be made. *Arteria renalis* and all its branches were filled with resin in two concentrations, which made them clearly distinguished (**Fig. 1**). Besides, the glomeruli with afferent and efferent arterioles were also filled and well visible which proved that the resin due to its low viscosity and easy penetration can fill the smallest vessels of the microcirculatory bed (**Fig. 2**). However, comparing the results of the two concentration of Duracryl® Plus using stereo microscope, it was established that significantly (approximately 2 times) more glomeruli were filled and visible by applying the lower (1:5) concentrated resin (**Figs. 3 and 4**) than 1:2 one than the other one (1:2).

The degree of the collecting system filling with Duracryl® Plus was also detected. The macroscopic measurements revealed that the large diameter of major renal calices casts and the large and small diameter of small renal calices casts made from Duracryl® Plus used in concentration 1:5 were higher than those made from the higher concen-

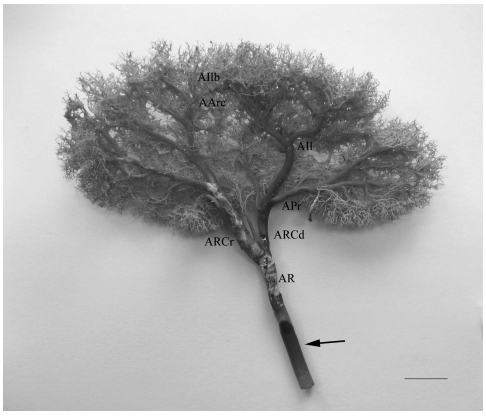


**Fig. 1.** Corrosion cast displaying arterial supply model of porcine kidney.
AR – renal arteria, ARCd – caudal renal artery, ARCr – cranial renal artery, Apr – prelobar artery, AII – interlobal artery, AArc – arcual arteria, AIIb – interlobular arteria, Bar = 1cm

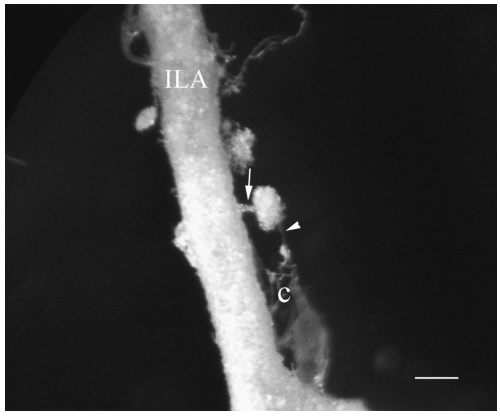


**Fig. 2.** Corrosion cast of interlobular arteria (ILA), afferent arteriole (arrow), cortical glomerulus and efferent arteriole (arrowhead) with capillary network (c). Concentration of the resin used (1:5). Bar = 140 μm

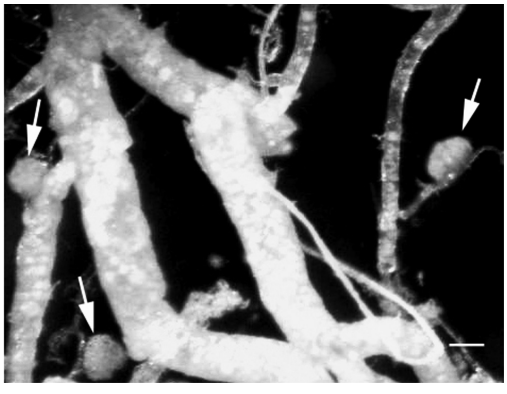

**Fig. 3.** Corrosion casts of cortical glomeruli (arrows) with higher concentrated resin. Bar = 100 μm

**Fig. 4.** Corrosion casts of cortical glomeruli (arrows) with lower concentrated resin. Bar = 100 μm

trated resin (**Table 1**). Our stereo microscope observations showed that the collecting tubules system of renal medulla and cortex of the entire kidney was more precisely filled with the lower concentrated resin (1:5) (**Fig. 5**). Higher concentrated resin filled the medullar and cortical parts of the collecting system in the cranial and caudal poles only (**Fig. 6**).

**Table 1.** Density (number/field ×42) of glomeruli, large and small diameters of major and small calices corrosion casts of porcine kidneys using two different concentrations of Duracryl® Plus as a medium. Data are presented as mean ± SD

| Parameters | Duracryl® Plus (concentration 1:5) | Duracryl® Plus (concentration 1:2) |
|---|---|---|
| Number of glomeruli | 4.28 ± 0.97 | 2.55 ± 1.04*** |
| Large diameter of major calices | 7.60 ± 1.47 | 9.63 ± 2.05 A |
| Small diameter of major calices | 6.30 ± 1.92 | 6.56 ± 2.23 |
| Large diameter of small calices | 11.99 ± 0.61 | 15.91 ± 1.58 B |
| Small diameter of small calices | 9.09 ± 0.62 | 11.42 ± 2.35 b |

*** $P < 0.001$ – statistical significant difference versus the number of glomeruli in lower concentration of Duracryl® Plus.
A – $P < 0.05$ – statistical significant difference versus the large diameter of major calices casts in lower concentration of Duracryl® Plus.
B – $P < 0.001$ – statistical significant difference versus the large diameter of small calices casts in lower concentration of Duracryl® Plus.
b – $P < 0.05$ – statistical significant difference versus the small diameter of small calices casts in lower concentration of Duracryl® Plus.

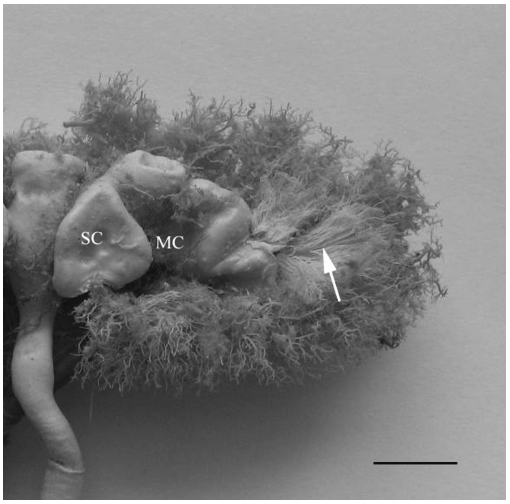


**Fig. 5.** Corrosion casts of major (MC) and small (SC) calices, collecting tubules (arrows) of renal cortex and medulla in lower concentration (1:5) of Duracryl. Bar = 12 mm

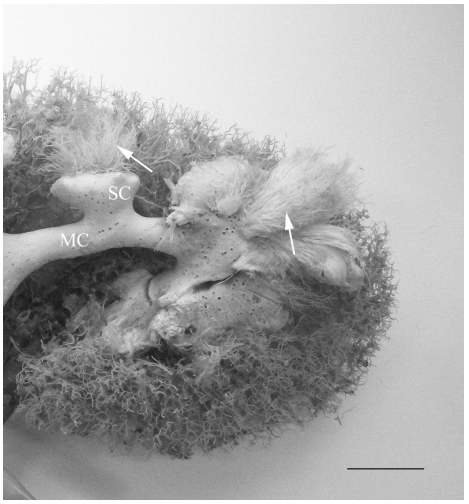


**Fig. 6.** Corrosion casts of major (MC) and small (SC) calices, collecting tubules (arrow) of renal cortex and medulla in higher concentration (1:2) of Duracryl. Bar = 15 mm

## Discussion

In this study, two concentrations of Duracryl® Plus (1 to 2 and 1 to 5 of base and catalyst, respectively) were compared in order to make more adequate corrosion casts of the renal arterial tree and collecting system. The application of Duracryl® Plus as a medium of corrosion casting technic on kidneys was established for the first time. This comparatively cheap resin allows to study entire arterial tree including glomeruli together with afferent and efferent arterioly arterioles similar to other certain, but more expensive resins such as Technovit 7100, Batson's # 17 and Mercox CL-2B [14]. The main advantage of Duracryl is that, among the resins, it is the cheapest. Many authors, who have studied the mechanical requirements of the dental materials, refer to their resistance to various types of forces and stresses, to surface hardness, to abrasion and compression forces for long time [2, 11, 15]. Our results showed that the mechanical properties of Duracryl® Plus also make this resin suitable for performing corrosion casting method in order to study in detail the features of the arterial tree and collecting system of the kidneys**.** Its low viscosity, rapid polymerization, minimal shrinkage during hardening, resistance to corrosion, cleaning, dissection and drying procedures, allow adequate replication of micro- and macrovessels, and collecting system, as well as in porcine kidney. This fact correlates with the results of Mazensky and Danko [6] that successfully used Duracryl in studying origin and course of the arteria vertebralis in rabbit. The authors conducted maceration in 2-4% KOH solution for a period of 2 days at 60-70 ºC. However, in our study the best results about this step of the corrosion technic technique was received using 20% NaOH solution for 24 h at 60 ºC. Based on these facts, it can be concluded that species and tissue dependence exist.

So far, the anatomical relationships between the intrarenal arteries and the kidney collecting system in swine have been detected by Pereira-Sampaio et al. (2004) using polyester resin and methyl ethyl ketone peroxide as a catalyst.

The authors described the arterial tree without glomeruli and the collecting system consisted of pelvis, major and minor calices without medullar and cortical collecting tubules. It should be mentioned that, unlike them, we found that the number of cortical glomeruli in kidney, which arteries were injected with casting media with higher dilution, was significantly higher than the lower dilution. With regard to collecting system, the higher concentrated resin with higher viscosity allowed the filling predominantly of major and small calices which were bigger in diameter than those from the lower concentrated resin. Furthermore, media with a higher dilution filled the collecting system in the medulla and even in the cortex on the entire renal surface. The described differences of the resin can be explained by the better penetrating ability of the lower concentrated Duracryl® Plus. In this regard, we recommend lower concentrated Duracryl® Plus (1:5) in making corrosion casts. On the one hand, the differences between our corrosion technic with Duracryl® Plus and that used by Pereira-Sampaio et al. [10] can be explained by distinct penetration which is specific for each resin type. On the other hand, the concentration of the resin is also important.

## Conclusion

The results of the present study proved that the Duracryl® Plus is one of the most suitable resin for making three-dimensional casts of the renal arteries and collecting tubules and also microvascular corrosion casts for stereomicroscopy and scanning electron microscopy. The concentration of the resin is very important for preparing accurate casts.

Further investigations are needed to prove the suitability of this resin as a medium for corrosion casting method conducting on different organs of animals and humans.

## References


1. **Aharinejad, S. H., A. Lametschwandther.** Microvascular corrosion casting in scanning electron microscopy. Techniques and applications. Springer-Verlag, Wien, New York, 1992, p. 13.
2. **Combe, E. C., C. Brandon, A. Owen, J. S. Hodges.** A protocol for determining the surface free energy of dental materials. – Dent. Mater., **20**, 2004, 262-268.
3. **Hossler, F. E., J. E. Douglas.** Vascular corrosion casting: review of advantages and limitations in the application of some simple quantitative methods. – Microsc. Microanal., **7**(3), 2001, 253-264.
4. **Joniau, S., K. V. Eeckt, H. Van Poppel.** The Indications for Partial Nephrectomy in the Treatment of Renal Cell Carcinoma. – Nat. Clin. Pract. Urol., **3**(4), 2006, 198-205.
5. **Kondo, S.** Microinjection methods for visualization of the vascular architecture of the mouse embryo for light and scanning electron microscopy. – J. Electron. Microsc., **47**(2), 1998, 101-113.
6. **Mazensky, D., J. Danko.** The importance of the origin of vertebral arteries in cerebral ischemia in the rabbit. – Anat. Sci. Int., 85, 2010, 102-104.
7. **Motta, P. M., R. Heyn, S. Makabe.** Three-dimensional microanatomical dynamics of the ovary in postreproductive aged women. – Fertil. Steril., **78**(2), 2002, 360-370.
8. **Murakami, T., T. Itoshima, K. Hitomi, A. Ohtsuka, A. L. Jones.** A monomeric methyl and hydroxypropyl methacrylate injection medium and its utility in casting blood capillaries and liver bile canaliculi for scanning electron microscopy. – Arch. Histol. Jap., **47**(2), 1984, 223-237.
9. **Murakami, T.** Application of the scanning electron microscope to the study of the fine distribution of the blood vessels. – Arch. Histol. Jap., **32**(5), 1971, 445-454.
10. **Pereira-Sampaio, M. A., L. A. Favorito, F. J. Sampaio.** Pig kidney: anatomical relationships between the intrarenal arteries and the kidney collecting system. Applied study for urological research and surgical training. – J. Urol., **172**(5 Pt 1), 2004, 2077-2081.
11. **Pflug, K.** 2004. Dental materials having a nanoscale filler. (Available at www.google.com/patents/US6693143).
12. **Sampaio, F. J., M. A. Pereira-Sampaio, L. A. Favorito.** The pig kidney as an endourologic model: anatomic contribution. – J. Endourol., **12**(1), 1998, 45-50.
13. **Vasiliu (Diaconu), M., D. I. Tomita, D. Spridon, N. Dumitrascu, G. Costin, C. Stadoleanu.** Surface energetic characteristics of acrylic biomaterials. – Biomaterials, **1**(3), 2011, 242-246.
14. **Vodenicharov, A.** Scanning electron microscopic study on renal glomerular arterioles in pigs. – Bulg. J. Vet. Med., **10**(3), 2007, 147-154.
15. **Wang, L., P. H. P. D'Alpino, L. G. Lopes, J. C. Pereira.** Mechanical properties of dental restorative materials: relative contribution of laboratory tests. – J. Appl. Oral. Sci., **11**(3), 2003, 162-167.



*Corresponding author:
*Nikolay Tsandev*
*e-mail: drcandev@abv.bg*

Institute of Experimental Morphology, Pathology and Anthropology with Museum
Bulgarian Anatomical Society

Acta morphologica et anthropologica, 22
Sofia ● 2015

*Review Articles*

# Briefly about Bone Defects and New Strategies to Treat Them: Review

*R. Alexandrova[1], A. Abudalleh[1], T. Zhivkova[1], L. Dyakova[2], B. Andonova-Lilova[1], O. Alexandrov[3], N. Saha[4]*

[1]*Institute of Experimental Morphology, Pathology and Anthropology with Museum, Bulgarian Academy of Sciences*
[2]*Institute of Neurobiology, Bulgarian Academy of Sciences*
[3]*Health Service, Gorna Malina, Bulgaria*
[4]*Tomas Bata University in Zlin,* Czech Republic

Treatment of severe bone defects, resulting from trauma or resorption, remains a major challenge in orthopaedic surgery and traumatology. These pathological conditions significantly decrease the quality of life of people affected and have a high social and economic costs. In the presented minireview we summarize data of both current therapy for bone regeneration and the perspectives in the field of bone tissue engineering.

## Introduction

Bone disease is a serious health problem that directly impacts on the quality of life of patients. It has been predicted that the percentage of persons over 50 years of age affected by bone disease will double by 2020, especially in populations where aging is coupled with increased obesity and poor physical activity. Bone and joint degenerative and inflammatory problems, bone fractures, low back pain, osteoporosis, scoliosis ant other musculoskeletal problems need to be solved by using permanent, temporary or biodegradable devices [28, 30].

### *Bone structure, role and properties*

Bone is a highly complex and specialized form of connective tissue which is composed of an organic matrix strengthened by deposits of calcium phosphate crystals. The organic matrix is composed of collagen type I fibers (approximately 95%) and of proteoglicans and numerous non-collagenous proteins (5%). This organic matrix, calcified

by calcium phosphate minerals embeds bone cells (**Table 1**), which participate in the maintenance and organization of bone, namely osteoprogenitor cells, osteoblasts, osteocytes, and osteoclasts [1, 4]. The cellular origin of bone was recognised in the early 19th century, and the term "osteoblast" was first used by Gegenbaur in 1864 to refer to the "granular corpuscles found in all developing bone as the active agents of osseous growth" [16].

**Table 1.** The cellular components of bone

| Cell type | Origin | Function and phenotype |
|---|---|---|
| OSTEOBLASTS | Mesenchymal stem cells | Can have one of four different fates: 1) become embedded in the bone as **osteocytes**, (2) transform into inactive osteoblasts and become **bone-lining cells** – found along the bone surfaces that are undergoing neither bone formation nor resorption, inactive cells that are believed to be precursors osteoblasts, (3) undergo programmed cell death (apoptosis), or in some situations (4) transdifferentiate into cells that deposit chondroid or chondroid bone. **Active osteoblasts** are mononuclear cells with cuboidal shape; rich in alkaline phosphatase; synthesize and secrete collagen type I and glycoproteins (osteopontin, steocalcin), cytokines, and growth factors into a region of unmineralized matrix (osteoid) between the cell body and the mineralized matrix; produce calcium phosphate minerals extra- and intracellularly within vesicles. **Inactive osteoblasts** are elongated cells, undistinguishable morphologically from the bone-lining cells |
| OSTEOCYTES | Osteoblasts | An important role of osteocytes and their network of cell processes is to function as strain and stress sensors, signals that are very important for maintaining bone structure |
| OSTEOCLASTS | Hematopoietic stem cells | Polynuclear cells responsible for bone resorption (by acidification of bone mineral leading to its dissolution and by enzymatic degradation of demineralized extracellular bone matrix; important for growth and development |
| CHONDROCYTES | Mesenchymal stem cells | Cells found in cartilage that produce and maintain the cartilaginous matrix |

According to [4, 14, 27, 43].

Despite its hard structure, bone actually exists in a constant state of dynamic turnover known as bone remodeling even once growth and modeling of the skeleton have been completed [21].

*Bone defects*

Bone defects often result from tumor resection, congenital malformation (such as osteogenbesis imperfects, osteopetrosis), trauma, fractures, surgery, or periodontitis in dentistry, as well as from diseases, such as osteoporosis or arthritis [15, 24, 39].

Osteogenesis imperfecta or brittle bone disease is the most common of the inherited disorders primarily affecting bone. It occurs in 1 in 10 000 to 20 000 live births and is associated with mutations in type I collagen genes (*COL1A1* and *COL1A2*) in ~ 90% of the patients [37, 40, 41].

Osteopetrosis is a rare genetic condition (with both autosomal recessive and autosomal dominant forms) characterized by an increase of bone mass due to defective osteoclast formation and function and spontaneous fractures [8, 42].

Osteoporosis, a major public health burden that affects millions of people (especially women) around the world, is defined as "a skeletal disorder characterized by risk of fractures of the hip, spine, and other skeletal sites." It is a systemic skeletal disease characterized by low bone mineral density and micro-architectural deterioration of bone tissue, leading to bone fragility and increased in risk of fracture [11, 31].

Bone health may be impaired in many patients being treated for cancer. Primary tumors that reside in (osteosarcoma and Ewing's family tumours) or form metastases (such as breast, prostate, lung cancers, myeloma) to bone can result in compromised skeletal integrity [17, 44]. Several medical conditions and medications significantly increase the risk for bone loss and skeletal fragility. These include androgen-deprivation therapy for prostate cancer and aromatase inhibitor therapy for breast cancer, among others. Hypogonadism induced by many of these cancer treatments results in bone loss and increases the risk of osteoporosis and fractures. Glucocorticoid-induced osteoporosis is the most common form of secondary osteoporosis [7, 32].

Fracture healing is a complex, unique physiological process of repair, where, unlike in other tissues, the majority of bone injuries recover without the formation of scar tissue, and bone is regenerated with its pre-existing properties largely restored [13]. However, there are cases of fracture healing in which bone regeneration is impaired due to various factors leading to pathologies such as delayed union or fracture non-union [3]. The unsuccessful bone regeneration still results in many people never recovering fully their function and quality of life; with all the social, financial and psychological implications [38]. For example there are data demonstrating that old people suffering from femoral fractures will die within a year (15-25%) or become dependent (50%) [11, 31].

*The techniques used to repair damaged bones*

When an area of damaged bone is too large for self-repair, the damaged bones must be repaired by using alternative materials, such as autografts, allografts and artificial materials.

Autografts, which are transferred from healthy parts of the bones of the same patient, are widely used because they show high performance. Autologous bone remains the "gold standard" for stimulating bone repair and regeneration, but its availability may be limited and the procedure to harvest the material is associated with complications (e.g. additional surgical trauma). On the other hand, allografts, which are transferred from other people, have problems related to not only limited availability but also with foreign body immune reactions and infections (for example risk of HCV or HIV transmission to the recipient). In addition, they have a poor degree of cellularity, less revascularisation, and a higher resorption rate compared to autologous grafts, resulting in a slower rate of new bone tissue formation [26, 28, 30].

As a result there is a need for the development of artificial bone substitute materials with improved characteristics that are safe for patients, (relatively) easily produced and can be supplied at any time and in any amount.

**Biomaterials for bone implants**

A variety of materials with different structure, composition and mechanism of action are available or under development to enhance the repair of bone defects (Some of them are presented in **Table 2**).

**Table 2.** Brief description of some biomaterials for bone implants

| BIOMATERIAL | SHORT CHARACTERISTIC | |
|---|---|---|
| | **ADVANTAGES** | **DISADVANTAGES** |
| **CERAMICS**<br>Based mainly on hydroxyapatite, since this is the inorganic compound of bone | Able to form bone apatite-like material or carbonate hydroxyapatite on their surface, enhancing their osseointegration;<br>Hardness, high compression strength and excellent wettability that result in low incidence of biologically significant particle generation and clinically significant osteolysis.<br>Able to bind and concentrate cytokines, as in the case of natural bone.<br>Used as a bearing surface in total hip arthroplasty (THA) for more than 30 years | Brittleness and slow degradation rates; low fracture toughness and linear elastic behavior which make them prone to breakage under stress. There are data that the addition of carbon nanotubes remarkably improves the mechanical characteristics of alumina. |
| **BIOACTIVE GLASS**<br>based on a random network of silica tetrahedra containing Si–O–Si bonds. The network can be modified by the addition of modifiers such as Ca, Na and P. | The first man-made material to bond to living tissues;<br>biocompatible and osteoconductive (especially glasses with $SiO_2$ content < 60% in weight), bond to bone without an intervening fibrous connective tissue; in vivo, there is a dynamic balance between intramedullary bone formation and bioactive glass resorption. | Low mechanical strength and decreased fracture resistance that can be easily overcome by modifying the composition and application in low load-bearing areas. |
| **METALS**<br>Mainly stainless steel and titanium alloys (i.e. Ti-6Al-4V) | Excellent mechanical properties, which makes them the most widely applied implant material used in bone surgical repairs | The lack of tissue adherence and the low rate of degradation results either in a second surgery to remove the implant or in permanent implantation in the body with the related risks of toxicity due to accumulation of metal ions due to corrosion |
| **NATURAL POLYMETS**<br>Collagen and glycosaminoglycans | Biocompatibility and biodegradability, since they compose the structural materials of tissues. | Low mechanical strength and high rates of degradation (they are used in composites or in chemical modification by cross-linking. These changes make cause cytotoxic effects and reduce compatibility). |
| **SYNTHETIC POLYMERS** | The versatility of chemically synthesized polymers enables the fabrication of scaffolds with different features (forms, porosities and pore size, rates of degradation, mechanical properties) to match tissue specific applications | |
| **COMPOSITES** | Can combine a synthetic scaffold with biologic elements to stimulate cell infiltration and new bone formation. Each individual material has advantages for osteogenic applications, each also has drawbacks associated in certain properties (i.e. brittleness of ceramics) that can be overcome by combining different materials. | |

According to [2, 12, 18, 30, 34, 46].

Historically, these materials belong to the following three generations:

**First generation** – Bioinert materials. They are represented by alumina ($Al_2O_3$) and zirconia ($ZrO_2$) and played an important role for substitution purposes due to their low reactivity. This is not surprising because at the very beginning the main goal of investigators was to achieve substitution with the lowest tissue response, perhaps because the only expected tissue response was inflammation and material rejection [25,45];

**Second generation** – Bioactive and biodegradable materials. To this group belong bioactive glasses – synthetic silica-based materials with bone bonding properties due to the formation of a carbonate substituted hydroxycarbonate apatite layer (similar to the apatite layer in bone) on the surface of the materials after immersion in body fluid [18, 19, 25];

**Third generation** – Materials designed to stimulate specific cellular responses at the molecular level [19, 33]. They appeared at the same time as scaffolds for tissue engineering applications started to be developed.

*Bone tissue engineering*

Tissue engineering approaches have recently been devised to repair large bone losses. Three main players take part in this technology: i) stem cells (for example mesenchymal stem cells) that are having the potential to form the organ of interest; ii) scaffold (where the stem cells will be transferred into) – a three-dimensional porous structures that serves as a template for cell interactions and the formation of bone-extracellular matrix to provide structural support to the newly formed tissue; iii) signals stimulating proliferation and appropriate differentiation of the stem cells [1, 25]. Scafold materials must meet a number of requirements including biocompatibility, adequate mechanical properties, biodegradability, etc. [25, 47]. Among the most important properties that they should possess are osteoinduction (the ability to stimulate the differentiation of osteoprogenitor cells into mature bone cells and then the formation of new bone), osteoconduction (the physical property of the graft to serve as a scaffold for viable bone healing - osteoblasts from the margin of defect that is being grafted, utilize the bone graft material as a framework upon which to spread and generate new bone), and osteogenesis (the ability of the graft to produce new bone, this process is dependent on the presence of vital bone cells in the graft) [29].

*Mesenchymal stem cells*

Adult mesenchymal stem cells (MSCs) are non differentiated multipotent cells with self-renewal capacity that have the potential to differentiate towards lineages of mesenchymal origin, including bone and cartilage. Although originally isolated from bone marrow, MSCs have since been obtained from many other tissues such as adipose tissue, synovial fluid, periosteum, umbilical cord blood and several fetal tissues [5, 9, 22, 23, 48].

MSCs have several advantages that are of interest for bone tissue engineering:

• These cells can be relatively easily obtained from different sources including fat tissue, bone marrow, cord blood;

• MSCs can be extracted from patient's own tissue than can prevent the development of immune rejection;

• In comparison to embryonic stem cells there are no ethical concerns for their application;

• MSCs do not develop into teratomas when transplanted, a consequence observed with embryonic stem cells and induced pluripotent stem cells [20].

There are some difficulties in working with these cells which should also be mentioned:

• Lack of commonly accepted surface markers, which can be used for the identification of MSCs. A set of minimal criteria for MSC was recommended, which includes the capability of adherence to plastic surfaces, the expression of CD73, CD90 and CD105 and the absence of major histocompatibility complex (MHC) class II surface molecules (HLA-DR), endothelial (CD31) and hematopoietic-specific antigens (CD34, CD45, CD14) [10, 23, 35]. In culture their cell surface antigens may vary depending on the isolation and expansion methods used [23].

• The small percentage of MSCs in some tissues such as bone marrow – the amount of BM-MSCs varies between 0.001% and 0.01% of the total mononuclear cell. Such low frequency of BM-MSC requires prolonged cultivation of the cells in laboratory conditions, thus increasing the risk of differentiation induction and epigenetic alterations [20]. In addition, age-related changes in number, proliferation capacity and differentiation potential of MSCs have been reported [6].

• The protocols for isolation and cultivation of MSCs are complicated and not suitable for routine clinical practice [20]. Human MSCs are sensitive to serum and oxygen deprivation, which resulted in cell death in vitro when applied in combination for 48 hours. This fact must be taken into consideration when working with them [36];

• The biological activity of these cells is not fully clarified;

• And finally – MSCs can be obtained from various tissues but there is still no definite answer to the question what is the best source for their isolation.

## Conclusion

Tissue engineering is one of the most rapidly developing and promising areas of science and medicine. The first successful steps in this exciting direction have already been made. Before its entry into routine clinical practice, it is necessary to overcome a number of challenges including establishment of scaffolds with improved properties that meet the requirements for these type biomaterials, identification of the most appropriate stem cells, optimizing strategies for their isolation, cultivation and directed differentiation.

*Acknowledgements:* This work was supported by the a COST Action MP1301 and by Grant No T 02/5 from 2014, National Science Fund at the Bulgarian Ministry of Education and Science.

## References

1. **Amini, A. R., C. T. Laurencin, S. P. Nukavarapu.** Bone tissue engineering: recent advances and challenges. – Crit. Rev. Biomed. Eng., **40**(5), 2012, 363-408.
2. **Arcos, D., I. Izquierdo-Barba, M. Vallet-Regi.** Promising trends of bioceramics in biomaterials field. – J. Mater. Sci: Mater. Med., **20**, 2009, 447-455.
3. **Audigé, L., D. Griffin, M. Bhandari, J. Kellam, T. P. Rüedi.** Path analysis of factors for delayed healing and nonunion in 416 operatively treated tibial shaft fractures. – Clin. Orthop. Relat. Res., **438**, 2015, 221-232.
4. **Barrere, F., C. A. van Blitterswijk, K. de Groot.** Bone regeneration: molecular and cellular interactions with calcium phosphate ceramics. – Int. J. Nanomedicine, **3**, 2006, 317-332.
5. **Bieback, K., S. Kern, H. Kluter, H. Eichler.** Critical parameters for the isolation of mesenchymal stem cells from umbilical cord blood. – Stem Cells, **22**, 2004, 625-634.
6. **Bellantuono, I., A. Aldahmash, M. Kassem.** Aging of marrow stromal (skeletal) stem cells and their contribution to age-related bone loss. – Biochim. Biophys. Acta., **179**(2), 2009, 364-370.
7. **Cannata, D. H., A. Kirschenbaum, A. C. Levine.** Androgen deprivation therapy as primary treatment for prostate cancer. – J. Clin. Endocrinol. Metab., **97**(2), 2012, 360-365.

8. **Coudert, A. E., M. C. de Vernejoul, M. Muraca, A. Del Fattore.** Osteopetrosis and its relevance for the discovery of new functions associated with the skeleton. – J. Int. Endocrinol., 2015, ID 372156. doi: 10.1155/2015/372156.
9. **De Bari, C., F. Dell' Accio, F. P. Luyten.** Human periosteum-derived cells maintain phenotypic stability and chondrogenic potential throughout expansion regardless of donor age. – Arthritis Rheum., **44**, 2001, 85-95.
10. **Dominici, M., K. Le Blanc, I. Mueller, I. Slaper-Cortenbach, F. Marini, D. Krause, et al.** Minimal criteria for defining multipotent mesenchymal stromal cells. The In ternational Society for Cellular Therapy position statement. – Cytotherapy, **8**, 2006, 315-317.
11. **D' Amelio, P., G. C. Isaia.** Male Osteoporosis in the Elderly. – Int. J. Endocrinol., 2015, ID 907689. doi: 10.1155/2015/907689.
12. **El-Ghannam, A.** Bone reconstruction: from biocermamics to tissue engineering. – Expert. Rev. Med. Devices, **2**, 2005, 87-101.
13. **Einhorn, T. A.** The cell and molecular biology of fracture healing. – Clin. Orthop. Relat. Res., **355**, 1998, S7-S21.
14. **Franz-Odendaal, T. A., B. K. Hall, P. E. Witten.** Buried alive: How osteoblasts become osteocytes. – Developmental Dynamics, **235**(1), 2006, 176-190.
15. **Forlino, A., W. A. Cabral, A. M. Barnes, J. C. Marini.** New perspectives on osteogenesis imperfecta. – Nat. Rev. Endocrinol., 7(9), 2011, 540-557.
16. **Gegenbauer, C.** Untersuchungen zur vergleichenden Anatomie der Wirbeltiere. – Heft 1. Carpus und Tarsus. Leipzig*:* Schultergtel, 1864.
17. **Gaspar, N., D. S. Hawkins, U. Dirksen, I. J. Lewis, S. Ferrari , M. C. Le Deley, H. Kovar, R. Grimer, J. Whelan, L. Claude, O. Delattre, M. Paulussen, P. Picci, K. Sundby Hall, H. van den Berg, R. Ladenstein, J. Michon, L. Hjorth, I. Judson, R. Luksch, M. L. Bernstein, P. Marec – Bérard, B. Brennan, A. W. Craft, R. B. Womer, H. Juergens, O. Oberlin.** Ewing Sarcoma: Current Management and Future Approaches Through Collaboration. – J. Clin. Oncol., **33**(27), 2015, 3036-3046.
18. **Hench, L. L.** The story of Bioglass®. – J. Mater. Sci: Mater. Med., **17**, 2006, 967-978.
19. **Hench, L. L., J. M. Polak.** Third-generation biomedical materials. – Science, **295**(5557), 2002, 1014-7.
20. **Hilfiker, A., C. Kasper, R. Hass, A. Haverich.** Mesenchymal stem cells and progenitor cells in connective tissue engineering and regenerative medicine: is there a future for transplantation? – Langenbecks Arch. Surg., **396**(4), 2011, 489-97.
21. **Hill, P. A.** Bone remodelling. – J. Br. Orthod., **25**(2), 1998, 101-107.
22. **In't Anker, P. S., S. A. Scherjon, K. C. Kleijburg – van der Keur C, W. A. Noort, F. H. Claas, R. Willemze et al.** Amniotic fluid as a novel source of mesenchymal stem cells for therapeutic transplantation. – Blood, **102**, 2003, 1548-1549.
23. **Jacobs, S. A., V. D. Roobrouck, C. M. Verfaillie, S. W. Van Gool.** Immunological characteristics of human mesenchymal stem cells and multipotent adult progenitor cells. – Immunol Cell Biol., **91**(1), 2013, 32–39.
24. **Jimi, E., S. Hirata, K. Osawa, M. Terashita, C. Kitamura, H. Fukushima.** The current and future therapies of bone regeneration to repair bone defects. – Int. J. Dent., 2012, ID 148261.
25. **Jones, J. R., P. D. Lee, L. L. Hench.** Hierarchical porous materials for tissue engineering. – Philos. Trans A Math. Phys. Eng. Sci., **364**(1838), 2006, 263-81.
26. **Kalfas, I. H.** Principles of bone healing. – Neurosurg. Focus, **10**(4), 2001, 1-10.
27. **Karageorgiou, V., D. Kaplan.** Porosity of 3D biomaterial scaffolds and osteogenesis. – Biomaterials, **26**, 2005, 5474-5491.
28. **Kokubo, T., H. Kim, M. Kawashita.** Novel bioactive materials with different mechanical properties. – Biomaterials, **24**(13), 2003, 2161-75.
29. **Kumar, P., B. Vinitha, G. Fathima.** Bone grafts in dentistry. – J. Pharm. Bioallied. Sci., **5** (Suppl. 1), 2013, S125-S127.
30. **Le Guéhennec, L., P. Layrolle, G. Daculsi.** A review of bioceramics and fibrin sealant. – Eur. Cell Mater., **8**, 2004, 1-10.
31. **Lane, N., S. Morris.** New perspectives on parathyroid hormone therapy. – Curr. Opin. Rheumatol., **17**(4), 2005, 467-474.

32. **Mirza, F., E. Canalis.** Management of endocrine disease: Secondary osteoporosis: pathophysiology and management. – Eur. J. Endocrinol., **173**(3), 2015, R131-R151.
33. **Navarro, M., A. Michiardi, O. Castaño, J.A. Planell.** Biomaterials in orthopaedics. – J. R. Soc. Interface, **5**(27), 2008, 1137-58.
34. **Ogihara, N., Y. Usui, K. Aoki, M. Shimizu, N. Narita, K. Hara, K. Nakamura, N. Ishigaki, S. Takanashi, M. Okamoto, H. Kato, H. Haniu, N. Ogiwara, N. Nakayama, S. Taruta, N. Saito.** Biocompatibility and bone tissue compatibility of alumina ceramics reinforced with carbon nanotubes. – Nanomedicine (Lond), **7**(7), 2012, 981-993.
35. **Pittenger, M. F., A. M. Mackay, S. C. Beck, R. K. Jaiswal, R. Douglas, J. D. Mosca, et al.** Multilineage potential of adult human mesenchymal stem cells. – Science, **284**, 1999, 143-147.
36. **Potier, E., E. Ferreira, A. Meunier, L. Sedel, D. Logeart-Avramoglou, H. Petite.** Prolonged hypoxia concomitant with serum deprivation induces massive human mesenchymal stem cell death. – Tissue Eng., **13**(6), 2007, 1325-31.
37. **Primorac, D., D. Anticević, I. Barisić, D. Hudetz, A. Ivković.** Osteogenesis imperfecta – multisystemic and life-long disease that affects whole family. – Coll Antropol., **38**(2), 2014, 767-72.
38. **Shekkeris, A. S., P. K. Jaiswal, W. S. Khan.** Clinical applications of mesenchymal stem cells in the treatment of fracture non-union and bone defects. – Curr Stem Cell Res Ther., **7**(2), 2012, 127-33.
39. **Scaramuzzo, L., L. Messuti, P. F. Manicone, L. Raffaelli, B. Rossi, P. Gallenzi, D. Berardi, G. Maccauro.** Clinical and histological modifications in osteopetrotic bone: a review. – J. Biol. Regul. Homeost. Agents, **23**(2), 2009, 59-63.
40. **Scaramuzzo, L., L. Raffaelli, M. S. Spinelli, G. Damis, G. Maccauro, P. F. Manicone.** Orthopaedic and dental abnormalities in osteogenesis imperfecta: a review of the literature. – J. Biol. Regul. Homeost Agents., **25**(3), 2011, 313-321.
41. **Shaker, J. L, C. Albert, J. Fritz, G. Harris.** Recent developments in osteogenesis imperfecta. – Faculty Rev., **681** 2015,. doi: 10.12688/f1000research.6398.1. eCollection.
42. **Sobacchi, C., A. Schulz, F. P. Coxon, A. Villa, M. H. Helfrich.** Osteopetrosis: genetics, treatment and new insights into osteoclast function. – Nat. Rev. Endocrinol., **9**(9), 2013, 522-536.
43. **Tuan, R. S., G. Boland, R. Tuli.** Adult mesenchymal stem cells and cell-based tissue engineering. – Arthritis Res. Ther, **5**(1), 2003, 32-45.
44. **Terpos, E., C. B. Confavreux, P. Clézardin.** Bone antiresorptive agents in the treatment of bone metastases associated with solid tumours or multiple myeloma. – Bonekey Rep., **4**(744), 2015, doi: 10.1038/bonekey.2015.113.
45. **Thamaraiselvi, T. V., S. Rajeswari. Biological Evaluation of Bioceramic Materials – A Review.** – Trends Biomater. Artif. Organs, **18**, 2004, 9-17.
46. **Välimäki, V. V., H. T. Aro.** Molecular basis for action of bioactive glasses as bone graft substitute. – Scand. J. Surg., **95**(2), 2006, 95-102.
47. **Williams, D. F.** On the mechanisms of biocompatibility. – Biomaterials, 29, 2008, 2941-2953.
48. **Zuk, P. A., M. Zhu, P. Ashjian, D. A. De Ugarte, J. I. Huang, H. Mizuno, et al.** Human adipose tissue is a source of multipotent stem cells. – Mol. Biol. Cell, **13**, 2002, 4279-4295.

Institute of Experimental Morphology, Pathology and Anthropology with Museum
Bulgarian Anatomical Society

Acta morphologica et anthropologica, 22
Sofia ● 2015

# Fibroblast Activation Protein α and Its Role in Cancer with a Focus on Breast Carcinoma: Review

*M. Dimitrova[1], I. Iliev[1], V. Pavlova[1], V. Mitev[2], I. Ivanov[2]*

[1]*Institute of Experimental Morphology, Pathology and Anthropology with Museum, Bulgarian Academy of Sciences, Sofia*
[2]*Department of Medical Chemistry and Biochemistry, Medical University of Sofia, Sofia, Bulgaria*

Fibroblast activation protein α (FAP-α) is a plasma membrane serine proteinase belonging to the S9b family of post-proline cleaving proteases. The enzyme is generally missing in normal tissues of adult humans and mammals but is up-regulated in the reactive stromal fibroblasts in tumors of epithelial origin and many types of sarcomas. For that reason, at present FAP-α is considered as an important marker molecule in oncology. However, the relationship between elevated enzyme activity/expression and prognosis is not always conclusive. Thus, in breast cancer, the connection between higher expression levels of FAP-α and prognosis varies from better to very poor in different studies. Obviously, despite the extensive studies by many research teams all over the world, the enzyme role in cancer is not elucidated yet. The aim of the present mini-review is to summarize the existing data about the role of FAP-α in cancer by focusing on its involvement in breast cancer.

*Key words:* fibroblast activation protein α, breast cancer, enzyme marker, Ehrlich ascites carcinoma, *in vivo* model.

## General information about FAP-α

Fibroblast activation protein-α (FAP-α; EC 3.4.21.B28) is a serine type integral membrane protease belonging to the S9b family of post-proline cleaving enzymes. FAP-α is also known as Seprase (from ***S***urface ***E***xpressed ***PR***ote***ASE***). Its soluble form, which enters the blood plasma after shedding from cell surface [3], has been recently recognized to coincide with **A**nti**P**lasmin **C**leaving **E**nzyme (APCE) [22]. The active enzyme is a 170 kDa homodimer composed of two 97 kDa glycoprotein subunits [32].

FAP-α is a highly conservative protein, e.g. the mouse enzyme has 89% similarity to its human analogue [27]. Additionally, human and murine FAP-α genes show very similar genomic organization [28]. On the other hand, FAP-α is the most closely related to dipeptidyl peptidase IV (DPPIV, EC 3.4.14.5) which is the best studied member of S9b family. They share 50% sequence identity in the entire sequence and 70% identity in the catalytic domain [2] – a fact which impedes the design of specific substrates and/

or inhibitors for the two enzymes. Amino acids of the catalytic triads of FAP-α and DPPIV are arranged in one and the same manner and have very close positions: Ser624, Asp702, His734 for FAP-α and Ser630, Asp708, His740 for DPPIV [reviewed in 9]. The human FAP-α gene is located on chromosome 2q23 and is organized similarly to the DPPIV gene which maps to chromosome 2q24.3. For this reason, some authors believe that the two enzymes have a common origin, one arising by duplication of the other's gene [25]. Comparison of the crystal structures of FAP-α and DPPIV reveals that the major difference in the active sites is that FAP-α possesses Ala657 instead of Asp663 in DPPIV. This variation proves to be enough to lessen the acidity and increase the size of the active center pocket, thus making FAP-α capable of endopeptidase activity [26]. Substrates [21] and inhibitors [6] for FAP-α have been developed that utilize the above difference and are selective for the enzymes.

FAP-α is well known to possess a gelatinase activity; one of its most characteristic substrates is collagen type I [31]. The endopeptidase activity of soluble FAP-α cleaves α2-antiplasmin [22], which is involved in blood clotting. Amongst the most recently found enzyme's natural substrates are neuropeptide Y, B-type natriuretic peptide, substance P and peptide YY [14].

## Tissue distribution of FAP-α

FAP-α is known to have a distinctive tissue distribution since it is usually absent from normal adult tissues as revealed by immunohistochemical analyses using specific monoclonal antibodies [7]. *In silico* electronic northern blot analysis also shows that normal tissues generally lack FAP-α mRNA expression [5]. In normal human and mammalian tissues, the enzyme activity is restricted to single reactive fibroblasts, glucagon producing A-cells in pancreatic islets and separated endometrial cells [reviewed in 38]. Comparatively high enzyme levels are found in mesenchymal cells during embryogenesis. However, FAP-α knockout mice have a normal phenotype in histological and hematological analysis [29]. Therefore, other compensatory pathways probably exists involving molecules with functional similarity to FAP-α, such as DPPIV or other S9b family members or matrix metalloproteases (MMPs).

Alternatively, FAP-α expression is highly induced during different pathological processes. For example, the enzyme is up-regulated in inflammatory diseases like rheumatoid arthritis and osteoarthritis, where it is found in fibroblast-like synovial cells. Also, FAP-α is expressed by activated but not by resting hepatic stellate cells of cirrhotic liver. Additionally, the enzyme is highly expressed by fibroblasts at the remodeling interface in human idiopathic pulmonary fibrosis as well as in liver fibrosis [reviewed in 38].

The most characteristic feature of FAP-α, however, is that it is up-regulated in stromal fibroblasts of over 90% of human epithelial tumors and in lots of sarcomas, but not in benign tumors [reviewed in 9 and 18]. Although the enzyme name "FAP" implies that it is to be found only on reactive stromal fibroblasts, lots of studies show that this is not the case. In fact, FAP-α has been identified in many tumor cells like melanoma cells, human colorectal cancer cells, breast cancer cells, human gastric and intestinal carcinomas, etc. [18]. Moreover, in certain types of carcinomas, the enzyme has not been restricted to plasma membrane, but intracellular cytoplasmic pools have also been discovered.

## The dual role of FAP-α in cancer

*FAP-α as a tumor promoter*

Epithelial cancers (carcinomas), just like other solid tumors, induce the formation of abundant stromal compartments which, in some cases, may comprise more than 50% of the mass of the tumor. Tumor stroma consists of newly formed blood vessels, connective tissue cells such as activated fibroblasts or cancer-associated fibroblasts (CAFs), infiltrating inflammatory cells and a network of matrix proteins. Resting fibroblasts of normal adult tissues usually do not synthesize proteins neither expresses FAP-α. On the contrary, CAFs are known to synthesize and secrete proteins which promote cancer cells' invasion and angiogenesis and regulate the immune response to the tumor growth. Additionally, a common characteristic of CAFs in almost all types of carcinomas and lots of sarcomas is that they express FAP-α. It has been shown that lack of FAP-α in the CAFs of lung tumors in FAP-α knockout mice causes a dramatically increased accumulation of type I collagen around tumor cells which impairs cell motility, tumor growth and angiogenesis [34]. These experiments are indicative for the important role of the enzyme in tumor progression.

Furthermore, FAP-α molecule of CAFs, endothelial cells of tumor blood vessels and cancer cells is situated in the invadopodia – membrane protrusions that contact and degrade extracellular matrix (ECM) – together with other proteolytic enzymes, mainly MMPs [15]. More recent works have shown that heterodimeric complexes FAP-α–DPPIV are formed in the invadopodia, which are able of hydrolyzing collagen type I and are responsible for the invasive phenotype of CAFs and cancer cells [19].

According to the recent studies [23], FAP-α expression by fibroblasts results in alterations of organization and composition of the ECM that favors invasion. Thus, the matrix produced by the FAP-α-positive cells promotes tumor cell motility and directs migration.

FAP-α has been shown to be highly expressed in endothelial cells of newly forming tumor blood vessels in different types of cancers [reviewed in 18]. Taken together with the enzyme ability to cleave off collagen type I, this fact is in favor of FAP-α supposed role in promoting angiogenesis. In fact, in an *in vivo* mouse model of human breast cancer expressing FAP-α, a much higher micro-vessel density has been reported in comparison to the same experiment but with human breast carcinoma cells with low levels of the enzyme [11]. Moreover, the lack of FAP-α-positive CAFs in FAP-α knockout mice carrying lung tumors results in a significant reduction of micro-vessel density in the tumor stroma [34]. All these findings confirm the involvement of FAP-α in the mechanisms underlying angiogenesis in solid tumors.

Various studies have shown that up-regulation of FAP-α in epithelial tumors is one of the main factors responsible for the inhibition of antitumor activity by the immune system. Thus, application of DNA vaccine to FAP-α which causes CD8+ T cells killing of FAP-α-positive CAFs has been shown to improve antitumor immune function and increase sensitivity of tumor cells to chemotherapeutics [24]. In another experiment with mice carrying lung or pancreatic carcinoma cells, the ablation of FAP-α expressing cells has led to a rapid necrosis of both cancer and stromal cells [20]. Hence, FAP-α seems to insert some kind of protective effect on tumor and stromal cells against the immune response.

*FAP-α as a Tumor Suppressor*

Certain results of experimental research have shown that in some types of tumors FAP-α may play a role as a tumor suppressor. In that respect, particularly convincing

are the recent studies on mouse melanoma cells and on human non-small cells lung carcinoma (NSCLC) cells [36, 37]. Initially, it has been shown that the lack of DPPIV activity in the two types of cells is directly linked to the tumor phenotype. Restoration of DPPIV activity by virus vectors in both cases leads to a re-expression of FAP-α on the cell surface, followed by a profound suppression of the tumor phenotype and return to the dependence of the cell growth on exogenous growth factors. Moreover, the re-establishment of dependence on growth factors occurred even when a catalytically inactive mutant of DPPIV was expressed, which according to the authors may be due to the re-expression of endogenous FAP-α molecule. Other studies have provided direct evidence of FAP-α as a tumor suppressor at least in the case of malignant melanomas [33]. It has been observed that FAP-α re-expression resulted in decreased tumorogenicity of mouse melanoma cells and restored contact inhibition and growth factor dependence.

From the above-mentioned data it is obvious that a significant discrepancy exists between FAP-α function as tumor promoter or tumor suppressor. Thus, the role of FAP-α in cancer either depends on the tissue origin of the cancer cells or the mechanisms of the enzyme involvement in tumor diseases are much more complex and not well understood thus far.

## FAP-α in breast cancer

FAP-α was first discovered in the mid-1980s as the protein binding the mouse monoclonal antibody F19 that labeled the reactive stromal fibroblasts of epithelial tumors, fibroblasts in fetal mesenchymal tissues and tumor cells of sarcomas. In one of the pioneer studies on FAP-α, using F19 antibody the enzyme was localized immunohistochemically in tissue sections of frozen malignant and benign breast tumors of 27 patients [7]. In this experiment, only reactive fibroblasts of malignant breast carcinomas were found to be FAP-α-positive, whereas stromal fibroblasts of the benign tumors as well as tumor epithelial cells were negative for the enzyme. After this work, many studies on FAP-α and its role in breast cancer have been carried out, however, with dissimilar results. For example, using the above antibody (F19) and three other clones recognizing monomeric or dimeric enzyme, retrospective immunohistochemical analyses were performed on tissue sections from invasive ductal carcinoma (IDC) of the breast of female patients who underwent mastectomy [1]. According to the authors, FAP-α was co-localized with type I procollagen, i.e. it was restricted to stromal fibroblasts adjacent to tumor-cell nests but not cancer cells. This result confirmed the early study on FAP-α in breast carcinoma [7]. On the other hand, FAP-α expression was reported in several human breast cancer cell lines [8]. Moreover, immunohistochemical analysis of the enzyme expression using FAP-specific antisera in 41 formalin-fixed and paraffin-embedded specimens of human breast tissue [16] revealed immunoreactivity also in malignant cells of invasive ductal carcinomas and in lymph node metastases. Neoplastic cells in ductal carcinomas in situ (DCIS) exhibited variable levels of staining, but epithelial cells of benign fibroadenomas and benign proliferative breast disease had no immunoreactivity. Epithelial cells of normal breast tissues were not stained, as well. These controversial results may be due to different antibodies used in the above studies. Obviously, F19 recognizes FAP-α on stromal cells, whereas the FAP-antisera may have a broader specificity [18].

Results from different studies on FAP-α expression and its connection with prognosis in breast carcinoma are also controversial. For example, retrospective clinicopathological analyses performed on 112 cases of IDC of the breast revealed that more

abundant FAP-α expression was associated with longer overall and disease-free survival [11]. The authors proposed the enzyme as an independent prognostic factor for mammary gland carcinoma. This result, however, contradicts all the later observations in breast cancer.

In a later study [11], to investigate the role of FAP-α in breast cancer, human mammary adenocarcinoma cells were engineered to over-express the enzyme. The cells were implanted into mammary fat pads of female immunodeficient mice and the xenografts were tested for tumorogenicity, growth rates and micro-vessel density. According to the results, control transfectants not expressing FAP-α grew slowly whereas cells over-expressing the enzyme formed fast growing highly vascular tumors. This observation is consistent with the hypothesis that FAP-α facilitates tumor growth and stimulates angiogenesis.

Later, using the above mouse model of human breast cancer, the authors investigated the role of proteolytic activity of FAP-α in promoting tumor growth, matrix degradation and invasion [12]. It was shown that breast cancer cells expressing a catalytically inactive mutant of FAP-α also produced rapidly growing tumors. Moreover, the FAP-specific inhibitor Val-boroPro (talabostat) given to the animals through oral gavage did not decrease substantially the growth rates of FAP-α expressing tumors. From these results it seems logical to conclude that proteolytic activity of FAP-α is not necessary for tumor promoting effects of the enzyme. In the same study [12], gelatin films with immobilized FITC-fibronectin and type I collagen gels were used for *in vitro* evaluation of the cells' capacity to degrade ECM and their invasive potential. Surprisingly, cells expressing inactive FAP-α molecules degraded gelatin films and invaded collagen gels with similar rates as did the cells expressing wild type FAP-α. The authors commented that the presence of FAP-α molecule, no matter active or inactive, in tumor cells invadopodia may induce the expression and secretion of MMPs like MMP-9 thus making the cells to acquire invasive phenotype. Actually, it was shown that FAP-α was co-localized with MMPs in tumor cells invadopodia [15, 19]. Nevertheless, the role of FAP-α activity in breast cancer remains controversial since other researchers have shown that FAP-α protease activity is abnormally high in extracts of patient tumors indicating that increased expression in real situations is always connected with increased FAP-α protease activity [17].

In another study [13], FAP-α was characterized in primary breast tumor samples and in cell lines, along with the potential interaction of FAP-α with other signaling pathways. These results showed that FAP-α once again was significantly increased in patients with poor outcome and survival. Another important observation was that the over-expression of FAP-α is closely related with the levels of focal adhesion kinase (FAK) – an enzyme known to coordinate adhesion and migration processes thus providing tumor cells migration. It was concluded that FAP-α promotes proliferation and migration of breast cancer cells, potentially by regulating the FAK pathway. These experiments tend to elucidate the intimate mechanisms of FAP-α over-expression on tumor growth.

Further on, attempts were made to specify the possible FAP-α diagnostic capacity for mammary gland carcinoma [10]. As it is well known, diagnosis of ductal carcinomas *in situ* (DCIS) in breast cancer is challenging for pathologists due to the large variety of artefacts, which could be misinterpreted as stromal invasion. Micro-invasion is usually detected morphologically by the presence of malignant cells outside the limits of the basement membrane and myoepithelium. In a recent study, FAP-α capacity as a diagnostic marker to distinguish DCIS from DCIS with micro-invasions (DCIS-MI) was evaluated. Evidence was provided that simultaneous immunostaining for FAP-α

(a cellular marker for invasiveness) and Calponin (a marker for myoepithelium layer integrity) could serve for pathologically diagnosing whether DCIS had micro-invasion. Thus, the presence of CAFs positive for FAP-α and interrupted myoepithelial layer (revealed by intermittent staining for Calponin), would indicate a high probability for DCIS-MI and vice versa.

## Animal models for studying FAP-α in breast cancer

As it becomes clear from the above, most of the recent studies on the role of FAP-α in breast cancer have been performed using human breast cancer cells implanted in the fat pad of immunodeficient mice and a subsequent tracking of the development of the tumor formation. However, such xenografts in standard mouse models express stromal and vessels elements of murine origin. This limitation was recently overcome by the development of a human skin/mouse chimeric model established by transplanting human foreskin on to the lateral flank of severe combined immunodeficient mice (SCID). The subsequent inoculation of breast carcinoma cells within the dermis of the transplanted human skin resulted in the production of xenografts expressing stromal and vessel elements of human origin [35].

Another, yet unexploited possibility, are the mouse models of Ehrlich carcinoma (EC) – ascites or solid form. EC is a spontaneous murine mammary adenocarcinoma adapted to ascites form and carried in outbred mice by serial intraperitoneal (i.p.) passages. EC is used both as ascites and as solid form, that is, if tumor cells are injected i.p., the ascites form is obtained; if they are administered subcutaneously (s.c.), a solid form is obtained [30]. Thus, one of the main advantages of Ehrlich carcinoma is that same tumor cell line could be used in *in vivo* experiments both with ascites or solid form of the tumor. Moreover, EC is known to possess great resemblance to highly undifferentiated human mammary gland carcinomas and is widely used to evaluate innovative anti-cancer therapies [reviewed in 30]. EC (solid form) allows researchers to trace the volume of the tumor on a daily basis without sacrificing the laboratory animals. Also, it could be studied by the application of histology methods aiming to determine the crosstalk between tumor and surrounding tissues or the necrotic or apoptotic areas of the tumor. Additionally, changes in enzymatic activities of tumor cells or the extracellular matrix could be obtained.

Recently, we developed a fluorogenic substrate for the histochemical studies of FAP-α - 4-(β-Ala-Gly-Pro-hydrazido)-N-hexyl-1,8-naphthalimide (βAGP-HHNI) [4]. Using this substrate, we studied the localization of the enzyme in cryostat sections of normal mouse mammary gland and in EC-solid form, obtained by s.c. inoculation of $1\times10^6$ tumor cells in 0.2 ml PBS in mature female mice (**Fig. 1**).

According to the results, alveolar epithelial cells and dense connective tissue in healthy mice were FAP-α-negative (**Figs. 1a, b**). Haematoxyline-eosin staining of cryosections from EC showed tumor cells in different stages of cell division as well as necrotic foci within the mass of cell (**Fig. 1c**). All the tumor cells, however, were FAP-α-positive (**Fig. 1d**). The result indicates that normal mouse mammary glands do not express the enzyme just like in humans, whereas mouse breast carcinoma cells do express FAP-α. This is additional evidence that the mouse model of EC can be successfully used to study FAP-α role in breast cancer.

In conclusion, research results obtained thus far show beyond any doubt that FAP-α is an important marker for many types of tumors including breast cancer. The enzyme is involved in tumor growth and dissipation throughout different mechanisms which are

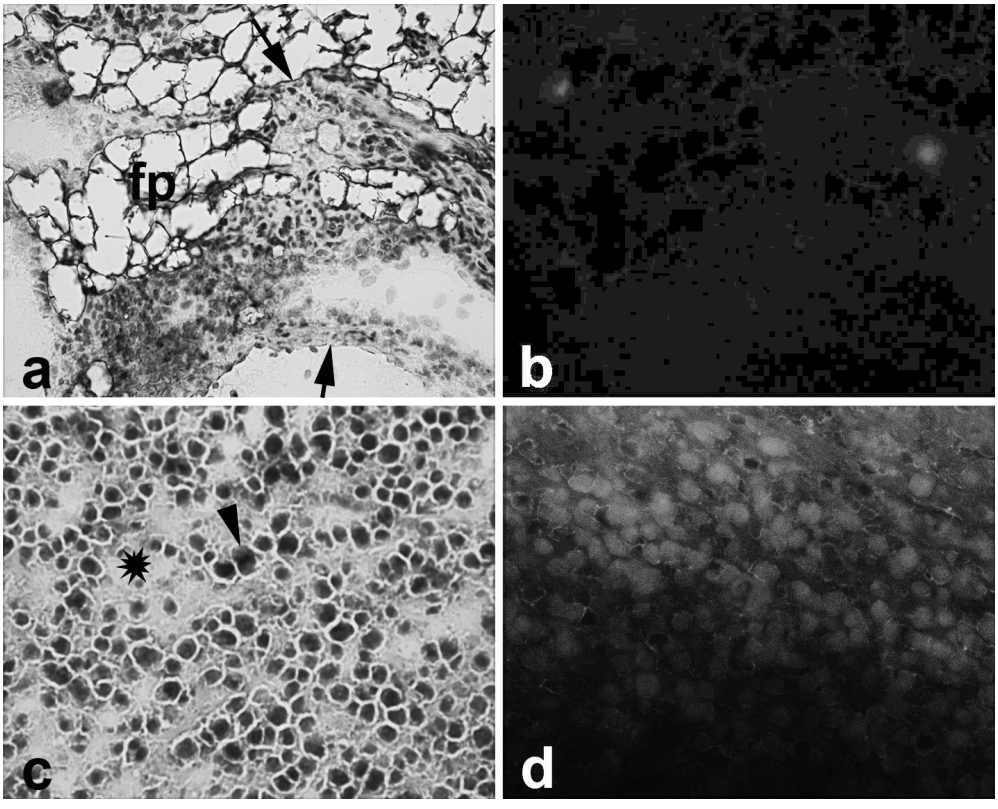


**Fig. 1.** FAP-α activity in normal mouse mammary gland (a, b), and in a mouse model of EC – solid form (c, d); a, b – No FAP-α activity in healthy mouse mammary gland (fp – fat pad; arrows – glandular epithelium and surrounding dense connective tissue); c – haematoxylin-eosin staining of solid EC with cells in mitosis (arrowhead) and necrotic foci (asterisk); a, c – light microscopy; b, d – fluorescent microscopy. a, b –200×; c, d – 400×

not fully elucidated yet. The use of animal models might be useful in biomedical studies on FAP-α involvement in cancer pathology as well as to evaluate the enzyme capacity as diagnostic and/or prognostic marker in cancer.

*Acknowledgements:* This work is financially supported by the National Science Fund of the Bulgarian Ministry of Education and Science, Grant No T02/25 2014.

## References

1. **Ariga, N., E. Sato, N. Ohuchi, H. Nagura, H. Ohtani.** Stromal expression of fibroblast activation protein/seprase, a cell membrane serine protease and gelatinase, is associated with longer survival in patients with invasive ductal carcinoma of breast. – Int. J. Cancer, **95**, 2001, 67-72.
2. **Cheng, J. D., M., Valianou, A. A Canutescu, E. K. Jaffe, H. O. Lee, H. Wang et al.** Abrogation of fibroblast activation protein enzymatic activity attenuates tumor growth. – Mol. Cancer Ther., **4**, 2005, 351-360.
3. **Collins, P. J., G. McMahon, P. O'Brien, B. O'Connor.** Purification, identification and characterisation of seprase from bovine serum. – Int. J. Biochem. Cell Biol., **36**, 2004, 2320-2333.

4. **Dimitrova, M., I. Iliev, V. Pavlova, V. Mitev, S. Dimitrova, D. Aleksandrova, I. Ivanov.** Development and application of a specific fluorogenic substrate for the cytochemical study of fibroblast activation protein alpha. – Proceedings of VIth Workshop on Experimental Models and Methods in Biomedical Research, 2015, in press.
5. **Dolznig, H., N. Schweifer, C. Puri, N. Kraut, W. J. Rettig, D. Kerjaschki, P. Garin-Chesa.** Characterization of cancer stroma markers: in silico analysis of an mRNA expression database for fibroblast activation protein and endosialin. – Cancer Immunity, **5**, 2005, 10-18.
6. **Edosada, C. Y., C. Quan, T. Tran, V. Pham, C. Wiesmann, W. Fairbrother, B. B. Wolf.** Peptide substrate profiling defines fibroblast activation protein as an endopeptidase of strict Gly(2)-Pro(1)-cleaving specificity. – FEBS Lett., **580**, 2006, 1581-1586.
7. **Garin-Chesa, P., L. J. Old, W. J. Rettig.** Cell surface glycoprotein of reactive stromal fibroblasts as a potential antibody target in human epithelial cancers. – Proc. Natl. Acad. Sci. USA, **87**, 1990, 7235-7239.
8. **Goodman, J. D., T. L. Rozypal, T. Kelly.** Seprase, a membrane-bound protease, alleviates the serum growth requirement of human breast cancer cells. – Clin. Exp. Metastasis., **20**, 2003, 459-470.
9. **Gorrell, M. D., J. E. Park.** Fibroblast activation protein α. – In: Handbook of proteolytic enzymes (Eds. N. D. Rawlings, G. S. Salvesen), Elsevier Ltd, 2013, 3395-3400.
10. **Hua, X., L. Yu, X. Huang, Z. Liao, Q. Xian.** Expression and role of fibroblast activation protein-alpha in microinvasive breast carcinoma. – Diagnostic Pathology, **6**, 2011, 111-117.
11. **Huang, Y., S. Wang, T. Kelly.** Seprase promotes rapid tumor growth and increased microvessel density in a mouse model of human breast cancer. – Cancer Res., **64**, 2004, 2712–2716.
12. **Huang, Y., A. E. Simms, A. Mazur, S. Wang, N. R. Leon, B. Jones, N. Azur, T. Kelly.** Fibroblast activation protein-α promotes tumor growth and invasion of breast cancer cells through non-enzymatic functions. – Clin. Exp. Metastasis, **28**, 2011, 567-579.
13. **Jia, J., T. A. Martin, L. Ye, W. G. Juang.** FAP-α (Fibroblast activation protein-α) is involved in the control of human breast cancer cell line growth and motility via the FAK pathway. – BMC Cell Biol., **15**, 2014, 16-25.
14. **Keane, F. M., N. A. Nadvi, T.-W. Yao, M. D. Gorrell.** Neuropeptide Y, B-type natriuretic peptide, substance P and peptide YY are novel substrates of fibroblast activation protein-a. – FEBS Journal, **278**, 2011, 1316-1332.
15. **Kelly, T., S. C. Mueller, Y. Yeh, W. T. Chen.** Invadopodia promote proteolysis of a wide variety of extracellular matrix proteins. – J. Cell. Physiol., **158**, 1994, 299-308.
16. **Kelly, T., S. Kechelava, T. L. Rozypal, K. W. West, S. Korourian.** Seprase, a membrane-bound protease, is overexpressed by invasive ductal carcinoma cells of human breast cancers. – Mod. Pathol., **11**, 1998, 855-863.
17. **Kelly, T.** Evaluation of seprase activity. – Clin. Exp. Metastasis, **17**, 1999, 57-62.
18. **Kelly, T., Y. Huang, A. E. Simms, A. Mazur.** Fibroblast Activation Protein-a: a key modulator of the microenvironment in multiple pathologies. – In: International review of cell and molecular biology, Academic Press – Elsevier, USA, UK, The Netherlands, 2012, 83-116.
19. **Kennedy, A., H. Dong, D. Chen, W. T. Chen.** Elevation of seprase expression and promotion of an invasive phenotype by collagenous matrices in ovarian tumor cells. – Int. J. Cancer, **124**, 2009, 27-35.
20. **Kraman, M., P. J. Bambrough, J. N. Arnold, E. W. Roberts, L. Magiera, J. O. Jones et al.** Suppression of antitumor immunity by stromal cells expressing fibroblast activation protein-alpha. – Science, **330**, 2010, 827-830.
21. **Lai, K. S., N.-H. Ho, J. D. Cheng, C.-H. Tung.** Selective fluorescence probes for dipeptidyl peptidase activity - fibroblast activation protein and dipeptidyl peptidase IV. – Bioconjug. Chem., **18**, 2007, 1246-1250.
22. **Lee, K. N., K. W. Jackson, V. J. Christiansen, C. S. Lee, J. G. Chun, P. A. McKee.** Antiplasmin-cleaving enzyme is a soluble form of fibroblast activation protein. – Blood, **107**, 2006, 1397-1404.
23. **Lee, H. O., S. R. Mullins., J. Franco-Barraza, M. Valianou, E. Cukierman, J. D. Cheng.** FAP-overexpressing fibroblasts produce an extracellular matrix that enhances invasive velocity and directionality of pancreatic cancer cells. – BMC Cancer, **11**, 2011, 245.
24. **Loeffler, M., J. A. Kruger, A. G. Niethammer, R. A. Reisfeld.** Targeting tumor associated fibroblasts improves cancer chemotherapy by increasing intratumoral drug uptake. – J. Clin. Invest., **116**, 2006, 1955-1962.

25. **Mathew, S., M. J. Scanlan, B. K. Mohan Raj, V. V. Murty, P. Garin-Chesa, L. J. Old, W. J. Rettig, R. S. Chaganti.** The gene for fibroblast activation protein alpha (FAP), a putative cell surface-bound serine protease expressed in cancer stroma and wound healing, maps to chromosome band 2q23. – Genomics, **25,** 1995, 335–337.
26. **Meadows, S. A., C. Y. Edosada, M. Mayeda, T. Tran, C. Quan, H. Raab,| C. Wiesmann, B. B. Wolf.** Ala657 and conserved active site residues promote fibroblast activation protein endopeptidase activity via distinct mechanisms of transition state stabilization. – Biochemistry, **46**, 2007, 4598-4605.
27. **Niedermayer, J., M. J. Scanlan, P. Garin-Chesa, C. Daiber, H. H. Fiebig, L. J. Old, W. J. Rettig. A. Schnapp.** Mouse fibroblast activation protein: molecular cloning, alternative splicing and expression in the reactive stroma of epithelial cancers. – Int. J. Cancer, **71**, 1997, 383-389.
28. **Niedermeyer, J., B. Enenkel, J. E. Park, M. Lenter, W. J. Rettig, K. Damm et al.** Mouse fibroblast-activation protein – conserved Fap gene organization and biochemical function as a serine protease. – Eur. J. Biochem., **254**, 1998, 650–654.
29. **Niedermeyer, J., M. Kriz, F. Hilberg, P. Garin-Chesa, U. Bamberger, M. C. Lenter, J. Park, B. Viertel, H. Puschner, M. Mauz et al.** Targeted disruption of mouse fibroblast activation protein. – Mol. Cell. Biol., **20**, 2000, 1089-1094.
30. **Ozaslan M., I. D. Karagoz, I. H. Killic, M. E. Guldur.** Ehrlich ascites carcinoma. – Afr. J. Biotech., **10**, 2011, 2375-2378.
31. **Park, J. E., M. C. Lenter, R. N. Zimmermann, P. Garin-Chesa, L. J. Old, W. J. Rettig.** Fibroblast activation protein, a dual specificity serine protease expressed in reactive human tumor stromal fibroblasts. – J. Biol. Chem., **274**, 1999, 36505–3651.
32. **Pineiro-Sanchez, M. L., L. A. Goldstein, J. Dodt, L. Howard, Y. Yeh, H. Tran, W. S. Argraves, W. T. Chen.** Identification of the 170-kDa melanoma membrane-bound gelatinase (seprase) as a serine integral membrane protease. – J. Biol. Chem., **272**, 1997, 7595-7601.
33. **Ramirez-Montagut, T., N. E. Blachere, E. V. Sviderskaya, D. C. Bennett, W. J. Rettig, P. Garin-Chesa, A. N. Houghton.** FAP alpha, a surface peptidase expressed during wound healing, is a tumor suppressor. – Oncogene, **23**, 2004, 5435-5446.
34. **Santos, A. M., J. Jung, N. Aziz, J. L. Kissil, E. Pure.** Targeting fibroblast activation protein inhibits tumor stromagenesis and growth in mice. – J. Clin. Invest., **119**, 2009, 3613-3625.
35. **Tahtis, K., Lee F.-T., Wheatley J. M., P. Garin-Chesa, J. E. Park, F. E. Smyth, Y. Obata, E. Stockert, C. M. Hall, L. J. Old, W. J. Rettig, A. M. Scott.** Expression and targeting of human fibroblast activation protein in a human skin/severe combined immunodeficient mouse breast cancer xenograft model. – Mol. Cancer Ther., **2**, 2003, 729-737.
36. **Wesley, U. V., A. P. Albino, S. Tiwari, A. N. Houghton.** A role for dipeptidyl peptidase IV in suppressing the malignant phenotype of melanocytic cells. – J. Exp. Med., **190**, 1999, 311-322.
37. **Wesley, U. V., S. Tiwari, A. N. Houghton.** Role for dipeptidyl peptidase IV in tumor suppression of human non-small cell lung carcinoma cells. – Int. J. Cancer, **109**, 2004, 855-866.
38. **Yu, D. M. T., T.-W. Yao, S. Chowdhury, N. A. Nadvi, B. Osborne, W. B. Church, G. W. McCaughan, M. D. Gorrell.** The dipeptidyl peptidase IV family in cancer and cell biology. – FEBS Journal, **277**, 2010, 1126-1144.

Institute of Experimental Morphology, Pathology and Anthropology with Museum
Bulgarian Anatomical Society

Acta morphologica et anthropologica, 22
Sofia ● 2015

# Mammalian Balbiani Body As a Sign of Ancestral Oocyte Asymmetry: Review

*V. Hadzhinesheva, V. Nikolova, I. Chakarova, S. Delimitreva, M. Markova, R. Zhivkova*

*Department of Biology, Medical Faculty, Medical University – Sofia, Bulgaria*

Eutherian eggs underwent a secondary loss of the ooplasmic gradient of yolk and maternal morphogens. However, the oocytes of mammalian primordial follicles display an asymmetric organelle cluster recognized as Balbiani body. Distribution of components of this aggregate might be a clue for the function of Balbiani body in eutherians and some alterations of its dynamics could be associated with ovarian pathology, particularly in human.

*Key words:* oocyte polarity, mitochondria, Golgi complex, Xenopus, mouse.

Mammalian evolution is characterized by secondary loss of the ancestral amniotic egg with its cytoplasmic gradients. As a result, blastomeres of eutherians (placental mammals) lack morphogenetic signals of maternal origin, and their fates are determined solely by embryonic induction. In this respect, eutherians are a rare exception. In all other metazoan groups, embryonic cell fates are determined by two mechanisms, ooplasmic segregation of maternal morphogens being at least as important as embryonic induction [8]. Ooplasmic segregation, i.e. the specification of preformed mRNAs, regulator proteins and other important oocyte components (e.g. yolk) into gradients, is important because these components can perform their morphogenetic function only if they are unevenly distributed into the early blastomeres during cleavage. For that reason, the establishment of oocyte asymmetry is a key prerequisite for successful development throughout the metazoan kingdom, with eutherians as a secondary exception.

The oocyte structure thought to be responsible for determination of cytoplasmic polarity is the so called Balbiani body, first decribed more than a hundred years ago. It is found in oocytes of different invertebrate and vertebrate species – insects, echinoderms, fishes, amphibians and birds [9, 13, 20, 23]. The Balbiani body is a transient collection of organelles, inclusions, proteins and mRNAs located adjacent to the nucleus. In frogs and fishes, it assembles in oogonia or early primary oocytes and disperses prior to stage II of oogenesis [17, 18], while in eutherians, it is observed first in oogonia and then in primary oocytes until dictyate stage [15].

The main constituent organelles of the Balbiani body are endoplasmic reticulum, Golgi cisternae and mitochondria. In the model amphibian *Xenopus*, where it is best studied, it is an aggregation composed mostly of mitochondria, endoplasmic reticulum,

clustered Golgi cisternae and germinal granules. Other animals may have somewhat different structure and composition of this complex. For example, the Balbiani body of mouse oocytes contains a much smaller quantity of mitochondria and no germinal granules [19]. Another difference is that mRNAs are an important component of the Balbiani body in oocytes of Xenopus but have not yet been found in its mouse counterpart [18].

A number of studies have addressed the relation of the Balbiani body to cytoskeletal structures. It is invariably associated with the centrosome. In frog oogonia, Balbiani body formation starts with aggregation of mitochondria and germinal granules around the centrosome. During mitosis, its components associate with the centrosome in the vicinity of the cytoplasmic bridges interconnecting the daughter cells. At a later stage, in the oocyte, the position of Balbiani complex marks the vegetal pole [14]. Ultrastructural and immunocytochemical studies of mouse oocytes also suggest involvement of microtubules in the dynamics of Balbiani body formation and disassembly. In ovaries of newborn mice, where meiosis is still ongoing, elements of Balbiani body are associated with centrosomes in primordial follicles [15].

Among other cytoskeletal elements, intermediate filaments have been reported to colocalize with the Balbiani body, particularly in amniote oocytes. A recent study on bird eggs (Japanese quail, *Coturnix japonica*) shows the presence of vimentin and cytokeratin 5, in the mitochondrial aggregation of Balbiani [20]. In the human, presence of cytokeratin 19 has been shown as a single perinuclear aggregation in oocytes from developing and adult ovaries [21] which is likely to correspond to the Balbiani body. However, the presence and dynamics of intermediate filaments in mammalian oocytes is still insufficiently studied and subject to controversy [16].

The evolutionary conservation of the Balbiani body across so many animal phyla suggests important functions of this structure in oogenesis. Based on the regular presence of mitochondrial aggregates in this complex, some authors have suggested that it plays a role in selection of good-quality mitochondria for the zygote [6, 10]. However, other data indicate importance of the Balbiani body for the transport of RNAs towards the vegetal pole of fish and frog eggs and its involvement in segregation and/or storage of regulatory proteins and mRNAs encoding them [12, 14, 22]. Notably, some maternal mRNAs required at later stages to establish the germline of the embryo (*vasa, nanos, gasz, dazl*) localize to the Balbiani body of fish and frog oocytes [18]. This strongly suggests a morphogenetic function of this transient organelle at least in mesolecithal and telolecithal eggs.

Unlike *Xenopus*, eutherians have secondarily isolecithal eggs. Despite the well-known asymmetrical position of the spindle, they have no specific yolk accumulation and no known gradients of morphogens; the ancestral cytoplasmic gradients have been lost. Nevertheless, a transient perinuclear complex of cytoplasmic organelles, apparently corresponding to the Balbiani body of other vertebrates though not always explicitly identified with it, has been observed in oocytes from primordial follicles of eutherians [11, 15]. This complex includes Golgi cisternae, endoplasmic reticulum, mitochondria and proteins; however, no RNAs have been detected so far [3, 5, 7, 14, 15, 19]. In mouse primordial follicles, Balbiani body is formed by aggregation of Golgi cisternae surrounded by mitochondria and endoplasmic reticulum (EPR). Perinuclear mitochondrial accumulation occurs just before ovarian tissue differentiates into primordial follicles, and is present for a short period in early primordial follicles. In later follicle stages (growing follicles), mitochondria and EPR disperse and Balbiani body is not present [19]. Hence, as a dynamic structure, the Balbiani body found in immature eutherian oocytes corresponds to those of eggs with cytoplasmic gradient as well as to a hypothetic ancestral model of polar egg [15].

What about the function of the eutherian Balbiani body? Is it just an evolutionary relic of the polarity-establishing structure that was important in the ancestral amniotic egg? The failure to detect mRNAs in the mouse Balbiani body, as well as the dispersal of key regulatory proteins such as Dazl throughout the cytoplasm of primary oocytes, seems to point to that direction [2]. However, in accordance with the general rule that conservation of structure indicates preservation of function, new data cast doubt on the old concepts; particularly the Vasa regulator protein, initially thought to lack specific localization in the oocyte, has recently been reported to associate with the Balbiani body in prepubertal and pubertal human ovaries [1].

Clues for the function of Balbiani body may come also from alteration of its dynamics associated with pathology. Our study of ovarian tissue from patients with ovarian polycystosis has demonstrated atypical structure corresponding to the Balbiani body – a semicircular or circular granular aggregate at the nuclear periphery in immature oocytes [24]. The Golgi complex, endoplasmic reticulum, mitochondria and associated proteins as important cytoplasmic components presumably affect the development of mammalian follicles, and their intracellular distribution may be important for some aspects of ovarian pathology during prenatal and postnatal mammalian development.

Perspectives of future investigation on the Balbiani body in mammals are related to localization and dynamic changes of its structures in oocytes from different species and at different developmental stages. Ultrastructural and immunocytochemical studies must be done on fetal and neonatal as well as adult ovaries. In this respect, the mouse is the most convenient object, particularly with its temporal shift in oocyte meiotic maturation allowing observation of active prophase I oocytes in the first days after birth [4]. Studies on humans are more difficult because of practical and ethical considerations, but at the same time they provide the opportunity to investigate the Balbiani body not only in norm but also in pathology.

*Acknowledgements:* The work was supported by Medical University – Sofia, Grant MU-16 / 2015.

## References

1. **Albamonte, M. I., M. S. Albamonte, I. Stella, L. Zuccardi, A. D Vitullo.** The infant and pubertal human ovary: Balbiani's body-associated VASA expression, immunohistochemical detection of apoptosis-related BCL2 and BAX proteins, and DNA fragmentation. – Hum. Reprod., **28**(3), 2013, 698-706.
2. **Anderson, R. A., N. Fulton, G. Cowan, S. Coutts, P. T. Saunders.** Conserved and divergent patterns of expression of DAZL, VASA and OCT4 in the germ cells of the human fetal ovary and testis. – B.M.C. Dev. Biol., 7, 2007, 136.
3. **Billett, F. S., E. Adam.** The structure of the mitochondrial cloud of Xenopus laevis oocytes. – J. Embryol. Exp. Morphol., **36**(3), 1976, 697-710.
4. **Bristol-Gould, S. K., P. K. Kreeger, C. G. Selkirk, S. M. Kilen, R. W. Cook, J. L. Kipp, L. D. Shea, K. E. Mayo, T. K. Woodruff.** Postnatal regulation of germ cells by activin: the establishment of the initial follicle pool. – Dev. Biol., **298**(1), 2006, 132-48
5. **Bukovsky, A., M. R. Caudle, M. Svetlikova, N. B. Upadhyaya.** Origin of germ cells and formation of new primary follicles in adult human ovaries. – Reprod. Biol. Endocrinol., 2, 2004, 20.
6. **Cox, R. T., A. C. Spradling.** A Balbiani body and the fusome mediate mitochondrial inheritance during Drosophila oogenesis. – Development, **130**, 2003, 1579-1590.
7. **de Smedt, V., D. Szöllösi, M. Kloc.** The balbiani body: asymmetry in the mammalian oocyte. – Genesis, **26**(3), 2000, 208-12.
8. **Gilbert, S. F.** Developmental Biology. 6th edition. Sunderland (MA): Sinauer Associates, 2000.
9. **Gupta T., F. L. Marlow, D. Ferriola, K. Mackiewicz, J. Dapprich, D. Monos, M. C. Mullins.** Microtubule actin crosslinking factor 1 regulates the Balbiani body and animal-vegetal polarity of the zebrafish oocyte. – PLoS Genet., **6**(8), 2010, e1001073.

10. **Guraya, S. S.** Recent advances in the morphology, cytochemistry, and function of Balbiani's vitelline body in animal oocytes. – Int. Rev. Cytol., **59**, 1979, 249–321.
11. **Hertig A. T., E. C. Adams.** Studies on the human oocyte and its follicle. I. Ultrastructural and histochemical observations on the primordial follicle stage. – J. Cell Biol., **34**(2), 1967, 647-675.
12. **Kloc, M., L. D. Etkin.** Two distinct pathways for the localization of RNAs at the vegetal cortex in Xenopus oocytes. – Development, 121, 1995, 287-297.
13. **Kloc, M., C. Larabell, A. P. Chan, L. D. Etkin.** Contribution of METRO pathway localized molecules to the organization of the germ cell lineage. – Mech. Dev., **75**(1-2), 1998, 81-93.
14. **Kloc, M., S. Bilinski, L. D. Etkin.** The Balbiani body and germ cell determinants: 150 years later. – Curr. Top. Dev. Biol., **59**, 2004, 1–36.
15. **Kloc, M., M. Jaglarz, M. Dougherty, MD. Stewart, L. Nel-Themaat, S. Bilinski.** Mouse early oocytes are transiently polar: three-dimensional and ultrastructural analysis. – Exp. Cell Res., **14**(17), 2008, 3245-54.
16. **Markova, M., S. Delimitreva, R. Zhivkova, V. Nikolova, D. Dimitrova.** Intermediate-cytoplasmic filaments in mammalian gametes. – Andrology, **19**(3), 2010, 14-16.
17. **Marlow, F., M. Mullins.** Bucky ball functions in Balbiani body assembly and animal–vegetal polarity in the oocyte and follicle cell layer in zebrafish. – Dev. Biol., **321**(1), 2008, 40-50.
18. **Marlow, F. L.** Oocyte Polarity and the Embryonic Axes: The Balbiani Body, an Ancient Oocyte Asymmetry. – Maternal Control of Development in Vertebrates: My Mother Made Me Do It! San Rafael (CA): Morgan & Claypool Life Sciences, 2010.
19. **Pepling, M. E., J. E. Wilhelm, A. L. O'Hara, G. W. Gephardt, A. C. Spradling.** Mouse oocytes within germ cell cysts and primordial follicles contain a Balbiani body. – Proc. Natl. Acad. Sci. USA, **104**(1), 2007, 187-92.
20. **Rodler, D., F. Sinowatz.** Expression of intermediate filaments in the Balbiani body and ovarian follicular wall of the Japanese quail (Coturnix japonica). – Cells Tissues Organs, **197**(4), 2013, 298-311.
21. **Santini, D., C. Ceccarelli, G. Mazzoleni, G. Pasquinelli, V. M. Jasonni, G. N. Martinelli.** Demonstration of cytokeratin intermediate filaments in oocytes of the developing and adult human ovary. – Histochemistry, **99**(4), 1993, 311-9.
22. **Wilk, K., S. Bilinski, M. T. Dougherty, M. Kloc.** Delivery of germinal granules and localized RNAs via the messenger transport organizer pathway to the vegetal cortex of Xenopus oocytes occurs through directional expansion of the mitochondrial cloud. – Int. J. Dev. Biol., **49**, 2005, 17-21.
23. **Yakovlev, K. V.** Localization of germ plasm-related structures during sea urchin oogenesis. – Dev. Dyn., 2015, doi: 10.1002/dvdy.24348
24. **Zhivkova R., M. Panevska, S. Delimitreva, M. Markova, V. Nikolova, I. Chakarova, T. Tenev, V. Hadzhinesheva, K. Mainhard, I. Vatev.** Investigation of cytokeratin and vimentin intermediate filaments in polycystic ovaries (PCOS) – presence and specific structure of Balbiani body in primordial follicles. – Akush. Ginekol. (Sofia), **52**(7), 2013, 7-12.

Corresponding author:
*Ralitsa S. Zhivkova*
*e-mail: rzhivkova@yahoo.com*

Institute of Experimental Morphology, Pathology and Anthropology with Museum
Bulgarian Anatomical Society

Acta morphologica et anthropologica, 22
Sofia ● 2015

# Contraception and *In Vitro* Fertilization in Young Women with Multiple Sclerosis: Review

*V. Kolyovska, V. Pavlova*

*Institute of Experimental Morphology, Pathology and Anthropology with Museum, Bulgarian Academy of Sciences, Sofia*

Multiple sclerosis (MS) is a chronic neurological disorder characterized by myelin sheaths damage, focal inflammation, gliosis and axonal degeneration. It affects predominantly women and the onset of the disease is at their child-bearing age. Myelination, a form of neural plasticity represents an important but poorly understood step to the process of repair. Unfortunately, cells that produce myelin can also be damaged which limits the ability of the brain to recover affected areas. The risks and benefits of using disease-modifying therapy during the various stages of a woman's reproductive life are topics that need attention. Since MS predominantly affects young women and is a hormone-dependent disease, then hormonal methods of contraception should be carefully discussed. Additionally, *in vitro* fertilization that also uses hormonal agents should be avoided. For that reason the pursuit of personalized medicine requires development of reliable biomarkers to predict the course of the disease and the response to therapies of this socially significant disease.

*Key words:* multiple sclerosis, contraception, contraceptives, *in vitro* fertilization, sex hormones.

Multiple sclerosis (MS) is the most common autoimmune inflammatory demyelinating disease of the central nervous system (CNS). Many young individuals are affected. Although the basic pathology of MS was already recognized in the 18$^{th}$ century, its causes and pathogenesis remain elusive. Relapsing-remitting multiple sclerosis (RRMS) accounts for approximately 80-85% of all MS cases. It affects 3 to 4 times more women than men, and many of these women are of child-bearing age. MS is characterized by intermittent or chronic damage to the myelin sheaths, focal inflammation, gliosis and axonal degeneration. The disease is both related to age (decreasing in elderly patients) and to sexual dimorphism [4]. Myelination, the process in which oligodendrocytes coat CNS axons with a myelin sheath, represents an important but poorly understood form of neural plasticity that may be sexually dimorphic in the adult CNS [6]. In response to demyelination oligodendrocyte precursor cells (OPCs) also considered as a type of adult neural stem cell, become activated. They proliferate, migrate and fill up the demyelinated lesions causing remyelination.

Addressing the reproductive concerns of women with MS is vital for comprehensive care [1]. Contraception, pregnancy, and breast-feeding remain disturbing questions to the woman with MS. The risks and benefits of using disease-modifying therapy dur-

ing the various stages of a woman's reproductive life are topics of great importance. Although physician's primary duty is to the patient, it is vital also to consider the fetus and later the child. Thus, the medical decisions that the patient is making should be guided by the physician after taking into account the patient's motivation for those decisions, including family obligations, cultural norms, and patient values [11]. Nowadays, it is considered that oral contraceptives are capable of offering health benefits beyond contraception. Some studies were designed to test the hypothesis that hormonal contraception brings certain health benefits. These were documented for several medical disorders including rheumatoid arthritis, multiple sclerosis, menstrual migraine and in perimenopause. Despite the benefits though, it is still outside the product license to use them in the majority of cases.

Recently, it has been suggested that hormones, including sex hormones, can affect and be affected by the immune system. Sex hormones have been linked to the disease activity in multiple sclerosis. Since they have major influence on brain and spinal neurons possible effect of the hormonal treatments used during assisted reproductive techniques may trigger some short-term disease processes. There is an increasing body of evidence that estrogen, progesterone, and testosterone provoke immune responses and influence damage repair in the nervous system and play an important role in neuroprotection following brain injury both *in vivo* and *in vitro* [3]. Estrogens and progestin may be the basis for such a new therapeutic approach and could help protect against myelin loss. Both types of hormones have been shown to promote the viability of neurons and the formation of myelin [5]. Sex steroids (particularly estrogen, androgen, and progesterone) also play an important role in neuroprotection following brain injury both *in vivo* and *in vitro* [9]. Moreover, hormones such as prolactin, vitamin D, leptin and gherlin may be used to modulate the immune response and may also influence the course of MS [12]. On the other hand, the role of male steroids in neuroprotection is less clear. For example, higher estradiol levels in men with MS were linked to a greater degree of brain tissue damage whereas testosterone proved to exert a protective role. Higher levels of testosterone in men may partially account for the fact that women with MS outnumber men. Apart from the protective role of testosterone a protective role of the pregnancy hormone estriol in pregnant women has been reported [14].

Infertility and MS might coincidentally come together and, therefore, these women might undergo assisted reproductive treatment (ART). Exogenous sexual steroids together with pregnancy have been shown to influence the risk of relapses in MS. Treatments used during assisted reproductive techniques may consequently influence the short-term evolution of MS by modifying the hormonal status of the patient thus increasing the risk of developing relapses or exacerbations in women with MS after *in vitro* fertilization (IVF) [10]. Other mechanisms involved in the worsening include temporary interruption of disease modified therapies, stressful events associated with infertility, and immunological changes induced by hormones such as increase in pro-inflammatory cytokines, as well as an increase in immune cell migration across the blood-brain-barrier. Women with MS who undergo IVF via hormonal injections may have an increased risk for relapse, a new study suggests. It is proposed that the increased risk is correlated with the use of GnRH (gonadotropin-releasing hormone) agonists leading to IVF failure [2]. The increased risk of relapse is particularly if the procedure does not result in a pregnancy. Furthermore, because there is a reasonable doubt that gonadotropin-releasing hormone agonists may make patients more prone to such an increase in relapse rate, gonadotropin-releasing hormone antagonists might be preferred for IVF protocols [10]. Prolactin (PRL) is a neuroendocrine peptide with potent immunomodulatory properties. Hyperprolactinemia enhances several autoimmune disorders and may play a role in the pathogenesis of MS. Significantly higher prolactin levels in serum

and cerebrospinal fluid (CSF) were found in female RRMS patients compared to males. The elevated PRL levels could be the result of an increased predisposition of females to synthesize and release PRL [3].

It is known that in women the artificial termination of pregnancy and childbirth leads to new attacks of the disease. Therefore, for women suffering from multiple sclerosis it is important to choose appropriate contraception on the advice of a gynecologist. Contemporary medicine has gained sufficient knowledge in the treatment of multiple sclerosis, unfortunately there are still no radical methods to treat it.

Women with MS or clinically isolated syndrome (CIS) were more likely to have used oral contraceptives in the 3 years before their diagnosis than women who did not have MS or CIS, the results of a new case-control study show. Independent of age, smoking status and obesity, there was a link between the use of oral contraceptives and the development of the first symptoms of MS. These findings suggest that using hormonal contraceptives may be contributing at least in part to the rise in the rate of MS among women. Hormones play an important role in many diseases, and it is known that pregnancy – which is associated with high estrogen levels – is protective against relapses in women who already have MS, so hormones appear to be involved in some way in this disease. Hughes noted that one idea is that low estrogen levels may trigger autoimmune disease, but there is no information on possible thresholds necessary for a protective or harmful effect. The researchers did not measure other factors associated with the lifestyle of modern women, such as diet, activity levels, or how long they spent outside, so several potential confounders were probably not accounted for [8].

The roles of progesterone (Pg), an immunomodulatory sex steroid, are poorly understood. Pg's immunomodulatory effects differ from those of estrogens and androgens. At pregnancy levels, Pg may suppress disease activity in MS [7].

POP (progestin only pills) is usually preferred during the postpartum period for its minimally suppressive effect on lactation. Considering the effect of progesterone on the myelin sheaths, it can be argued that POP can be an effective choice of contraception for MS patients during the postpartum period [13]. Because MS is usually observed among women of the reproductive age, the question about the most reliable contraceptive option for these patients will always be the first one for clinicians to answer. While in earlier studies the idea of using hormonal contraceptives in MS patients was not opposed, a recent study suggested that certain hormonal methods may increase the risk of developing MS or MS-like symptoms. Angiogenesis in MS causes neovascularization and a rise in the vascular supply of nutrients and migration of inflammatory cells to demyelinating lesions. Based on recent findings, it is recommended that clinicians should prescribe selective nonhormonal contraceptives such as copper-containing intrauterine devices (IUDs) in all phases of MS disease to be on the safe side. Those IUDs release free copper and copper salts into the uterine cavity without increasing serum copper levels in women with IUDs. Early analyses suggested that IUDs cause pelvic inflammatory disease (PID) in women. However, more recent studies have found no increased risk of PID in monogamous women with IUDs. It can be assumed that MS attacks can be triggered by the presence of infection in the genital tract. Based on the data in literature, it can be concluded that copper-containing IUDs can be safely used by MS patients. Additionally, the use of diaphragms increases urinary tract infections in women and can induce MS symptoms with mechanisms similar to those mentioned above. Additionally, when counseling about contraception methods for MS patients, each case should be individually evaluated on the basis of the severity of the disease and patient' s lifestyle. It proves logical that further studies are needed to come to a definitive conclusion regarding the identification of potential adverse effects of various hormonal and nonhormonal contraceptive methods [13].

In conclusion, all these findings can help establish a differential therapeutic concept in MS, which would allow treating MS women selectively according to their pathogenetic subtype and disease status. Advances in the understanding of the diagnostic significance of woman with multiple sclerosis may lead to novel therapeutic strategies in the future. Since MS is a hormone-dependent disease, then in the choice of contraceptive methods for young women diagnosed with MS should be carefully chosen.

## References


1. **Alwan, S., I. M. Yee, M. Dybalski, C. Guimond, E. Dwosh, T. M. Greenwood, R. Butler, A. D. Sadovnick.** Reproductive decision making after the diagnosis of multiple sclerosis. – Mult. Scler., **19**(3), 2013, 351-358.
2. **Boughton, B.** Women With MS May Have Increased Relapse Risk After IVF. – Medscape Neurology, July 11, 2012.
3. **Deleva, D., V. Kolyovska, B. Sultanov.** Influences of sex hormones and pregnancy in multiple sclerosis. – Acta morphol. et anthropol., **18** 2012, 140-142.
4. **Deleva, D., V. Kolyovska, B. Sultanov.** Multiple sclerosis and pregnancy: Disease biomarkers. – Compt. rend. Acad. bulg. Sci., **65**(6), 2012,865-870.
5. **El-Etr, M., A. Ghoumari, R. Sitruk-Ware, M. Schumacher.** Hormonal influences in multiple sclerosis: new therapeutic benefits for steroids. – Maturitas, **68**(1), 2011, 47-51.
6. **Gregg, C.** Pregnancy, prolactin and white matter regeneration. – J. Neurol. Sci., **285**(1-2), 2009, 22-27.
7. **Hughes, G.** Progesterone and autoimmune disease. – Autoimmun. Rev., 2011, Dec. 13.
8. **Hughes, S.** MS Linked With Use of Hormonal Contraceptives. – Medscape, March 06, 2014.
9. **Liu, M., M. Kelly, P. Herson, P. Hum.** Neuroprotection of sex steroids. – Minerva Endocrinol., **35**, 2010, 127-143.
10. **Michel, L., Y. Foucher, S. Vukusic, C. Confavreux et al.** Increased risk of multiple sclerosis relapse after in vitro fertilization. – J. Neurol. Neurosurg. Psychiatry, June 2012.
11. **Morgan-Followell, B. N., J. A. Nicholas, P. Weisleder.** Reproductive issues in women with multiple sclerosis: ethical considerations. – Continuum (Minneap Minn)., **20**(1) 2014, 177-180.
12. **Shuster, E.** Hormonal influences in multiple sclerosis. – Curr. Top. Micribiol. Immunol., **318**, 2008, 267-311.
13. **Türkyılmaz, E., M. Yıldırım, A. Filiz, Y. Avşar.** Multiple sclerosis; a disease of reproductive-aged women and the dilemma involving contraceptive methods. – J. Turk. Ger. Gynecol. Assoc., **16**(1), 2015, 49-53.
14. **Voskuhl, R.** Gender issues and multiple sclerosis. – Curr. Neurol. Neurosci. Rep., **2**(3), 2002, 277-286.

Institute of Experimental Morphology, Pathology and Anthropology with Museum
Bulgarian Anatomical Society

Acta morphologica et anthropologica, 22
Sofia ● 2015

# Protective Role of Germinal Angiotensin I Converting Enzyme (gACE) for Sperm and Fertilization: Review

*M. Pencheva[1], Y. Koeva[1], N. Atanassova[2]*

*[1] Department of Anatomy, Histology and Embryology, Medical University of Plovdiv, Bulgaria*
*[2] Institute of Experimental Morphology and Anthropology with Museum, Bulgarian Academy of Sciences, Sofia, Bulgaria*

The present review is focused on the processes in male reproductive system associated with the motility and maturation/capacitation of sperm and it is related to the fact that about 40% of male infertility cases have unclear nature, i.e. idiopathic infertility, which often results from compromised maturation of sperm in the epididymis and other portions of reproductive ducts. One of the enzymes involved in realization process is germinal isoform of angiotensin I converting enzyme (gACE), also known as testicular ACE (tACE). Our study revealed the key role of gACE in spermatogenesis and later in the process of fusion of sperm and eggs, suggesting a possible remodeling and protective function of the enzyme toward male gametes. This study is an attempt to demonstrate the importance of gACE in fertilization process and male reproductive health.

*Key words:* gACE, testis, reproduction, sperm, male infertility.

## Introduction

Semen is a complex organic fluid containing sperm and a complex of proteins that are produced and secreted by male reproductive tract and its accessory glands. Much of proteins produced act in specific areas, while others accompany sperm in their long way of spermatogenesis, ducts of male and female reproductive system to final destination oocytes/ova. During that process, sperm undergo series of physiological and biochemical events associated with sperm motility and capacitation. Investigations on such key proteins are essential for better understanding of the evens responsible for infertility and more specifically called idiopathic infertility.

The present study examines the role of germinal isoform of angiotensin I-converting enzyme (gACE) in male reproduction, in particular its function in male reproductive tract. A number of different cell surface proteins, such as membrane-anchored enzymes, receptors, and adhesion molecules, are targets of specific proteolytic processing that releases their extracellular domain and may function as a posttranslational switch for their biological activity [2, 19, 51].

## Structure and Function of ACE

In male mammals ACE is expressed in two isoforms encoded by a single gene and transcribed from two alternative promoters [5, 9]: a somatic ACE (sACE), which is expressed in numerous tissues (vascular endothelium, renal tubule, and intestinal epithelium), and gACE (also known as testicular ACE), which is located on the plasma membrane of sperm released from the testis [48, 55].

The structure of the ACE gene is a result of gene duplication in the distant past. ACE molecule consists of an intracellular domain, a transmembrane domain, N- and C- terminal domains. ACE is anchored to the plasma membrane near the C-terminus of the enzyme. ACE also exists in a soluble form (in blood plasma, amniotic and cerebrospinal fluid and seminal plasma). The soluble form of the enzyme is released with the mediation of unknown protease known as secretory ACE as a result of process called "shedding" [4, 20].

ACE is zinc metalloproteinase that hydrolyses multiple substrates exerting multiple specific functions, some of them are still unknown. Acting as a non-specific dipeptidase, by liberating di- and tripeptides from various proteins, the enzyme may participate, in general processes as peptide metabolism, detoxification and absorption of amino acids at cell surfaces [11].

Angiotensin converting enzyme is an integral part of renin-angiotensin-aldosterone system (RAAS) [36]. The system consists of a cascade of precursors which are transformed into final bioactive products. The main peptides involved are as follows: angiotensinogen, which is converted to angiotensin I (Ang I) by the enzyme renin secreted by the kidney. Ang I is converted by somatic isoform of ACE to potent vasoconstrictor angiotensin II [Ang II or Ang (1-9)]. Therefore, sACE has been implicated in the control of blood pressure and fluid-electrolyte balance [4, 11]. Somatic ACE also played role in male reproduction catalyzing degradation of bradykinin, which stimulated germ cell proliferation [1]. The enzyme is a marker for germ cell neoplasia [37]. Ang II is involved in Leydig cell steroidogenesis via cleavage of LHRH and substance P. Epididymal sACE is responsible for remodeling of seminal fluid [12].

There is another form of ACE named ACE 2. ACE 2 is involved in generation of alternative angiotensin peptides in particular, conversation of Ang (1-9) to Ang (1-7), which is vasodilatator [43].

RAS involved prorenin, renin, angiotensinogen, Ang I and II and ACE and they have been reported in reproductive organs, particularly in the ovary, epididymis and testis [50, 53]. Ang II participated in several important functions for male gametes as sperm motility, acrosome reaction and binding of sperm to the zona pellucida [54, 34].

ACE acts through two G protein coupled receptors, AT I and AT II. Activation of AT I receptors is responsible for vasoconstriction and aldosterone release while AT II receptors are proposed to mediate antagonizing effects and apoptosis [6, 8, 13, 22, 40]. AT1 receptor is present in seminiferous tubules, in particular Sertoli cells and germ cells and as well as in tails of spermatids. In mature sperm AT1 receptor is localized at the base of the tail and in the acrosome area.

## Role of gACE in the Testis

Germinal isoform of angiotensin I converting enzyme (gACE) is germ cell specific isoform of male reproductive system that is a key factor for male fertility [53]. In contrast to sACE, gACE does not generate vasoconstrictor peptide AngII and substrate for gACE has not been identified [12]. Germinal ACE is expressed at high level by

developing germ cells and it is also present in mature sperm. Germinal ACE activity is possibly linked with androgens and is involved with spermatogenesis and sperm maturation.

During spermatogenesis the enzyme is detected in germ cells in rodents (mouse, rat) and men. Although, gACE mRNA present in spermatocytes, the gACE protein is found in post-meiotic germ cells (spermatids) during elongation steps in gradually increasing pattern [3, 32, 47]. In adult rat stage specific pattern of protein expression revealed [3]. Faint immunoreactivity appeared in the cytoplasm of round spermatids step 8 (stage VIII of the cycle) in a round shape manner. Later that stage, the immunostaining progressively increased and was located in caudally organized cytoplasm of elongating spermatids. Immunoexpression of gACE became strong later than steps 12 of spermiogenesis (stage XII of the cycle) and reached maximum in steps 17-19 (stages IV-VIII of the cycle). No immunoexpression of gACE was observed in other germ cell types (spermatogonia, spermatocytes) as well as in somatic cells (peritubular cells, Leydig and Sertoli cells). Similar pattern of cellular localization of and distribution gACE was described in mice [32, 47].

Stage-specific expression of gACE was demonstrated in human testis where gACE protein was found only in adluminal membranes of post meiotic germ cells later than step 3 round spermatids corresponding to step 7 round spermatids in rat [38]. Maximal expression of human gACE occurred in step 7-8 elongated spermatids. Germinal ACE mRNA expression was detected in pachytene spermatocytes and round spermatids. The gACE protein was always strictly confined to the adluminal membrane of differentiating spermatids, leaving the head and acrosomal regions free of detectable immunoreactivity [45]. After sperm release, gACE protein localized to residual bodies and the neck and midpiece region of normal spermatozoa within the seminiferous tubules and ejaculates.

High gACE activity has been determined in human seminal plasma [46]. Immunoelectron microscopy demonstrated that ACE is mainly located at the plasma membrane of the acrosomal region, equatorial segment, postacrosomal region and midpiece [28]. A role of the gACE in capacitation, acrosome reaction and binding to zona pellucida has been suggested by several authors [10, 49].

In spermatozoa the protein is localized in the neck and middle part of ejaculated mature spermatozoa [45]. Dipeptidase activity of gACE is responsible for release of GPI proteins from sperm membrane that is important for sperm-zona pellucida binding, necessary for fertilization. Acting like a GPI-anchored protein releasing factor, gACE shed various GPI-anchored proteins, mostly PH-20 and Tesp5 from the cell surface of germ cells [27, 29]. Therefore, gACE may serve as marker for fertilizing ability of spermatozoa.

Stage specificity of gACE localization during spermatogenic cycle characterizes gACE as a good marker for stage of spermatid differentiation [3]. In rat testis expression of gACE starts and reaches maximum in androgen dependent stage VIII of spermatogenic cycle that implies androgen regulation of enzyme production in germ cells. Localization pattern of gACE revealed the importance of elongation phase of spermatids in male germ cell differentiation with respect to gene expression and not only to morphological modifications. Expression of gACE in post meiotic germ cells is an example for specific gene activation and translation during spermiogenesis [12].

Expression of gACE was investigated by application of various experimental models in rat as spontaneous hypertension (SHR), androgen deprivation and hyperglycaemia (diabetes mellitus) [3, 31]. Data suggested that gACE can be used as a marker for germ cell depletion in experimental and pathological conditions. In particular, gACE can be recommended for precise visualization and evaluation of spermatid loss that is not optional by routine histological technique.

Developmentally, with the advent of puberty, gACE increased significantly in the testes and ductuli efferentes and to a lesser extent in the more distal regions of the male reproductive tract. The gACE concentration in the testicles is the highest among of the all organs [15].

Studies on human males revealed time-related changes in the cell specific expression of sACE. Switch of both ACE isoforms in human germ cells occurred: sACE is found in foetal gonocytes but only gACE is exclusively expressed in spermatids and spermatozoa. Generally, Sertoli cells show only a weak and markedly diffuse immunoreactivity for sACE. This labelling disappears towards the end of gestation but may be maintained in some seminiferous tubules for months after birth. Both of Leydig cell populations – fetal and adult expressed sACE [38].

## Role of gACE in the Epididymis

Once sperm have undergone process of formation and differentiation in the testis, they enter the epididymis. Epididymis is divided into three regions: caput, corpus and cauda. The proximal part of caput epididymis is designated as initial segment. Segmentation of epididymis contributed to establishment of morpho-functional compartments, each of them maintain unique microenvironment due to segment-specific expression of genes encoding signaling molecules, transcription factors, receptors, regulatory and transport molecules. Such segment-specific microenvironment is essential for adequate response of epididymal epithelium to hormones and regulatory factors [52].

Epididymis is a target androgen regulation that is important for segment specific physiology and stimulation of production and secretion of factors interacting with surface proteins located on sperm membrane [15].

Turner et al. suggested that whole amount of gACE in luminal fluid of the epididymis derived from the testis resulting from an active proteolytic process and release of extracellular domain of the enzyme from the sperm surface occurred in the initial segment. Using PCR and Northern blot the author did not found mRNA of gACE suggesting that gACE protein is not produced in the epididymis [14, 35]. Moreover, the amount and sACE mRNA is very low in the epididymis and the protein is hardly discernible. Germinal ACE is absent from the liquid fraction in the epididymis in azoospermic men thereby demonstrating that ACE in luminal fluid of the epididymis is derived from membrane-binding gACE of the sperm [14, 39].

High ACE activity has been determined in human benign prostatic hyperplasia, whereas normal prostates apparently have low enzymatic activity [46]. Vas deferens and seminal vesicles showed low ACE activity [18].

## Role of ACE in Female Reproductive Physiology

ACE plays a significant role in ovarian physiology as follicular development, steroidogenesis and formation of corpus luteum, egg maturation, ovulation and follicular atresia. Appearance of ACE in the ovary is regulated by gonadotropins. Angiotensin II bioactive octa-peptide is involved in paracrine and autocrine regulation of different phases of female reproductive cycle [17]. Angiotensin II receptors are AT2 subtype and they are located primarily on granulosa and theca interna cells of atretic follicles [7, 41]. Kuji et al. [30] reported that Ang II facilitates follicular development and ovulation in the rabbit via AT2 receptor, since an AT2 receptor antagonist inhibited hCG- and Ang

II-induced ovulation, oocyte maturation in vitro, as well as, Ang II-induced estrogen and prostaglandin production.

High concentrations of renin and Ang II were found in all utero-placental tissues. The presence of renin mRNA in the endometrium, choroid and fetal part of the placenta proves local renin synthesis. Ang II is important for the contraction of uterine muscles. Ang II is also committed in the regulation of utero-placental blood flow [16].

## Germinal ACE and Male Infertility

*Role in sperm–zona pellucida binding*

Experiments with genetically manipulated mice provided new data about essential role of gACE for male reproduction and fertility. For better understanding of the role of gACE and sACE in the male reproduction, an insertional disruption of the somatic but not the testicular ACE gene was generated. Males homozygous for this mutation have normal amounts of testicular ACE mRNA and protein but completely lack of somatic ACE (equal to complete knockout of sACE) is responsible for severe kidney pathology. Nevertheless, homozygous for sACE mutation males have normal fertility, proving conclusively that somatic ACE in males is not essential for their fertility. ACE null mice lacking both somatic and testicular ACE are infertile suggesting that only gACE has critical importance for male fertility by acting differently compared to sACE. Infertility, independently of normal testis weight, sperm count and morphology, is due to altered sperm migration in the oviduct and their ability to bind zona pellucida. In mutant mice lack of expression of gACE on sperm membrane may result in lack of processing of some cell surface proteins of the sperm. Mutants exhibit also low blood pressure and renal dysfunction. Experiments with transgenic expression of testicular ACE in ACE null mice restored fertility, whereas transgenesis of somatic ACE in ACE mutants did not and mice were infertile. Therefore, sACE cannot substitute gACE in male reproduction [42].

Sperm phenotype, i.e., failure of sperm to bind to the zona pellucida, was found not only in mice deficient in ACE gene but in genetic model of disruption of a number of genes, e.g., calmegin (CLGN), calsperin (CALR3), fertilin alpha (ADAM1) and beta (ADAM2) and ADAM3. Data from these knockout models provided new understanding of molecular mechanisms of gACE function in male fertility. In particular, gACE is not a direct mediator of the connection between sperm-zona pellucida. Interactions and relationships of ADAMs proteins with calmegin and calsperin are possibly responsible for zona binding ability of sperm. Because calmegin functions as a testis-specific molecular chaperone for membrane transport of target proteins, there is a possibility of misfolding of membrane surface ADAMs proteins of sperm from CLGN-/- mice. As gACE showed normal activity in CLGN-/- mice, CLGN seems to be not involved in transporting ACE to the sperm membrane. The role of ADAM3 protein and its regulation was investigated using both of GLGN- and ACE- deficient mice. ADAM3 was absent from GLGN-/- and ACE-/- sperm suggesting that both of gACE and GLGN are involved in distributing ADAM3 to a location on the sperm surface where it can participate in sperm-zona pellucida binding [21, 24, 56].

*Role in sperm–egg fusion*

Similar approach of genetic mouse models was applied for identification of genes responsible for sperm-egg fusion. It is known that only acrosome reacted sperm have an ability to fuse with eggs. During acrosome reaction, sperm shed the plasma membrane

in their acrosomal cap area and expose their inner acrosomal membrane. So far, two essential proteins have emerged to be involved in sperm-egg fusion – CD9 on egg membrane and IZUMO1 on sperm [25]. IZUMO1 is a transmembrane protein with an extracellular region, a single transmembrane region and a short cytoplasmic tail [26]. Mice lacking IZUMO gene (IZUMO -/-) were healthy but males were sterile. They produced normal-looking sperm that bound to and penetrated the zona pellucida but were incapable of fusing with eggs. Human sperm also contain Izumo and addition of an antibody against human Izumo left the sperm unable to fuse with zona-free eggs [23]. In attempt to find an IZUMO1-interacting protein, Inoue et al. [26] proposed gACE3 that has been previously reported by Rella et al [44] as a novel homologue of testis specific, but only at mRNA level. In mice lacking ACE3, the only phenotype found in ACE3-deficient sperm is that the localization of IZUMO1 extended to a broader area than in wild-type sperm having no effect on sperm fertilizing ability. Therefore, elimination of gACE3 did not result in a loss of sperm fertilizing ability, differing from the case of gACE disruption.

Recent data by Li et al. [33] outlined a possible application of gACE as a marker for sperm selection for assisted reproductive technologies. Using Western blot and immunofluorescence, the author suggested that absence of gACE expression is responsible for total fertilization failure and lower fertilization rates by in vitro fertilization (IVF). Therefore, sperm lacking gACE may be recognized before commencing IVF and that the patients may be directed instead to consider intracytoplasmic sperm injection.

In conclusion, our review provides broad understanding of the role of gACE as a novel marker for male fertility. Protein interactions between gACE and other important key factors located on sperm surface underlie molecular events/mechanisms of fertilization. The identification and understanding of the role of gACE in maturation mechanisms of key sperm proteins will pave the way toward novel approaches for both contraception and treatment of unexplained male infertility. Clinical application of gACE in assisted reproductive technologies promises new perspective for development of reproductive medicine.

## References


1. **Atanassova, N., L. Kancheva, B. Somlev**. Bradykinin stimulates prepubertal rat germ cell proliferation in vitro. – Immunopharmacology **40**(3), 1998, 173-178.
2. **Arribas, J., L. Coodly, P. Vollmer, T. Kishimoto, S. Rose-John, J. Massague.** Diverse cell surface protein ectodomains are shed by a system sensitive to metalloprotease inhibitors. – J. Biol. Chem., **271**, 1996, 11376-11382.
3. **Atanassova, N., E. Lakova, Y. Bratchkova, G. Krasteva, M. Donchev.** Expression of testicular angiotensin-converting enzyme in adult spontaneously hypertensive rats. – Folia Histochem. Cytobiol., **47**(1), 2009, 117-122.
4. **Carey, R. M., H. Siragy.** Newly recognized components of the renin-angiotensin system: Potential roles in cardiovascular and renal regulation. – Endocrine Rev., **24**, 2003, 261-271.
5. **Corvol, P., A. Michaud, F. Soubrier, T. Williams.** Recent advances in knowledge of the structure and function of the angiotensin I converting enzyme. – J. Hypertension Suppl., **13**(3) 1995, 3-10.
6. **Crawford, K. W., E. Frey, T. Cote.** Angiotensin II receptor recognized by Dup753 regulates two distinct guanine nucleotide-binding protein signaling pathways. – Mol. Pharmacol., **41**, 1992, 154-162.
7. **Daud, A. I., F. Bumpusand, A. Husain.** Evidence for selective expression of angiotensin II receptors on atretic follicles in the rat ovary: an autoradiographic study. – Endocrinology, **122**, 1988, 2727-2734.
8. **Dingh, D. T., A. Frauman, C. Johnston, M. Fabiani.** Angiotensin receptors: distribution, signaling and function. – Clin. Sci., **100**, 2001, 481-92.

9. **Ehlers, M. R., J. Riordan**. Angiotensin-converting enzyme: new concepts concerning its biological role. – Biochemistry, **28**(13), 1989, 5311-5318.
10. **Florman, H. M., M. Jungnickel, K. Sutton.** Shedding light on sperm phertility. – Cell, **140**, 2010, 310-312.
11. **Franke, F. E., K. Pauls, L. Kerkman, K. Steger, T. Klonisch, R. Metrger, F. Alhenc-Gelas, E. Burkhardt, M. Bergmann, S. M. Danilov.** Somatic isoform of angotensin I converting enzyme in the pathology of testicular germ cell tumors. – Hum. Pathol., **31**, 2000, 1466-1476.
12. **Franke, F. E, K. Pauls, R. Metzger, S. M. Danilov.** Angiotensin I-converting enzyme and potential substrates in human testis and testicular tumours. – APMIS **111**, 2003, 234-44.
13. **Fraser, L. R., M. Pondel, G. Vinson.** Calcitonin, angiotensin II and FPP significantly modulate mouse sperm function. – Mol. Hum. Reprod., **7**(3), 2001, 245-253.
14. **Gatti, J. L., X. Druart, Y. Guerin, F. Dacheux, J. Dacheux.** A 105- to 94-kilodalton protein in the epididymal fluids of domestic mammals is angiotensin I-converting enzyme (ACE): evidence that sperm are the source of this ACE. – Biol. Reprod., **60**, 1999, 937–945.
15. **Ghyselinck, N. B., C. Jimenez, Y. Courty, J. Dufaure.** Androgen-dependent messenger RNA(s) related to secretory proteins in the mouse epididymis. – J. Reprod. Fertil., **85**, 1989, 631-639.
16. **Hagemann, A., A. Nielsen, K. Poulsen.** The uteroplacental renin-angiotensin system: a review. – Exp. Clin. Endocrinol., **102**(3), 1994, 252-61.
17. **Herr, D., I. Bekes, Chr. Wulff.** Local renin-angiotensin system in the reproductive system. Front. Endocrinol. (Lausanne), **4,** 2013, 150.
18. **Hohlbrugger, G., H. Schweisfurth, H. Dahlheim.** Angiotensin I converting enzyme in rat testis, epididymis and vas deferens under different conditions. – J. Reprod. Fertil., **65,** 1982, 97-103.
19. **Hooper, N. M., E. Karran, A. Turner.** Membrane protein secretases. – J. Biochem., **321**(2), 1997, 265-279.
20. **Hubert, Chr., An. Houot, P. Corvol, Fl. Soubrier**. Structure of the angiotensin I-converting enzyme gene. – J. Biol. Chem., **266**(23), 1991, 15377-15383.
21. **Ikawa, M., K. Tokuhiro, R .Yamaguchi, A. Benham, T. Tamura, I. Wada, Y. Satouh, N. Inoue, M. Okabe.** Calsperin is a testis-specific chaperone required for sperm fertility. – J. Biol. Chem., **286**, 2011, 5639-5646.
22. **Inagami, T., N. Iwai, K. Sasaki, Y. Yamano, S. Bardhan, S. Chaki, D. Guo, H. Furuta.** Cloning, expression and regulation of angiotensin II receptors. – J. Hypertension, **10**, 1992, 713-716.
23. **Inoue, N., M. Ikawa, A. Isotani, M. Okabe**. The immunoglobulin superfamily protein Izumo is required for sperm to fuse with eggs. – Nature, **434**, 2005, 234–238.
24. **Inoue, N., R. Yamaguchi, M. Ikawa, M. Okabe.** Sperm-egg interaction and gene manipulated animals. – Soc. Reprod. Fertil. Suppl., **65**, 2007, 363-371.
25. **Inoue, N., M. Ikawa, M. Okabe.** The mechanism of sperm-egg interaction and the involvement of IZUMO1 in fusion. – J. Asian Androl. **13**(1), 2011, 81-87.
26. **Inoue, N., T. Kasahara, M. Ikawa, M. Okabe.** Identification and disruption of sperm-specific angiotensin converting enzyme-3 (ACE3) in mouse. – PLoS One, **5**, 2010, e10301.
27. **Kirchhoff, C., G. Hale.** Cell-to-cell transfer of glycosylphosphatidylinositol anchored proteins during sperm maturation. – Mol. Hum. Reprod., **2**, 1994, 177-184.
28. **Kohn, F. M., I. Dammshauser, C. Neukamm, H. Renneberg, W. E. Siems, W. B. Schill, G. Aumuller.** Ultrastructural localization of angiotensin- converting enzyme in ejaculated human spermatozoa. – Human. Reproduction, **13**(3) 1998, 604–610.
29. **Kondoh, G., H. Tojo, Y. Nakatani, N. Komazawa, C. Murata, K. Yamagata, Y. Maeda, T. Kinoshita, M. Okabe, R. Taguchi, J. Takeda.** Angiotensin-converting enzyme is a GPI-anchored protein releasing factor crucial for fertilization. – Nat. Med., **11**, 2005, 160-166.
30. **Kuji, N., K. Sueoka, T. Miyazaki, M. Tanaka, T. Oda, T. Kobayashi, Y. Yoshimura**. Involvement of angiotensin II in the process of gonadotropin-induced ovulation in rabbits. – Biol. Reprod., **55**, 1996, 984-991.
31. **Lakova E., S. Popovska, I. Gencheva, M. Donchev, G. Krasteva, E. Pavlova, D. Dimova, N. Atanassova.** Experimental model for streptozotocin-induced diabetes mellitus neonatally or in adulthood – comparative study on male reproduction in condition of hyperglycaemia. – Acta Morphol. Anthropol., **19**, 2012, 122-126.
32. **Langford, K. G., Y. Zhou, L. Russell, J. Wilcox, K. Bernstein**. Regulated expression of testis angiotensin-converting enzyme during spermatogenesis in mice. – Biol. Reprod., **48**, 1993, 1210-1218.

33. **Li, L. J., F. B. Zhang, S. Y. Liu, Y. H. Tian, F. Le, L. Y. Wang, H. Y. Lou, X. R. Xu, H. F. Huang, F. Jin**. Human sperm devoid of germinal angiotensin-converting enzyme is responsible for total fertilization failure and lower fertilization rates by conventional IVF. – Biol. Reprod., **90**(6), 2014, 125.
34. **Mededovic, S., L. Frase.** Mechanisms of action of angiotensin II on mammalian sperm function. – Reproduction, **129**(2), 2005, 211-218.
35. **Metayer, S., F. Dacheux, J. Dacheux, J. Gatti.** Germinal angiotensin I-converting enzyme is totally shed from the rodent sperm membraneduring epididymal maturation. – Biol. Reprod. **67,** 2002, 1763-1767.
36. **Paul, M., A. Mehr, R. Kreutz.** Physiology of local rennin-angiotensin system. – Physiol. Rev., **86**, 2006, 747-803.
37. **Pauls, K., L. Fink, F. Franke.** Angiotensin-converting enzyme (CD143) in neoplastic germ cells. – Lab. Invest., **79**, 1999, 1425-35.
38. **Pauls, K., R. Metzger, K. Steger, T. Klonisch, S. Danilov, F. Franke.** Isoforms of angiotensin I-converting enzyme in the development and differentiation of human testis and epididymis. – Andrologia, **35**, 2003, 32-43.
39. **Perttula, T. V., J. Mather, C. Bardin, S. Moss, A. Bellve.** Localization of the antigotensin-converting enzyme activity in testis and epididymis. – Biol. Reprod., **33,**1985, 870-877.
40. **Pobiner, B. F., J. K. Northup, P. H. Bauer, E. D. Fraser, J. C.** Garrison. Inhibitory GTP-binding regulatory protein Gi3 can couple angiotensin II receptors to inhibition of adenylyl cyclase in hepatocytes. – Mol. Pharmacol., **40**(2), 1991, 156-67.
41. **Pucell, A. G., J. Hodges, I. Sen, F. Bumpus, A. Husain.** Biochemical properties of the ovarian granulosa cell type-2-angiotensin II receptor. – Endocrinology, **128,** 1991, 1947-1959.
42. **Ramaraj, P., S. P. Kessler, C. Colmenares, G. C. Sen.** Selective restoration of male fertility in mice lacking angiotensin-converting enzymes by sperm-specific expression of the testicular isozyme. – J. Clin. Invest., **102**(2), 1998, 371-378.
43. **Reis, A. B., F. Araújo, V. Pereira, A. Reis, R. Santos, F. Reis.** Angiotensin (1-7) and its receptor Mas are expressed in the human testis: Implications for male infertility. – J. Mol. Histol., **41**, 2010, 75-80.
44. **Rella, M., J. L. Elliot, T. J. Revett, J. Lanfear, A. Phelan, R. M. Jackson, A. J. Turner, N. M. Hooper.** Identification and characterisation of the angiotensin converting enzyme-3 (ACE3) gene: a novel mammalian homologue of ACE. – BMC Genomics, **8**, 2007, 194.
45. **Ryan, J. W., U. Ryan, D. Schultz, C. Whitaker, A. Chung.** Subcellular localization of pulmonary angiotensin-converting enzyme (kininase II). – J. Biochem., **146,** 1975, 497-499.
46. **Sande, M. V., J. Inokuchi, A. Nagamatsu, S. Scharpe, H. Neels, K. Camp.** Tripeptidyl carboxypeptidase activity of angiotensin-converting enzyme in human tissues of the urogenital tract. – Urol. Int., **40**, 1985 100-102.
47. **Sibony, M., D. Segretain, J. Gasc**. Angiotensin-converting enzyme in murine testis: step-specific expression of the germinal isoform during spermiogenesis. – Biol. Reprod., **50**, 1994, 1015-1026.
48. **Sibony, M., J. Gasc, F. Soubrier, F. Gelas, P. Corvol.** Gene expression and tissue localization of the two isoforms of angiotensin I-converting enzyme. – Hypertension, **21,** 1993, 827-835.
49. **Singh U. S., M. Kumar, J. Panda**. Angiotensin converting enzyme in semen and its possible role in capacitation. – Andrologia, **17**, 1985, 472-475.
50. **Speth, R. C., D. Daubert, K. Grove.** Angiotensin II: a reproductive hormone too? – Regul. Pept., **79**, 1999, 25-40.
51. **Thimon, V., S. Métayer , M. Belghazi, F. Dacheux, J. Dacheux, J. Gatti**. Shedding of the germinal angiotensin I-converting enzyme (gACE) involves a serine protease and is activated by epididymal fluid. – Biol. Reprod., **73**(5), 2005, 881-890.
52. **Turner, T., T. Bomgardner, J. Jacobs, Q. A. Nguyen.** Association of segmentation of the epididymal interstitium with segmented tubule function in rats and mice. – Reproduction, **125**, 2003, 871-878.
53. **Vinson G. P., E. Saridogan, J. Puddefoot, O. Djahanbakhch.** Tissue renin-angiotensin systems and reproduction. – Hum. Reprod., **12,** 1997, 651-662.
54. **Wennemuth, G., D. Babcock, B. Hille.** Distribution and function of angiotensin I1 receptors in mouse spermatozoa, Department of Physiology and Biophysics, University of Washington, Seattle, USA.

55. **Williams, T. A., K. Barnes, A. Kenny, A. Turner, N. Hooper**. A comparison of the zinc contents and substrate specificities of the endothelial and testicular forms of porcine angiotensin converting enzyme and the preparation of isoenzyme-specific antisera. – J. Biochem., **288**(3), 1992, 875-881.
56. **Yamaguchi, R., K. Yamagata, M. Ikawa, St. B. Moss, M. Okabe.** Aberrant distribution of ADAM3 in sperm from both angiotensin-converting enzyme (Ace)- and calmegin (Clgn)-deficient mice. Biol. Reprod., **75**(5), 760-766.